Alternative Binder Systems for the Immobilisation of Waste Streams

Robin Shirley

Submitted in accordance with the requirements for the degree of Doctor of Philosophy

The University of Leeds
School of Civil Engineering

March, 2012

The candidate confirms that the work submitted is his own and that appropriate credit has been given where reference has been made to the work of others.

Acknowledgements

First and foremost I have to thank my supervisor Dr Leon Black for giving me the opportunity to undertake this work and for his constant support throughout. I could not have completed the work without his guidance and encouragement. Thanks must also go to Viridor, and in particular Andrew Goddard and Roy Griffin for their support and contributions helping me gain a better understanding of the waste management industry and helping to guide the work.

Many thanks are also offered to the technical staff at the university who have put up with me in the laboratories and always been there with good advice, a helping hand and morale support. The help of all the technical staff I have bothered during my study is appreciated and particular thanks go to Leslie Arkless, Peter Flatt and Steve Holmes. Thanks also go to the other academics within the department whom I have troubled with questions and have helped me out with their knowledge and experience, and to the other members of the department who have supported me not only with advice but with friendly faces and understanding.

Thanks are also due to the EPSRC for their support with funding of the work.

Finally I thank my family, friends and Ale for their support not only over my time in Leeds but throughout my life, and for reminding me that there is life outside work which must not be neglected.

Abstract

This work aimed to assess the potential for valorisation of waste materials in order to minimise the environmental impact of hazardous air pollution control residues by solidification/stabilisation. The potential for immobilisation in a primarily pozzolanic matrix was examined. Pulverised fuel ash resulting from the co-combustion of coal and biomass, which did not meet end of waste criteria for construction purposes, and a waste caustic solution resulting from the cleaning of aluminium extrusion dyes were utilised as reagents.

A range of variables were examined with regards to mix design and curing conditions. The mineralogy, reaction kinetics and pore structure of the samples were examined and performance assessed based on physical tests and leaching performance with regard given to current legislation within the UK. A detailed understanding of the treatments potential was thereby developed along with an understanding of the factors determining the observed performance.

The treatment option proved unsuccessful primarily due to the lack of potential for immobilisation of the high levels of soluble chloride salts present in the air pollution control residues and the gas production typically observed when blending air pollution control residues with a caustic solution. Compared to more traditional cement based solidification/stabilisation systems other disadvantages were observed relating to slower reaction kinetics and therefore the need for increased curing temperatures, matrix durability, and increased sulphate leaching. Nevertheless the reagents showed some potential and may be suitable for use treating alternative waste streams, providing an economic option which is beneficial for the environment as a whole.

In addition the impact of the known variability in air pollution control residue composition, on the potential treatment by solidification/stabilisation with cement was assessed. Significantly different performance was observed which implied the necessity to modify any such treatment.

Table of Contents

List of Figures

List of Tables

List of Abbreviations

AAS, Alkali activated blast furnace slag

AFm, Al_2O_3-Fe_2O_3-mono, reference to hydrated calcium-aluminium/iron minerals containing a single divalent or two monovalent anions

AFt, Al_2O_3-Fe_2O_3-tri, reference to hydrated calcium-aluminium/iron minerals containing three divalent anions (or equivalent)

ANC, Acid neutralisation capacity

APC, Air pollution control

BSE, Back scattered electron

C-A-S-H, Calcium aluminium silicate hydrate

C-S-H, Calcium silicate hydrate,

DIW, De-ionised water

DOC, Dissolved organic carbon

DTA, Differential thermal analysis

EDX, Energy dispersive x-ray spectroscopy

EfW, Energy from waste

EWC, European waste catalogue

GGBS, Ground granulated blast furnace slag

I/LC, Ion/liquid chromatography

ICP OES, Inductively coupled plasma optical emission spectroscopy

IPPC, Integrated pollution prevention and control

LOI, Loss on ignition

MSW, Municipal solid waste

NOx, Nitrogen oxides

PFA, Pulverised fuel ash

RIR, Reference intensity ratio

ROC, Renewable obligations certificate

(G)SE, (Gaseous) Secondary electron

(E)SEM, (Environmental) Scanning electron microscopy

SNR, Stable-non reactive

S/S, Solidification/stabilisation

STA, Simultaneous thermal analysis

TDS, Total dissolved solids

TGA, Thermogravimetric analysis

UCS, Unconfined compressive strength

WAC, Waste acceptance criteria

WC, Waste caustic

WFD, Waste framework directive

WID, Waste incineration directive

XRD, X-ray diffraction

XRF, X-ray fluorescence

1 Introduction

Within this thesis a potential treatment option for hazardous air pollution control (APC) residues, collected when controlling the flue gas emissions created during solid waste incineration in a modern energy from waste (EfW) facility, was examined. This chapter aims to provide a background to the work which is presented, including a brief summary of waste policy and the regulatory framework surrounding waste management within the UK. The importance of incineration of waste within this policy along with the negative implications in terms of residue production, and the obligations for management of these residues are discussed. From this, the aims and objectives of the work here reported are established.

1.1 Introduction

The overarching framework for waste management within the European Union is established in the waste framework directive (WFD), the first drafts of which appeared in 1975 [1], and which was last updated in 2008 [2]. This document sets out a hierarchy of management options for waste which is also discussed and represented graphically (Figure 1.1) in the Waste Strategy for England [3], the 2011 Review of Waste Policy in England [4] and Waste (England and Wales) Regulations 2011 [5].

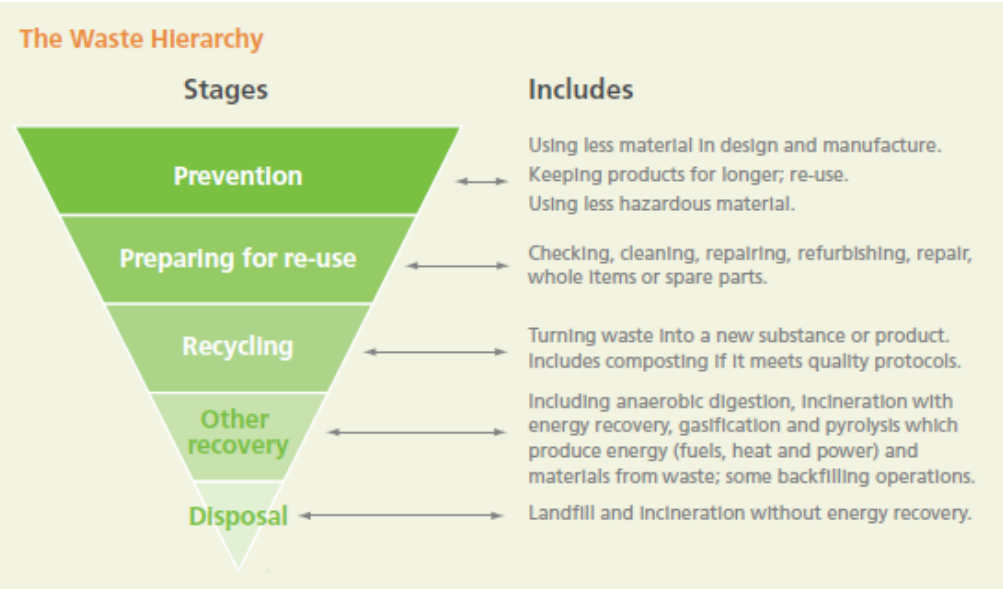

Figure 1.1 Waste Hierarchy, [4]

The UK aims to become a ‘zero waste economy’ [4]. This refers to zero landfilling of waste being achieved by employing processes further up the waste hierarchy. The waste fraction which is not re-used, recycled or composted is labelled as residual waste [6] and is subject to energy recovery methods or disposal in a landfill site.

The generation of residual waste is unavoidable in a modern society. In 2008 ~54 million tonnes of waste was sent to landfill which included 19 million tonnes of commercial and industrial waste [6]. In the Waste Strategy for England (2007) published by DEFRA [3], the target quantity for municipal waste not re-used, recycled or composted in 2020 was given as 12.2m tonnes, a 50% reduction per person on the quantity in 2000 [6]. This waste may be subject to landfilling or energy from waste (EfW) processes such as incineration. Waste incineration is a rapidly growing choice of processing these wastes in many developed countries [6-8] due to its many advantages such as energy recovery and reduction in volume and mass of waste requiring disposal. Whilst there are other methods which can achieve this such as anaerobic digestion, pyrolysis and gasification, incineration is by far the most common because it is suitable for processing the bulk of the residual waste whilst other EfW processes may be suitable for only a small fraction of the waste composition e.g. anaerobic digestion requires organic waste [9]. Additionally EfW incineration is commercially proven.

Residues are created during the waste incineration process. These include bottom ash which may represent around 25% by weight of initial waste and air pollution control (APC) residues which represent ~3% by weight of incinerated waste [10]. Rani *et al* [11] estimated UK APC residue production in 2008 to be 128,000 tonnes and, due to increasing use of EfW incineration this figure is rising [8]. Should government targets be met, in 2020 12.2m tonnes of waste would require either disposal directly to landfill or via EfW processes. Assuming half of this 12.2m tonnes is incinerated (which would result in much being sent directly to landfill unless new technologies are developed) production of these residues in 2020 would be close to

- 305,000 tonnes of APC residue
- 1.22m tonnes of bottom ash

Whilst bottom ash is often classed as inert, APC residues have an absolute hazardous classification in the European Waste Catalogue (EWC) (19 01 07*). Therefore despite the advantages of EfW incineration over sending waste directly to landfill, there are residues remaining which require characterisation, treatment and disposal/valorisation accordingly. The WFD [2] requires wastes are managed such that:

- the risk to human health or the environment is minimised, in particular the risks to water (groundwater and surface water), air, soil, plants or animals,
- nuisance (noise or odours) is avoided
- countryside or places of special interest are not adversely affected.

These obligations should be met using the best available technique, i.e. that which is considered to provide the most effective high general level of protection for the environment as a whole [12]. The strategy for hazardous waste management in England [8] outlines a framework to assist with decision making in order that this be achieved and sets out a hierarchy for hazardous waste management with similar principles to those presented in Figure 1.1 (Figure 1.2).

There is currently a lack of sustainable, cost effective treatment options capable of recycling, valorising or stabilising the hazardous APC residues to a level suitable for disposal in landfill sites according to emissions limits set out in the landfill directive [13]. Consequently, development of potential treatment options is an area of great research interest.

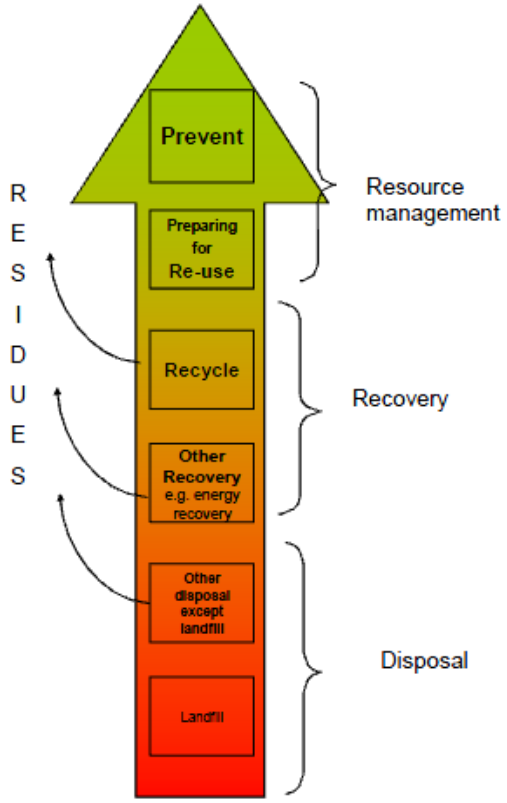

Figure 1.2 Hazardous waste management hierarchy [8]

The aim of this study was to investigate the potential stabilisation of APC residues using other waste materials which would be subject to either disposal or treatment and subsequent disposal. Valorising waste materials as reagents for minimising the environmental impact of hazardous waste would have significant economic and environmental advantages, avoiding the need for raw material extraction and processing to produce reagents, and avoiding direct disposal of the wastes.

Mixing of hazardous waste with other waste materials purely to meet emissions limits by dilution is banned by the WFD and Landfill regulations in order that dilution is not seen as a treatment. The UK government interpretation of the landfill regulation [14] defines a treatment as a physical/chemical/thermal or biological process, including sorting, which changes the characteristics of the waste in order to reduce its volume, reduce its hazardous nature, facilitate its handling or enhance its recovery. Mixing of hazardous waste with other waste may therefore be allowed, as long as it induces these changes in the waste and is shown to be the best

available technique for achieving the management objectives established in the WFD.

With these considerations in mind, the primary objectives of the research included

- Mineralogical and morphological characterisation of APC residues, including identification of principal environmental concerns,
- Identification of suitable waste materials for use as stabilising reagents,
- Investigating performance properties which are required to meet the regulatory limits for stable non-reactive hazardous waste sites and produce an industrially feasible treatment, with a view to optimisation of the treatment.
- Chemical and microstructural characterisation of the treated waste, allowing an understanding of the performance by identifying contaminant immobilisation methods and structural development.
- Examination of treatment robustness i.e. its ability to handle inevitable changes in composition which occur with wastes.

2 Literature Review

This chapter reviews the current literature to give a more comprehensive picture of the operation of EfW incineration, the nature of the residues produced and the current waste management options. Particular attention is paid to treatment by solidification/stabilisation, including the science underpinning its performance, because this was the primary treatment option investigated throughout this study.

2.1 The Incineration Process

Figure 2.1 shows a schematic of a typical EfW incinerator. The incineration of waste is a carefully controlled process with very stringent emissions limits which are important for pollution control and public perception. The EU waste

incineration directive (WID) [15] dictates the operation of waste incinerators although this has been superseded by the large combustion plant directive [16] which applies to all combustion plants with a rated thermal input exceeding 50MW. In concurrence with the integrated pollution prevention and control (IPPC) directive [12] there are best available technique reference documents to complement these directives [17, 18]. These directives are concerned with the efficiency of fuel use and the by-products of the incineration process, such as emissions to the atmosphere, contaminated wastewater and contaminated ash residues.

Primary concerns with respect to emissions to the atmosphere include, particulates, heavy metals, pollutant gases such as HCl, HF, SOx and NOx, and organic pollutants (occurring as products of incomplete combustion) such as dioxins, furans and polycyclic aromatic hydrocarbons (PAH). Measures are taken to keep these emissions below the levels dictated in the WID which affect the operation of the incinerator and result in the production of air pollution control (APC) residues.

Waste can be incinerated as a principle fuel or in co-combustion with other fuels [19]. Co-combustion would primarily be undertaken should the waste be burning at insufficient temperatures (<850℃ or 1100℃ for at least 2 seconds for certain hazardous wastes) and therefore additional, more combustible fuels are used to encourage incineration. This is rare, generally waste can be left to burn self sufficiently once the process is started. However, during start up and shut down additional fuels are required to control emissions before the required temperatures are met. These temperatures are prescribed in order to maximise efficiency and ensure complete combustion thereby avoiding production of the aforementioned organic pollutants. Additional to these temperature restrictions complete combustion is assisted by incinerating the waste on a slow moving grate to provide turbulence and time for complete combustion, as well as ensuring a sufficient oxygen supply [17, 20, 21]. Non-volatile material (bottom ash and metals) is moved along the grate and quenched. Ferrous metals are separated from the bottom ash by a magnetic separator and recycled.

The gases in the combustion chamber (~850˚C) pass through water tube boilers, generating steam and cooling the gases (~140˚C). Cooling is rapid in order to minimise *de novo* synthesis of organic pollutants which occurs primarily when cooling through the temperature range 250-400℃ [21].

The high pressure steam produced during cooling of the incinerator gasses can be used to power turbines and thereby create electrical energy for internal power demands and export to the national grid. The schematic in Figure 2.1 shows distribution of this steam into two turbines. Steam can also be transferred to a heat transfer station where it can be passed through heat exchangers, creating high pressure hot water which can be used for industrial and district heating. When both electricity production and heating are employed the facility is considered a combined heat and power (CHP) plant [21].

Values for residues and energy production for a typical EfW plant are given in Table 2.1. Due to the significant energy recovery possible it is now incredibly rare for a waste incinerator to operate without EfW capability. In addition to the reduction in mass and volume of waste previously mentioned, the recovery of energy from waste in this manner has environmental benefits; recovering value from the waste and reducing the need for raw, finite material consumption in energy production. There are also potential economic benefits for the operator, as it is possible to earn renewable obligation certificates (ROCs) from waste incineration, although the criteria are complicated. The energy efficiency must be high enough for the process to be defined as recovery (calculated as set out in annex II of the WFD [2]). Additionally, unless the waste is a solid recovered fuel the facility must be a qualifying CHP plant and only the energy content in the biomass fraction of the waste is counted [22].

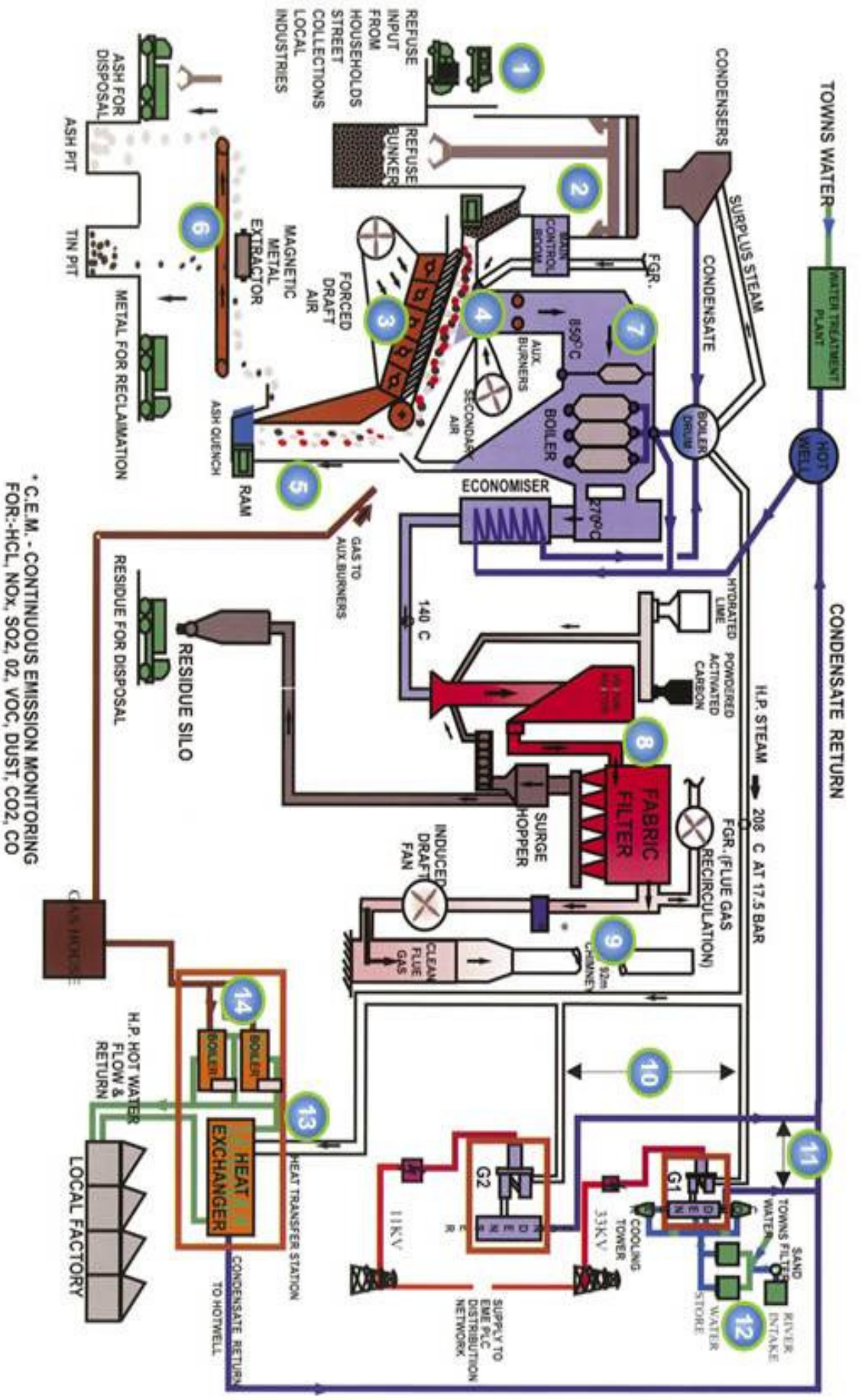

Figure 2.1 Schematic of an EfW incinerator [23]

Waste Incinerated	240,000	tonnes per annum
Energy Exported	85,000	MWh per annum
Metals Recovered	5,000	tonnes per annum
Bottom Ash	46,000	tonnes per annum
APC Residues	8,000	tonnes per annum

Table 2.1 Typical figures for energy and residue production from Coventry EfW incinerator [23]

Following the boiler the gases may pass through an economiser, as shown in Figure 2.1, producing further hot water. The cooled gases are then cleaned. Particulates may initially be removed by an electrostatic precipitator or cyclone. The gases then pass into a reactor tower where an alkaline scrubber and activated carbon are injected to absorb pollutants. Lime is most commonly used to neutralise acid gases such as HCl and SO_2 as shown in equations 2.1-2.4 [24, 25].

Equation 2.1 $Ca(OH)_2 + HCl \rightarrow CaClOH + H_2O$

Equation 2.2 $CaO + HCl \rightarrow CaClOH$

Equation 2.3 $2Ca(OH)_2 + 2SO_2 + O_2 \rightarrow 2CaSO_4 + 2H_2O$

Equation 2.4 $2CaO + 2SO_2 + O_2 \rightarrow 2CaSO_4$

Carbon is typically added at concentration levels between 0.1 and 0.5gm^{-3} of waste gas in order to absorb organic pollutants and metals, particularly those which may be present in the vapour phase such as Hg or Se [18, 21, 26]. Other metals may condense as the gases cool post-furnace, either heterogeneously on the surface of the particulates or via homogeneous condensation [19, 21]. The gases then pass through a fabric filter to remove the carbon and fine particulates. A large proportion of the gas may be re-circulated to optimise the cleaning process.

Additionally treatment is necessary to control the amount of NOx gases (NO and NO_2) released. Treatment for NOx can be separated into two categories, primary measures which prevent the production of NOx gases in the combustion chamber, and flue gas treatments which involve addition of

compounds to remove NOx from flue gases. Primary measures may include treatment such as re-circulation of a proportion of the cleaned, cooled gases to the combustion chamber, reducing the temperature peaks, in turn reducing thermal NO production, a major contributor to NOx emissions, which depends on the reactions shown as equations 2.5-2.7 [27].

Equation 2.5 $N_2 + O \rightarrow NO + N$

Equation 2.6 $N + O_2 \rightarrow NO + O$

Equation 2.7 $N + OH \rightarrow NO + H$

Production of thermal NO is highly dependent on temperature and oxygen concentration. Keeping the combustion temperature below 1400˚C significantly reduces thermal NO production [27].

Flue gas treatments involve the addition of compounds such as ammonia, urea or cyanuric acid to reduce the NOx to molecular nitrogen (Equations 2.8 and 2.9) [27].

Equation 2.8 $4NO + 4NH_3 + O_2 \rightarrow 4N_2 + 6H_2O$

Equation 2.9 $2NO_2 + 4NH_3 + O_2 \rightarrow 3N_2 + 6H_2O$

These processes may be used alongside primary measures in order to meet NOx emissions limits. Additionally there are other methods of controlling NOx emissions such as wet scrubbing with water, or processes which simultaneously treat SOx and NOx such as the copper oxide process or dry absorption onto activated carbon [27].

2.2 Residues Created by Waste Incineration

2.2.1 Bottom ash

Production of bottom ash is around 25% by weight and 10% by volume of waste input [10, 28] a proportion of this, such as large metal fragments, can be recovered and recycled. The remaining bottom ash consists of the ash collected from the grate and the hoppers beneath the grate. It therefore includes the incombustible waste fragments and non-volatile elements [19]. Generally a significant amorphous phase is present as well as siliceous/aluminosilicate crystalline phases such as quartz, anorthite, gehlenite and hydrocalumite, along with iron oxides such as hematite and magnetite [20, 28-31]. Fresh bottom ash frequently contains CaO which, on storage, reacts with moisture to form $Ca(OH)_2$. As a result, the pH of bottom ash before aging can be as high as 12.6 [20, 28, 29, 32]. The acid neutralisation capacity (ANC) to pH 4.5 of fresh bottom ash observed by various authors ranges between 1.2-4.1mEq/g [20, 31, 32] although may be slightly higher [29].

The elemental composition of bottom ash is unsurprisingly affected by the composition of the waste being incinerated as well as the incineration conditions. Typically however, bottom ash is rich in Ca, Si, Al and Fe, and may also contain significant concentrations of Na, K and Mg [20, 29-31, 33-36]. Table 2.2 shows concentration of selected elements reported in [20] for worldwide bottom ash composition. A proportion of the toxic and heavy metals present in the waste remain present in the bottom ash [20, 28, 30, 37]. However, only a small fraction is generally available for leaching, even under acidic conditions [31]. There is also a variable organic content in bottom ash, including the possibility of carcinogenic compounds such as dioxins and furans, although this should be minimised by proper operation of the incinerator i.e. conditions which allow complete combustion [20, 21, 28, 38]. The WID dictates that incinerators should be operated such that the total organic carbon content of the bottom ash is <3% or loss on ignition (LOI) <5% of the dry material [15].

Element	mg/kg
Al	21,900-72,800
Ca	370-123,000
Cl	800-4190
Fe	4120-150,000
K	750-16,000
Mg	400-26,000
Na	2870-42,000
S	1000-5000
Si	91,000-308,000

Table 2.2 Typical concentration of selected elements in bottom ash [20]

The major elements viewed in bottom ash from a hospital incinerator reported by Kougemitrou *et al* [37], Idris *et al* [39] and Whittaker *et al* [40], were similar to those typically found in bottom ash occurring from a municipal solid waste incinerator. There may be differences in the minor and trace element contents e.g. Cu, Cr, Ba, Ni. Hospital incinerators may be subject to operation at higher temperatures (>1100℃ [15, 37]) which affects the composition. This is perhaps the reason for the particularly low unburnt material present in the ash examined by Kougemitrou *et al* [37], indicated by a loss on ignition (LOI) of 0.1%. One noticeable difference between the bottom ash characterised by Kougemitrou *et al* [37] and those resulting from municipal waste incinerators presented throughout other literature here referenced is the lack of any clear crystalline phases in the XRD analysis. This was possibly a result of the operating conditions of the incinerator, specifically the rate at which the ash is cooled by quenching rather than the waste composition, although no specific details were provided. The ash studied by Idris *et al* [39] was also largely amorphous although showed evidence of similar crystalline phases to those found in MSW bottom ash, including quartz, kaolinite, albite, and gibbsite. Hospital waste incinerator ashes were also studied by Genazinni *et al* [41, 42] which showed some similar crystalline phases to municipal waste bottom ash (quartz, hematite, calcite, portlandite, feldspars, anhydrite) but significantly different elemental

composition including higher concentrations of calcium and sulphur, and much lower Si concentration (SiO_2=0.39%). It is noted that despite this low SiO_2 concentration quartz was listed as one of the main XRD peaks. Such compositional variation surely reflects variation in feedstock composition although it is unclear why variation was so large.

Bottom ash has a mirror entry in the European waste catalogue (EWC) (19 01 11* and 19 01 12), thus its hazardous nature must be assessed. Typically the concern is ecotoxicity due to its metal content and possibly Cl or SO_4 salts. However bottom ash may exhibit other hazardous properties, for example it may be carcinogenic, or classed as an irritant/corrosive due to elevated alkalinity [43]. When classed as inert, bottom ash is relatively cheap to landfill, subject to a lower rate of landfill tax.

When end of waste criteria are met, bottom ash may also find uses in such as concrete or asphalt pavements, road bases, fill or embankment applications [34, 44]. Bottom ash is highly heterogeneous with a very large particle size distribution [33]. Before use the ash is often pre-treated to adjust particle size distribution or by aging to reduce the pH and enhance physical and chemical stability. This process reduces the chance of release of metals or salts which may be contained [20, 28, 34, 44, 45]. A significant amount of research has also been done looking into the thermal treatment of bottom ash to improve stability [29, 31, 33, 36, 46, 47]. Such treatment causes mineralogical and physical changes in the bottom ash, reducing the leaching potential and therefore improving the safety and improving the potential for reuse. The ANC of the bottom ash is however reduced after sintering, therefore use in applications in which the ash may contact acidic environments can results in undesired leaching [29, 31, 46]. A possible application studied for the reuse of thermally treated bottom ash is blending with a binder (clay), pellitising, and utilisation as a synthetic aggregate in concrete, which may give improved workability and only slightly lower strength than a comparable natural aggregate mix [47].

The high Si, Al and Ca content of bottom ash has also prompted research into its potential use as a cement replacement material although a linear decrease in strength with %w/w cement replacement was observed along with a reduction in workability, rendering the potential limited to lower strength applications [35]. The increased water demand for a given workability when including bottom ash in a mix was probably due to the high capacity for water absorption as demonstrated by various authors [20, 31], owing to the mineralogical composition and high surface area of the bottom ash. The reduction in strength was most likely a result of the large fraction of the ash which was of low reactivity, or did not react to produce phases which positively contribute to the strength of the cement. Oxidation of the aluminium and iron in bottom ash may also cause swelling and therefore degradation of cement/concrete [48]. Hydrogen production evolved from the aluminium in bottom ash, when blended with concrete has previously caused accidents meaning its use must be carefully controlled [49].

Life cycle risk assessment performed by Shih and Ma [50] showed that reuse of bottom ash presented risk to labourers, primarily due to Cr and Cd inhalation and dermal contact. However, due to the reduction in population size affected by the risk, this was considered easier to control than that presented through disposal and potential pollution of groundwater and therefore ingestion by drinking or food chain contamination. Reuse of bottom ash in road construction, embankments, and other civil works was reported in 2007 to be greater than 70% in Denmark, France, Germany and the Netherlands [44].

2.2.2 Fly Ash

Fly Ash results from the particulates entrained in the gases created during incineration. The ash contains volatile elements such as Na, K, Pb, Zn, Cl and S. These elements condense as the temperature in the incinerator is decreased after the furnace [19, 21]. Fly ash can be recovered from the gas stream by a combination of precipitators and cyclones but is generally incorporated into the air pollution control (APC) residues [11, 20]. Fly ash

would typically contain higher concentrations of Al and Si than APC residues. This is largely due to the incidental dilution which occurs when adding lime and carbon and absorbing the acid gases.

2.2.3 Air Pollution Control Residues

APC residues including fly ash are produced in quantities close to 3% by weight of waste input [10]. They are collected by the injection of an alkaline scrubber, usually lime, in order to neutralise and collect acid gases (HCl, HF, SO_2) and particulates when controlling incinerator emissions. The scrubber also contains activated carbon to absorb heavy metals, dioxins and furans [21, 51].

The variety of possible NOx treatments as discussed in 2.1 adds to the variability in the composition of APC residues, which is also significantly affected by other factors, including:

- Varying waste composition which changes with place and season although no particular trends can be distinguished for seasonal variation. Figure 2.2 [10] demonstrates seasonal changes in the concentration of various metals in APC residues resulting from different plants. Whilst most EfW incinerators operate with a municipal solid waste input, incineration is also used for treatment of, and energy recovery from many other types of waste including for example clinical waste [52], hospital waste [37, 38, 53], animal waste [53, 54], or sewage sludge [55-58].

- Scrubber systems may be dry (injection of powdered lime), semi-dry (injection of a lime slurry) or wet. The wet scrubbing process involves removal of the fly ash by cyclones or electrostatic precipitation, and collection of acid gases and trace elements such as metals by bubbling through an alkaline effluent. The effluent is dewatered and frequently mixed with the fly ash resulting in a scrubber sludge [11, 20]. The water content of wet scrubber sludges is clearly much higher

than dry or semi-dry systems, which produce powdered material. Loss of soluble salts in the waste water stream also occurs in wet scrubber systems, resulting in a much lower content of certain elements, notably Cl [20]. The effluent may however be recycled, by circulating it back into the gas stream after the boiler in order to cool the gases. By this process the water is evaporated and the soluble salts are retained on bag filters. This circulation of the effluent produces residues with much greater concentration of chlorides and associated cations but avoids discharge of the scrubber effluent [59]. The residues resulting from semi-dry and dry scrubber systems appear very similar in physical properties and chemical composition although some morphological differences can occur. Some results suggest than a finer particle size distribution occurs from semi-dry scrubber systems [20].

- Different grades of lime are available for use in scrubber systems. This choice varies between plants and has a significant effect on the APC residue composition. Variation in the scrubber occurs in factors such as surface area. Higher surface area lime used in scrubbers is much more absorbent therefore less has to be used to meet emissions regulations. This results in residues with much lower % w/w Ca content. Very occasionally alternative alkaline scrubbers are used instead of lime which may include NaOH, $NaHCO_3$ or Na_2CO_3 [60, 61].

- Storage conditions of the collected residues also have a large effect on the residue composition. One obvious example of this is carbonation which can occur if the residues are left exposed to ambient conditions. Hydration reactions and leaching may also occur due to exposure to water during weathering. These changes affect both the physical and chemical characteristics of the residue, for example altering the density, particle morphology, initial pH and buffering behaviour, leaching behaviour, and reactivity.

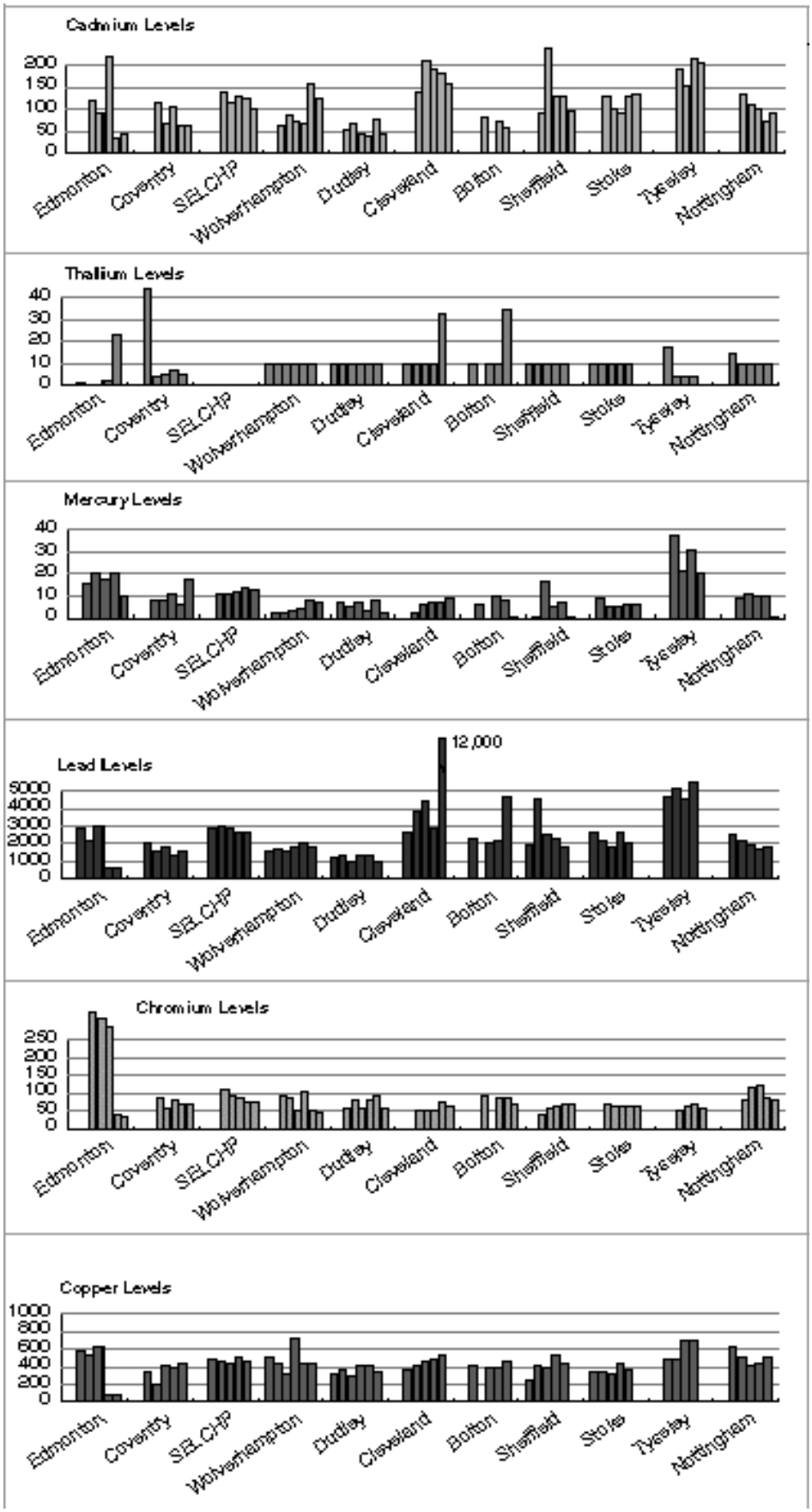

Figure 2.2 Variability in composition of APC residues produced from different incinerators between July-Decemember 2001. Y axis units in mg/kg [10]

Despite the many variations which can occur, commonly APC residues will contain high levels of Ca due to the scrubber, and Cl, with intermediate levels of Na, K, S, Al and Si. Trace contents of heavy and toxic metals such as Pb, Zn, Cu, Cd, and Cr may are also present in variable concentrations [10, 20, 28, 51, 62-70]. A guide for the bulk elemental composition of residues resulting from the incineration process is given in Table 2.3 [20]. The Al and Si contents shown for semi-dry and dry residues in Table 2.3 appear high compared to values observed in more recent literature, as do the concentrations for Mg, Zn and Pb. The composition of APC residues has changed over time as different portions of the waste stream entering EfW incinerators may be removed for treatment further up the waste hierarchy such as recycling or reuse. One example of this is the removal of PVC window frames (uPVC) and PET. Because Pb is commonly used as a stabiliser in PVC and PET, Pb concentration in APC residues has decreased considerably with their removal [71, 72]. PVC is also a source of Cd in the APC residues [61, 71] and since it is typically between 25-53% weight chlorine, is also a significant contributor to the concentration of Cl and other elements associated with the scrubber and scrubber products [61].

In addition to variations in chemical composition, there are also variations in mineralogy. Major crystalline phases typically include $Ca(OH)_2$, $CaCO_3$ and CaClOH, whilst in lower concentrations NaCl, KCl, and $CaSO_4$ are also frequently observed [19, 24, 37, 51, 59, 62, 64-67, 73-79]. Occasionally quartz is observed along with other aluminosilicate species [51, 64, 73, 77, 79].

It has been suggested that at the typical operational temperature of 850℃ melting of the ash is not significant therefore the amorphous content tends to be low [62]. However, other authors have shown a significant glass content in APC residues [24, 67, 80] which together with crystalline phases present below XRD detection limits may be as high as 50%w/w [24]. Le Forestier *et al*, [80] suggested APC residues to include a calcium-rich aluminosilicate glass phase. Based on infrared (FTIR) observations Bodenan and Deniard [24] suggested ‘the form of the non-crystalline Ca phases is not necessarily

different from that of the crystalline phases'. Electrostatically precipitated fly ash may have a more significant glass content [19, 80] which is diluted when blended with the more crystalline scrubber residue.

Element	Range for Fly Ash (mg/kg)	Range for Dry/Semi-dry APC System Residues (mg/kg)	Range for Wet APC System Residue without Fly Ash (mg/kg)	Range for Wet APC System Residue/Fly Ash Mixture (mg/kg)
Ag	2.3 - 100	0.9 - 60	-	53
Al	49,000 - 90,000	12,000 - 83,000	21,000 - 39,000	71,000 - 81,000
As	37 - 320	18 - 530	41 - 210	130 - 190
Ba	330 - 3,100	51 - 14,000	55 - 1,600	330 - 1,900
Be	-	0.5 - 0.9	-	1.5 - 1.9
C	-	-	-	-
Ca	74,000 - 130,000	110,000 - 350,000	87,000 - 200,000	93,000 - 110,000
Cd	50 - 450	140 - 300	150 - 1,400	220 - 270
Cl	29,000 - 210,000	62,000 - 380,000	17,000 - 51,000	48,000 - 71,000
Co	13 - 87	4 - 300	0.5 - 20	14 - 22
Cr	140 - 1,100	73 - 570	80 - 560	390 - 660
Cu	600 - 3,200	16 - 1,700	440 - 2,400	1,000 - 1,400
Fe	12,000 - 44,000	2,600 - 71,000	20,000 - 97,000	15,000 - 18,000
Hg	0.7 - 30	0.1 - 51	2.2 - 2,300	38 - 390
K	22,000 - 62,000	5,900 - 40,000	810 - 8,600	35,000 - 58,000
Mg	11,000 - 19,000	5,100 - 14,000	19,000 - 170,000	18,000 - 23,000
Mn	800 - 1,900	200 - 900	5,000 - 12,000	1,400 - 2,400
Mo	15 - 150	9.3 - 29	1.8 - 44	20 - 38
N	-	-	1,600	-
Na	15,000 - 57,000	7,600 - 29,000	720 - 3,400	28,000 - 33,000
Ni	60 - 260	19 - 710	20 - 310	67 - 110
O	-	-	-	-
P	4,800 - 9,600	1,700 - 4,600	-	6,000 - 7,400
Pb	5,300 - 26,000	2,500 - 10,000	3,300 - 22,000	5,900 - 8,300
S	11,000 - 45,000	1,400 - 25,000	2,700 - 6,000	11,000 - 26,000
Sb	260 - 1,100	300 - 1,100	80 - 200	-
Se	0.4 - 31	0.7 - 29	-	12
Si	95,000 - 210,000	36,000 - 120,000	78,000	120,000
Sn	550 - 2,000	620 - 1,400	340 - 450	1,000
Sr	40 - 640	400 - 500	5 - 300	200
Ti	6,800 - 14,000	700 - 5,700	1,400 - 4,300	5,300 - 8,400
V	29 - 150	8 - 62	25 - 86	62
Zn	9,000 - 70,000	7,000 - 20,000	8,100 - 53,000	20,000 - 23,000

Table 2.3 General range of elemental composition of APC residues [20]

Morphological and physical characterisation of APC residues has shown a high surface area, agglomerated material consisting of irregular, polycrystalline and occasional spherical particles [51, 66, 67, 74, 77, 81]. Particle size has shown a trimodal distribution [51, 73] with the majority of particles having an effective diameter <400µm. The fineness and irregular

particle morphology results in a high BET specific surface area, as determined by nitrogen adsorption of ~5.92m^2/g [51].

The composition discussed above applies to incineration of municipal waste, but a fairly similar composition appears to occur when clinical waste and medical waste is combusted [24, 37] due to the similarity in the composition of ~80%w/w of the waste [39, 71]. However, clinical waste is generally expected to contain a higher PVC content than MSW [61] and therefore a greater amount of scrubber is required and residues may show higher concentrations of elements such as Ca and Cl [61]. Residues from sewage sludge or animal waste incinerators may contain much higher contents of P, Fe, Si and Al as well as higher concentrations of metals such as Cd, Cr, Cu, Mn, Ni, Pb and Zn due to the very different composition of the initial waste stream [53, 55-58].

APC residues are classified under chapter 19 of the European Waste Catalogue (EWC) 'Wastes from Waste Management Facilities, off-site Waste Water treatment Plants and the Preparation of Water Intended for Human Consumption and Water for Industrial Use' and specifically classified as 19 01 07* 'solid wastes from gas treatment'. This is an absolute hazardous entry in the catalogue, i.e. there is no non-hazardous mirror entry. APC residues therefore do not have to be characterised before they are classified as hazardous, although common hazardous characteristics include

- H8/H4 - corrosive/irritant due to the high pH and alkalinity, evident from an initial pH of a distilled water batch extraction>11.5 [20, 51, 67, 73, 76] and ANC to pH 4.5 ~8-16mEq/g [20, 59, 69, 82, 83]. Such characteristics result primarily from the use of excess alkaline scrubber to ensure neutralisation of the acid gases. The wide range of ANCs recorded for APC residue is largely a result of the concentration of excess scrubber present. This is an effect of plant operating conditions, the amount of scrubber injected, and the extent to which the scrubber is recycled through the flue gases [20].

- H14 - ecotoxic, harm to the aquatic environment and organisms, flora and fauna may result from release of metals and soluble salts from the APC residues if incorrectly disposed of [84, 85].

The hazards posed by disposal of APC residues are largely due to the high solubility of some of the components of the residues. Residues typically have a soluble content of 270,000-380,000mg/kg (27-38%w/w) [20] releasing soluble chloride and sulphate salts along with toxic and heavy metals [63, 65, 67, 86-90]. The release of soluble salts and metal species poses significant risk to the environment, particularly to groundwater, which is an important resource for agriculture and for provision of safe drinking water [91].

As such, APC residues cannot be considered safe for landfill and require treatment in order to either valorise or stabilise them to a level where disposal in a landfill cell can be undertaken without risk to the environment. There are numerous management options proposed and currently in use, as detailed in the following section.

2.3 Options for Management of APC Residues

2.3.1 Landfilling with Derogated Waste Acceptance Criteria

The EU landfill directive [13] defines separate classes of landfill in order to avoid co-disposal of hazardous and non-hazardous waste. Landfill cells are distinguished by accepting either

- hazardous waste
- stable non-reactive hazardous waste and non-hazardous waste deposited in the same cell with such waste,
- or non-hazardous/inert waste

In assessing the suitability of waste for a specific type of cell, waste acceptance criteria (WAC) are defined according to the Landfill (England and Wales) (Amendment) Regulations 2005 [92]. These criteria consist of limits for the leaching of contaminants during specified testing procedures and are discussed in more detail later. APC residues may exceed several of the limits established for acceptance at hazardous waste landfill cells. Cl and Pb are

the most common problematic elements [59, 67, 88]. Wastes which do not meet acceptance criteria, and for which there is no recognised, efficient and effective waste management option for minimising the environmental impact can be sent to sites with derogated WAC (up to a factor of 3). This is conditional to a site specific risk assessment and annual reports in order that waste management options for the waste are frequently reviewed [93]. A significant proportion of APC residues are currently sent to sites with such WAC derogations, between 1996-2000 88% of air pollution control residues were sent directly to landfill [10]. This is certainly not considered a long term option.

2.3.2 Storage in Deep Salt Mines

Due to the fact they are dry and therefore leaching is avoided, deep salt mines are used as an option for storing several types of hazardous waste including APC residues [11, 28, 94, 95]. The waste is left in sealed capsules or bags, or occasionally blended with other wastes or cement and placed in the mines. Prevention of infiltration and percolation of water is assisted by an impermeable geology, as such no pathway is available for pollutants to enter the biosphere [95]. Such treatment is referred to as ‘total containment’ or ‘entombment’ [95]. In Germany filling of salt caverns with APC residues has even been considered utilisation [28].This method of treatment is clearly limited by available space. The mine currently operated by Veolia in Cheshire, UK for example can take a maximum annual input of 75,000-100,000 tonnes per year [96, 97] -less than the current annual production of APC residues [8]. Furthermore, with a planned life of around 20 years [96], space becomes problematic, particularly as there is competition from other waste producers.

2.3.3 Waste Acid Treatment

Between 1996-2000 ~12% of APC residues produced in the UK were used in treatment of acidic liquid or sludge waste such as emulsion paint residues, latex, waxes and greases [10]. The APC residues act as sorbents for these types of waste due to their hygroscopic nature and large surface area [51,

67, 73, 74, 81]. The waste can then be handled as a solid waste, typically pressed into a filter cake and landfilled. Adding the alkali APC residue neutralises the acid and certain compounds are converted to those with lower risk classification. An example of this is the conversion of calcium hydroxide to calcium chloride shown in equation 2.10 [11].

Equation 2.10 $2HCl + Ca(OH)_2 \rightarrow CaCl_2 + 2H_2O$

Due to such reactions, and the incidental dilution which occurs during this process, the concentration of hazardous compounds can drop below the limits for hazardous waste. APC residues which have been blended with waste acids in this way are assessed for hazardous properties and classed as either 19 02 05*- 'sludges from physico/chemical treatment containing dangerous substances' or the non-hazardous mirror entry 19 02 06- 'sludges from physico/chemical treatment other than those mentioned in 19 02 05'. When non-hazardous criteria are met the resultant waste can be landfilled at a non-hazardous site without the need for leach testing. However, more commonly the waste remains hazardous and is sent to a site with derogated WAC. Despite this, the treatment goes some way to minimising the environmental impact of the residues and the acidic waste. Greater amounts of APC residues are not treated in this way due to the limited quantities of waste acid available.

The EA permits a process in the UK carried out by 'Future Industrial Services' which involves first washing the residue before reacting it with sulphuric acid to produce gypsum which can be used in industrial applications such as cement manufacture. The gypsum produced is contaminated with low levels of metals which are then incorporated into the cement. The level of acceptable contamination in the gypsum is defined by the cement producer and due to the low amounts of gypsum added to cement [98], coupled with the low metal concentration in the gypsum, is often not problematic. The wash eluate has to be treated and recovery of components is difficult due to the impurity. The eluate may however be reused several times for the washing stage [99].

2.3.4 Chemical Stabilisation

Chemical stabilisation processes may prevent leaching of contaminants by conversion to insoluble/sparingly soluble species or adsorption processes. Various chemical stabilisation processes have been or are being developed including:

The Ferrox® Process developed by Lundtorp *et al* [68] involves the addition of a ferrous sulphate solution and recycled water to the APC residue. Insoluble iron oxides are formed before the suspension is filtered to separate the residue and waste water. Most of the salts are removed with the waste water whilst the metals remain. The leachability of many of the metals (Pb, Cd, Zn, Cu) is significantly reduced, attributed to the surface bonding of iron oxides [68]. Such work is based on the principal that iron oxides are stable in terrestrial and aquatic environments and able to bind significant quantities of heavy metals [68]. As such iron oxides may be used to remove heavy metals from waste water [100]. Immobilisation of Cr and Hg is however much less effective [11, 68, 101].

The VKI process involves washing to remove soluble salts and addition of carbon dioxide or phosphoric acid to stabilise the residue. This process reduces leaching as metal carbonates and phosphates have low solubility. Treated residues meet the relevant EU WAC for hazardous landfill sites and in most cases for non hazardous sites [11]. Due to the potential formation of stable and sparingly soluble minerals, several authors have examined the use of phosphates to immobilise metals [83, 102-107]. The WES-PHix process [103] is reportedly used in the USA and does not involve a washing stage. Whilst many divalent metals such as Pb, Zn, Cu, and Ni can be stabilised by the addition of phosphates [83, 104], leaching of Cl salts from the resultant waste is unaffected and therefore remains high [83, 106] and Cr leaching may in fact be increased [83].

Acid extraction sulphide stabilisation (AES) is used in Japan and treats incinerator fly ash residue to a level which meets the required landfill limits

[11]. This is achieved by washing to remove soluble salts, acid extraction of soluble heavy metals using HCl and addition of NaHS to stabilise those remaining as insoluble metal sulphides. The process produces waste water from the removal of salts, which is treated by evaporation/crystallisation with both the solid salt residue and waste water being reportedly recycled. The process is therefore only suitable for plants with high level waste water treatment equipment [108]. The process also produces a waste stream from the acid extraction of heavy metals. It is unclear how heavy metals in the waste water are treated.

Quina *et al* [83] examined the potential of various chemical additives for immobilisation of metals (Pb, Zn, Cu, Ni, Cr, Cd) in APC residues, concluding that the addition of soluble phosphates (H_3PO_4) and silicates ($Na_2O{\cdot}SiO_2$) were the most efficient and cost effective. Although it is possible to reduce the mobility of metals by such treatment methods, they do little for the immobilisation of chlorides which is why they tend to involve a separation stage such as washing. In order to be economically and environmentally sound, when separating fractions of waste like this, the aim has to be to recover value from the separated waste stream or at the very least increase the ease with which it can be treated. Introducing a separation stage into a treatment process increases the monetary cost of the treatment process and, unless a fraction can be valorised increases the volume of waste and is in contrast to the IPPC directive since pollutants are moved from one environmental media to another.

In order to valorise a separated fraction of the waste it is desirable to separate a fairly pure stream of the target fraction. A washing stage capable of removing solely the chloride salts from APC residue for example, would produce an eluate which could be easily treated to produce a recyclable material. Several of these processes go some way towards achieving this. However, without further treatment to immobilise metals, removal solely of chloride salts from APC residues is not feasible [64, 65, 89, 109]. In order to increase the ease with which metals can be recovered from separated eluates it is also desirable to increase the concentration of the target element

[110]. Concentrations can be increased by methods such as re-circulating the wash eluate or modifying the eluant to increase the solubility of target elements. Acid washing, as used during the AES process previously discussed, can increase the level of metals removed due to their highly pH dependent solubility [69, 90, 111-113].

2.3.5 Thermal Treatment

Thermal treatment of APC residues has been examined in the form of vitrification which may be followed by crystallisation to form glass ceramics [114-117]. This high temperature treatment (~1400˚C) has been shown to immobilise certain hazardous elements, destroy organic pollutants with an efficiency of 99.9% [114, 117] and significantly reduce the volume of the waste [115, 117]. Vitrification may require addition of glass formers if Si content of the waste is low [115, 116]. In 2000 melting technology was reportedly in use in 24 waste incinerator plants in Japan [117].

This stabilisation of metals by vitrification has been attributed to the formation of a compact, highly polymerised glass [115]. Treatment with heat and silica has also been reported to improve APC residue leaching behaviour by reduction of chemically instable phases such as the water soluble CaClOH, and an increase in silicate phases such as $CaSiO_2$ which keep the material structurally stable and may incorporate the heavy metals [118]. Treatment of the residues at elevated temperatures causes volatisation of Cl and many of the metals present in APC residue [78, 117, 119]. Therefore this treatment itself requires air pollution control measures.

Thermal treatment may be performed using fuel burning furnaces or electric melting systems. An example of the latter is a plasma melting furnace in which a high temperature plasma is formed, usually from air or an inert gas, which is then directed at the waste [117, 120]. In the process commercialised by Tectronics ltd. the APC residues are mixed with a source of silica and alumina (e.g. quartz and corundum) to encourage glass formation, and a feed of typically ~70%w/w APC residue is treated [120]. A significant fraction

of the chlorides volatilised can be recovered by bubbling through solution to produce HCl which can be used for applications such as steel pickling [121]. Despite this recovery, the process produces a secondary APC residue which has a high concentration of chlorides and contains a large fraction of the metals present in the initial APC residue [120].

Thermal treatments can be an effective way of treating hazardous residues and may produce useful by products for re-use in civil engineering applications such as fill for road surfaces, additives in asphalt or concrete mixture, or use in products such as bricks and tiles [114, 117]. Nishida *et al* [114] crystallised the vitreous slag produced from the melting process to improve the mechanical properties and produce stones suitable for use as an aggregate for concrete or asphalt, showing mechanical properties equal to or better than using natural crushed stone aggregates. The crystallised slag material was also shown suitable for producing permeable pavement blocks, with 1800m² of these blocks used commercially in a park in Chiba Prefecture [114]. The inert glassy slag produced by plasma melting referred to as 'Plasmarok' by Tectronics ltd. may find application as an aggregate, ceramic product or as a raw material for production of geopolymers [122, 123]. Due to the high temperatures required thermal treatments have very large energy and cost demands and may concentrate volatile hazardous elements in by-products. With escalating landfill tax however, the cost of such a treatment is becoming more feasible and if the concentration of metals in the by-products is high enough recovery may become viable.

2.3.6 Bitumen Encapsulation

Bitumen encapsulation is an effective way of immobilizing many hazardous and radioactive waste streams. This is generally coupled with storage in steel drums [11]. Despite its effectiveness there are serious cost and sustainability issues with a treatment which is so dependent on crude oil.

2.3.7 Carbonation

Carbonation is used for pre-treatment of bottom ash and APC residues and may be considered a chemical stabilisation method although the treatment is usually performed using gaseous CO_2 either simply by exposure to the atmosphere or accelerated by exposure to higher CO_2 concentrations. To be effective carbonation must be comprehensive [124]. This may require addition of water, since an initial presence of water is essential for carbonation to proceed (equations 2.11 and 2.12) [125]. If insufficient water is present the potential for carbonation is much lower [126, 127].

Equation 2.11 $CO_2 + H_2O \leftrightarrow H_2CO_3$

Equation 2.12 $Ca(OH)_2 + H_2CO_3 \rightarrow CaCO_3 + 2H_2O$

Carbonation of air pollution control residues causes a drop in pH [74, 81, 82, 124, 126, 128] primarily due to the conversion of $Ca(OH)_2$ to $CaCO_3$. This pH drop, to below 11.5, ensures that the residues are not classified as corrosive [84]. The mobility of some of the problematic metals such as Pb and Zn may also be reduced [74, 77, 81, 82, 124, 126, 128] due to formation of their less soluble carbonate forms, which may occur via dissolution and precipitation of calcium carbonate polymorphs [129]. The reduced solubility of the amphoteric metals such as Pb and Zn with carbonation is also assisted by the pH reduction, since these metals have a minimum solubility at pH around 8-10 [69, 82, 112]. Additionally, adsorption onto calcium carbonate polymorphs may occur [75, 129, 130].

The carbonated residues agglomerate and form solids with reduced porosity due to the expansive formation of calcite from $Ca(OH)_2$ [81, 126, 128]. This can also assist in preventing leaching of contaminants by reducing the infiltration of water and therefore active surface area. The reduced mobility of toxic and heavy metals reduces the ecotoxic potential of the residues. However, carbonation may not reduce the leaching potential of all metals. An increase in mobility of Sb when carbonating APC residues has been observed [74, 75, 82, 128, 131] which eventually led to leach limits for

hazardous waste landfill sites being exceeded by the APC residue treated by Cappai *et al* [75] despite an inert classification according to release from the untreated residue. Increase in release of Cd was also observed [128, 132] and Cr when carbonating bottom ash [131], primarily due to the pH drop caused by carbonation. These effects may result in the need for additional treatment if using carbonation as a treatment for APC residues.

If aiming to meet WAC a washing stage would also be required to remove chlorides. Whilst a reduction in chloride leaching from APC residues due to carbonation has been reported [81, 132] this did not reduce chloride release to acceptable levels for landfilling and generally chloride release is reported as unaffected or negligibly affected [74, 75, 128]. This is not surprising since other than the physical changes which occur to the residue, reducing active surface area, the only chemical change which would affect chloride release would be the carbonation of CaClOH as shown in equation 2.13.

Equation 2.13 $2CaClOH + H_2CO_3 \rightarrow CaCl_2 + CaCO_3 + 2H_2O$

Whilst this reaction was also proposed by Wang *et al* [128], XRD analysis of the carbonated residue instead showed $KCaCl_3$, possibly due to a complex reaction with KCl. $CaCl_2 \cdot 4H_2O$ has been observed in carbonated APC residue containing less KCl [133]. These chloride bearing reaction products are all highly soluble however, such that the reaction has very little effect on chemical immobilisation of Cl.

Despite the negligible effect carbonation has on chloride mobility, and the negative effect it may have on release of some other pollutants such as antimony and other oxyanions, a process is employed by the UK based company carbon8 to produce aggregate, which has been granted end of waste status by the EA. The residue is carbonated and pellitised by mixing with a filler such as sand and often cement (in a worst case scenario incorporating 50%w/w APC residue). The pellets are classed as a product and can be used for concrete block manufacture. The pellets are unsuitable for monoliths containing reinforcement due to the risk of corrosion due to Cl.

However, due to the environment in which the monoliths would find application, surrounded by cladding etc, exposure to water would be minimal and, assisted by the dilution factor as the aggregate is bound in the concrete block, leaching is not a concern [134, 135].

Additionally the treatment of APC residues has the advantage of sequestration of CO_2, offering potential use and capture of the greenhouse gas. Total sequestration capacity may be very low compared to CO_2 emissions associated with EfW incineration however [124]. The CO_2 sequestration capacity of APC residues varies on the residue and operation conditions but may be as high as 250g/kg [74, 75, 81, 124, 126, 136].

2.3.8 Cement Manufacture

A study by Wu *et al* [78] examined the suitability of replacing raw material in sulphoaluminate cement clinker production with APC residue. The replacement of raw material resulted in a decrease in compressive strength of the resultant cement but reasonable compressive strengths were still obtained with APC residue content up to ~45% weight of the raw materials. No problems were observed from leach testing the resultant cement pastes after 28 days curing for a range of metals and oxyanions including Pb, Zn, Cu, Cd, Cr, Ni, As and Se. This was assisted by the temperatures (>1150℃) used for the cement formation, at which it was demonstrated that >80% of the Cd, Zn, Pb, As, Se were volatilised, whilst >80% of the Cr, Cu and Ni remained in the clinker. Cl release was not studied, though it is reasonable to assume the majority of the Cl would have been volatilised. Chloride volatisation during the production of the cement can cause significant corrosion to equipment [78, 137].

Although the majority of the chlorides would be volatile, increasing replacement of raw materials with the waste did result in formation of a $C_{11}Al_7{\cdot}CaCl_2$ phase in the clinker [78]. The $C_{11}Al_7{\cdot}CaCl_2$ cement clinker phase has been shown to hydrate to form Friedel's salt, calcium aluminate hydrates and $Al_5Cl_3(OH)_{12}{\cdot}7.5H_2O$ [138] and is often found alongside alinite

[119, 137, 139-144]. The utilisation of APC residues as a raw material for alinite cement production perhaps holds some potential. Such cements utilise the addition of chloride salts in the raw materials, which allows the clinkering temperature to be reduced to ~1100°C [137, 139, 142, 144]. Typically $CaCl_2$ is used although other salts may be used with implications on the resultant clinker [140, 143, 145]. Following hydration, the Cl may be water soluble, particularly when excessive Cl is included [140, 141, 146] and therefore such cements are unsuitable for use with reinforcement or applications where leaching is of concern [137, 144, 147].

Although the elemental complexity of APC residues may play an important role due to the incorporation of additional elements in the cement, alinite has been said to form well in 'dirty' systems containing different elements [142]. Substitution of Cl with Br and F is possible [142] and other studies have shown the potential substitution of Mg for Zn which appeared to remain bound within the alinite structure and therefore immobile [141]. Fe may also replace Al although the ionic size difference had significant implications on the clinker phases formed [141]. As such alinite formation with waste materials has previously been examined [119, 143, 148] including the use of MSWI bottom ash and fly ash or APC residue [119, 143]. Additional $CaCl_2$ had to be added alongside the chlorides present in the fly ash, along with $CaCO_3$ and additional sources of Si, Al and Mg. Increasing the APC residue content in the raw mix beyond 30% weight was shown by XRD analysis to be detrimental to alinite formation [119]. With 30% APC residue content in the raw mix, the alinite cement had lower water demand, shorter setting times, higher 1 day and lower later age compressive strength than ordinary Portland cement (CEM I 42.5). Addition of gypsum increased the later age compressive strength to values similar to that of the ordinary Portland cement but also increased the water demand and reduced the setting time further [119, 143]. Leaching was not observed to be a problem, largely assisted by similar volatisation as was observed when attempting to produce the aforementioned sulphoaluminate cements [78, 119]. Due to the volatisation of the metals, chlorides and sulphates, further air pollution control measures

would be required if using APC residues as a raw material for manufacture of cements, producing a secondary residue.

Saikia *et al* [149] examined the potential use of MSWI fly ash for production of ordinary Portland cement clinker, with the addition of $CaCO_3$, Fe_2O_3 and SiO_2. Washing of the fly ash was beneficial to this process and utilisation for the production of alinite appears a more suitable management option. Such results suggest further work is merited to investigate the performance of the cements resulting from this management option. Work would have to consider the secondary residue produced and equipment corrosion as well as the durability of the resultant cements and the implications of the variability in APC residue composition.

2.3.9 Solidification/Stabilisation

Solidification/Stabilisation (S/S) involves both chemical and physical immobilisation methods. Solidification of waste materials by mixing with reagents to form a monolithic product changes the physical form of the waste increasing the ease with which it can be handled, and reducing the risk of redistribution by wind. Conversion to a monolith also reduces the exposed surface area, therefore offering some physical encapsulation of contaminants. Typically the encapsulation is assisted by the micro or nanoporous nature of the products [20, 150, 151]. Since fluids will follow the path of least resistance, when the hydraulic conductivity of the monolithic product is sufficiently low, leaching by an advection or percolation mechanism is avoided in favour of a slower, diffusion controlled process during which leaching occurs predominantly from the surface of the product [20, 87, 152].

Stabilisation is the process of converting contaminants into less soluble, mobile or toxic forms. This involves processes such as precipitation, adsorption and diadochy i.e. substitution of contaminant ions into mineral structures [111, 150, 153-156]. The potential for immobilisation by adsorption is dependent on the surface and pollutant ion charges as well as the

available surface area and competing ions within the pore solution. Sorption may be physical, resulting from unsatisfied surface charges, or more specific chemical adsorption in which molecules have a high affinity and may covalently bond [154]. The potential for diadochy is dependent on the charge of the ion along with its size and geometry, thus specific minerals present a greater potential for immobilisation of specific pollutant ions [111]. Matrix pH is a particularly important factor during s/s, determining the speciation and therefore solubility of contaminants, particularly metals [69, 112, 157, 158].

Treatment by s/s therefore reduces leaching to a diffusion controlled process for which the rate of contaminant diffusion through the matrix is governed by physical and chemical retardation due to the permeability and tortuosity of the matrix, along with chemical retardation factors [87].
Solidification/stabilisation has proven an effective method of minimising the environmental impact of both inorganic and organic waste materials [150, 159, 160] in accordance with the IPPC regulations and Landfill directive. There are several forms of s/s involving different reagents and treatment conditions however the reagents used in almost all s/s systems are one of the following [159]

- Portland cement
- Cement/fly ash
- Cement/soluble silicate
- Lime/fly ash
- Kiln dust
- Phosphate-based processes

Reportedly [159] the first s/s treatments were performed in the 1950s for radioactive nuclear waste materials which were blended with large amounts of cement and disposed of at sea or in deep underground storage in drums. In attempts to combat the retarding effects the waste often had on the cement setting and increase the waste/binder ratio, thereby reducing the costs of disposal due to a reduction in volume and weight, the technology developed by the inclusion of other reagents such as sodium silicate, fly ash

and clay. S/S processes were also developed using lime blended with fly ash, soil or cement in order to neutralise acidic wastes, treat APC residues resulting from scrubbing SOx gases with lime in power plants, and increase ease of handling/landfilling. Cement/fly ash blends and ground granulated blast furnace slag were also used as reagents for treating high volume sludge from electric power plants. Before the introduction of regulations such as the WFD (1975), and landfill directive (1999) in Europe, and the resource conservation and recovery act (1976) in the USA, no strict quality controls were implemented. The introduction of these legislative guidelines drove the development of the technology forwards from the mid 1970s.

The effectiveness of an s/s product can be judged based on its physical characteristic such as compressive strength, permeability, porosity and durability, along with chemical characteristics, in particular the leachability of contaminants from the waste form. This is the primary concern for stabilised waste and forms the dominant part of the waste acceptance criteria for landfill acceptance [92]. Concerns relating to durability stem from the risk of increased, unsafe leaching of pollutants resulting from changes in the waste form which may be dramatic after environmental exposure [161, 162]. Defra refer to stable non-reactive waste forms as those for which “the leaching behaviour of the waste will not change adversely in the long-term in the waste alone or under the impact of water, air, temperature or by other wastes including leachate or gas.” [8]. Tests can be conducted in the laboratory to simulate the typical threats to the integrity of an s/s product, such as measuring the products acid corrosion resistance or acid neutralisation capacity (ANC). Exposure to acidic groundwater can have serious implications for the leaching of contaminants due to the heavily pH dependent solubility of metals and the dissolution of minerals which may be chemically immobilising pollutants or offering physical encapsulation [163-165]. As such an initial pH between ~11.9-12.2 determined by a distilled water batch extraction test [157] and an ANC to pH=9 of >1 or >3 mEq/g depending on the precise disposal scenario are recommended [152]. Exposure to carbonic acid results in carbonation which significantly affects the pH and leaching of pollutants. Carbonation of s/s monoliths can be

particularly disruptive. This is due to the affects of carbonation on calcium silicate hydrates (C-S-H), the principal binding phase in cementitious or pozzolanic systems (utilising cement or lime/fly ash). Decalcification of C-S-H, results in the destruction of the primary binding phase responsible for immobilisation [166-168]. Other durability concerns may relate to factors such as the ability of the product to withstand freeze/thaw and wet/dry cycles without physical degradation such as cracking, which increases the surface area available for leaching [152].

The effectiveness of an s/s system for immobilising certain pollutants, mainly those which form oxyanions, is also dependent on the potential for reduction-oxidation reactions (or redox reactions) within the matrix. Certain elements show much greater solubility and mobility in certain oxidation states. Cr^{3+} for example is known to be much less mobile and therefore hazardous than Cr^{6+} [111, 155]. S/S is further aided by the greater ability of Cr^{3+} to form insoluble Ca minerals [111, 155]. Oxidation is the process of an atom loosing electrons whilst reduction is the process of an atom gaining electrons. These reactions must therefore take place simultaneously i.e. something must be reduced for something else to oxidise. The redox potential (Eh, with units mV) is therefore dependent on the presence of species which can be readily reduced or oxidised. A reducing environment displays a negative Eh, whilst an oxidising environment displays a positive Eh. Common reducing species (species which are readily oxidised and therefore cause reduction) include organic matter and reduced forms of iron, aluminium and sulphur [111]. The addition of these species can be used to control the Eh within matrices. For example the addition of iron blast furnace slag which may contain reduced forms of iron (Fe^{2+}) can cause a reducing environment [155]. The redox potential is also correlated with the amount of dissolved oxygen, becoming more reducing with lower oxygen content [169]. Redox reactions may also commonly be facilitated by bacteria, which use them to gain energy [169].

Figure 2.3 [20] summarises the key factors influencing leaching from a monolithic s/s product.

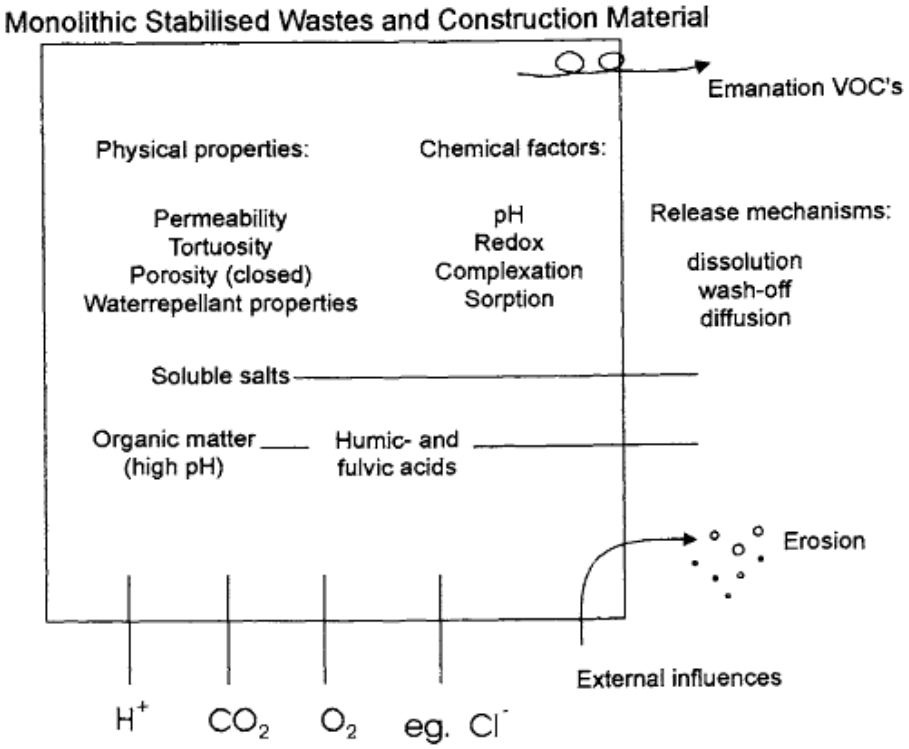

Figure 2.3 Factors affecting leaching from a monolithic s/s product [20]

In order to meet UK WAC monolithic products resulting from s/s treatment must also demonstrate a 28 day compressive strength of at least 1MPa. This enables them to support their own weight and overbearing loads such as vehicular traffic [157]. Several other parameters also need to be considered to ensure the treatment is feasible on a commercial scale [157]. These considerations include workability, setting time and potential for bleeding of the blend, all of which play an important role in the ease and cost with which the treatment can be applied. The amount of waste which can be incorporated should also be considered. This is inherently related to the increase in mass and volume the waste will undergo by the s/s process and therefore influences disposal as well as treatment costs. According to the IPPC directive [12], environmental as well as economic costs should be considered in order to truly manage the waste in a way which is beneficial for the environment as a whole. This implies consideration of the environmental costs of the reagents used and process conditions (including transport) [152, 157].

Treating APC residues and similar wastes by s/s has been studied using various reagents. The choice of reagent is very important due to the mineralogical and microstructural variations which are achieved as well as the economic implications. These processes are reviewed in the following sections in order to identify key concerns.

2.3.9.1 Solidification with Water

Todorovic *et al* [170] mixed APC residue with demineralised water and tested compressive strength and leaching behaviour. Compressive strengths close to 7MPa were achieved when cured at 100˚C for 29 days (l/s=0.35). Leach results showed release of 95% of available Cl, 88% of K, 89% Na, 40% Cr. WAC for stable non-reactive (SNR) sites or hazardous sites without derogated WAC was not met. However, release of Pb, Zn, and Mn was 0.31% or less of availability, and that of Hg was only 1.7%. Carbonation conditioning the pH of the leach test was perhaps the greatest influence on the observed release. Leachate fractions were observed to produce pH between 8.7 and 11.8, close to the minimum solubility range for Pb and Zn [69, 112, 157, 158].

Mixing APC residues with waste water has the advantages of producing a solidified product which is less susceptible to redistribution by the wind and has a lower specific surface area, somewhat slowing leaching. However, long term behaviour and durability of the resultant solidified waste is not known [11] but would be expected to be very low due to the high fraction of water soluble solids. This treatment option is clearly not ideal as the waste has not been stabilised sufficiently to meet the recommended leach limits and still has to be sent to specific sites with derogated WAC.

2.3.9.2 Cement Based S/S

For the purpose of this literature review the term ‘cement’ will be used to refer to CEM I as defined in BS EN 197-1:2011. Cement is one of the most common reagents used for s/s application and the implications of its use are

therefore discussed here. Hydration of cement (CEM I) produces the following primary reaction products [155].

- C-S-H (50-60%)
- $Ca(OH)_2$ (20-30%)
- AFm phases (0-10%)
- AFt phases (0-10%)

C-S-H is cement shorthand for calcium silicate hydrate (C=CaO, S=SiO_2, H=H_2O) [155]. C-S-H produced from cement hydration at ambient temperatures is an amorphous or poorly crystalline phase, consisting of various morphologies, often distinguished by their position relative to the original cement clinker particle [154, 171, 172]. This phase is primarily responsible for the high compressive strength and low porosity of cementitious materials [172-174]. The hyphens indicate the variable composition of this phase [173] which, in neat cement pastes, may have a Ca/Si ratio between ~1.2 to~2.3 with a mean ~1.75 [171]. In blended systems this ratio may vary.

Unless there is a significant alkali presence in the waste, at 28 days, when testing against WAC is generally conducted, the pH in cement/waste blends will be predominantly controlled by $Ca(OH)_2$ produced form the cement hydration. However, the Ca/Si ratio also has implications for the resulting pH of liquid in equilibrium with the C-S-H. A high Ca/Si can produce a pH as high as ~12.5 whilst low Ca/Si reduces the pH to as low as 10.5 [155, 164, 173, 175] or even 9.9 [175]. The pH of the C-S-H is significant since it is the main binding phase and as such plays an important role in the buffering capacity of the matrix [164], determining the pH at which buffering will occur. The large range in C-S-H pH values has important implications for the solubility of metal contaminants in the system [69, 112, 158]. According to the literature [173, 175] a Ca/Si ~1.1-1.4 would condition pH to within the preferential range for s/s products (11.9-12.2) [157]. But pH during batch extractions is unlikely to be a result of only the C-S-H.

The Ca/Si ratio of C-S-H also affects the surface charge, which is appriximately 0 when the Ca/Si is ~1.2 [150], with a high Ca/Si ratio the surface charge becomes positive, encouraging adsorption of anionic species, SO_4 and Cl being those of greatest concern in APC residues. At low Ca/Si the surface charge of C-S-H is negative, encouraging adsorption of cations from solution [155, 176]. All C-S-Hs have a range of sorption sites however, regardless of the Ca/Si, and therefore never adsorb solely cations or anions [155].

Substitution of elements into the C-S-H structure may also occur. Trivalent cations such as Fe^{3+} or Al^{3+} may be included in C-S-H, replacing Si in the bridging tetrahedra [177]. Elsewhere it has been suggested that Si may be substituted by Cr^{3+} or other oxyanions [111, 154, 155, 178-181]. The potential for incorporation of Cr^{6+} is much more limited and not the primary mechanism of immobilisation [182, 183]. Substitution of a trivalent cation for the Si^{4+} cation results in a more negative charge which must be balanced. This is generally achieved by the inclusion of Na^+, K^+ or Ca^{2+} in the interlayer [177]. The sorption of alkali metal cations removes them from liquid in contact with the solid, lowering the pH [155].

Literature suggests C-S-H may also immobilise other cations, including Zn [156, 184-189] and Pb [156, 184-186, 190, 191], amongst others [150, 154-156, 192]. The precise mechanism of immobilisation of these cations, whether they balance surface charge by inclusion in the interlayer, sorption on the outer surfaces, or substitution of the structurally bound Ca ions is unclear. Interlayer incorporation would perhaps be more dependent on the size and geometry of the ions. Substitution of structurally bound Ca appears to be more likely in crystalline calcium silicate hydrates [185, 193, 194] therefore the immobilisation of metal cations by substitution into the amorphous C-S-H structure created by hydration of cement appears to play a minor role. The primary mechanisms of immobilisation by C-S-H clearly depend on the precise contaminant but appear to be the pH, resulting in the precipitation of sparingly soluble compounds including metal hydroxides [150, 154, 155, 168, 180, 182-184, 195-197], along with the low permeability

providing physical encapsulation, and the large specific surface area of C-S-H [144, 150] encouraging surface adsorption. As discussed, adsorption is dependent on the surface charge and therefore the Ca/Si ratio and the extent of Si substitution.

C-S-H plays a much smaller role in the immobilisation of anions, such as Cl, although may offer encapsulation of anion salts, reducing contact with water. Surface sorption and interlayer incorporation of Cl in C-S-H may occur, particularly at high Ca/Si [198, 199]. This Cl remains easily removed by water however. The amount of Cl held by C-S-H such that it cannot be removed by leaching is very low (<0.25% weight) [199] and as such C-S-H can make little contribution to the chemical immobilisation of the Cl present in APC residues.

A non-comprehensive summary of species which have been shown to experience some level of immobilisation in C-S-H gel is shown in Table 2.4 [192].

Species Reported as Immobilized by Calcium Silicate Hydrate Gel (C–S–H)
Li, Na, K, Rb, Cs
Mg, Ni, Co, Hg, Zn, Cd
Al, Fe, Cr
Pb, U
Cl, I
OH^{-1}, CO_3^{-2}, SO_4^{-2}

Table 2.4 Species reported as immobilised by C-S-H [192]

The AFm and AFt phases formed in CEM I binders constitute lower percentage weight than C-S-H but can play an important role in immobilising a range of pollutant ions.

Ettringite is one of the AFt group of minerals which can be considered as having the formula $[Ca_3(Al,Fe)(OH)_6 \cdot 12H_2O]_2 \cdot Y_3 \cdot XH_2O$, in which X is usually ≤2 and Y is occupied by a divalent, or occasionally two monovalent anions [144]. The trivalent metal is usually Al or Fe but may also be, for example, Cr^{3+} [200]. Several articles review the incorporation of pollutants into ettringite

[111, 192, 201]. Gougar *et al* [192] described ettringite as a very 'forgiving' structure, meaning it can withstand significant compositional changes without changing structure. A summary of the ions which have been shown to substitute into the ettringite structure is shown in Table 2.5.

$(Ca^{+2})^{VIII}$ site	$(Al^{+3})^{VI}$ site	(SO_4^{+2}) site	(OH^{-1}) site
Sr^{+2}	Cr^{+3}	$B(OH)_4^{-1}$	O^{-2}
Ba^{+2}	Si^{+4}	CO_3^{-2}	
Pb^{+2}	Fe^{+3}	Cl^{-1}	
Cd^{+2}	Mn^{+3}	OH^{-1}	
Co^{+2}	Ni^{+3}	CrO_4^{-2}	
Ni^{+2}	Co^{+3}	AsO_4^{-3}	
Zn^{+2}	Ti^{+3}	SeO_4^{-2}	
		VO_4^{-3}	
		BrO_3^{-1}	
		NO_3^{-1}	
		MoO_4^{-2}	
		ClO_3^{-1}*	
		SO_3^{-2}*	
		IO_3^{-1}*	

Table 2.5 Possible ionic substitutions into ettringite[192]

Although it displays significant potential for immobilising pollutants, ettringite only persists when the anion/trivalent cation ratio is high. In a pure CEM I paste the ettringite converts to the monosulphate AFm phase once the $Al(OH)_4/SO_4$ concentration is reduced [111, 144, 202]. Ettringite occurs in cement pastes as a result of gypsum addition in a process designed to slow the hydration of the calcium aluminate phase and thereby avoid excessively fast setting times which hinders the ease with which the cement or concrete can be cast [203, 204]. Ettringite formation at later ages is often seen as problematic because the reaction can be expansive which can cause cracking in hardened pastes [203, 204]. Ettringite is also susceptible to carbonation [166], is not stable below a pH~10, and is destabilised at pH higher than ~12.8 [201, 205-207].

The AFm phase formed from conversion of the ettringite has also been shown to offer immobilisation of several pollutant ions by substitution [111, 150, 156, 201], and has been reported to possess a greater capacity for incorporation of monovalent anions [150]. The AFm phase in cement can be described with the general formula $[Ca_2(Al,Fe)(OH)_6]^+Y^-\cdot mH_2O$ in which the

square brackets enclose a positively charged layer unit which is charge balanced by anions (Y) in the interlayer [144]. AFm phases tend to be more soluble than AFt phases, although solubility depends on the exact chemical composition [201] as well as environmental conditions (temperature, pressure, composition of pore water or aqueous environment). These factors will also dictate the formation of AFt or AFm phases. The solubility of AFm and AFt phases are much lower than those of minerals more commonly found in as-collected APC residue, particularly Cl and SO_4 salts such as NaCl, KCl, CaClOH, gypsum and anhydrite Table 2.6.

Mineral	**logK_{sp} (approximate)**	**Reference**
Ettringite	-44-45	[200, 202, 205, 208]
AFm (SO_4)	-28-29	[202, 205]
Gypsum/Anhydrite	-4.5/-4.3	[205, 209]
AFm (Cl)	-27.1	[210]
NaCl	1.57	Based on solubility of 357g/L [209]
KCl	1.33	Based on solubility of 347g/L [209]

Table 2.6 Solubility data for a range of chloride and sulphate bearing minerals

The formation of Friedel's salt, an aluminium containing AFm phase in which the anion position is occupied by Cl, is of interest for cement and concrete scientists because it provides a possible binding mechanism for chlorides [210-212] which can cause corrosion of reinforcement. It is therefore also of interest in waste management since chloride release must be monitored when testing against WAC. The Fe containing analogue of Friedel's salt also possesses chloride binding potential [211, 213]. The anion site in AFm minerals may also be occupied by SO_4, as is more commonly found in cement and concrete due to the gypsum addition. SO_4 must also be monitored for WAC compliance. AFm phases are very sensitive to changes in material composition and service environment, which affect the aqueous phase in contact with the AFm containing solid. This results in formation of various phases including possible solid solutions dependent on the local environment [198, 213, 214]. Whilst this means that similar materials can be

used to initially stabilise a range of waste materials containing different anions, some studies suggest that when the activity is similar, uptake of ions occurs preferentially. For example, formation of Friedel's salt only occurs following nearly total uptake of SO_4 [166, 215, 216], making immobilisation of chloride ions more difficult. The ease with which AFm phases can change also creates the risk of contaminant release over time as the local environment changes, e.g. by infiltration of CO_2 or ion rich water [214, 217, 218].

Contaminants present in waste materials may significantly affect the cement hydration process [180, 184, 190, 219-222], the behaviour of the blend in its plastic state [67, 157] and the resultant properties of the solidified product, such as the pH and ANC [164, 165, 223], compressive strength [180, 219, 221, 222, 224, 225] and porosity [67, 180, 183, 226, 227].

More often than not wastes contain a mix of different metals, oxyanions and salts, which may have individual effects on the product and interactions between these effects may be significant [165, 221]. Cheeseman and Asavapisit [228] studied the effects of calcium chloride, a known accelerator of cement hydration [229], on cement containing Pb, known to retard setting time [180, 190, 220], and observed the competing processes. The $CaCl_2$ addition reduced the retarding effect of the Pb, encouraging formation of $Ca(OH)_2$ therefore reducing OH concentration, and in turn, preventing dissolution of the Pb and formation of $Pb(OH)_3^-$. The adsorption of $Pb(OH)_3^-$ onto hydrating cement forms a barrier to continued hydration, hence the retarding effect of Pb [228]. Blends of inorganic industrial wastes with cement would become more complicated still due to an increased variety of contaminants which would chemically interact with the process. A brief summary of the effect of some metals on cement hydration is presented in Table 2.7 [150].

Metal	Interference effect
Pb	Retards hydration due to precipitation of impermeable coating. Weakens lime/fly ash and cement/fly ash mixtures.
Zn	Prevents hydration at high concentrations. Reduces compressive strength. May increase ettringite formation and reduce porosity.
Hg	Does not retard, carbonate formation is enhanced.
Cd	Associated with increased ettringite formation, expansion and compressive strength loss.
Cr	Cr^{3+} associated with increased ettringite formation, and compressive strength loss in C_3A/gypsum blends[230] and may promote C_3S hydration [184]. Strength loss after 7 days with Cr^{6+} may not be significant in cement matrices [231].

Table 2.7 Summary of effects of some metals on cement adapted from [150]

The presence of high concentrations of anions in APC residues, such as Cl and SO_4, also alter the nature of the products. As previously discussed, their relative availabilities may encourage formation of various AFt or AFm phases. Cl, the anion of key concern in APC resides, has also been shown to affect the pore structure of cementitious blends [227, 232-235]. Several studies have shown the addition of chlorides to cement pastes, mortars or hydrated C_3S at the time of casting, to result in a greater pore volume and coarser pore size distribution [232-234]. Others have shown a reduction in the mean pore diameter and pore volume when chloride admixtures were added [227, 235]. Which was attributed to a change in the morphology of the

C-S-H to a denser structure after exposure to chloride solutions [227]. The effect is dependent on the cation originally associated with the Cl solution [227, 233]. Perhaps hydration of cement in the presence of Cl results in a smaller average pore radii but greater overall porosity which is consistent with the reduced strength observed for Cl exposed samples when the extent of hydration was equal [234]. Additionally calcium leaching is increased in Cl solutions which can increase the rate of C-S-H dissolution and therefore the integrity of the pore structure [236].

Cement pore solutions tend to show oxidising conditions [155, 237, 238] but these may be readily modified with the addition of reductive or oxidative agents, as may be found in supplementary materials or wastes [155, 238].

2.3.9.2.1 S/S of APC Residue with Cement

Several authors have reported results for blends of APC residues with CEM I including [67, 76, 104, 166, 239, 240]. There is a notable reduction in mix consistency with increased APC residue addition [67] or increased water demand for standard consistency [166]. This is attributed to the deliquescent nature along with the high specific surface area of the residue [67, 241]. High lime content of the APC residue would also increase the water demand.

APC residue addition up to a threshold has been shown to accelerate the hydration of cement, and reduce the setting time [67, 166]. This can be explained by the Cl content in the APC residue behaving as an accelerator [229] or has been attributed to the formation of gypsum resulting in ‘false set’ [166]. Perhaps a combination of the effects is present, and the magnitude would depend on the composition of the specific waste, certainly the compositional variation has an influence on the measured properties, hence the variation in the threshold level observed in the literature (30% [67] or 50% [166]). Above the threshold the setting time of the blends is increased [67, 166] and very little hydration is evident by calorimetery [67]. The acceleratory behaviour of chloride salts is concentration dependant [242], in higher concentrations chlorides such as NaCl retard setting time and cement

hydration [242]. This may then explain the threshold behaviour observed as the APC reisdue:CEM I ratio is adjusted. Additionally retardation of the cement hydration by the metals present in the APC residue may occur [220, 228].

Samples containing higher levels of APC residue exhibited greater porosity [67] with a reduction in unconfined compressive strength (UCS) [67]. Despite the lack of evidence by calorimetery for hydration reactions for blends containing more than 30%w/w_{solid} APC residue [67], blends containing up to 90% APC residue still showed compressive strengths greater than the 1MPa required to satisfy WAC. Importantly samples with greater than 50% APC residue suffered a decrease in compressive strength as a result of 7 days submersion in de-ionised water. This is a result of the loss of solids owing to the large soluble content. With addition of less than 50% APC residue no significant compressive strength loss was observed [67], a result of lower soluble solid content and therefore lower release coupled with further cement hydration.

The significant quantity of soluble solids in the CEM I/APC residue blends was apparent from the leach results obtained. Chloride release was always especially high [67, 166] and well above WAC unless incidental dilution was achieved by including very low quantities of the waste, or a pre-washing stage was implemented [239, 240]. This is due to the very low potential for chemical retention of chlorides in a CEM I/APC residue waste forms, owing to the paucity of insoluble chloride containing minerals which can be formed. Chemical retention is dependent on the low sorption capacity of C-S-H, and formation of AFm phases such as Friedel's salt, Kuzel's salt and solid solutions [198, 199, 210, 212]. The potential for formation of AFm phases in a CEM I system is limited by the low availability of aluminium in the clinker, which is typically made up of the equivalent %w/w of CaO~67%; SiO_2~22%; Al_2O_3~5%; Fe_2O_3~3%; Other~3% [144]. The Al content in cement is controlled in order to allow ettringite formation, preventing flash setting but also avoid problems associated with sulphate attack. The limited binding capacity of such systems was demonstrated by XRD analysis [243] which

showed retention of the CaClOH and NaCl phases with low CEM I addition and evidence of $Ca_2Al(OH)_7 \cdot 2H_2O$. This indicates that not all of the available aluminium was involved in chloride binding, possibly due to solid solution formation, and the high availability of OH [198, 244] in the pore solution. The chloride anion would also be competing with sulphate anions [198, 214, 245] which would be present in the CEM I and maybe also in the APC residue. XRD analysis by Alba *et al* [166] showed significant ettringite presence which appeared to form preferentially before Friedel's salt, consistent with other work [215, 216].

The potential for immobilisation of the chlorides in an APC residue/CEM I blend is therefore limited almost entirely to the physical encapsulation offered by the monoliths. High waste/binder ratios result in a very large water demand, high porosity and compressive strength loss upon leaching [67]. Therefore with high waste/binder ratios the physical retardation of chloride diffusion is not sufficient to meet WAC. Very low waste/binder ratios would be required to meet WAC and produce a stable product, rendering the treatment unfeasible due to the implied costs and volume increase in the waste.

Potential for immobilisation of metals including Pb, Zn and Cd has been reported in cement/APC residue matrices [76, 104, 166, 243] although Pb release has been shown to exceed monolithic WAC for hazardous waste landfill cells with a waste/binder ratio>1 [243] and granular WAC with waste/binder between 2 and 10 depending on the APC residue [76, 104] (using similar leach test to that required by WAC but with particle size <10mm rather than 4mm therefore perhaps slightly greater retention would be expected). The availability of the metals in the specific batch of APC residue appears to play a significant role.

The most significant drawback with the use of cement for immobilisation of APC residues is the limited ability to immobilise the high levels of chlorides. The potential for formation of Friedel's salt can be greatly enhanced by the addition of supplementary materials containing high concentrations of available aluminium [212]. The addition of such materials in theory may also

increase the capacity of chemical retention of Pb and Zn by sorption processes owing to a more negative surface charge through substitution of Al for Si in C-S-H [177].

2.3.9.3 Alternative Cementitious Binders

This section reviews the use of alternative cementitious binders for stabilisation of APC residues. This includes material such as ground granulated blast furnace slag (ggbs) and pulverised fuel ash (PFA). These materials were initially considered waste materials however due to their chemical composition are frequently used as a partial replacement for cement. Many types of cement include a significant weight fraction of such materials [98]. Since they are industrial by-products, use of these materials has environmental benefits including the avoidance of raw material extraction and processing, and the disposal of the by-products which may themselves contain the potential for release of contaminants into the environment [246, 247]. Due to their well established suitability for use as a cement replacement there may still be significant economic costs associated with them, particularly blast furnace slag. However, materials which do not meet end of waste quality criteria [248] e.g. EN 450-1:2005 [249] for PFA as a cement replacement material, may be particularly cost and resource efficient, and suitable for s/s applications [226, 250-253].

The use of alternative materials for s/s matrices is not uncommon [160] however due to their inconsistent composition, is less reliable than the use of cement. Often when used in the absence of cement e.g. lime/fly ash matrices, these blends may take a considerable amount of time to react and therefore set and develop strength [160], hindering their applicability commercially. This reactivity can be accelerated by methods such as curing at elevated temperatures [254-256]. Elevated curing temperatures can increase the rate at which a matrix reacts and therefore reduce setting time and increase early age strength, however, the ultimate compressive strength developed by the product may be lower and porosity greater than that which can be achieved at lower temperatures [255-257]. This occurs because the

rapid solidification of reaction products behaves as a barrier, hindering the diffusion of reactants throughout the matrix, resulting in uneven distribution of hydration products and less reacted material [256-258]. Curing of binders containing significant quantities of Al and SO_4 at temperatures greater than~70℃ may also result in problems with delayed ettringite formation, causing expansion and cracking of the solidified product [259].

Despite the possible slower reactivity, there may be advantages to the use of alternative materials to CEM I for s/s binders. As discussed previously, increasing the availability of reactive Al (or Fe^{3+}) in the blend can increase the potential for immobilisation of chlorides and sulphates by binding into AFt and AFm phases [212] and also encourage sorption of cations onto C-S-H through charge balancing of Si substitution with trivalent cations [177, 193]. The C-S-H in such blends may also have a lower Ca/Si ratio [155, 171] resulting in a more negative surface charge [150, 155, 176], and lower pH of the C-S-H [173, 175, 260], the reduction of which is also assisted by the sorption of alkali metals [155, 260].

At early ages the pH of blended systems is still likely to be controlled by the presence of $Ca(OH)_2$. The production of $Ca(OH)_2$ as cement hydrates results in pH buffering ~12.4-12.6 which is above the preferential range of ~11.9-12.2 suggested by Stegemann and Zhou [157]. However, in the presence of a pozzolan, the $Ca(OH)_2$ is consumed, producing further hydration products resulting in lower pH values of blended systems than pure cement systems. The rate at which this consumption occurs will depend primarily on the rate of the dissolution of the pozzolan. This is both temperature and pH dependant [261]. Consumption of $Ca(OH)_2$ also reduces the buffering or ANC of the matrix therefore blended systems tend to display a lower ANC than CEM I/waste matrices [223, 260]. The pozzolanic reactions which consume the pH also result in a denser microstructure due to the formation of the C-S-H which is more beneficial for reduced permeability and increased UCS, and consequently blended cements tend to perform better in these respects at later ages [204]. This is assisted by the ‘foil like’ morphology of the C-S-H

with low Ca/Si which results in less well connected capillary pores than the 'fibrillar' C-S-H with high Ca/Si [171].

The pore solutions for alternative binders may also display different redox potential than that of CEM I due to the presence of reductive or oxidising agents [155, 238, 260].

Several advantages and disadvantages for using alternative binders have been discussed which may be summarised as

Advantages

- Economic and environmental benefits of using industrial by-products and avoiding cement manufacture.
- Greater potential for formation of calcium-aluminate minerals including AFm and AFt phases, which may offer chemical immobilisation of anions and cations.
- More negative surface charge beneficial for sorption of metal cations owing to reduced Ca/Si ratio and replacement of Si with Al in C-S-H.
- Less permeable microstructure at later ages, offering enhanced physical retardation of contaminant diffusion.
- Reduced pH below the excessive 12.4-12.6, owing to consumption of $Ca(OH)_2$, sorption of alkali metals and reduction in Ca/Si ratio of C-S-H.

Disadvantages

- Less consistent material composition and therefore less reliable than cement.
- Slower reactivity, delaying setting time, strength development and immobilisation potential.
- Lower ANC due to $Ca(OH)_2$ consumption.

It is important to consider that the range of materials which may be used as alternative binders is extensive and each material has a different composition

and behaviour. Additionally waste materials are, of course, variable and therefore the most effective binder for one waste is not necessarily the most effective for another. Due to this reasoning some of the factors listed as ‘advantages’ or ‘disadvantages’ may alternate between lists depending on the waste being treated. The lists above were drawn up considering APC residue. The range of available binders makes it possible to tailor an s/s treatment to a specific scenario, although a detailed understanding of the scenario and as such the behaviour of the s/s product is essential for successfully achieving this.

2.3.9.3.1 Alternative Cementitious Binders for S/S of APC Residue

The use of ground granulated blast furnace slag (ggbs) has been studied by several authors for s/s treatment of APC residues [76, 241, 243, 262, 263]. Lampris *et al*, [241, 263] blended APC residue with ggbs utilising the high lime content in the APC and its inherent alkalinity, coupled with the high Si and Al content in ggbs, allowing pozzolanic reactions to occur when hydrated. Albino *et al* [262] blended ggbs with cement and $CaSO_4 \cdot 1/2H_2O$ to encourage ettringite formation, whilst Geysen *et al* [76] utilised CEM II, CEM III A, CEM III B and CEM III C. CEM II contains a minimum of 65%w/w clinker and up to 35%w/w pozzolanic material which is unspecified in the paper. CEM III A, B and C contain %w/w clinker of 35-64, 20-34 and 5-19 respectively, with the rest of the weight (except for 0-5% ‘minor additional constituents’) accounted for by ggbs [98].

As with APC residue/CEM I blends, compressive strengths reduced with increasing APC residue content [241, 262] and higher APC residue addition resulted in dissolution of the matrix upon submersion in water for 7 days [241]. Setting time of APC residue/ggbs blends increased with increased waste/binder whilst workability was reduced [241]. Similar curing conditions and mix proportions applied to APC residue/ggbs blends showed considerably slower setting times than that of the CEM I blends [263] which is

due to the nature of the raw materials and reactions occurring. The ggbs blends also had a greater water demand for a given level of workability.

As with cement stabilised samples, chloride immobilisation was minimal. XRD showed evidence of Friedel's salt [243] however quantification for comparison with CEM I blends was not possible. Granular leach tests showed greater chloride release from ggbs samples [263] which may suggest lower chemical immobilisation of the chlorides, although other factors may affect the results such as adjustments to the density of the dry matter through chemically binding water which may adjust the availability of chlorides (mg/kg) despite similar initial mixture proportions. Chloride release exceeded granular hazardous WAC limits [241] and the limited chemical fixation meant release from monolithic samples was primarily controlled by physical retardation which was insufficient for meeting the monolithic WAC leach limits. Release from ggbs blends was slower than release from cement blends [67, 241] perhaps due to the greater potential for Friedel's salt production and therefore chemical retardation of diffusion, or improved physical encapsulation.

Along with slower Cl release, measured release of Pb and Zn during monolithic leach testing on 28 day old samples has been observed to be lower from APC residue/ggbs samples than equivalent CEM I blends with similar waste:binder [243]. Monolithic WAC for stable non-reactive (SNR) hazardous waste cells was satisfied [243]. The pH of the leachates produced were lower for ggbs blends than CEM I blends [263] which, as previously discussed, is a result of the consumption of lime by the pozzolanic reactions occurring in the ggbs blends in comparison to hydration of the CEM I which produces $Ca(OH)_2$. This reduction may have contributed to the lower release of the amphoteric Pb and Zn in the ggbs matrices than the CEM I blends [243]. The immobilisation potential of binders containing ggbs during granular leach testing was lower than that of a CEM I matrix after 7 days curing [76], likely due to the slower reaction kinetics. After 5 weeks curing performance was similar [76].

Albino *et al*, [262] examined the release of metals from blends of APC residue with ggbs/cement/$CaSO_4 \cdot 1/2H_2O$ as well as PFA/cement/$Ca(OH)_2$/$CaSO_4 \cdot 1/2H_2O$, such blends were designed to encourage ettringite formation. Blends made with ggbs performed better than the PFA blends in terms of compressive strength and leach performance. Both ggbs and PFA blends showed sufficient compressive strength for WAC (1MPa). A higher waste:binder ratio could be achieved using the ggbs blends whilst still meeting US legal limits from granular testing. US legal limits were satisfied with waste:binder up to 3:2 using ggbs whilst limits were met with waste :binder up to 2:3 using the PFA blend. Direct comparison of the effectiveness of PFA and ggbs was not possible however since the concentration of other reagents used differed. Blends were designed based on optimum physico-mechanical performance [262].

The EPA leaching test used for assessment against US legal limits is considered to be a more aggressive leach procedure than that required for UK WAC [264]. The EPA test involved buffering to pH 5.2 [262] at l/s=20 as opposed to use of de-ionised water and l/s=10 for UK granular WAC, which is therefore undertaken at the sample's natural pH. It is therefore considered that the legal limits for granular UK WAC could be met.

Quina *et al*, [106] examined a range of CEM types including CEM IV (pozzolanic cement) and CEM II (65% clinker +pozzolan) a 1:1 blend of CEM I and PFA for the immobilisation of an APC residue, with waste:binder=1:0.62 showing release from all types which would satisfy waste acceptance criteria for hazardous cells for Cd, Cr, and Pb but exceed WAC for Cl.

2.3.9.3.2 Summary of Alternative Cementitious Binders for S/S of APC Residue

Consistent with the work which utilised CEM I, the main concern for s/s of APC residues with alternative binders is the poor immobilisation of the chlorides, which remain present as highly soluble salts or associated with the

C-S-H. Formation of Friedel's salt is the principal immobilisation mechanism, which is increased with increasing calcium and aluminium concentration and as such may be higher when using alternative binders than CEM I. The molar ratio of Ca:Al:Cl in Friedel's salt is 2:1:1 [210] i.e. a weight ratio of 80:27:35.5. Considering the interaction of Ca and Al with other reaction products formed in APC residue blends including the formation of C-S-H and the reported preferential formation of SO_4 phases before Cl, a considerable excess of Ca and Al would be necessary to bind enough of the Cl to meet WAC limits. Any s/s treatment for unwashed APC residues must therefore utilise a binder with considerable Al content whilst the Ca may, at least in part, be contributed by the APC residue itself.

Additionally there are concerns about the slower reaction kinetics of pozzolanic binders. Physical encapsulation and immobilisation of contaminant metal cations may ultimately be as good as or superior to more costly CEM I binders at later ages. However, the longer curing times required to set, develop strength and attain these levels of leach performance can hinder the feasibility of such systems commercially, implying the need for significant storage time before monoliths are physically stable enough for handling and can be safely disposed of. The demand for large quantities of binder and water to produce a workable mix, and structurally stable block observed in previous work, also increases the cost of such a treatment both in terms of binder cost and the increase in the volume and mass of the waste sent to the landfill cell.

2.3.9.4 Alkali Activated S/S Systems

Before discussing the materials analysed in this section it should be stressed that the majority of s/s systems are alkaline, resulting from the often alkaline nature of the binders and wastes used. As such, blending APC residues with pozzolanic materials, which require a high pH to react, can result in reaction even when the liquid phase is water. This was demonstrated by the work of Lampris *et al* [241] who took advantage of the alkalinity in order to blend APC residues with ggbs as previously discussed. This section however examines

the use of alkali metal solutions as the liquid phase in s/s matrices, the use of which can have several effects depending on a range of factors, such as solution type and concentration and raw material composition, as will be discussed.

Shi and Fernandez-Jimenez [265] reviewed the use of alkali activated cements for s/s of hazardous and radioactive wastes. These were discussed in two groups dependent on the starting materials and therefore the reaction products.

2.3.9.4.1 Alkali Activated Cementitious Systems

The first group discussed is cementitious or pozzolanic materials which result in C-S-H formation. The typical example used by Shi and Jimenez [265] is alkali activated blast furnace slag (AAS) but other matrices such as lime/fly ash blends fall into the same category. The effects of alkali activation on such systems may include increasing the rate of (or initiating) reaction, encouraging dissolution of the aluminosilicate glass network [261, 266, 267]. Setting time is therefore shortened compared to water activation [268] and strength development may be accelerated [256, 269] particularly when coupled with increased curing temperatures.

The combined effect of activator addition and temperature on compressive strength and pore structure may be detrimental [256]. The detrimental effect has been attributed to excessively fast reaction resulting in hindered diffusion and thereby non-uniform distribution of hydration products which can prevent complete hydration, reducing strength and also hindering crystal growth due to spatial constraints [256]. Such conditions may affect the nature of the reaction products. NaOH addition has been observed to suppress ettringite formation, with sulphate instead present as Na_2SO_4, a more soluble salt than ettringite and a disadvantage when trying to meet waste acceptance criteria (WAC) limits [256]. The production of Na_2SO_4 as opposed to ettringite may have been a result of the reduced ettringite stability due to the high pH [205, 207] and Na availability, and perhaps spatial constraints due to the rapid

reaction rate at early ages. The additional ions introduced into the chemically active system can be incorporated into hydration products therefore the nature of the activator affects the products formed [270-272]. The nature of the activator including type, concentration and pH also affects the extent to which the reaction kinetics [267, 268, 273-275] and mechanical performance [256, 268, 270, 276] are influenced. In addition the nature of the activated material determines the effectiveness of a specific activator type or concentration [270, 272].

The hydration products of alkali activated ggbs have been studied by several authors including [277-279]. The high pH appears to result in a semi-crystalline C-S-H (I) i.e. poorly crystalline tobermorite with a low Ca/Si (<1.2) [172, 277, 279] which is more crystalline at higher curing temperatures [279] and, due to the high Al availability in ggbs, may show significant substitution of Si at later ages, when the silicate chains are more polymerised. The Ca/Si, being below 1.2, would encourage sorption of metal cations and have a pH of ~11.5 [173]. This is below the threshold suggested by Stegemann and Zhou (11.9-12.2) [157]. However, the C-S-H would not be the only phase influencing pH when produced in a waste matrix, particularly not one involving APC residues. Secondary hydration products such as AFm phases may also be present [277-279] the nature of which is clearly dependent on the nature of the local chemical environment and as such varies depending on the composition of the activated material. Lime/fly ash [271] and lime/metakaolin [273, 280] blends also produce C-S-H when alkali activated with low concentration (<~5M) solutions, along with secondary reaction products which may include AFm, AFt or zeolitic phases. As discussed in the next section, the effect of activator concentration can be decisive for the reaction products obtained.

AAS may effectively immobilise Cd, Zn, Pb and Cr^{6+} cations [281, 282], release of which may be lower than that from a Portland cement matrix [281]. Immobilisation of Hg and Zn in AAS matrices by formation of silicates, calcium minerals and incorporation in C-S-H has also been demonstrated [283, 284] although higher concentrations (2% by mass of ggbs) were seen

to significantly retard the formation of C-S-H. The lower porosity of the alkali activated slag matrices relative to those of typical Portland cement was stressed [282]. Physical encapsulation appeared to play a particularly important role for Cr^{6+} immobilisation since good correlation between the observed diffusion coefficient for Cr^{6+} and the pore structure were demonstrated [281].

Work by Shi *et al* [285] showed high concentrations of Pb, Zn, Cr, Hg, Ni and B present in electric arc furnace dust to have less effect on the hydration of alkali activated blast furnace slag than water activated CEM I. This was shown by a much lower reduction of the maximum heat evolution rate when the arc furnace dust was added. The retardation of setting time was greater for the activated slag however. Other work [281, 282] has shown the addition of Pb and Cr^{6+} to alkali activated slags to have little effect on compressive strength development or pore size distribution of activated ggbs. Pb is known to retard cement hydration and strength development as previously discussed [150, 231]. Cr^{6+} may not have significant implications for the compressive strength of cement matrices after 7 days [231]. Additionally alkali activated slag materials or lime/fly ash pastes may show superior resistance to acid corrosion than CEM I pastes despite the lower ANC, due to the production of a protective siliceous layer of low permeability [163].

As previously mentioned sulphates may be more mobile in alkali activated blends due to depressed ettringite formation and instead formation of more soluble alkali sulphates [256]. Little literature is available on the mobility of chlorides in alkali activated cementitious or pozzolanic matrices. Roy *et al* [269] showed slower diffusion of external chlorides through alkali activated ggbs/CEM blends than water activated blends which was consistent with a lower porosity observed by mercury intrusion porosimetry. However, Shi [276] showed the strength, pore structure and permeability of alkali activated slags to vary considerably relative to that of a type III Portland cement, depending on the activator used. $CaCl_2$ can itself be used as an activator for lime/fly ash and lime/natural pozzolan blends, increasing compressive

strength and reducing setting time [272, 286]. NaCl has no such effect however, appearing inert or even reducing the strengths observed [272, 286].

2.3.9.4.2 Geopolymeric Systems

With low availability of Ca or very higher activator concentration, activation of aluminosilicates, such as metakaolin and PFA, with alkali metal solutions, such as NaOH or KOH, can result in the precipitation of zeolitic phases [287] or semi-crystalline aluminosilicate gels referred to as geopolymers by Davidovits [265]. These are the second group of alkali activated s/s matrices discussed by Shi and Jimenez [265]. The primary reaction products observed appear to be dependent on the nature of the raw materials used, in particular the dominant cation present i.e. the alkali metal/Ca ratio, and the concentration of the alkaline activator [273, 280, 288, 289]. Increasing the activator concentration would affect the alkali metal/Ca ratio, however, the high OH^- concentration encountered when using alkali hydroxide activators >~10M also encourages precipitation of $Ca(OH)_2$ which can result in formation of geopolymeric phases even when Ca is present in the activated material [273, 280, 288]. Without $Ca(OH)_2$ present, low concentration activators (<5M) result in insufficient OH^- concentration for rapid dissolution of the aluminosilicate material, preventing reaction and setting [280]. Temperature increase may encourage reaction in such conditions [261, 275, 290]. With low activator concentration and increased temperatures, crystalline zeolitic phases are likely to precipitate [287].

The use of geopolymeric matrices for the immobilisation of various waste ions has been studied by several authors [231, 265, 291, 292]. Such systems are considerably different to cementitious matrices and their applicability depends on the nature of the waste material. For example, Palomo and Palacios [231] examined the potential for immobilisation of Cr^{6+} and Pb in geopolymeric matrices, comparing the results with those for Portland cement. Geopolymeric matrices were vastly superior for Pb immobilisation showing low leaching and only a small loss of strength. The same addition of Pb to a cement matrix resulted in no strength development. The potential for Cr^{6+}

immobilisation was the reverse however. In high Ca systems such as alkali activated slag cements and Portland cement, calcium chromate ($CaCrO_4$ or $Ca_2CrO_5 \cdot 3H_2O$ [182]) can precipitate, with low solubility and little negative impact on compressive strength [231, 282]. In the low Ca alkali activated fly ash systems studied by Palomo and Palacios [231] Cr^{6+} formed the highly soluble $Na_2CrO_4 \cdot 4H_2O$ which prevented Na condensing with the silicoaluminates and therefore prevented any mechanical strength development. Pb is often a concern in APC residue treatment, however the concentration would be significantly lower than that studied by Palomo and Palacios [231] and the principal concern would be the Cl salts.

The effect of Cl addition to geopolymeric matrices, along with other inorganic salts, was studied by Lee and van Deventer [293]. Chloride addition increased early age strengths, but reduced the later-age compressive strength, consistent with other work [294]. Effects observed by Lee and van Deventer [293] were consistent with changes in mineralogy and morphology of the products and were very sensitive to the cation associated with the Cl and with the strength of the alkali solution used for activation. Higher solution concentrations resulted in lower strengths but were also less affected by chloride contamination.

When curing conditions of alkali activated aluminosilicates allow formation of crystalline reaction products, generally from curing hydrothermally with low concentration (<5M) alkali solutions, zeolites may form [265, 287]. The type of zeolite formed will depend on various factors including raw material composition (in particular the Si/Al ratio of the glass matrix), the curing time and temperature, activator type and concentration, and l/s ratio of the synthesis. Zeolites can have a cation exchange capacity (CEC) as high as $5meqg^{-1}$ [287] and therefore offer potential for immobilising hazardous metal cations [295-299]. However, in blends with high Ca availability zeolitic phases may not be stable as they may be consumed in pozzolanic reactions [295, 300, 301]. As discussed previously, alkali activation with an alkali solution ≤5M of cement or pozzolanic blends in which there is high availability of Ca, may not produce zeolites [254, 256, 277, 279], but rather C-S-H is the

primary hydration product. With the correct conditions however, zeolites may exist alongside Ca-bearing reaction products such as C-S-H [266, 295, 298, 302, 303].

2.3.9.4.3 Alkali Activated Matrices for S/S of APC Residues

The inclusion of APC residues or MSWI fly ash in geopolymeric matrices has been studied by several authors. Kourti *et al* [122, 123] examined the possibility of geopolymerisation of the glass collected from plasma melting of APC residues with quartz and corrundum as described in section 2.3.5 and [120]. As there are no leaching concerns associated with the plasma treated residue [120, 122], leaching from the produced geopolymer was negligable [123]. The study focused on optimising the mechanical and physical properties of the geopolymer, which were dependent on factors such as the alkali solution concentration and were shown for a range of properties to be suitable for various commercial applications [123].

Zheng *et al* [79] examined the possibility of geopolymerisation for immobilisation of an APC residue (referred to as fly ash but containing CaClOH therefore considered to include the scrubber residue and as such be APC residue according to the definitions of [20]) along with the implications of a pre-washing stage to remove the soluble salts. No supplementary materials were added by to encourage geopolymerisation, which was possible due to the extraordinarily high Si and Al concentration in the residue studied (SiO_2=15.4%, Al_2O_3=7.2%). Studies on the geopolymerisation of MSWI fly ash [304, 305] used additional alumino silicate sources despite typically higher concentration of Si and Al in the fly ash.

Compressive strengths up to ~26MPa were obtained from the washed APC residue geopolymer (made with 10M NaOH and 0.8M Na_2SiO_3 solution) with lower strengths observed at all ages for the unwashed residue [79]. This was most likely associated with the removal of Cl by washing, which as previously discussed may have a negative effect on the compressive strength of geopolymers [293, 294]. Washing also causes enrichment in the

concentration of the less soluble compounds present in the residue, resulting in an increased elemental concentration of Si, Al and Ca which would benefit geopolymerisation and/or C-S-H production thus improving strength development. Despite inevitably leaching during the washing stage, several metals were enriched in the washed residue including Cr. None of the negative impacts of Cr observed in other literature [231] were evident, most likely due to the significantly lower concentration.

The porosity, measured by mercury intrusion porosimetry, of geopolymers produced from the unwashed residue was initially slightly lower than those produced from the washed residue [79], attributed to the presence of the crystalline chlorides. During leaching however there was wash-out of the soluble salts and significant damage to the samples was observed. Thus the initial lower porosity was only temporary. XRD analysis of the geopolymers revealed large amounts of NaCl. These chlorides were therefore not chemically immobilised and, although Cl leach results were not presented, would be expected to exceed WAC limits. This was consistent with low levels of Cl retention by chemical immobilisation, observed through geopolymerisation of MSWI fly ash and fabric filter ash [305]. Due to the low Ca concentration, and high, Na and CO_3 concentration in the fabric filter ash studied in reference [305] it is suspected a Na based scrubber ($NaHCO_3$ of Na_2CO_3) was used.

Leaching of metals present in the APC residue and MSWI fly ash was generally below regulatory limits for SNR WAC [304] and low in comparison to their availability [79, 305]. Luna Galliano *et al* [304] compared the geopolymeric s/s products produced from geopolymerisation of MSW fly ash with Portland cement or Portland cement/lime blends. Sb was more successfully immobilised in the cementitious systems whilst other metals such as Pb and Ba appeared to be better retained in the geopolymeric matrices. Both matrices showed pH dependent leaching and significantly different ANC due to the different reaction products. Greater buffering at pH~12 was observed for cementitious blends which was a result of the increased $Ca(OH)_2$ content.

Zheng *et al* [79] observed crystalline ettringite and calcium aluminate hydrates alongside the amorphous fraction of the products. As previously discussed ettringite production in alkali activated products may be suppressed due to the pH [207]. Zheng *et al* utilised a very low l/s ratio however (2.5ml solution/12g residue), and the NaOH appeared to be neutralised by reaction with the CaClOH to produce NaCl and $Ca(OH)_2$. The samples prepared using the washed APC residue contained no CaClOH and did not produce ettringite with sulphates instead identified as Na_2SO_4. Sodium sulphate formation would also neutralise the NaOH. Potentially the ettringite formation was then dependant on the availability of the Na to combine with the SO_4 which was lower in the unwashed samples due to the formation of NaCl. It is likely that amorphous C-S-H was also present alongside the geopolymeric gel as discussed by Yip *et al* [289] and appeared to be evident in the alkali treated plasma product studied by Kourti *et al* [123] due to the high availability of Ca in the residue.

2.3.9.5 S/S of EfW Fly Ash

Whilst the review so far has focused on papers which report treatment of APC residues, many papers report treatment of fly ash collected from EfW incinerator by s/s. A selection of these papers includes [166, 215, 216, 306-314]. As discussed in 2.2.2, the fly ash is collected before the addition of the alkaline scrubber to absorb the acid gases and therefore typically contain lower concentration of Ca, Cl and SO_4 and higher concentration of Si and Al. The mineralogy is also different, without the formation of CaClOH and lower $Ca(OH)_2$ and (therefore potentially) $CaCO_3$ content [20]. Some similarities may be considered however as fly ashes may still contain high levels of chloride and sulphate salts including NaCl, KCl and $CaSO_4$ along with metal pollutants [20, 215, 216, 310, 311].

Work on s/s of MSW fly ash demonstrates the potential for immobilisation in various cementitious or pozzolanic systems including with cement [166, 311] pozzolanic cement [312, 313], a lime/pozzolan matrix [216] and using

calcium aluminate cement [215]. Immobilisation of metals including Pb and Zn within such binders has been demonstrated [166, 215, 311, 312]. Leach results for chlorides remain high from CEM I matrices [166] and are not presented in the studies using alternative binders. Based on characterisation the release is expected to remain high, although reduced, with the use of high Ca and Al binders which results in significant formation of Friedel's salt [215, 216, 312]. Remond *et al* [310] observed greater evidence for Friedel's salt production when using a cement with higher C_3A content.

Other authors performed very energy, resource and economically expensive pre-treatments on MSW fly ash before s/s treatment including melting at 1400°C and pulverising [314], or washing followed by addition of phosphoric acid, and calcination at >600°C [306, 307], or performing washing stages [309]. As previously discussed, whilst washing is a simple method of removing soluble salts from the APC residue, unless the contaminants in the effluent can be recovered this process appears not to satisfy the IPPC directive [12] since the pollutants are moved from one media to another. And therefore the treatment may not be considered beneficial for the environment 'as a whole'.

In a novel approach Massiardier *et al* [308] extruded MSW fly ash with melted polymers to produce pellets which were then solidified in mortar. Pb release was increased when PVC was included as a polymer for pellitisation due to the Pb stabiliser in PVC. Some immobilisation of Zn was observed. The possibility of including waste plastic in such a treatment reduces the economic costs and increases resource efficiency although removes the high calorific materials from the incinerator.

Work has also been performed on the geopolymerisation of EfW fly ash [304, 305]. These papers were discussed in chapter 2.3.9.4.3.

2.3.10 Summary of APC Residue Treatment Options

Despite the many treatment methods reviewed there is not yet an inexpensive, sustainable solution for treating the quantities of APC residue which are being produced to a level suitable for landfill sites which are not classed as hazardous. With residue production expected to continue rising it is important that such a treatment, or preferably a method of valorising the waste, is developed. This problem results in ~90% of UK APC residue being sent to hazardous landfill sites with derogated WAC. Table 2.8 [110] shows the global nature of this problem by a summary of primary treatment methods in various countries.

Treatment options may be categorised into two types. The first type of treatment would include methods of encapsulating the waste, preventing liquid contact with the waste and therefore avoiding leaching of contaminants. A typical example of this type of treatment would be bitumen encapsulation, or storage in deep salt mines. The second type of treatment involves chemically incorporating the hazardous elements in insoluble (or less soluble) compounds. Included in this category would be treatment by carbonation and the various chemical stabilisation methods such as the Ferrox process, VKI and AES. Although most treatment options bridge both categories to some extent, this is most clear with s/s and thermal treatments including cement production. The amount of chemical immobilisation and physical encapsulation vary depending on the materials and treatments used.

Whilst immobilisation of metals and oxyanions by various methods seems to be achievable to limits required by the WAC, Cl leach seems to be a consistent problem for all kinds of treatment due to the very high concentrations present in the residues. Many treatment methods therefore require a washing stage in order to remove a large proportion of the soluble salts from the waste prior to additional treatment. Thermal treatments similarly remove the salts by volatisation and offer more potential for their recovery than a water washing stage. Removal of salts adds expense and results in a further waste stream (the wash eluate or secondary APC

residue). Unless the elements present in wash eluates can be recovered, such treatment appears contradictory to the IPPC regulations because the pollutants are being moved from one environmental media to another. Though they may be recirculated, recovery of wash eluates is difficult due to the solubilised metals and oxyanions alongside the chloride and sulphate salts.

Based on the literature review it was decided to examine the potential use of a pulverised fuel ash, high in Si and Al, as a reagent for s/s of APC residue, utilising the reactive Ca contents in the residue for consumption in pozzolanic reactions and production of AFm/AFt minerals. The high concentration of reactive aluminium present in PFA was considered to perhaps offer potential for immobilisation of significant proportions of the chloride ions by incorporation within the Friedel's salt AFm phase. Such lime/fly ash systems are not uncommon for s/s binders and the involvement of the Ca present in the APC residue could allow for a high waste:binder ratio, increasing the efficiency of the treatment. Activation of the system with an alkali solution, and using elevated curing temperatures were considered primarily in order to increase the reaction kinetics which are otherwise slow causing commercially unfeasible setting times and microstructure development.

A PFA was identified which did not meet end of waste criteria established in EN 450. The use of such a PFA has several advantages, reducing economic and environmental costs associated with reagents and avoiding disposal of the PFA. Conversely, there are also potential disadvantages to the use of such materials, including high water demand and addition of pollutant ions which require monitoring for WAC and may have detrimental influence on the matrix integrity. A waste alkali solution resulting from cleaning of extrusion dyes in an aluminium plant was also identified. Such a waste would require treatment and disposal which is avoided by its use as a reagent. A perceived additional advantage of using such a waste was the contained soluble aluminium content which can contribute alongside the aluminium present in the PFA to sparingly soluble mineral production.

Waste management of FA/APC residues from MSWI processes in various countries

Country	Management strategies for FA/APC residues
USA	APC residues and bottom ash are mixed at most MSW incineration (MSWI) plants and disposed as a "combined ash". The most frequent dumping option is disposal in landfills which receive only MSWI residues (monofills)
Canada	APC residues are disposed in a hazardous waste landfill after treatment
Sweden	APC residues are disposed in secure landfills after treatment
Denmark	APC residues and fly ashes are classified as a special hazardous waste and are currently exported or stored temporarily in big bags. Significant efforts are being spent to develop treatment methods which can guarantee that APC residues can be landfilled in a sustainable way
Germany	The APC residues are mainly disposed of in underground disposal sites, such as old salt mines
Netherlands	Flue-gas cleaning wastes are disposed temporarily in large sealed bags at a controlled landfill until better options are available. The utilization of APC residues is presently not considered. The re-use of the waste is subject to investigation
France	After industrial solidification and stabilization processes based on the properties of hydraulic binders, the waste is stored in confined cavities in a specific landfill (French class I and II). The high cost of this treatment is promoting the companies to search alternatives to disposal
Italy	Various technologies have been proposed, but the most widely adopted comprehends solidification with a variety of hydraulic binders (such as cement and/or lime, blast furnace slag, etc.)
Portugal	APC residues are treated with hydraulic binders (solidification/stabilization method) and landfilled in specific sites (monofills)
Japan	MSWI fly ash and APC residues are considered as hazardous, and before landfill intermediate treatments must be performed, such as melting, solidification with cement, stabilization using chemical agents or extraction with acid or other solvents. Melting slag may be used in road construction and the materials of S/S with cement are landfilled

Table 2.8 Overview of management of EfW incineration residues internationally [110]

3 Experimental Techniques

3.1 Sample Preparation

Samples were prepared as 50 mm cubes by mixing dry materials, adding the liquid phase and blending until homogenous before compacting using a vibrating table or hand tamping as necessary. Samples were cured at various constant temperatures. Humidity was controlled by sealing in plastic bags to prevent excessive drying until test age.

3.2 Chemical Characterisation Techniques

This section reviews test methods which were undertaken in order to characterise, the chemistry and morphology of the reactants and products studied. Characterisation was undertaken in order to offer insight into reasons for the achieved level of performance. Characterisation of the treated waste products was also important since 'the government considers that simple physical dilution, without any concurrent chemical or physico-chemical changes, is not an acceptable treatment process' [14]. It is therefore necessary when testing an s/s product to ensure that physico-chemical changes in the waste form occur, which reduce its hazardous nature. Whilst leach tests may give some indication of chemical changes, confirmation can be achieved with characterisation techniques.

3.2.1 Hydration Stopping Techniques and Sample Storage

Before analysis by XRD and SEM samples were hydration stopped, a technique designed to drive water from the sample in order to allow storage of samples without further reactions which depend on the presence of water, such as hydration reactions and carbonation, occurring before analysis. Additionally, during the present study, hydration stopping was necessary in order to observe the soluble reaction products as can be seen in Appendix A.

Several techniques can potentially be used to initially remove water from samples such as oven drying, freeze drying and solvent replacement. These techniques all have implications on the mineralogy and pore structure of the

sample which must be considered [315-321]. In this study hydration stopping was undertaken by submersion in isopropyl alcohol (IPA) for 24 hours followed by vacuum drying for a further 24 hours which was sufficient to result in a %weight change over 4 hours of <0.1% classed as dry according to BS EN 1924-2:1990 [322].

This technique was decided upon based on a review of the literature which suggested replacement of pore water with a solvent of lower surface tension and greater volatility enables relatively rapid drying in a vacuum with less damage to the pore structure than removal of water directly [315, 320]. This is discussed further in (3.3.9). Solvent replacement may alter the mineralogy of cementitious samples, thereby giving misleading results from subsequent chemical analysis, particularly by thermal analysis [315-319, 321]. The extent of this influence appears dependant on the solvent used. IPA was decided upon for the solvent since according to the referenced literature there appeared to be less chemical influence on mineralogy similar to that present in the samples examined in the present study.

The minimal effect of submersion in isopropanol and vacuum drying was confirmed by results presented in appendix A. It was shown that other than the appearance of the highly soluble phases, x-ray diffraction (XRD) patterns obtained for a typical sample dried by submersion in IPA and vacuum drying showed little to no deviation from that obtained for the undried sample. This technique was therefore considered suitable for hydration stopping of samples when storage was necessary. Once water was removed, samples were stored in sealed plastic bags over a hygroscopic self indicating silica gel in a desiccator to prevent re-absorption of water from the atmosphere.

3.2.2 Simultaneous Thermal Analysis (STA)

STA was undertaken in order to gain insight into the chemical/mineralogical composition of samples. The STA applied involved the use of thermogravimetric analysis (TGA) and differential thermal analysis (DTA).

TGA monitors the weight change of the sample as a function of temperature or time. Weight changes occur as substances decompose and gases are given off. TGA curves may be presented with temperature or time along the x axis and weight, %weight or relative molecular mass plotted on the y axis [323]. Results may also be presented as a first derivative of the TGA curve, known as derivative thermogravimetric (DTG) curve. DTG curves may be used to achieve greater clarity when weight losses due to different processes overlap. A change in sample mass due to a known decomposition can be used to quantify the amount of a particular phase in the sample (%w/w).

DTA monitors the temperature of the sample relative to that of an inert reference material subjected to equal conditions. In this way exothermic and endothermic reactions which occur as samples suffer physical and chemical changes as a function of time and/or temperature can be observed. This is achieved by plotting chamber temperature (or time) along the x axis and temperature difference between sample holder and inert reference material holder on the y axis. This information can inform on the compounds present in the sample. Peaks are most distinguishable for crystalline phases present in high concentrations due to the large concentration of material undergoing the changes simultaneously.

STA has been widely used throughout scientific literature due to its relative simplicity and in particular the quantitative analysis which can be achieved with the use of TGA curves. The extent of cement hydration for example is frequently undertaken via STA by monitoring the presence of $Ca(OH)_2$ [144]. Similarly monitoring of the $Ca(OH)_2$ peak has been used to observe pozzolanic reactivity, in which the $Ca(OH)_2$ is consumed [324-326].

Whilst qualitative anaylsis of materials with the use of STA is possible, it should ideally be used alongside additional, complementary techniques such as XRD which is more sensitive to subtle changes in phase composition, or only when there is already a relatively sound understanding of the materials and the phases which are likely to be present. Many phases suffer

physical/chemical changes at similar temperatures and therefore identification of an unknown material by STA alone is unadvisable.

Several factors can affect the results obtained by STA and therefore must be considered in order to achieve meaningful, reproducible results, these factors have been summarised in [323].

- Heating rate- Peaks corresponding to phase changes will occur at lower temperatures when using a lower rate of heating, the temperature range of a reaction (from start to finish) may also appear to be lower at lower heating rates. The heating rate can be lowered in order to achieve higher resolution of STA curves, generally a compromise is made between curve resolution and analysis time.
- Furnace atmosphere- The atmosphere within which heating of a sample takes place has significant consequences on the behaviour of the sample. Ideally the atmosphere should remain constant throughout the experiment. This is hindered by the evolution of gases from the sample and convection currents which occur within the furnace. These issues are generally overcome by allowing flow of a controlled gas through the furnace, maintaining a constant pressure. The selection of the type of gas used and therefore the atmosphere in which heating takes place is an important one. Different atmospheres may affect the temperature at which physical/chemical changes occur, e.g. decomposition of $CaCO_3$ occurs at much higher temperatures in a CO_2 atmosphere than N_2 [323]. Heating in an atmosphere which contains oxygen also allows combustion of the sample which is not possible in oxygen free, inert atmospheres such as N_2. This behaviour can be taken advantage of. For example Paya *et al* [327] suggested a method for determining the organic carbon content of PFA by first heating in an inert N_2 atmosphere to remove mass due to water, hydrated lime and $CaCO_3$, before cooling, switching to a reactive atmosphere and re-heating the sample to allow mass loss due to organic carbon combustion. This method offers a more accurate determination of organic carbon content than more traditional loss on ignition methods

of determination such as BS EN 12879:2000. Atmospheres may be chosen and manipulated depending on the information desired from the analysis.

- Crucible geometry- The geometry of the crucible used to hold the sample during analysis has implications on the diffusion of evolved gases and therefore may affect the atmosphere in which the sample is heated.
- Sample preparation- Care must be taken when preparing samples for STA in order to obtain reproducible results. The weight and volume of sample used may affect the diffusion of evolved gases and heat during reactions. Particle size also has significant impact on the behaviour of a sample during thermal analysis. Criado and Ortega [328] showed activation energy for decomposition of $CaCO_3$ to decrease with decreasing particle size.

3.2.2.1 STA methods used in the present study

STA was performed throughout this study using a Stanton-Redcroft STA 1500. Whilst it is possible to increase the chamber temperature of this equipment to 1500˚C which may give further information on sample composition, this was avoided due to the possible corrosion of equipment which may occur as chlorides and sulphates are volatilised, which are present in large quantities in APC residues. Equipment was calibrated by a contract worker due to the difficulty of the process. Calibration was checked running materials of known behaviour such as $CuSO_4 \cdot 5H_2O$ and Zn. Periodically laboratory reagent grade $Ca(OH)_2$ was also used in order to check the calibration. Since the STA equipment was readily available hydration stopping of samples as described in section 3.2.1 was not necessary and therefore avoided due to the possibility of obtaining erroneous results.

Samples were prepared by first grinding to a fine powder with a pestle and mortar in order to normalise particle size. Analysis was performed immediately after preparing the sample as a fine powder. A mask was worn

in order to mitigate against carbonation of the sample during preparation which may be accelerated due to the increased surface area after grinding the sample. Between 15-18mg of sample was used for each run which generally consisted of heating from 20-1000℃ at a rate of 20℃/min in a N_2 atmosphere at a flow rate of 58ml/min.

Attached to the STA was a mass spectrometer. This collected gases evolved during the heating of the sample and identified their masses. Identification of mass allowed identification of the gases produced, providing further information on decomposition processes and assisting with phase identification.

Quantification of phases identified by STA analysis was achieved by drawing tangents to the TGA curve at the start and end of the mass loss and measuring the loss at the midpoint as depicted in [144]. This method allows for a sloping baseline due to gradual loss of water from amorphous phases and subject to attractive surface forces [203]. Depending on pretreatment, C-S-H and hydrated aluminate phases may for example loose bound water from ~90℃ to beyond 550℃ [144]. The % value obtained at the midpoint was used as Δy in equation 3.1. Where mass losses overlapped this method could not be used to achieve accurate results.

Equation 3.1. $$\%w = \left(\frac{mw_c}{mw_v}\right) * \Delta y$$

In which %w= the % weight of the compound
mw_c= the molecular weight of the compound
mw_v= the molecular weight of the volatilised fraction
Δy= the % weight loss measured by TGA

Analysis of as received APC residues by STA presented overlapping peaks and mass losses due to the decomposition of $Ca(OH)_2$ and CaClOH. Several methods were evaluated for quantification which are discussed and compared in appendix B. The method used involved analysis of the DTA peak areas. Although particle size may affect the DTA peak area [144], good

linearity between DTA peak area and %w/w $Ca(OH)_2$ content determined by analysis of the TGA curve was observed for a range of samples studied within this work (Figure 3.1).

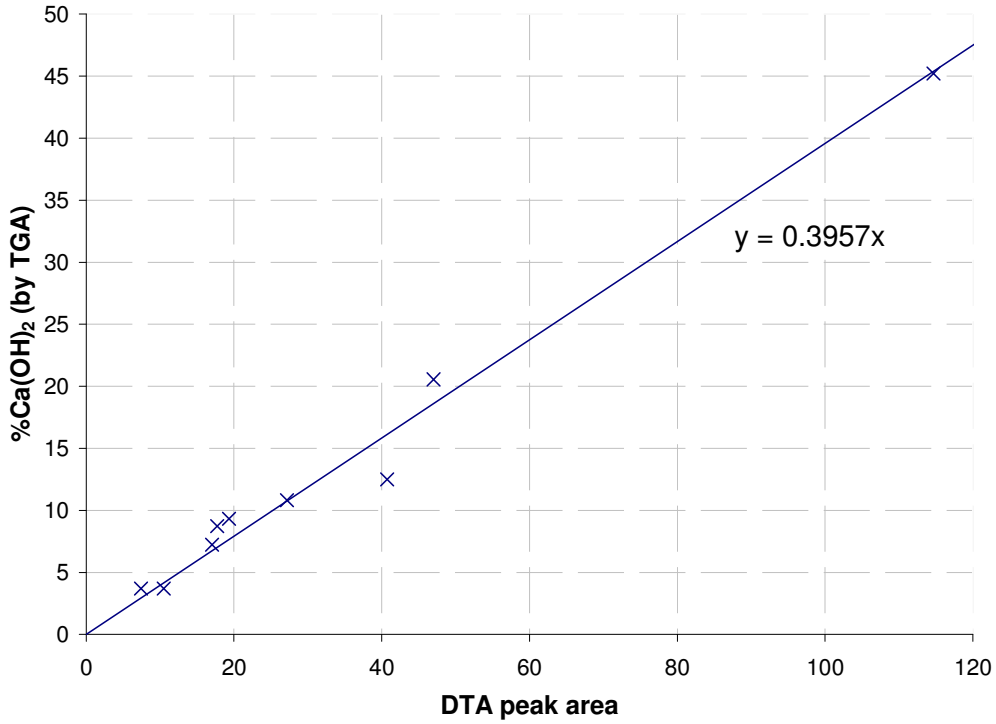

Figure 3.1 Response of DTA peak area to %w/w $Ca(OH)_2$ determined by analysis of the TG curve

The method of quantification by analysis of the DTA peaks involved first subtracting a baseline, created by drawing a tangent across the overlapping DTA peaks, before fitting a Gaussian peak to the DTA peak corresponding to $Ca(OH)_2$ using Origin Pro software. This peak was then integrated and the % weight $Ca(OH)_2$ calculated assuming the linear relationship shown in Figure 3.1. The weight loss due to $Ca(OH)_2$ could then be calculated. The rest of the loss observed by the TGA curve occurring within the range of the overlapping peaks was attributed to loss of water from CaClOH.

As is shown in Appendix B the different methods of analysing the overlapping peaks resulted in some variation in the observed concentrations. The quantification was therefore only considered suitable for comparison of the relative concentration of compounds within materials to which the same analysis method was applied. This technique was only necessary for analysis

of the APC residues as received. Quantification of the TGA curves for other samples could be undertaken by drawing tangents as previously described.

3.2.3 X-ray Diffraction (XRD)

XRD was used to characterise the crystalline phase of samples. This technique consists of directing x-rays at the sample. An intensity peak of diffracted x-rays occurs when the distance travelled by rays diffracting from consecutive atomic planes differs by an integral number of wavelengths of the x-ray, causing constructive interference. This occurs when atoms are periodically distributed throughout the sample i.e. the material is crystalline. Mathematically this is written as Bragg's law, (equation 3.2), derivation of which can be found in [329]. Plotting intensity against d-spacing or °2θ gives a pattern characteristic of the crystal structure which can be examined against databases of previously determined patterns to identify crystalline phases present [330].

Equation 3.2. $$2d\sin\theta = n\lambda$$

In which λ=x-ray wavelength
θ=scattering angle
d=inter plane distance of lattice
n=an integer representing the order of the diffraction peak.

The relative intensities of peaks can be used to give some indication of the $\%w/w_{crystalline}$ of a given phase. This process can be performed using computer software such as Phillips X'pert Highscore in which the Semi-quantitative, normalised reference intensity ratio (RIR) method is employed. RIR values are calculated from the intensity (height) ratio of the strongest line of the phase in question relative to the strongest line of corundum in a mixture of equal weight percentages [331, 332]. Chung [332] stated that three important factors for achieving high precision and accuracy when using this method included:

- Grinding to achieve optimum particle size and sample homogeneity. Alexander *et al* (1948) recommended a particle size <10µm [331]. Smaller particle or grain size generally increases the amount of crystals in all orientations which can be examined in the irradiated area, increasing the chances of correctly orientated crystals to reflect x-rays at each characteristic °2θ. “When the grains are too large there is not enough room within the irradiated volume for a sufficient number of crystals to lie in all possible orientations. The reflections will still lie on a curve of constant θ but the resulting powder reflection will no longer be a smooth line.” [333]. When reflections or ‘Debye rings’ become spotty the intensity becomes uneven which can affect the intensity registered by the detector [334]. However, if particles become too small, peak broadening or damage to crystals may occur [334, 335].
- Loading of sample into sample holder by free-fall in order to avoid preferred orientation. Preferred orientation has similar effects to large grain size in that the statistical distribution of crystals in each orientation is uneven, impacting on observed intensities and in severe cases causing the absence of peaks [331, 334, 335]. The effects of preferred orientation are most pronounced when analysing crystals with anisotropic shapes such as calcite or gypsum [334, 335].
- That the phase used for the reference intensity and the phase to be analysed have equal levels of perfection or imperfection in crystal structure. Differences in crystallinity can be seen in the width of the diffraction lines or peaks. The width of peaks can also vary depending on the crystal size. Analysis of peak widths can be performed to inform on the crystal dimensions [333].

In addition it is important to analyse a flat surface when performing powder diffraction. Without a level surface, errors in the observed °2θ may occur [329, 334].

Errors tend to occur when using this quantification method for materials which are not pure due to variations in crystallinity and non-perfect statistical

distribution/orientation of crystals. The method is therefore only considered to give a broad indication of relative proportion of phases present.

The restriction imposed by the need for periodic atom distribution, allowing only identification of crystalline phases by sharp peaks, allows the proportion of the sample which is crystalline to be calculated. This may be done by comparing the $\%w/w_{crystalline}$ of a phase as shown by XRD with the % weight in the total sample of the same phase as determined by alternative characterisation techniques (e.g. STA). Alternatively addition of a known weight of crystalline material to the sample can give similar information. This method is commonly referred to as the internal standard method and corundum is commonly use as the crystalline material added due to its low amorphous content, small grain size and because it generally shows little preferred orientation [336].

XRD has become a widely used method for characterisation of reactants and products. Though in cementitious and pozzolanic systems the primary reaction products are largely amorphous, XRD allows identification of secondary reaction products which may be of significant importance to the performance of the materials. Occasionally ‘semi-crystalline’ products may also be observed as broad peaks on XRD patterns for example semi-crystalline C-S-H (I) [277, 279].

It is also possible to derive some information on amorphous phases from XRD data. Amorphous phases give broad diffuse humps or ‘halos’, the position of which is ‘usually centred near the main peak of the crystalline compound that the glass would form if devitrified’ [337]. Identification of materials from amorphous XRD patterns is not generally undertaken, due to the simplicity of the patterns and difficulties in distinguishing materials. If a significant amount of information about the material is already known however, such that the range of possibilities is narrow, reasonable assumptions on the composition of amorphous phases can be made based on XRD analysis. Diamond [337] for example, noted correlations between the °2θ value corresponding to the maximum point of the amorphous hump in

PFA and the composition of the glassy material present. Analysis of amorphous materials can produce a radial-distribution function, informing on the density of atoms relative to any reference atom in the solid, and as such giving information on the local atomic environment [329].

3.2.3.1 XRD measurements made during the Present Study

Samples analysed by XRD in the present study were prepared by grinding with a pestle and mortar and backfilling, in order to avoid preferred orientation and obtain a level surface for analysis, into a sample holder with 10mm sample surface diameter. Samples were rotated during analysis, by this process “the number of crystals contributing to the formation of each powder line is considerably increased and the line becomes smoother” [333]. A spinner revolution time of 2-4 seconds per revolution was used.

XRD analysis was performed using a Phillips X’pert Pro diffractometer with X’celerator detector; Cu Kα x-ray source operated at 40kV and 40mA; Ni β filter, in place to absorb the Kβ wavelength, removing associated peaks and thereby simplifying results and avoiding incorrect assignment [329]; 0.04 radian Soller slits, used to minimise axial divergence of the beam which can result in peak asymmetry and misleading peak positions particularly at low angles [329, 334]; divergence and anti-scatter slits programmed to give an irradiated/observed length of 10mm. Data was typically collected with a step size of 0.0334°2θ and a time per step of 120 seconds. Most samples were analysed between 5-90°2θ although some deviation occurred depending on information gathered during trial runs performed with less time per step.

Samples were hydration stopped by submersion in isopropanol and vacuum drying prior to analysis by XRD as described in chapter 3.2.1.

3.2.4 X-ray Fluorescence (XRF)

Bulk analysis of the chemical composition of certain samples was performed by XRF. This technique gives the concentration of elements present as a

weight percentage. As in XRD an x-ray is aimed at the sample to be examined. Unlike XRD, XRF relies on absorption of the x ray. If the x-ray had sufficient energy electrons are ejected from the inner shells creating vacancies, this process is known as the photoelectric effect and is taken advantage of for techniques such as photoelectron spectroscopy. The vacancies left in the inner shells of the atom are filled by electrons moving in from the outer shells. This causes fluorescence of an x-ray photon of energy equal to the difference in the initial and final state of the atom. XRF measures the energy of, and counts these x-ray photons. Due to the unique energy levels of elements, composition identification is possible [338, 339]. By measuring the intensity of x-rays of discreet energies it is possible to quantify the concentration of each element in the material. This quantification can be quantitative or semi-quantitative dependant on sample preparation.

Samples prepared for XRF should ideally be homogeneous such that the analysed material is representative of the bulk material. This may mean controlling particle size prior to analysis [335, 339]. Semi-quantitative XRF involves pressing the powdered sample into a pellet generally with an organic binder. Quantitative analysis involves fusing the sample with typically borate fluxes at ~800-1200˚C [339]. More reliable information than semi-quantitative analysis may be obtained by fusion because matrix, particle size and mineralogy effects are reduced by the formation of a glass like homogeneous liquid which hardens when cooled [339]. The fusion temperature must be considered however. High temperatures can result in volatisation of a significant proportion of certain materials, APC residues for example, which consist of the volatile fraction of the waste at 850℃ may undergo a very high loss and therefore XRF results obtained by quantitative analysis would be misleading.

3.2.4.1 XRF measurements made during the present study

Samples analysed by XRF in the present study were sent away for analysis to Sheffield Hallam University, sample preparation was performed by pressing into a pellet with an organic binder. XRF analysis of APC residues

was not undertaken due to the risk of volatisation of certain fractions by quantitative preparation, and the need for greater accuracy in determining concentrations of trace elements. As such Bulk elemental analysis of APC residues was undertaken by acid digestion and ICP-MS or ICP-OES.

3.2.5 Scanning Electron Microscopy (SEM)

SEM analysis was performed in order to obtain greyscale images of samples magnified up to ~10,000* [340] allowing features to be seen in detail or in relation to their surroundings. At lower levels of magnification it is possible to study such as the arrangement of particles, defects in pastes and porosity. At higher magnifications it is possible to distinguish the morphology of reaction products and the extent of hydration [340]. Electron microscopy involves firing a beam of electrons at the sample and measuring the intensity of the return signal. Many signals may be measured including secondary electrons (SE) and back scattered electrons (BSE).

Backscattered electrons occur due to the return of incident beam electrons to the detector after interaction with the sample. They have energy between that of the primary electron (as aimed at the sample therefore elastic scattering) and, if multiple collisions within the sample have occurred resulting in energy loss before re-emergence, 50eV (by convention) [341]. BSEs offer information on average atomic number as this has a predominant effect on the intensity of the return signal. Areas of high average atomic number appear brighter on BSE images therefore when the contrast and brightness are carefully set, identification of compounds by their greyscale is possible and quantification of compounds (and pores) within the observed area can be performed [340]. This can be a useful technique, however, consideration must be given to the limited sample area being analysed as well as the 2D nature of the image which influences such as estimation of particle and pore size distribution [340]. Additionally the 2D nature of the BSE images means the connectivity of pores and therefore permeability of the sample cannot be deduced.

The greyscale response observed in BSE imaging is not only affected by the average atomic number but by the topography of the sample. In order to avoid the influence of the latter samples are prepared as flat, resin impregnated and polished surfaces which may affect pore structure. Additionally samples must be dried before analysis in high vacuum SEM which can have significant affects on the pore structure depending on the process used (discussed further in chapters 3.2.1 and 3.3.9) [340, 341]. Drying of samples can be avoided by the use of environmental or low vacuum SEM, this technique also avoids the need to apply a conducting coat to non-conductive samples in order to avoid charge build up as is necessary in a vacuum. In a low vac SEM the gas surrounding the sample includes positively charged ions which neutralise the negative charge build up on the sample after exposure to the electron beam [342].

Secondary electrons (SE) are sample atom electrons liberated through inelastic scattering of the incident beam electrons. They therefore have low energies (<50eV) and offer information on surface topography and films [341]. SE imaging has the advantages of clearer resolution than BSE imaging and therefore it is easier to distinguish morphology and voids, additionally three-dimensional morphology of particles may be observed which is not possible with BSE imaging due to the need for a flat, polished surface. Due to the low energy of SEs, this type of analysis is limited to a very thin area at the sample surface. SE imaging is commonly performed on fracture paths which are typically weak sections of the sample and are therefore unrepresentative of the bulk [341]. The surfaces observed by flattening and polishing as is typical for BSE imaging may be more representative [340].

If electrons in the incoming beam collide and eject an inner shell electron from a sample atom, such that an outer shell electron drops to the inner shell, analysis of the characteristic x-rays emitted from the sample (similar to that measured during XRF as previously discussed) can offer localised chemical analysis of the features in the paste which can be compared to the visual image produced. This type of analysis is known as energy dispersive x-ray spectroscopy (EDX) or energy dispersive spectroscopy (EDS). Due to the

extreme localised chemical analysis it can be possible to determine which elements are associated with one another in the reaction products. It is however important to consider the type of analysis with respect to the area of the sample which will be studied. This is summarised in Figure 3.2 [340]. Due to the higher energy of the electrons, BSE analysis penetrates deeper into the sample than secondary electron analysis. X-rays as measured in EDX are generated throughout an entire pear shaped interaction zone and therefore EDX analysis may not correspond directly to the image produced by BSE.

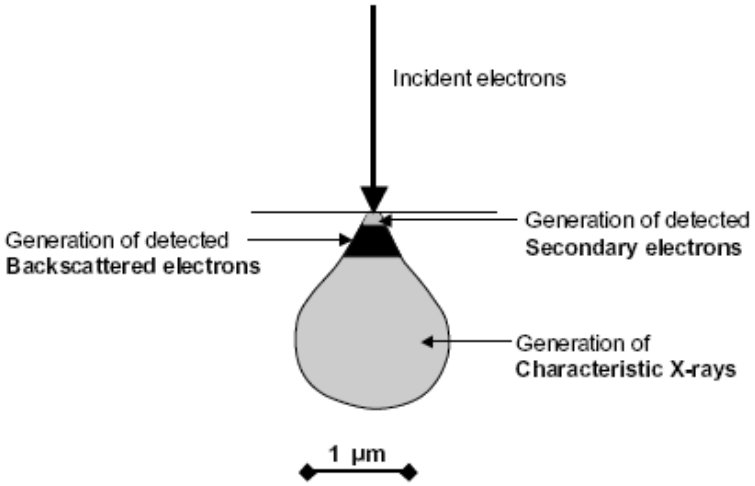

Figure 3.2 Interaction zone for SEM and EDX analysis [340]

SEM imaging has been used by several authors for analysis of waste matrices including [161, 167, 168, 178, 180, 262]. Observations have included, the impact of specific wastes on the reaction rate and products of the matrices [180], the influence of leaching on the matrices [167, 168], and the influence of carbonation and in-situ degradation [161, 167, 168]. Several authors have also used the technique to observe the presence of metals due to their bright response with BSE imaging coupled with energy dispersive x-ray (EDX) analysis [168, 178, 262]. This can inform on their behaviour during leaching and the reaction products with which they are associated. Due to the different interaction zones of the signals previously discussed, and the often fine intermixing of reaction products, such observations require additional evidence. SEM analysis is also commonly incorporated in a suite

of analysis techniques for raw materials, offering information on such as particle morphology and size distribution.

3.2.5.1 SEM analysis in the present study

Sample morphology was examined using an FEI XL-30 environmental SEM with an accelerating voltage of 20 kV. Although the use of an ESEM precludes the need to dry samples prior to analysis, the microscope was typically operated with a chamber pressure of 1 torr, effectively working in low vacuum mode. At this level the relative humidity would be reduced to such an extent that samples would be in a dry state as viewed. For example, at 20℃ the saturation vapour pressure of water is 17.54 torr, operation of the ESEM at a chamber pressure of 1 torr would therefore allow a maximum %RH of 100/17.54=5.7%. Use of the microscope at this level did however prevent the need for application of a conductive coating to prevent charge build up during analysis.

Fracture surfaces were viewed using a gaseous secondary electron detector. Raw materials were viewed by SE and BSE detection after sprinkling a thin coating onto a carbon pad. BSE imaging was also performed after resin impregnating flattened cross sections of samples with Struers Epofix resin and hardener. Following hardening of the resin, samples were polished with various grades of silicon carbide paper and cloths to which Struers DP-Stick P polish was added containing various size polycrystalline diamonds, along with a Kemet type OS lubricant. Polishing was performed mechanically using a Struers Rotopol-35 and PDM Force-20 in order to achieve regularity.

An EDX attachment was available for the FEI XL-30 ESEM equipment. However, due to the highly heterogeneous nature of the samples studied at the level viewed in the SEM, and the fine intermixing of the hydration products, EDX analysis was considered unreliable for phase identification [343]. Although it is possible to overcome this problem to an extent by extended use of EDX and plotting elemental ratios in order to determine

trendlines, as used in various previous studies e.g. [344] this type of analysis was not prioritised during the present study.

3.2.6 Calorimetry

Isothermal conduction calorimetry was used to measure the heat of hydration of the samples. This technique involves measuring the heat flow of the sample when both the sample and surrounding environment are maintained at approximately isothermal conditions [345]. Plots can then be obtained for the rate of heat evolution over time (W/g/sec). This is an important indicator of when critical reactions in the matrix development occur and therefore informs on when characterisation is best performed (e.g. before and after reactions). Results may show some correlation with setting time and strength development since both are largely dependant on the reaction kinetics [346]. Plots may also be obtained for cumulative or total heat evolution (W/g). The heat of hydration is an important factor in itself, if excessive heat is given off this has implications for the casting process should it be performed on an industrial scale, however, blends which do not show, or show minimal heat evolution may not be sufficiently reactive and therefore may not develop strength by formation of reaction products other than carbonation products and drying which would have severe implications for the integrity of the matrix [157].

For accurate interpretation of calorimetry results it is important to take into account the time interval between completion of mixing and beginning recording data, if the test specimen rapidly reacts this period could be of significant interest. Additionally the mixing method employed should be considered since heat may be imparted into the paste by mixing which has been shown to decrease the time to reach the maximum rate of heat evolution, and reduce the total het evolved [347, 348].

3.2.6.1 Calorimetry measurements made during the present study

In the present study, calorimetry was undertaken using an 8 channel TAM air 90℃ isothermal heat conduction calorimeter. In which the aluminium

calorimetric block sits inside an insulated chamber in which the air is conditioned with a thermostat to between 5-90℃. Reaction ampoules are twined with a reference ampoule which should be inert and was left empty for the measurements taken in the present study, the observed signal is the difference between the reaction and reference ampoules. Twined reactive and reference ampoule configuration reduces a significant quantity of external noise in the signal, allowing for high sensitivity and baseline stability. Signals were detected by Seebeck heat flow sensors positioned beneath the ampoules, as a voltage proportional to the heat flow.

Mixing of samples was performed by hand with each sample being subject to the same mixing time (until the driest mix became homogeneous) and rate (based on judgement) before loading into the calorimeter. Approximately 15g of sample was loaded into each reaction ampoule with each sample being run in duplicate. Two further reaction ampoules were left empty in order to check for cross heating within the calorimeter. In order to minimise the heat imparted by mixing, a large excess of material was mixed (300g mixed with 30g tested). Mechanical mixing was attempted in order to better normalise the mixing procedure although was insufficient to enable complete mixing of materials due to the dry nature of some of the samples.

3.3 Performance Related Tests

This section gives details of test methods which were used to directly determine the performance of the treated waste. Performance characteristics which were examined include workability, setting time, compressive strength, porosity, permeability, granular and monolithic leach behaviour and acid neutralisation capacity (ANC).

3.3.1 Workability

Workability is a measure of the ease with which the fresh blends can be cast and compact in order to remove the air and produce a solid product. It therefore has important implications for the applicability of the treatment on

an industrial scale. Blends which are excessively dry and cannot be poured or easily moulded are not suitable for casting monoliths however may be treated by compaction, e.g. rolling into place [157]. Excessively high workability also creates problems, resulting in a paste which is difficult to handle and pour safely. Since workability is largely a result of water content, consideration must be given to the influence a change in water content would have on the matrix. For example, limited water content may prevent optimum formation of hydration products through a lack of water which can be bound, and, since the volume of the freshly compact mix consists of the solid particles dispersed in the liquid, a lack of volume in which the expansive hydration products can form [144, 204]. Excessive water content on the other hand leaves residual water occupying volume within the hardened product which results in interconnected pores, increasing the porosity and permeability of the s/s product. A compromise is therefore necessary between minimising water to that required for optimum hydration of the binder, minimising permeability, and ensuring enough water is present to produce a workable paste. Stegemann and Zhou [157] suggested a workability corresponding to a flow measurement ~175mm as determined by BS EN 1015-3:1999 [349].

Since workability is a measure of the ease with which a paste consisting of solids suspended in a liquid will flow, and this type of assembly generally behaves as a fluid, the behaviour can be characterised by fundamental rheology [144, 330]. S/S matrices, similar to concrete, mortars and cement pastes, would tend to behave as Bingham plastics, such that flow begins (viscosity is reduced) after an initial application of stress, known as the yield stress [330]. Assuming constant temperature and pressure, several factors can affect the viscosity and yield stress of such pastes as discussed in [330] including

- The volume fraction of solids- since crowding restricts the ability of particles to flow, increased volume fraction of solids causes an increase in yield stress and viscosity.

- Particle shape- intrinsic viscosity is lower for spherical particles than non equant, higher specific surface area shapes. Spherical particles therefore have a lower water demand for a given workability (where other properties are equivalent).
- The degree of flocculation or dispersal- flocculation of particles increases the viscosity of the paste, and the yield stress since flocculations need to be dispersed in order to flow. Often breakdown of flocculations is not complete at the yield stress therefore suspensions show thixotropic behaviour i.e. viscosity is reduced with time under a constant stress level. After the applied stress is removed, particles may flocculate again causing a reversal in the viscosity decrease. Dispersed suspensions may behave as a Newtonian fluid in which no yield stress is required unless the volume fraction of solids is high.

3.3.1.1 Workability measurements made during the present study

The workability of the fresh mix was assessed using BS EN 1015-2:1999 'Determination of consistence of fresh mortar (by flow table)' [349]. This test involves filling a conical mould of known dimensions with the fresh mix before removing the mould and 'jolting' the cone of fresh material (standardised lifting and dropping of table) 15 times over approximately 15 seconds. The spread of the material which occurs as a result of the energy from the drop action is then measured with callipers in two directions perpendicular to each other. The mean of these measurements is given as the flow value in mm. Two cones are tested, if the flow values differ by more than 10% from their mean the test is repeated. The equipment required for the test is shown in Figure 3.3.

The test offers no simple indication of any fundamental rheological property but is an empirical indication which may be used to compare the relative workability of the mixes studied. There are many such tests however the flow table was considered the most suitable for the materials being studied due to the limited amount of material required and speed with which the test can be conducted.

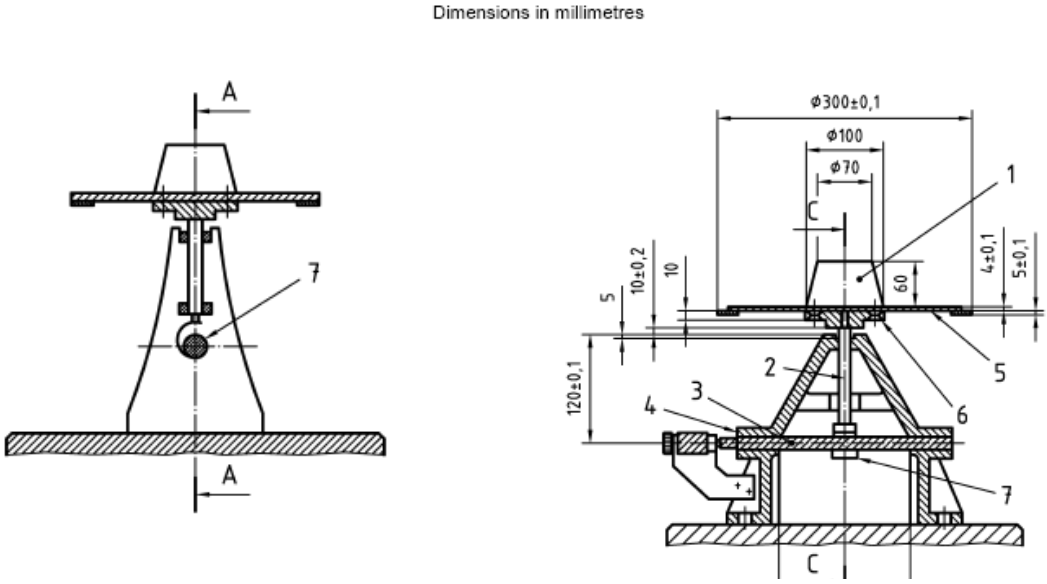

Key

1 Truncated conical mould
2 Disc
3 Rigid table plate
4 Lifting cam
5 Stand
6 Horizontal shaft
7 Lifting spindle

Figure 3.3 Equipment for flow table test, BS EN 1015-2:1999

3.3.2 Setting Time

The setting time of the mixes was determined using EN 480-2:2006 [350]. This test consists of periodically penetrating the sample (held in a mould of regulated dimensions) and measuring the depth of penetration. Initial setting time refers to the time at which the mix begins to stiffen i.e. there is a dramatic increase in the yield stress, and is determined by the time from completion of mixing until the time when the needle penetrates to a depth 4mm above the base plate (bottom of the sample). The sample is then inverted to determine the final setting time which is the time at which the plasticity of the mix is lost [346]. Final setting time is given as the time from completion of mixing until the needle no longer penetrates 2.5mm into the sample. Equipment required for this test is shown in Figure 3.4.

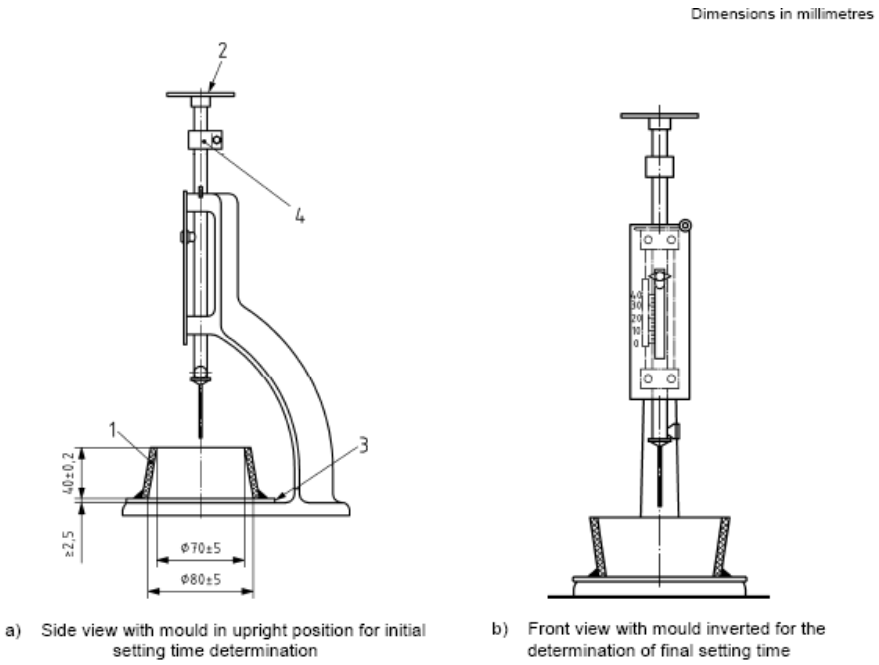

Figure 3.4 Determination of setting time, EN 480-2:2006

The standard was designed to compare setting time of mixes with a standard consistence. In the current work the test was employed to compare setting time of mixes which may vary in consistence but share other properties (e.g. equal APC residue content or l/s). Additionally the standard method dictates that the samples be stored underwater between measurements. This was not adhered to since such a curing regime would be unfeasible for the samples studied in the current work due to leaching.

Stegemann and Zhou [157] suggested an initial setting time between ~2-8 hours in order to offer sufficient time for casting of the blend, and final setting time <~24 hours in order that cast s/s monoliths need not be stored for excessive periods before they can be handled and moved. Stegemann and Zhou suggested determination of setting time by BS EN 196-3:2005 [351]. In this study BS EN 480-2:2006 was used. 196-3 was designed for testing of cement pastes whilst 480-2 was designed for testing of mortars. The principle differences include the use of a needle with 5mm diameter ring attachment 0.5mm from the tip, for determination of final setting time in 196-3 whilst in 480-2 the same needle is used for initial and final setting time (1.13mm tip). The penetration depths for initial and final setting time are also slightly different in BS EN 196-3:2005, initial set being specified as 6mm from the

base plate and final set as <0.5mm penetration (ring attachment leaves no mark). Values for initial and final set determined by the two tests would therefore vary (196-3:2005 giving slightly longer setting times) however the criteria suggested by Stegemann and Zhou [157] was still considered as a guide, with consideration given to the implied variations.

3.3.3 Compressive Strength

Compressive strength is of primary interest for construction materials due to the demanding loads they have to withstand. For s/s products the compressive strength is of less importance however monolithic WAC does require a 1 MPa compressive strength after 28 days [92] and products may be required to withstand the load of material placed above in the landfill cell and possibly vehicular traffic [157]. The compressive strength is however generally a good indicator of other properties of monoliths such as porosity [204] and the progression of reactions which contribute to a dense, durable microstructure [157].

Compressive strength was assessed using BS EN 12390-3:2009 [352] in which samples are loaded until failure under compression. The maximum load sustained by the sample was recorded and the compressive strength calculated as shown in equation 3.6. Three samples were tested for each determination of compressive strength allowing standard deviation calculations. Compressive strength was reported as the mean.

Equation 3.6 $UCS=F/A$

In which UCS= unconfined compressive strength (MPa)
F= Maximum load at failure (N)
A= Cross sectional area of test piece (mm^2)

50mm cubes were cast for compressive strength testing. This is a modification to the standard which was undertaken in order to avoid using

more material than is required. Such deviation is however allowed for in Annex B of BS EN 12390-3:2009.

3.3.4 Density

Various density measurements were made as are discussed in the following sections. Although the density of s/s products would have some impact on the handling ease and cost of landfilling, measurement of density was not undertaken for presentation but in order to use the values in calculations of such as availability and porosity.

3.3.4.1 Fresh mix density

Density of the fresh, compact mix was determined by monitoring the weight of moulds of known volume ($3*50mm^3$) after carefully compacting, levelling and ensuring excess mix was not present on the mould. This process is similar to that described in BS EN 1924-2:1990 section 2.1 'Determination of the dry density/moisture content relation' [322], without the subsequent determination of dry mass. Testing was performed at least in duplicate using separate batches and the average weight used for calculation of density.

3.3.4.2 Test piece density

Determination of the density at a given age was determined by weighing of a known volume of the test piece (usually $50mm^3$) and converting to density (kg/m^3).

3.3.4.3 Dry density of test pieces

Dry mass density was calculated by weighing a known volume (generally $50mm^3$) of test piece at a given age before drying a representative granular sub sample of the piece at 105℃ for 24 hours to determine percentage dry weight. Sub samples were typically 2-4g of granular material (<4mm), which gave a standard deviation in percentage dry weight low enough to be considered representative of the bulk sample (Table 3.1). Weight was

determined on analytical balance correct to 4dp giving a lower detection limit of 0.005-0.0025%. Percentages accurate to 1dp were used.

	Sample 1	Sample 2
sub sample 1	71.5	71.8
sub sample 2	71.3	71.5
sub sample 3	71.5	71.6
Standard Deviation	0.12	0.15

Table 3.1 Repeatability of % dry weight by drying for 24 hours at 105°C

This drying temperature may remove interlayer water from C-S-H [144, 279] as well as chemically bound water in, for example, ettringite and gypsum [144, 322], and therefore may result in an overestimation of free water. A comparison of dry mass determined by oven drying at 105℃ and submersion in IPA followed by vacuum drying, for a sample typical of those studied in the current work is presented in Table 3.2. Oven drying indicated significantly less dry mass. Additionally alkaline samples may undergo carbonation therefore gaining weight during the drying process which could result in an underestimation of free water. This can be avoided by the use of a N_2 atmosphere to exclude CO_2. This drying method, without the use of a N_2 atmosphere was considered accurate enough for determination of dry weights in this work however. It has been extensively used throughout the literature and is a standardised procedure [322, 353].

105℃	IPA+Vac
72.6	78.6

Table 3.2 Dry weight % according to different drying methods

The % dry weight was applied to the weight of the test piece to calculate the dry mass of the test piece which could be converted to density (kg/m^3).

3.3.4.4 Density of dry mass

The density of the dry mass was determined with a Quantachrome Ultrapycnometer 1000, helium pycnometer in which the volume of sample is determined by displacement of helium at a defined pressure. Granular samples were first submerged in isopropanol for 24 hours and vacuum dried

for a further 24 hours which was sufficient to dry the sample such that %weight change over 4 hours was lower than 0.1% (defined as dry in BS EN 1924-2:1990 [322]). This type of drying was used instead of oven drying to remove water before analysis in order to avoid removal of chemically bound water and alteration to the mineralogy and therefore density of the sample. The dried sample was finely ground with a pestle and mortar and weighed into the pyconometer cell using an analytical balance correct to 4dp.

3.3.5 Bulk Porosity

Bulk porosity was calculated using the dry mass density of test pieces and the dry mass density calculated using the helium pycnometer. Bulk density could be calculated as the volume of the test piece minus the volume occupied by the dry mass as shown in equation 3.7 [67]. Since dry mass density of the test piece was determined by drying the sample at 105℃ and density of dry mass determined after drying by solvent replacement and vacuum drying there may be some error in the results due to the discrepancy in these drying procedures (Table 3.2). With hindsight the author recognises the same drying procedure should have been used for both density determinations. However, since the same procedure was used for all samples analysed, results are still considered to give an indication of relative bulk porosity.

$$p = 1 - \left[\frac{BD * (1 - WC)}{SG * d} \right]$$

Equation 3.7. Calculation of bulk porosity [67]

This method for determination of bulk porosity has been used by several authors including [67, 226, 241, 354].

3.3.6 Leach Tests

There are many different leach tests available. Variations occur in such as [20]

- Sample type- Typically granular or monolithic of defined sizes. Granular leach tests are more aggressive due to increased surface area and negligible physical encapsulation. Granular tests can therefore be used for assessing the extent at which analytes are chemically immobilised. Monolithic tests conversely may be used for assessing the physical encapsulation offered by a solidified/stabilised waste form and the integrity of the matrix. Release from monoliths is typically analysed per unit surface area over time and by renewing the leachant in order to maintain a concentration gradient, can offer information on the diffusion rate of analytes through the waste form.

- Leach Medium- Often de-ionised water but may be acidic or basic solutions. The leach medium will have implications on the leach results due to the variation in solubility of compounds which can occur with variation in pH and the influence of ionic species present in solution.

- L/S (w/w)- Higher l/s result in a more aggressive leach test, reducing the risk of saturation and therefore solubility limitations. Whilst concentration of analytes in the leachate may be lower due to dilution, release of ions by concentration in the sample is greater. A higher l/s may also reduce the variation in pH of the leachant. This can be altered as elements in the solid are released into the solution and due to higher concentrations, may be more significant at lower l/s.

- Hydrogeological Conditions- The way the leachant flows around the samples. Higher speed flow of the leachant around the particles increases their rate of dissolution creating a more aggressive leach test. Flow rate can be incurred through agitation during testing. Agitation also ensures the solid phase is constantly mixed, preventing any encapsulation by settlement.

- Temperature may also affect the solubility of species and rate of reactions therefore has to be dictated and controlled in leach tests.

For assessment against WAC [92] a granular or monolithic test can be used both of which are performed at room temperature, using de-ionised water and therefore at the pH conditioned by the sample. The prescribed monolithic leach test is EA NEN 7375:2004 [355] which involves no agitation and leachant renewals at set intervals.

Granular WAC requires the use of the tests BS EN 12457/1-3 [356-358]. These tests are all performed on sample crushed so 95%w/w of the sample has a grain size less than 4mm. The sample is agitated in the leachant during the leaching period in order to avoid settlement and therefore any encapsulation. The granular test methods vary in the l/s ratio employed and procedure for addition of the water. Differences can be summarised as

- EN 12457-1, one stage leach test at l/s=2 (l/kg) for 24 hours
- EN 12457-2, one stage leach test at l/s=10 for 24 hours
- EN 12457-3, two stage leach test at l/s=2 for 6 hours and l/s=8 for 18 hours.

EN 12457-2 is more aggressive than 12457-1 due to the higher l/s. EN 12457-1 is not suitable for wastes with a moisture content greater than 33%w/w. EN 12457-3 results can be analysed as a cumulative release or as separate fractions, offering information on the rate of analyte release and possible solubility limits.

3.3.6.1 Leaching tests used in the present study

3.3.6.1.1 Granular tests

For convenience, granular leach testing was performed according to BS EN 12457-2:2002 [357]. The method was adapted to accommodate the use of a rotating table operating at 90rpm rather than an end-over-end tumbler. A brief test showed only slight differences in the chloride leach from as-recieved

APC residue with stirring as opposed to tumbling, with the former giving a mean release of 166,033 mg/kg with σ=26,565 mg/kg and tumbling releasing 160,000mg/kg. Thus, whilst it is appreciated that results from a rotating table will not be identical to those obtained with an end over end tumbler, the chloride release was similar, and the test still enabled the performance of the mixes to be compared with one another. A principal risk of using a horizontal stirrer was the settlement of sample and therefore some form of encapsulation during the test. In order to mitigate against this risk, sample size was reduced from the standardised 90g to 20g. Repeated testing suggested that this size sample was still representative of the bulk of the test pieces (Table 3.3).

	Cl release (mg/kg)
Sample 1	45,900
Sample 2	47,500
Sample 3	45,400
Standard Deviation	1097

Table 3.3 Reproducibility of granular leach results using modified 20g sample size

Crushing was achieved through repetitive impact followed by sieving with a 4mm sieve. The weight of sample required was calculated by first calculating the dry matter content as a %w/w, by drying a sub sample at 105˚C for 24 hours and applying equation 3.8.

Equation 3.8 $DR=100*M_D/M_W$

In which, DR= the dry matter content ratio (%)
M_D= the mass of the dried test portion (kg)
M_w= the mass of the undried test portion (kg)

The mass of the undried test portion to be used for leach analysis was then calculated by rearranging equation 3.8 and taking M_D as 20. DR % correct to 1dp was used. The test sample was then mixed with 18MΩ de-ionised water to establish the defined l/s ratio. The moisture content of the test sample was taken into consideration here. The resultant mixture was agitated for 24h +/-

0.5h at 20˚C before vacuum filtration using 0.45µm filters. Following filtration leachate pH was immediately measured. After determination of analyte concentrations (as discussed in chapter 3.3.7), interpretation was performed as shown in equation 3.9.

Equation 3.9. $A=C*[(L/M_D)+(MC/100)]$

In which, A= the release of a constituent (mg/kg of dry matter)
C= the concentration of a constituent in the eluate (mg/l)
L= the volume of leachant used (l)
MC= the moisture content ratio= $100*(M_w-M_D)/M_D$

Results could be compared with availability which was calculated by equation 3.10.

Equation 3.10. $U_t=(D_f/D_t)*U_f$

In which, U_t= Availability at test age (mg/kg dry mass)
U_f= Availability in fresh mix (mg/kg)
D_t= Dry mass density at test age
D_f= Density of fresh mix

In which densities were determined as described in sections 3.3.4.3 and 3.3.4.1.

3.3.6.1.2 Monolithic Leach Testing

Monolithic leach testing was performed according to the standard prescribed in the monolithic WAC, EA NEN 7375:2004 [355]. Leachant renewals are undertaken after 0.25, 1, 2.25, 4, 9, 16, 36 and 64 days resulting in 8 leachate fractions. 18MΩ de-ionised water was used as the leachant at a liquid/solid (by volume) ratio of 5. $50mm^3$ test pieces were used which were supported on stainless steel, mesh stands in sealable plastic containers in order to give the required clearance for the test, allowing release from the

entire surface area. A blank run was performed using 18MΩ de-ionised water exposed to the containers and stainless steel stand for 64 days (without leachate renewal) which showed no contamination with anions.

Leachates fractions from the test were stored and analysed individually as described in subsequent sections (3.3.7). Analysis of results obtained from such a monolithic leach test can be performed in order to observe measured cumulative release, and also calculate the mechanism controlling the release of the analyte. According to EA NEN 7375:2004, the mechanism is determined by analysis of the gradient of intervals on a plot of the log of derived cumulative release against the log of time. Derived cumulative release is given by equation 3.11 and as such equals the cumulative release which would have occurred from the start of the test to the end of the fraction being analysed, if release had occurred at a constant rate proportional to the square root of time, i.e. by a diffusive mechanism.

Equation 3.11
$$\varepsilon_n = \frac{E_i^* * \sqrt{t_i}}{(\sqrt{t_i} - \sqrt{t_{i-1}})}$$

In which ε_n = the derived cumulative leaching of a component for period comprising fraction i=1 to n (mg/m^2)

E_i^* = the measured leaching of the component in fraction i (mg/m^2)

t_i = the replenishment time of fraction i, i.e. time at the end of fraction i (s)

t_{i-1} = the replenishment time of fraction i-1 i.e. time at the start of fraction i (s).

Analysis of the gradient of the log-log plots therefore gives an indication of the change in the rate of leaching throughout the test. When release is diffusion controlled (proportional to the square root of time), the linear regression of the log derived cumulative release-log of time plot will give a gradient of 0.5. An increase in the rate of release indicates some dissolution

of the matrix and a reduced rate of release indicates depletion of the analyte or a possible change in the chemical form, resulting in greater chemical or physical retardation of release. Increments to be analysed and the interpretation of data is summarised in Table 3.4 [355].

Increment a-b	Slope, rc		
	≤ 0.35	> 0.35 and ≤0.65	> 0.65
Increment 2-7	Surface wash-off	Diffusion	Dissolution
Increment 5-8	Depletion	Diffusion	Dissolution
Increment 4-7	Depletion	Diffusion	Dissolution
Increment 3-6	Depletion	Diffusion	Dissolution
Increment 2-5	Depletion	Diffusion	Dissolution
Increment 1-4	Surface wash-off	Diffusion	Delayed diffusion or dissolution

Table 3.4 Interpretation of the gradient (rc) of log-log plots during EA NEN 7375 [355]

When a diffusion controlled increment is identified, the derived 64 day release can be calculated as equation 3.12, based on the rate of release during the diffusion controlled increment. When no diffusion controlled increment can be identified the derived cumulative leaching of a component over 64 days is equal to the measured release [355].

Equation 3.12

$$\varepsilon_{64} = \sqrt{64} * \left(\prod_{i=a}^{b} \frac{E_i^*}{\sqrt{t_i} - \sqrt{t_{i-1}}} \right)^{\frac{1}{1+b-a}}$$

In which ε_{64}= the derived cumulative leaching of a component over 64 days (mg/m^2)

a and b= dimensionless indices by which an increment a-b is indicated for which a diffusion mechanism is established according to criteria in Table 3.4

t_i and t_{i-1} = the replenishment time of fraction i and i-1 respectively (hours)

If leaching is diffusion controlled a diffusion coefficient may also be calculated as equation 3.13.

Equation 3.13 $$D_e = \left(\frac{\varepsilon_{64}}{2653 * \rho * U_{avail}} \right)^2 * f$$

In which D_e= the average, effective diffusion coefficient for a given component (m^2/s)

ρ= the dry density of the test piece determined as described in chapter 3.3.4.3 (kg/m^3)

U_{avail}= the leachable available quantity determined according to EA NEN 7371 (mg/kg)

f= a factor equal to 1/s

EA NEN 7371 is a granular leach test performed on finely ground material at l/s=50 and buffered to pH~7 for 3 hours followed by pH~4 for 3 hours with HNO_3 in order to determine availability. In order to determine availability of chlorides and sulphates in this work the release from granular samples buffered to pH<4 with HNO_3 at l/s=10 for 24 hours was used which was believed to give suitable indication of the leachable availability of chlorides and sulphates. Availability may also be taken as total availability which can lead to overestimations of the amount available for leaching since some of the analyte may be unavailable for leaching due to its chemical form [20]. This overestimation results in smaller diffusion coefficients. Importantly the same method should be used for determining availability in all samples such that diffusion coefficients are comparable. Diffusion coefficients illustrate the rate at which an analyte can diffuse through a matrix and therefore the chemical and physical retention of the anlayte [20].

Diffusion coefficients are reported as the –log (pD_e) and can be interpreted as

pD_e>12.5	component with low mobility
12.5>pD_e>11.0	component with average mobility
11.0>pD_e	component with high mobility

A pD_e value below 9.5 is said to have no physical significance as the material has no internal tortuosity [355].

Additionally, an approximate % release of analytes was calculated by determining the availability in a test piece in mg from the density of the fresh mix (3.3.4.1), analysis of the raw materials and dilution. Release was calculated in mg as the concentration in the leachate (ppm or mg/l) multiplied by the initial leachate volume (625ml). Compressive strength of samples following the monolithic test was also determined and the granular test BS EN 12457-2 performed in order to attain an indication of water soluble chlorides and sulphates retained.

3.3.7 Analysis of Leachate

3.3.7.1 pH

The pH of the leachate was determined using a Denver instrument ultrabasic pH meter with a range of pH 0-14, resolution of 0.01pH units and accuracy of +/- 0.01 pH units. All pH results were recorded to an accuracy of 1dp in a room with temperature ranging from 20-25℃ although pH was measured with a pH combination electrode with temperature, and auto pH temperature compensation was used to a default temperature of 25℃. The meter was calibrated with buffer solutions of pH=4, 7 and 9.2. Solutions were made periodically (every 4-8 weeks) from buffer tablets (Fisher Scientific UK catalogue numbers B/4760/77, B/4765/77 and B/4770/77 for pH 4, 7 and 9.2 respectively).

3.3.7.2 Total Dissolved Solids (TDS)

TDS were measured according to BS EN 15216:2007 [359]. A 25ml sub sample of leachate was used. The sample size prescribed in the standard is enough to leave a residue of 20-1000mg which was satisfied by 25ml samples. Samples were dried in glass evaporating dishes. After determining the weight of the dried dish, 25ml of leachate was added using a 5ml micropipette and weighed on analytical scales correct to 4dp. The leachate was dried at 105℃ +/- 3℃ to a constant mass to determine TDS.

3.3.7.3 Sample Storage

Leachate samples for analysis of individual ion concentrations were stored according to BS EN ISO 5667-3:2003 [360]. HDPE bottles were used, with caps of inert material to avoid contamination and minimal head space to exclude air. Samples to be analysed for chlorides and sulphates were stored in a fridge between 1-5℃.

3.3.7.4 Anion Analysis

Anion analysis was performed using liquid chromatography (LC). This technique involves the liquid sample being transported by a conductive eluent through an ion exchange separator column which separates ions of interest using exchange sites. For anion exchange separation these are positively charged sites whilst for cation exchange separation they are negatively charged. The different affinity of the ions for the ion exchange sites, largely as a result of radius and valence [361], results in ions eluting from the column separately over time. This allows identification of ion type by its retention time within the exchange column. Conductivity is plotted against time and peaks occur which correspond to the elution of different ions (Figure 3.5). The peak heights or areas can be compared with a calibration curve created using standard solutions with known ion concentrations, in order to offer quantitative analysis.

The eluent is degassed in order to prevent bubbles which cause noise in the detector cell and loss of pressure in the valves and pump heads [362]. The eluent is the source of competing anions which establish equilibrium with the analyte ions within the ion exchange column. As such greater eluent concentration reduces the retention time of analyte anions. Excessive concentration of eluent ions may cause poor resolution of peaks and a high baseline [361]. Other ions present in the matrix may also affect the peak heights and areas of analytes observed if for example, they are eluted from the column after a similar retention time. Matrix effects can be checked for using the standard addition method in which a sample is spiked to increase

the concentration a known amount [362, 363]. Responses (ppm) are plotted against the concentration added. If no matrix effects are present the results should plot in a linear correlation with an x intersect of –the original solution concentration such that the linear regression has the equation 3.14.

Equation 3.14 Y=X+SR

In which SR= the unspiked sample result (original solution concentration)

Acceptable limits (indicating no matrix effects) give %R=80-120 [363] where %R is determined as shown in equation 3.15.

Equation 3.15 $$\%R = \frac{(MSSR - SR)}{SA} * 100$$

In which MSSR= Matrix spike sample result
SA= Spike added

If %R lies within 80-120 then the linear regression for MSSR against SA will take equation 3.16.

Equation 3.16 Y=kX+SR

In which 0.8<k<1.2

The eluent containing the sample ions moves from the exchange column to a suppressor column which, for anion analysis, contains a cation exchange resin. This converts the highly conductive eluent and analyte ions to their acid forms, reducing background magnitude, enhancing peak height and resolution, and increasing detection sensitivity [361]. After passing through the suppressor column the conductivity of the sample is measured.

This type of analysis is restricted by several factors. Samples must be aqueous solutions without particulates. Any particulates must be filtered before injection into the chromatograph in order to avoid blockage. Samples must also be of very small size, typically ~50µl. Larger sample quantities should be avoided as they reduce column efficiency and increase the water dip which occurs as the water in the sample elutes. This water dip can be seen in Figure 3.5 and is due to the lower conductivity of water in the sample than the suppressed eluent which dictates the baseline conductivity [362]. For reliable quantification, analyte concentration must also be within the analytical range for which the response of the chromatograph is known to be linear. This often requires dilution of the samples.

3.3.7.4.1 LC measurements made during the present study

Anion concentrations in leachates were analysed with a Dionex DX500 liquid chromatograph system with IonPac AS14 anion exchange column, GP50 gradient pump and ED40 electrochemical detector. The leachate sample was transported by a conductive eluent comprising of 2mM Na_2CO_3 and 2.5mM $NaHCO_3$. The eluent was degassed with an inert gas (helium).

The calibration standard plot is shown in Figure 3.5. The response (peak area) was calibrated using a standard solution containing

- 5ppm Fl
- 10ppm Cl
- 25ppm Br
- 25ppm NO_3
- 40ppm PO_4
- 30ppm SO_4

which was periodically remade at 100* concentration and diluted in order to assist in accuracy when weighing reagents. No nitrite was added because nitrites were not of interest for the current study and readily oxidise to nitrates due to atmospheric O_2 exposure [364], disrupting the standard. An analytical balance correct to 4dp was used for weighing standard reagents. Fresh standard was tested against the old standard before acceptance.

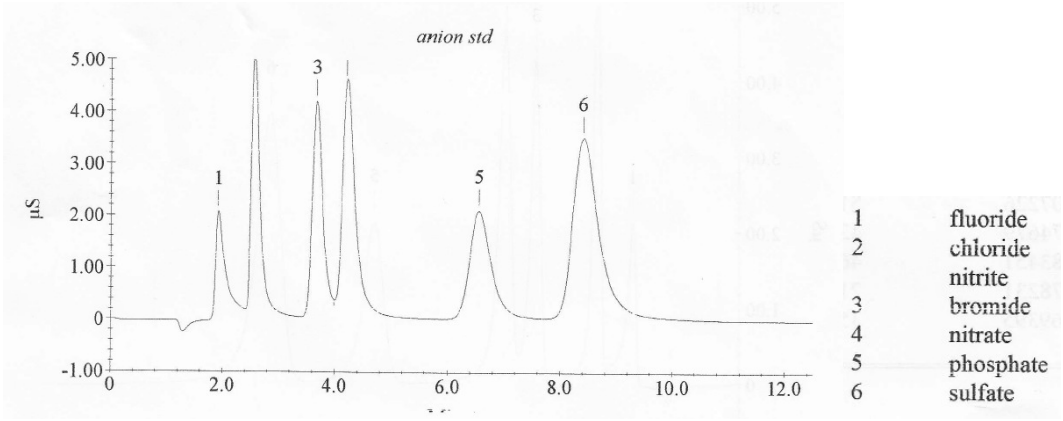

Figure 3.5 Ion chromatography plot for calibration standard

Before injection into the chromatograph samples were filtered with a 0.22 micron syringe filter. The equipment operates with a sample size of 0.25µl.

For Cl analysis of the leachates being studied, dilution was required in order to ensure the concentration lay within the analytical range. Dilution was also undertaken in order to avoid a residue building on the column which could produce false readings. In order to confirm residue had not collected on the column 18MΩ de-ionised water was periodically run through the chromatograph to check for peaks. Solutions studied were diluted using 18MΩ de-ionised water to produce ppm reading between 5-50ppm Cl. The calibration curve for this range, obtained with duplicate dilutions is shown in Figure 3.6. All dilutions were undertaken using micropipettes of various volume ranges and volumetric flasks. Pipette calibration was checked before use and periodically using a balance and de-ionised water.

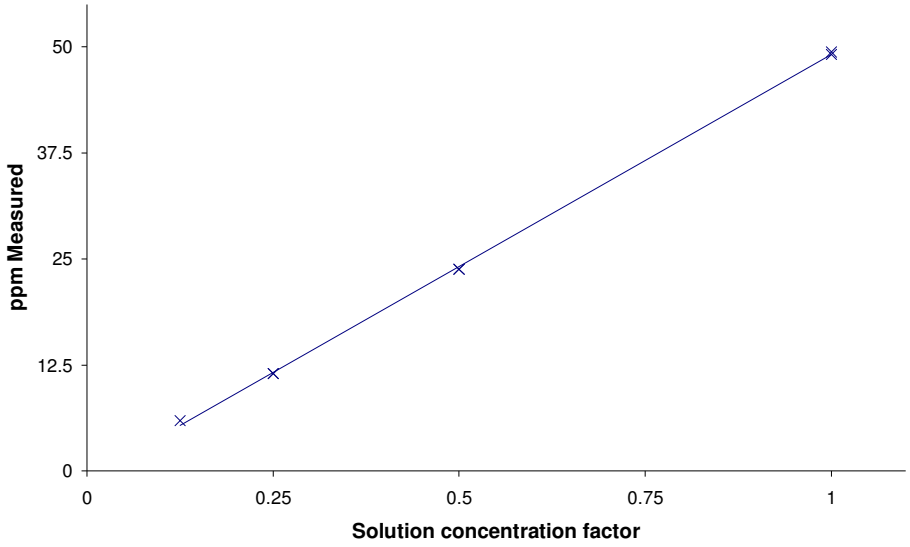

Figure 3.6 Cl calibration curve in the concentration range analysed

In order to check for matrix effects the standard addition method was performed in duplicate, using a leachate resulting from a granular leach test on a typical sample studied. As can be seen in Figure 3.7 the linear regression had the equation y=1.1106x+7.455, corresponding to %R=111.06 therefore EPA criteria were satisfied, showing no matrix effects [363].

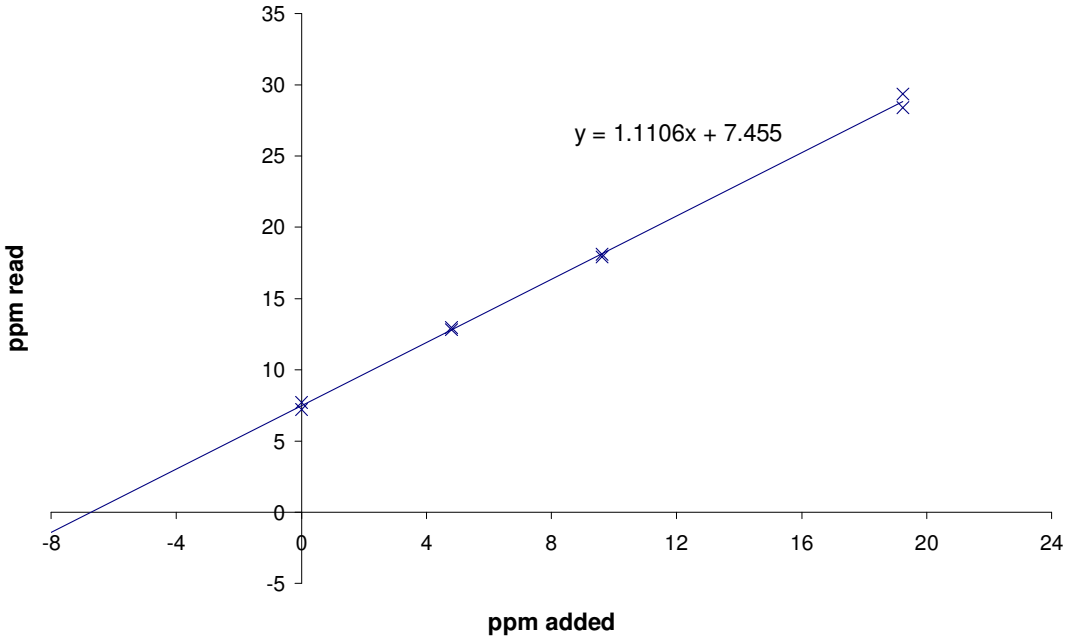

Figure 3.7 Results for standard addition (matrix spike) of leachate

Additionally the stability of the chromatograph was assessed over time by periodically running the anion standard. Result obtained by L.Arkless (University of Leeds) are presented in Figure 3.8. Based on the result equipment was left to stabilise for at least two hours before calibrating and beginning analysis.

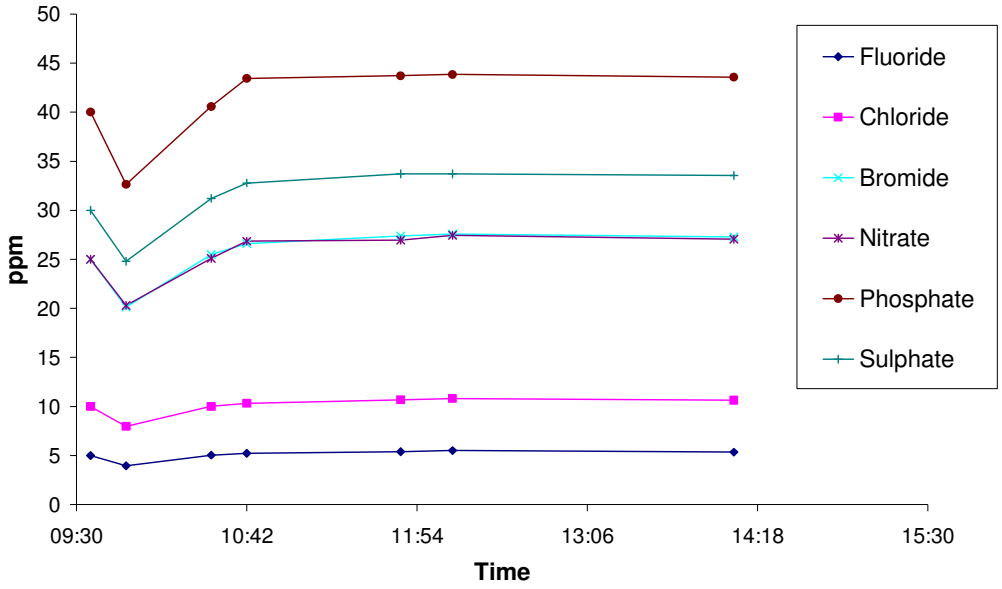

Figure 3.8 Chromatograph stability results obtained by L.Arkless

Results obtained as described above were compared with those obtained in an industrial lab in order to further validate accuracy which was confirmed (Table 3.5).

Result obtained in University	Result obtained by UKAS accredited lab	% difference
47,500	47,000	1
57,500	55,000	4.5
40,500	40,000	1
45,000	44,000	2.8

Table 3.5 Comparison of Cl release analysed on site and at a UKAS accredited laboratory

3.3.7.5 Additional Analysis

In addition to the analysis of anions described above, selected samples were analysed at a commercial laboratory for full WAC analysis which involved

determination of concentration of metals by ICP OES, and dissolved or total organic carbon (DOC or TOC respectively) by oxidation and infrared detection. Selected raw materials were also characterised by these methods after total acid digestion.

3.3.8 Acid Neutralisation Capacity

Acid neutralisation capacity, is a particularly important parameter regarding s/s waste products [152] because acidic exposure can corrode the matrix, reducing integrity [163], and because the solubility of contaminants is often pH dependant [69]. In the current study ANC was measured by two methods. First, the method described in DD/CEN TS 15364:2006 [365] in which a series of separate extractions with l/s=10 and different mEq/g acid addition (HNO_3) are undertaken for a minimum of 48 hours was used. Tests were conducted in HDPE bottles sealed to exclude CO_2. Atmospheric exposure during pH measurements was kept to a minimum. Bottles were agitated on a rotating table at 90rpm and agitated by hand after each pH measurement to avoid any encapsulation due to settlement. According to DD/CEN TS 15364:2006 [365] the pH of the sample is considered stable once a difference of less than 0.3pH units is observed over a period of 4 hours. Whilst this condition was satisfied by the samples analysed after several days agitation, it was observed that satisfying this criteria did not correspond to a pH equilibrium since sample pH continued to rise. To ensure pH stability was achieved, the criteria were adjusted such that the pH was considered stable if deviation over 48 hours was <0.3pH units.

Deviation from DD/DEN TS 15364:2006 occurred by the use of samples with dry mass=5g (determined as described in chapter 3.3.6.1.1) and allowing greater than 1.5 pH units deviation between extractions. Greater deviation was allowed due to the great number of extractions which would have been required to analyse all samples to pH<4 according to this criteria. This deviation, whilst still allowing comparison of the relative alkalinity of samples, did not allow for identification of plateaus for reaction products due to the low resolution of the resultant curves.

In order to obtain higher resolution curves, ANC was also tested by titration. This method is described by Young *et al* [366] and is recommended in technical guidance WM2 for assessment against H4/H8 corrosive/irritant thresholds [84]. This method is also described in appendix B of DD/CEN TS 15364:2006. Titrations were performed by initially establishing a l/s ratio of 9, with 5g dry weight of granular sample and 18MΩ de-ionised water, and adding 70% HNO_3 (15.8M HNO_3) in additions of 0.16 or 0.32ml, corresponding to addition of 0.5 or 1mEq/g respectively. Volume change resulting from the addition of the HNO_3 was considered negligible due to the logarithmic nature of the pH scale, and the small volume of acid added due to the use of 70% HNO_3. The effect of volume adjustment on pH (at both ends of the scale) by addition of 10mEq/g (3.2ml) is shown below for pH 12 and 4. The pH was recorded to 1dp.

Effect of volume adjustment for alkaline pH (12)

- Assuming 50ml has pH=12, then $H^+=10^{-12}M = 10^{-12}g/L = 5*10^{-14}g$
- If volume is adjusted +3.2ml then $H^+= 5*10^{-14}g$ in 53.2ml = $9.4*10^{-13}g/L$
- If $H^+= 9.4*10^{-13}$, pH=12.03

Effect of volume adjustment for acidic pH (4)

- 50ml has pH=4, $H^+=10^{-4}M = 10^{-4}g/L = 5*10^{-6}g$
- $5*10^{-6}g$ in 53.2ml $=9.4*10^{-5}g/L$
- If $H^+=9.4*10^{-5}g/L$, pH=4.03

Disadvantages of performing ANC by titration may include repeated exposure to atmospheric CO_2 due to repeated pH measurements, and the time required for the test to reach completion which may enable further reactions (e.g. hydration) to occur in the sample. The pH of all ANC samples was considered stable once deviation of less than 0.3pH units occurred over 48 hours. For titrated samples this generally took ~7 days (Figure 3.9).

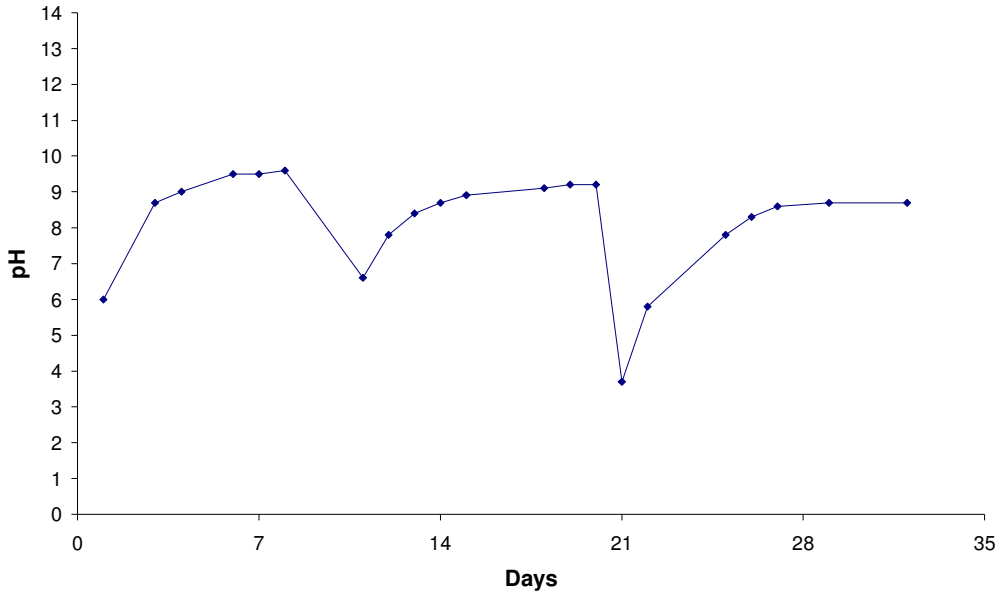

Figure 3.9 Example of pH development over time for titrated samples, showing time required to reach a stable pH. Drops in pH indicate addition of 0.5mEq/g HNO_3. Rapid drops indicate additions of 0.5mEq/g

ANC to pH 4.5 was calculated by linear interpolation of data points either side of pH 4. This value was used to calculate alkalinity as $\%CaCO_3$ equivalent assuming equation 3.17.

Equation 3.17 $2HNO_3 + CaCO_3 \rightarrow H_2O + CO_2 + Ca(NO_3)_2$

Since 1Eq of HNO_3 corresponds to 1M (63g), the mEq/g HNO_3 was converted to mg/g by multiplying by 63. Since 2M HNO_3 reacts with 1M $CaCO_3$ (100g) (equation 3.4) the mg/g $CaCO_3$ was calculated as equation 3.18 and converted to $\%CaCO_3$ equivalent.

Equation 3.18. $(100/126) * mg/g\ HNO_3 = mg/g\ CaCO_3$

3.3.9 Permeability

Permeability of s/s products is an important property which as discussed in chapter 2.3.9 and by Poon *et al* [367], governs the interrelated properties of durability and leachability. Bone *et al* [150] also mention the importance of permeability with regards to the release of gas from the waste into the

atmosphere. Since long term performance of construction materials is largely a result of durability, permeability measurements have received much attention in this field [144, 368].

Permeability is experimentally determined by measuring flow rate of a fluid of known viscocity, through a sample specimen of known dimensions. The intrinsic permeability of the sample can then be determined using D'arcy's law (equation 3.19)

Equation 3.19 $$K = \frac{v\eta L}{a\Delta p}$$

In which v =flow rate (m^3s^{-1})

K = intrinsic permeability (m^2)

a =cross sectional area (m^2)

Δp =change in fluid pressure (Pa)

η =fluid viscocity (Pa·s)

L =length of specimen (m)

Since the viscocity of the fluid is considered in the equation, intrinsic permeability is an indication only of the properties of the sample with units m^2. In contrast, results for hydraulic conductivity are presented as a velocity (m/s) and reflect the properties of the fluid and the sample. For s/s products the hydraulic conductivity is the primary property of interest as the transport of aqueous solutions has the most significant effects on leachability, and transporting dissolved, reactive ions such as sulphates and carbonates into the matrix. Carbonates may diffuse into the matrix as a gas, however solubilisation is necessary for carbonation reactions to occur therefore water must be present in the pores and carbonates ions may also be carried into the matrix after dissolving.

There are several difficulties which arise when attempting to measure the hydraulic conductivity of s/s products. Disadvantages discussed by Poon *et*

al [367] and Feldman *et al* [369] include the reactivity of water within a typical cementitious or pozzolanic matrix which coupled with long time periods required to reach a steady flow rate, results in continued hydration and therefore changes to the product during testing. Pores may also become blocked by transport and crystallisation of calcium hydroxide, formation of calcite and silting [368, 369]. Changes in solution composition may also affect the permeability results obtained [370]. These changes may be considerable due to leaching from s/s products during the experiment. Leaching would also clearly affect the pore structure of the sample and would occur whilst vacuum saturating the sample in order to avoid capillary forces [144] if using a high pressure permeability test. Whilst a steady state of flux could eventually be achieved, this may relate to a modified pore structure. S/S products may also have low strength relative to construction materials which can also affect the result obtained for hydraulic conductivity. Differences in the coefficient obtained may occur with eluted sample volumes and sample size Ganjian *et al* [370]. Low sample strength increases the probability of damage to sample when using high pressures for permeability testing, sample damage such as cracking can significantly affect data obtained [369, 371].

As long as a gas which is unreactive within the s/s matrix is used, measuring gas permeability at low pressures avoids many of these problems, including, of primary concern during the present study, leaching during testing. The relationship between the intrinsic permeability recorded using gas and liquids is however complicated due to effects such as the ‘slip’ phenomena otherwise known as the Klinkenberg effect.

The ‘slip’ or non-zero velocity of gas along pore walls described by Klinkenberg in 1941 [372, 373], as opposed to the zero velocity observed for liquids [372], was suggested to explain the consistently higher results obtained when measuring permeability with gas compared to liquid. This has also been noted by several other authors including Bamforth [374].

The Klinkenberg effect is more prominent when the Knudsen number (defined as mean free path/physical restraint e.g. pore diameter) is high, because collisions between molecules and the pore walls become dominant therefore the ‘wall velocity’ becomes more significant with respect to the average velocity [373]. The definition of the Knudsen number shows that the effects of slip, and therefore the discrepancy between liquid and gas permeability values, becomes more prominent as the pore diameter (reducing the physical restraint) or the pressure of the gas (increasing the mean free path) are reduced. Differences between liquid and gas permeability are therefore generally greater for less permeable media [374, 375]. Additionally a non linear relationship between pressure and flow rate occurs as experimentally observed by several authors including [375]. Whilst measurement at low pressures is beneficial as sample damage is avoided, results obtained at such pressure must be considered with this in mind.

Another important factor when measuring gas permeability is the moisture content of the samples. Liquid in pores hinders the flow of gas through the sample [367, 375]. Samples must therefore be dried before measurement of gas permeability or at least be prepared in such a way that moisture content can be assumed to be consistent in all samples as was relied upon by Bamforth [374]. Pore structure may be affected by drying in various ways depending on the method used therefore drying methods should be selected appropriately.

Lynsdale [375] and Sanjuan [376] investigated the effect of oven drying at various temperatures on the permeability coefficient obtained. Sanjuan [376] showed an increase in permeability with increased drying temperature. Somewhat in contrast, Lynsdale observed drying at 60℃ to result in greater permeability than 40℃ and 105℃. Residual water was said to be present in the samples dried at 40℃ whilst greater permeability of samples dried at 60℃ compared to 105℃ was attributed to the higher surface tension, resulting from the slower movement of water during drying, causing greater damage to the pore structure [375].

The results of Lynsdale [375] also show mix design to affect the changes in permeability with different drying temperatures. Increased reaction kinetics at higher temperatures can result in significant changes in permeability during the drying process due to continued reaction. The extent of reaction is dependent on the temperature and the time required to reach a constant weight. This process is more prominent in samples in which reactions may be significant even at later ages such as those in which pozzolanic reactions occur.

Damage to pore structure by oven drying has been observed by several authors including [315, 377]. Typically the process results in damage to smaller pores and as such a coarsening of the pore structure. Pore structure has also been studied after removal of water by freeze drying techniques [315, 377] evidence of damage to the microstructure and formation of cracks due to thermomechanical stresses is presented.

Other methods used for drying samples for gas permeability measurements in the literature include vacuum drying [369, 378]. Shafiq and Cabrera allowed moisture content to equilibrate in controlled humidity [379]. Submersion in isopropanol followed by drying at 38℃ has been suggested to cause the least disruption to pore structure [369]. As discussed in chapter 3.2.1 replacement of pore water with fluids of lower surface tension including isopropanol followed by drying was also observed to result in less damage to pore structure in several other studies [315, 320, 377].
Reviewing the literature suggests that whilst drying, or at least normalising moisture content is essential for measuring gas permeability, as stated by Hearn [371] “Any conditioning process that involves drying of the specimen introduces microcracking in the matrix, thus opening up the microstructure”. In the same paper Hearn highlighted that cracking caused by drying shrinkage, as opposed to mechanical loading, is not localised and therefore has a much more significant effect on the permeability.

Finally the temperature plays an important role in measurements, significantly affecting the analysis gas viscosity.

Due to the many effects discussed throughout this section, and reviewed in the referenced literature, permeability values obtained using both liquid and gas fluids should not be viewed as absolute or precise values, consistent methods should be used within any study in order that results can be used to offer a ranking of sample permeability. Neville [368] suggested that scatter of permeability results even on "similar concrete, at the same age, using the same equipment, is large. Differences such as between, say, $2*10^{-12}$ m/s and $6*10^{-12}$ m/s are not significant, so that reporting the order of magnitude, or at the most $0.5*10^{-1}$m/s, is adequate." Where comparison of values obtained with values presented in literature are desired, it is essential sample preparation and test methods are borne in mind and the likelihood of significant variations are accepted.

3.3.9.1 Permeability measurements made during the present study

During this study measurement of permeability was performed using the 'Leeds gas permeameter" (Figure 3.10) Designed by Cabrera and Lynsdale [380]. Varying input pressures between 1 and 4 bars were used. Measurements were made at room temperature with atmospheric outlet pressure. N_2 was used as the analysis gas and flow rates were measured on a bubble flow meter.

The equation used to calculate intrinsic permeability is shown in equation 3.20. This is a modified D'arcy equation in which the analysis gas volume is calculated at the average pressure within the sample.

Equation 3.20. $$K = \frac{2 p_{out} v L \eta}{a(p_{in}^2 - p_{out}^2)} * 10^{-11}$$

In which p_{in}= absolute pressure in (bar)

p_{out}=atmospheric pressure=1.01325 bar

v is measured in cm^3/s

L and a measured in m and m^2 respectively

η is the viscocity of N_2 at 25℃=1.77*10^{-5} Ns/m^2

Figure 3.10 Leeds gas permeameter (Image from [354])

Samples were cast as 52mm diameter cylinders, before testing samples were all measured using veneer callipers. After curing the pore structure was opened by sanding as cutting resulted in 'smearing' of the surface (Figure 3.11). After sanding high pressure air was aimed at the sample surface to remove any debris. The results of this method of sample preparation is shown in Figure 3.12.

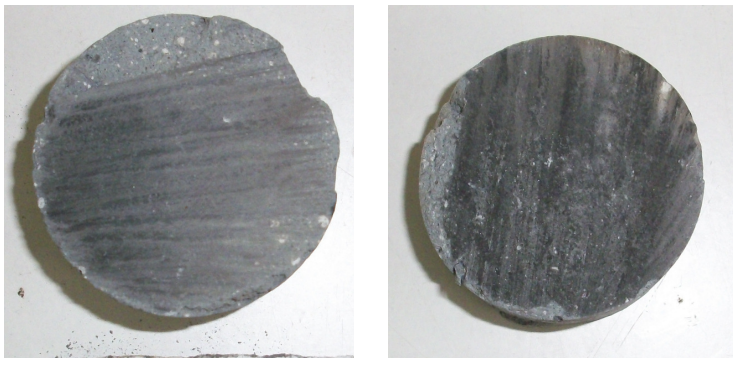

Figure 3.11 'Smearing' of sample surface after cutting to expose the internal pore structure

Figure 3.12 Sample as cast (left) and after exposing internal pore structure (right)

Several methods were attempted for drying samples in order to compare results. Samples were also tested without drying. Methods employed for drying included

- submersion in IPA followed by vacuum drying. Both the submersion and vacuum drying process were undertaken for a minimum of 3 days.
- Freeze drying was also undertaken which involved submersion in liquid N_2 until the liquid settled followed by storage in a vacuum at temperatures <-20°C.
- Oven drying was also undertaken at 60°C until a constant weight was achieved. Constant weight was defined as a difference in sample weight after cooling to room temperature of not more than 0.1% over a 4 hour period, as in BS EN 1924-2:1990. 60°C was chosen as drying temperature as a compromise between drying rapidly to avoid excessive additional curing, and avoiding temperatures at which reaction products of the samples were known to be altered.

For many of the samples studied oven drying and freeze drying resulted in cracking (Figure 3.13). The majority of the work was therefore performed by submerging samples in IPA for 3 days and vacuum drying for a further 3 days. This technique offered no guarantee that samples were fully dried or dry weight normalised. Results may be exaggerated since lower permeability samples would dry at a slower rate [381] and therefore retain more water at the time of testing. Several samples were also tested after submersion for 7 days in de-ionised water, similar to the procedure described by Stegemann and Zhou [157] coupled with measurement of UCS, for assessment of matrix integrity and strength development by methods other than drying. Such

samples were subjected to the same drying procedure, due to the initially much greater water content in such samples, if drying was not comprehensive permeability measurements would be expected to be underestimations. Due to the implications of this drying regime results obtained were considered qualitative rather than quantitative.

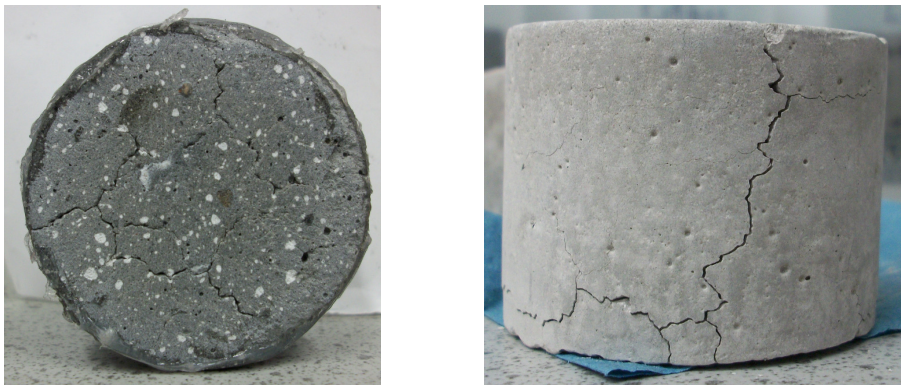

Figure 3.13 Examples of sample cracking after oven drying (left) and freeze drying (right)

Following drying samples were coated around the curved sides with a silicon rubber compound (RS Stock No. 555-558), this provided a more effective seal between the sample and gas permeameter and prevents leakage of gas through the curved face of the sample as described by Bamforth [374]. Coating by Bamforth was more important due to the permeameter used which did not otherwise constrain the samples curved face.

4 Results and Discussion- Analysis of Raw Materials.

4.1 Characterisation of as received air pollution control residues

Several APC residues were studied throughout this work, collected from different EfW incinerators. The residues are identified by the nomenclature A1-A5. A1 resulted from a clinical waste incinerator in which emissions limits for NO_x established in the WID could be met without flue gas treatment by injection of nitrogenous compounds. Other residues involved the injection of urea to reduce NOx gas emissions. Clinical waste is generally expected to have >1% halogenated organic substances (e.g. dioxins and furans) therefore a furnace temperature of 1100℃ for at least two seconds is required [15]. The other residues resulted from incineration of municipal solid waste (MSW) at ~850℃. All residues were collected from incinerators which used semi-dry scrubber systems in which $Ca(OH)_2$ was used as the scrubber.

As received residues were leach tested in duplicate according to BS EN 12457-2 from which water soluble Cl, SO_4, TDS and pH were determined (Table 4.1). Full WAC analysis by BS EN 12457-2 and total elemental content by acid digestion and ICP OES of A1 was determined at a commercial laboratory and are presented in Table 4.2 along with SNR and hazardous WAC limits. Values which exceed the limits for SNR WAC are highlighted in the table.

The mineralogy of the residues was characterised by STA and XRD. DTA and TGA plots for the residues are shown in Figure 4.1 and Figure 4.2 respectively. Quantification of compounds identified by STA including $Ca(OH)_2$, CaClOH and $CaCO_3$ are shown in Table 4.1 as a percentage of the dry weight determined by drying for 24 hours at 105℃. The minimum dry weight observed was 97.5%, corresponding to residue A5. The compounds were quantified as described in chapter 3.2.2.1. Figure 4.3 shows the STA of A1 together with the mass spectrometry curves for H_2O (mass 18) and CO_2 (mass 44) indicating the evolution of these gases as compounds were

thermally decomposed. XRD patterns for the residues are shown in Figure 4.4 with semi quantitative analysis according to the normalised RIR method presented in Table 4.3. Reference patterns for the matched phases are presented for the readers' convenience in Figure 4.5.

Several of the phases have overlapping diffraction peaks which can result in apparent broadening of peaks, peak asymmetry and intensity differences relative to the reference patterns. Peaks for $Ca(OH)_2$ and CaClOH for example overlap at 2Θ positions of ~18°, ~47°, ~51° and ~63° (Figure 4.5). A set of three peaks belonging to $CaCl_2{\cdot}2H_2O$ (hkl=(121), (113) and (004)) occur very close together ~29°2Θ and result in an apparently broad, asymmetric peak (Figure 4.5). $CaCl_2{\cdot}2H_2O$ was present in residue A5 with the presence of these peaks resulting in an apparent broadening and asymmetry to the (104) $CaCO_3$ peak occurring at a similar °2Θ (Figure 4.4). The most intense peak corresponding to the $CaCl_2{\cdot}2H_2O$ phase ((122) at ~32°2Θ) lay between peaks for NaCl (200) and CaClOH (102) and was therefore difficult to distinguish. However, the (111) and (102) peak doublet for $CaCl_2{\cdot}2H_2O$ could be clearly identified at 2Θ values of ~21° along with several other minor peaks including the (002) reflection at ~14.7°2Θ (Figure 4.4).

Overlapping of three $KCaCl_3$ peaks ((211), (031) and (112)) at ~28-29°2Θ, with peaks corresponding to KCl (200) and CaClOH (101), resulted in a broad asymmetrical feature in the pattern for residue A3 (labelled K (KCl) in Figure 4.4). Other $KCaCl_3$ reflections just above 29°2Θ were hidden beneath, or visible as shoulders on the strong $CaCO_3$ reflection (104). However, other peaks corresponding to these phases could be clearly identified, including $KCaCl_3$ peaks at 2Θ values of ~17° (101), 19° (111) and 24° (121) (Figure 4.4). The most intense reflection from $KCaCl_3$ ((040) at ~34°2Θ) could also be clearly distinguished due to the very minor concentration of $Ca(OH)_2$ present in residue A3 as evident from the XRD pattern and STA (Figure 4.4 and Table 4.1 respectively).

Importantly no RIR was available for the $KCaCl_3$ reference patterns (ICDD PDF- 21-1170 or 25-0625) therefore peaks for this compound remained unmatched during the analysis, resulting in an overestimation, and some error in the quantity of the other compounds. XRD was also performed on A1 following BS EN 12457-2 and vacuum drying (Figure 4.6).

Table 4.1 also includes the alkalinity of the APC residues, defined as ANC to pH 4.5 and presented as %w/w $CaCO_3$ equivalent. Titration curves are presented in Figure 4.7. Finally the morphology of A1 was studied by ESEM analysis using GSE and BSE detectors (Figure 4.8).

As discussed in the literature review APC residues may contain trace levels of organic pollutants including dioxins and furans. These were not evident in any of the residues studied in concentrations of concern and were not the subject of the current study.

	A1	A2	A3	A4	A5
Cl Release 12457-2 (mg/kg)	157,400	105,300	132,400	112,600	233,600
SO_4 Release 12457-2 (mg/kg)	3500	8500	11,800	12,300	5700
pH 12457-2	12.4	12.5	12.4	12.5	12.2
Alkalinity (%$CaCO_3$ equiv)	87.5	55	62.5	50	58.5
TDS 12457-2	333,300	235,130	304,670	271,800	460,480
$Ca(OH)_2$ (%w/w)	40.2	15.0	0.5	2.6*	3.8
CaClOH (%w/w)	15.3	8.6	9.8	18.4*	7.4
$CaCO_3$ (%w/w)	4.4	7.3	28.6	10.3	nd

Table 4.1 Release of Cl and SO_4, pH and TDS during BS EN 12457-2, Alkalinity and %w/w_{dry} of compounds identified by STA. nd-not determined. *suspected erroneous results, see text.

Analyte	HAZ WAC	SNR WAC	A1 total (mg/kg)	A1 12457-2 (mg/kg)
As	25	2	3	0.3
Ba	300	100	380	69.0
Cd	5	1	11	<0.1
Cr_{total}	70	10	27	2.0
Cu	100	50	590	1.4
Hg	2	0.2	26	**2.3**
Mo	30	10	<10	1.2
Ni	40	10	15	0.1
Pb	50	10	1700	**200**
Sb	5	0.7	29	<0.1
Se	7	0.5	<10	**0.5**
Zn	200	50	1900	8.2
Cl^-	25,000	15,000	200,000[b]	**157400[b]**
F^-	500	150	<1[b]	18.0[b]
SO_4^{2-}	50,000	20,000	19,500[a]	3500.0[b]
TOC	1000	800	6000[c]	520.0[c]
TDS	100,000	60,000		**333300[d]**

Table 4.2 Release from A1 during BS EN 12457-2 compared to total availability and WAC limits. Highlighted figures exceed SNR WAC limits. [a]determined by semi-quantitative XRF, [b]determined by IC, [c]determined by oxidation and infrared, [d]determined by gravimetric analysis, other results determined by ICP OES

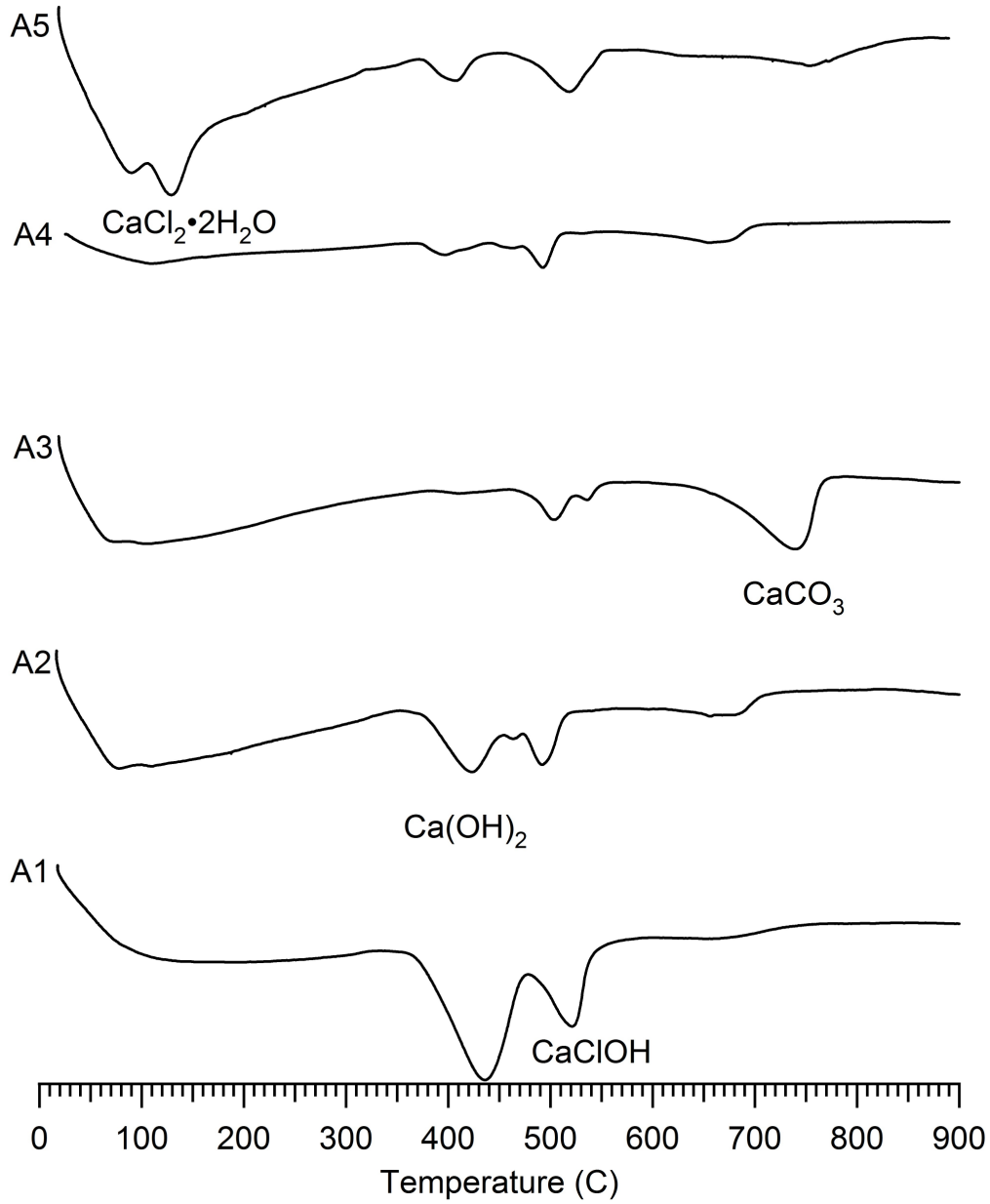

Figure 4.1 DTA curves (y axis range normalised) of as received APC residues heated at 20°C/min in a N_2 atmosphere

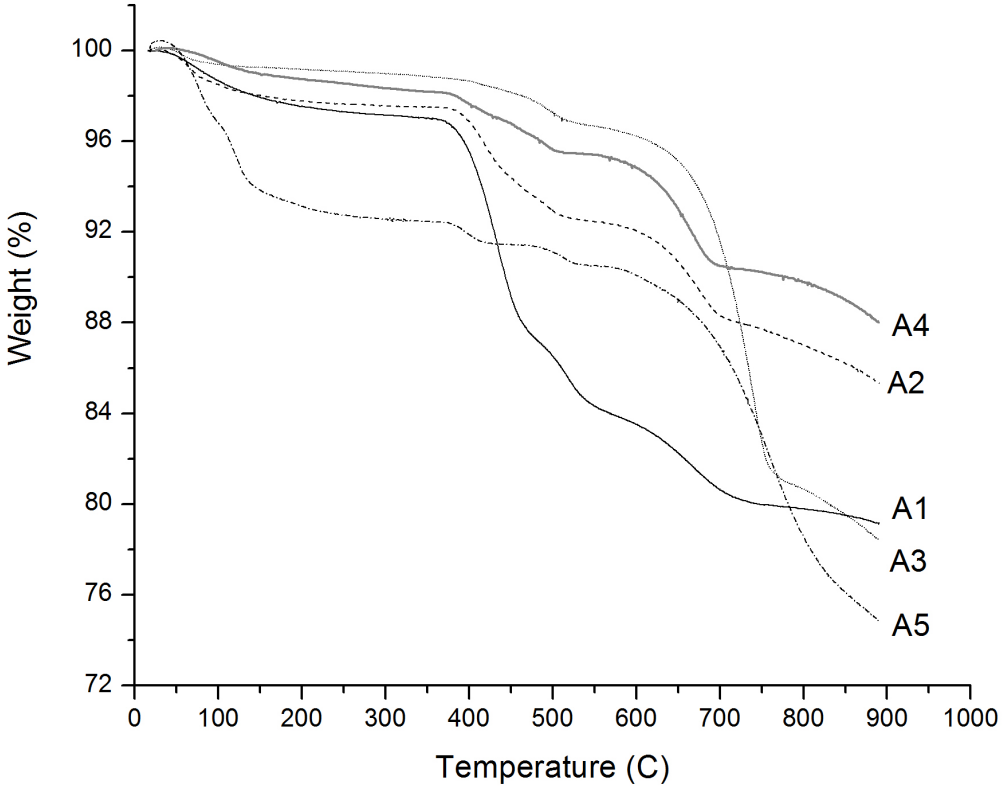

Figure 4.2 TGA of as-received APC residues

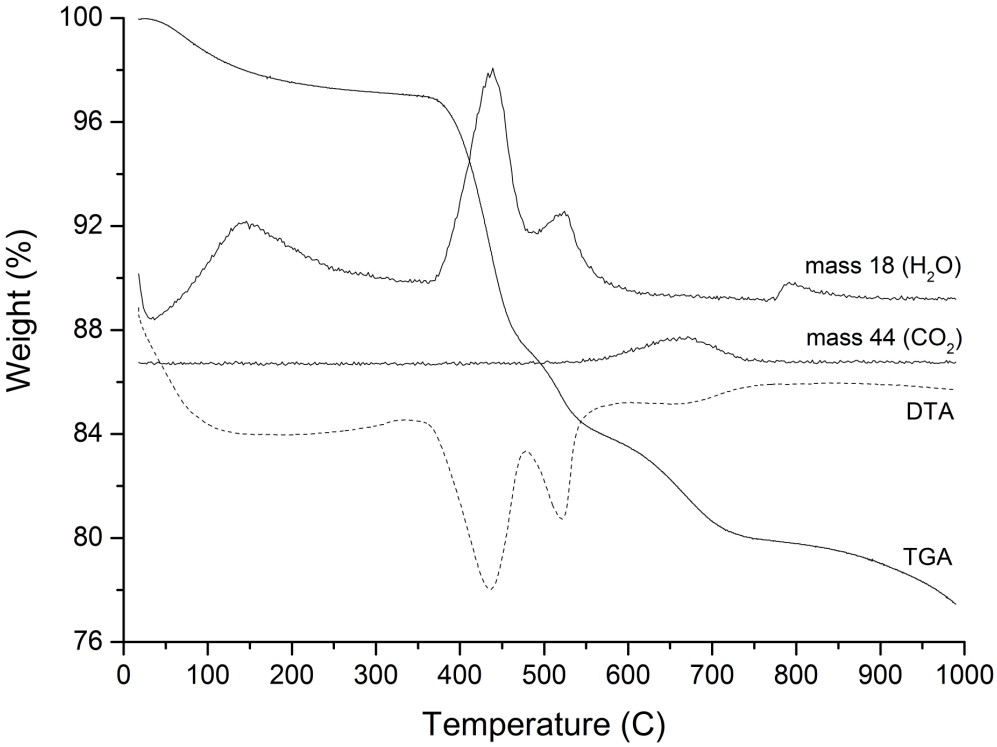

Figure 4.3 STA of as-received A1 showing TGA, DTA and mass spectrometry for H_2O (mass 18) and CO_2 (mass 44). Y axis for DTA and mass spec data not shown.

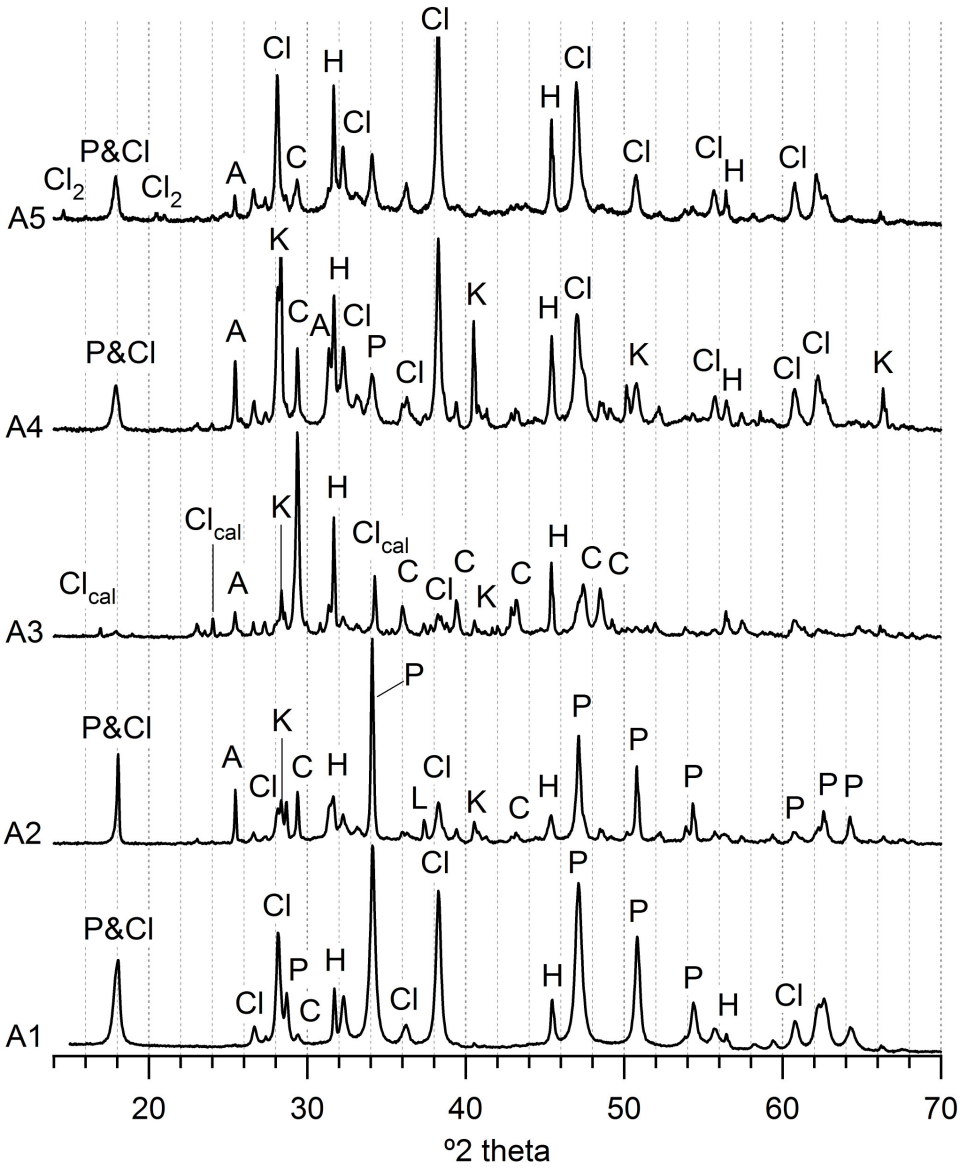

Figure 4.4 XRD patterns (y axis range not normalised) for as-received APC residues. P=$Ca(OH)_2$ (ICDD PDF=84-1264), C=$CaCO_3$ (ICDD PDF=72-1652), Cl=CaClOH (ICDD PDF=36-0983), Cl_2=$CaCl_2{\cdot}2H_2O$ (ICDD PDF=70-0385), H=NaCl (ICDD PDF=05-0628), K=KCl (ICDD PDF=75-0296), A=$CaSO_4$ (ICDD PDF=86-2270), L=CaO (ICDD PDF=82-1690), Cl_{cal}=$KCaCl_3$ (ICDD PDF=21-1170)

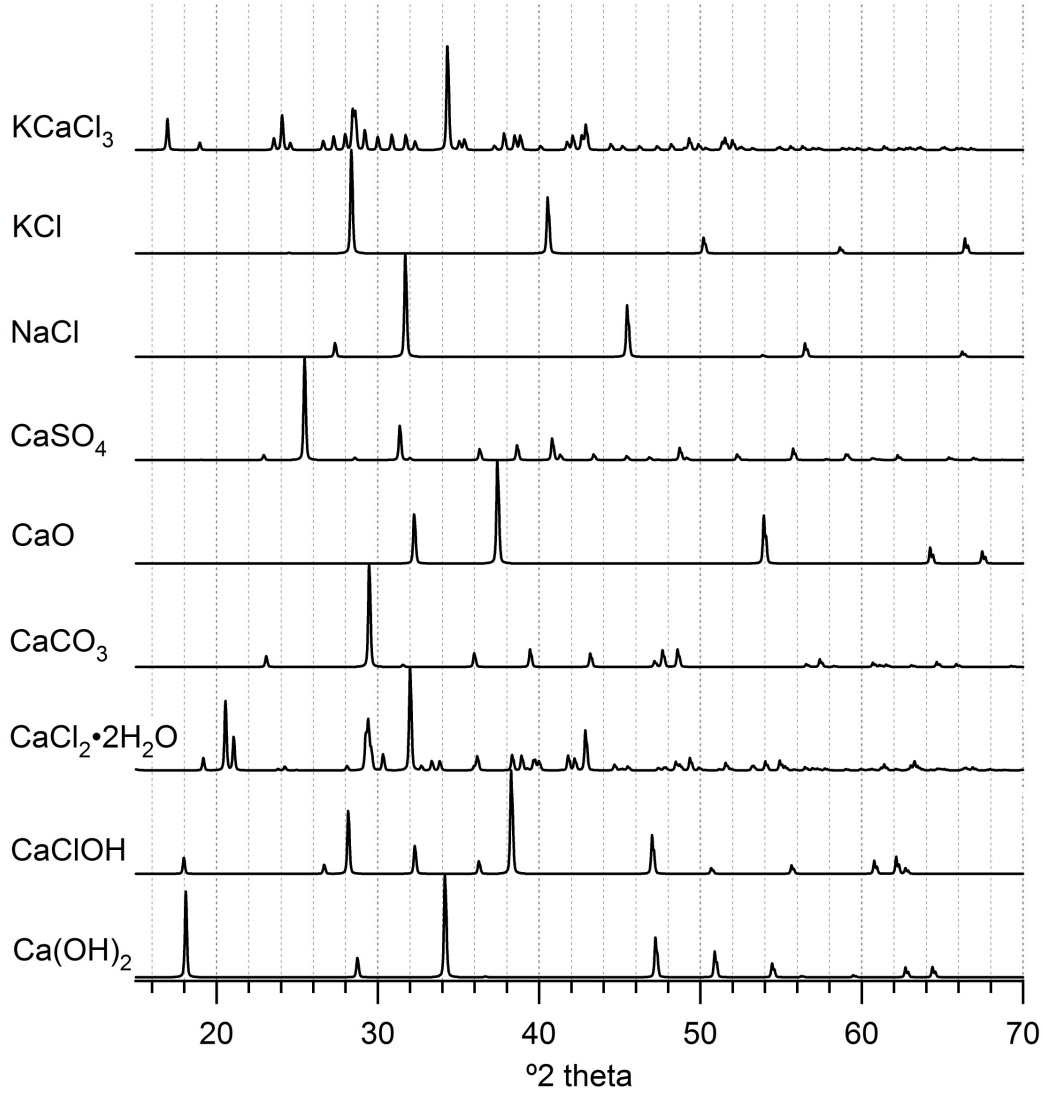

Figure 4.5 Reference patterns for phases identified in as-received APC residues (Figure 4.4)

	A1	A2	A3*	A4	A5
$Ca(OH)_2$	39	40	4	9	12
$CaCO_3$	9	13	47	14	7
CaClOH	41	14	6	28	37
$CaCl_2{\cdot}2H_2O$					10
NaCl	11	6	21	13	19
KCl		5	5	15	
$CaSO_4$		17	16	22	14
CaO		5			

Table 4.3 Semi-quantitative analysis of XRD patterns using normalised RIR. *No RIR was available for $KCaCl_3$ therefore results are given without accounting for this compound.

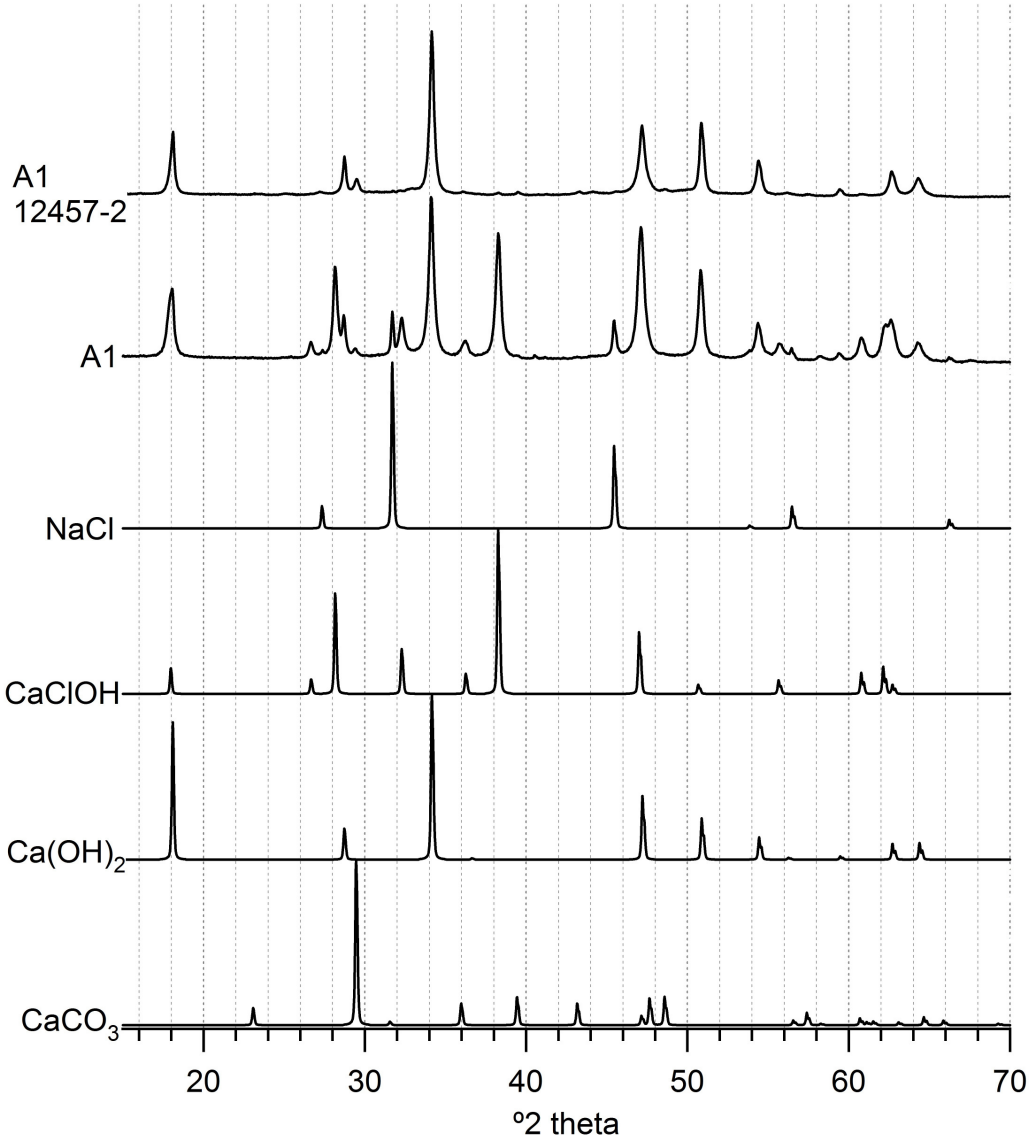

Figure 4.6 XRD patterns (y axis range not normalised) for residue A1 before and after leaching according to BS EN 12457-2 and vacuum drying

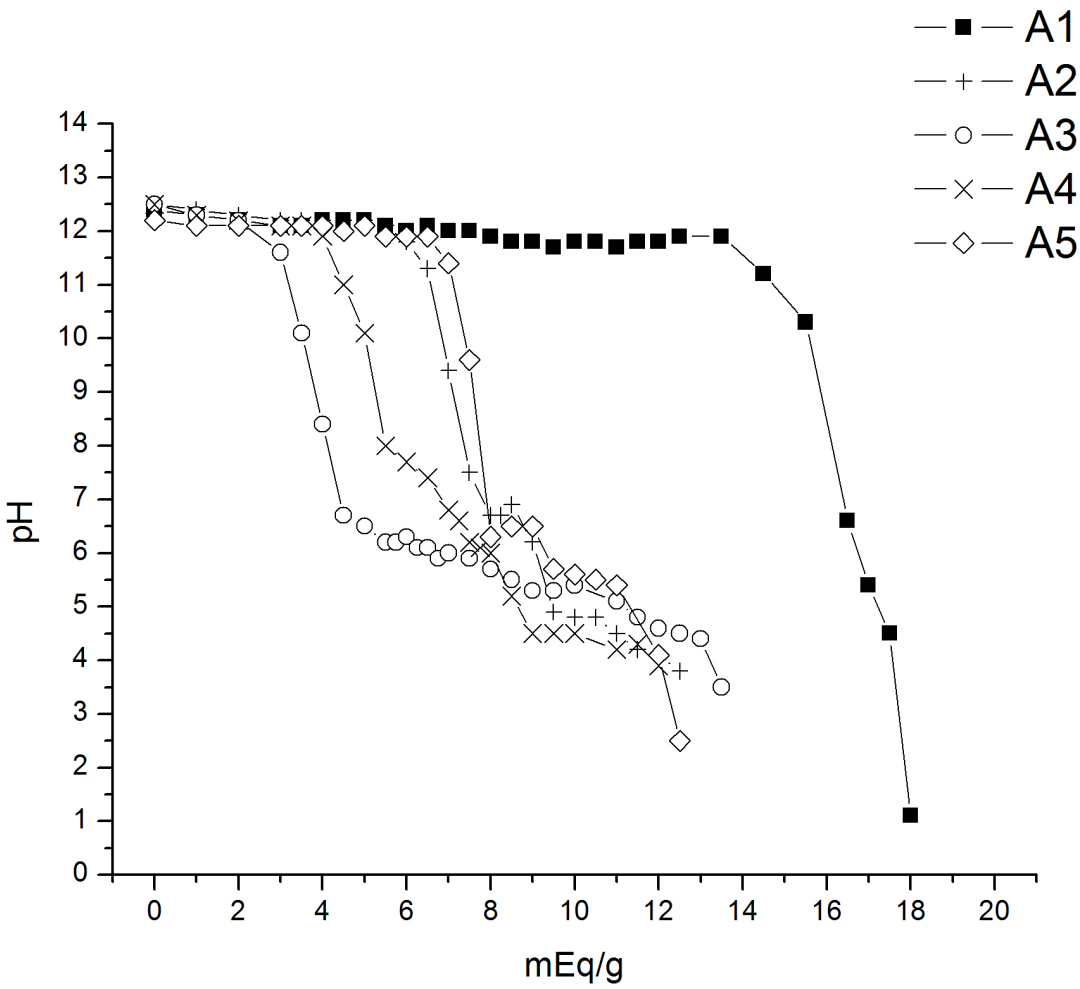

Figure 4.7 ANC titration curves for as-received APC residues

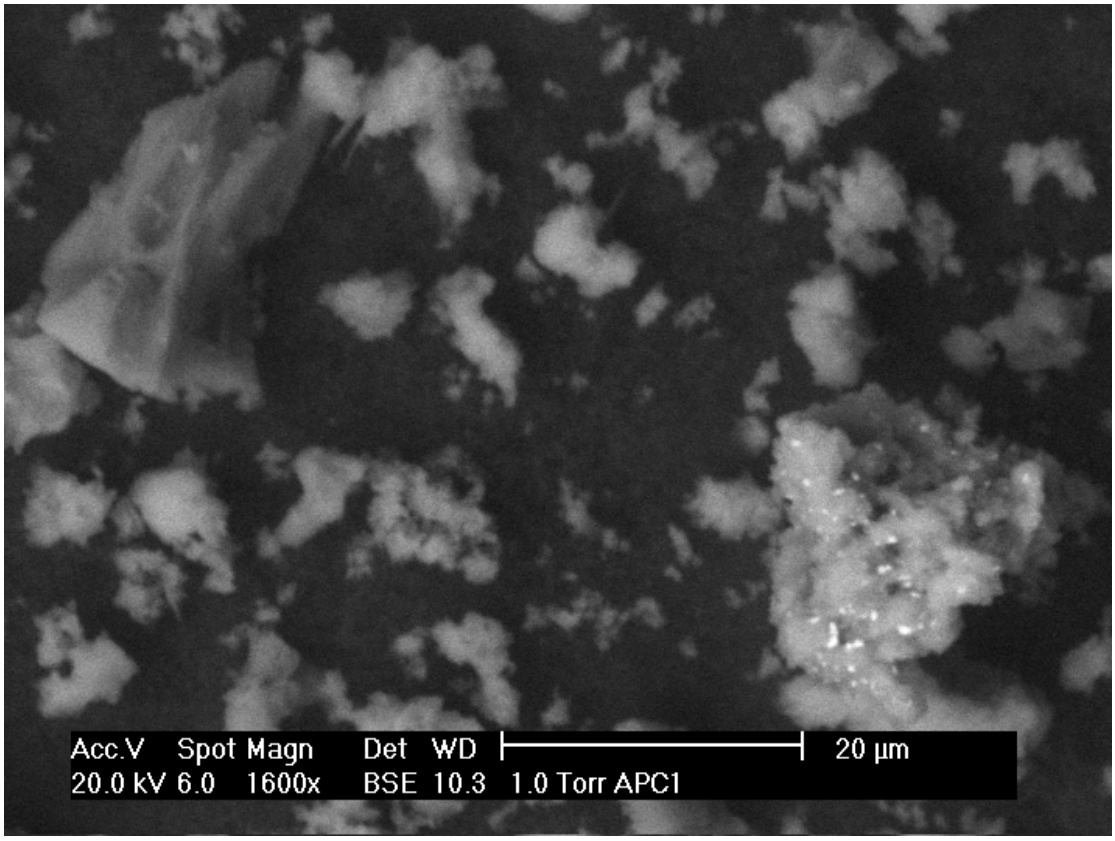

(a)

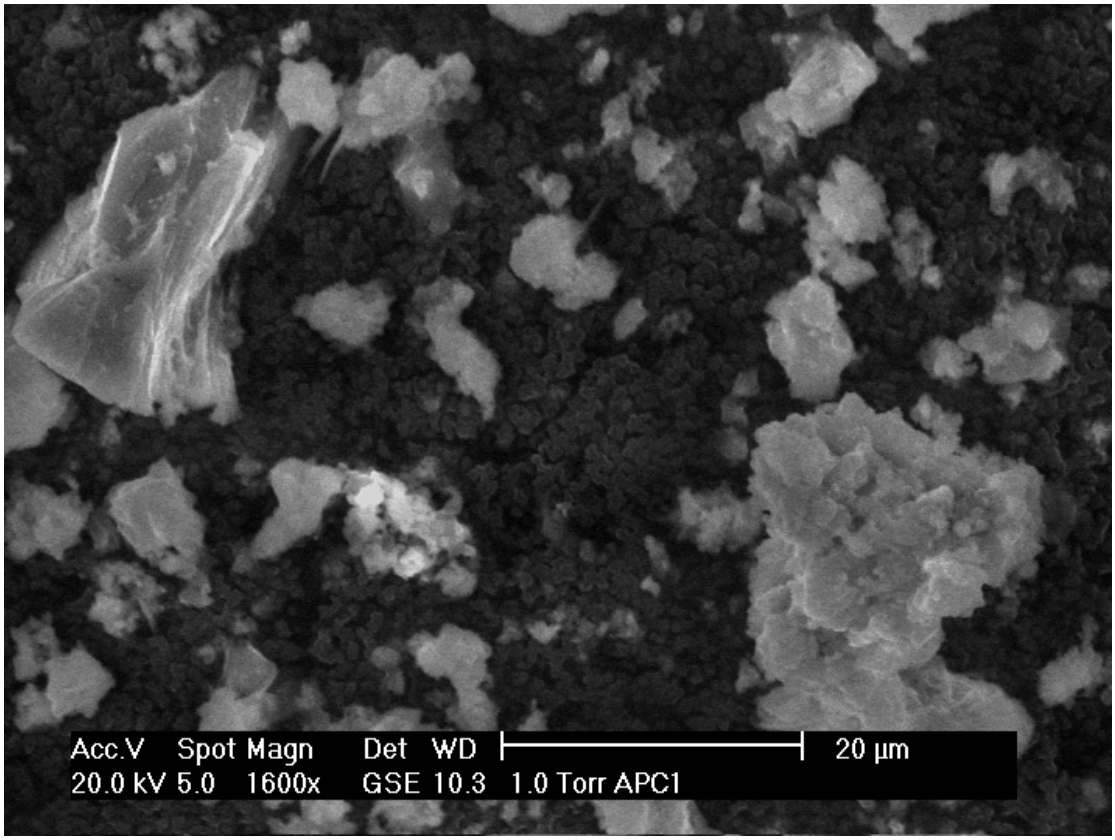

(b)

Figure 4.8 ESEM images of A1 including BSE(a) and GSE (b)

4.1.1 Discussion of as received APC residue characterisation results

The composition and leach behaviour of the residues studied here were consistent with those reported in the literature. As previously observed [24, 25, 51, 59, 74, 75] endothermic reactions and corresponding weight losses due to thermal decomposition of the scrubber related compounds $Ca(OH)_2$ (peak~400-450℃), CaClOH (peak~490-550℃), and $CaCO_3$ (peak~650-750℃) occurred during STA (Figure 4.1 and Figure 4.2). XRD analysis of the residues (Figure 4.4) confirmed the presence of the compounds identified by STA. In addition XRD analysis showed the APC residues to consist of other crystalline compounds which were not detected by STA and have been identified in previous literature [24, 59, 62, 66, 67, 73-79, 120] including alkali metal chlorides associated with the fly ash [61, 76], along with $CaSO_4$, $KCaCl_3$ and CaO. All of the residues had a noticeable amorphous content, evidenced by the baselines of the XRD patterns. This amorphous content was not quantified and therefore the semi-quantitative results presented in Table 4.3 were only suitable for comparison of the ratio of compounds. These ratios often showed discrepancies with those observed by STA (Table 4.1). This may have been a result of poor crystallinity of some of the compounds. It has previously been suggested that the amorphous Ca phases in APC residue may be similar to the crystalline [24].

Thermal decomposition of $Ca(OH)_2$, CaClOH and $CaCO_3$ resulted in volatisation of H_2O and CO_2 as shown by the mass spectrometry (Figure 4.3). No volatisation of HCl was observed (mass 36 or 38), confirming the decomposition of the CaClOH phase occurred according to equation 4.0 rather than equation 4.1 as proposed previously [51]. This has implications for the quantification of the mass loss observed by TGA. Mass spectrometry of gasses evolved during thermal analysis in an inert (argon) atmosphere was also reported by Bodenan and Deniard [24] showing similar results.

Equation 4.0. $2CaClOH \rightarrow CaCl_2 + CaO + H_2O$

Equation 4.1. $CaClOH \rightarrow CaO + HCl$

More than one DTA peak may appear within the range associated with CaClOH decomposition [24, 59]. This was most prominent in the plot for A3 (Figure 4.1) which showed peaks with maxima at ~500℃ and ~540℃. No other candidates could be identified by XRD analysis (Figure 4.4) which would decompose to produce this peak. Both peaks were attributed to CaClOH by Bodenan and Deniard [24]. Occurrence of a double peak may perhaps occur if particle size is not homogeneous. However, pestle and mortar grinding performed in the present study should have prevented this. A double peak may also occur if there is variation in the crystallinity/crystal unit cell dimensions [382]. Such variations would also explain the discrepancy between the ratios of compounds observed by STA and XRD. Alternatively, since the peak 540℃ appeared to occur after the weight loss recorded by TGA (Figure 4.2), it may be associated with a melting event. Melting temperatures of salts may be unpredictable in such a complex system. The melting of $CaCl_2$ for example, normally occurs ~772℃. However, an equimolar mixture of $CaCl_2$ and NaCl will melt at~550℃ [59]. No $CaCl_2$ was evident in the XRD patterns for the as received residues but $CaCl_2$ would be produced during the analysis due to the decomposition of CaClOH according to equation 4.0. The presence of $KCaCl_3$ in A3 would seem to coincide with the appearance of this endothermic event suggesting this compound may be involved in the melt. However, except for A5 the residues remained friable after analysis. If they had melted it is believed this would not be the case but instead the residues would be expected to cool as a solid mass, as was the case with residue A5. This observation would appear to therefore support the variation in crystallinity/crystal dimensions explanation of the double peak.

A5 showed evidence of two distinct endothermic peaks below 200℃ (Figure 4.1), the first of which can be attributed to the loss of free water and water subject to low, attractive surface forces in the sample. This is water which would be lost upon drying at 105℃ [203]. The second peak, occurring between 100-150℃ has occasionally been observed by other authors [24, 59]. Such a peak may be attributable to dehydration of $CaSO_4 \cdot 2H_2O$ or $CaCl_2 \cdot 2H_2O$ [25, 59]. Other authors have placed both peaks in the bracket of partially bound water [24]. Based on XRD analysis of the residues (Figure

4.4) and the water soluble Cl and SO_4 content of A5 (Table 4.1), the peak is considered primarily attributable to $CaCl_2{\cdot}2H_2O$. This compound occurs when the scrubber/HCl ratio is low as in equation 4.2 [25] and as such is not commonly found alongside excess $Ca(OH)_2$ [61]. Coupled with the very high soluble Cl content present in A5, the presence of $CaCl_2{\cdot}2H_2O$ suggested recirculation of the scrubber. Geysen *et al* [59] observed this compound alongside CaClOH in residue collected from a wet scrubber system in which the scrubber effluent is recycled to cool the gas stream, evaporating the water and leaving the salts on the bag filters. Such a process would reduce the scrubber/HCl ratio. The reasons for the simultaneous presence of $Ca(OH)_2$, CaClOH and $CaCl_2{\cdot}2H_2O$ in A5 are unclear, but perhaps is the result of blending residues collected at different times. The $CaCl_2{\cdot}2H_2O$ phase would not be expected to persist, reacting with the excess portlandite as equation 4.3 [25].

Equation 4.2 $Ca(OH)_2 + 2HCl \rightarrow CaCl_2{\cdot}2H_2O$

Equation 4.3 $Ca(OH)_2 + CaCl_2{\cdot}2H_2O \rightarrow 2CaClOH{\cdot}2H_2O$

Pure $CaCl_2{\cdot}2H_2O$ also shows an endothermic peak without a corresponding weight loss at ~780°C due to melting of $CaCl_2$ [59]. As previously mentioned the melting temperature may be altered in such a complex system. A5 showed a very diffuse endothermic peak ranging from ~560-900°C (Figure 4.1) which may well have encapsulated the endotherm associated with melting as well as volatisation of the Cl and SO_4 salts [19] and that associated with $CaCO_3$ decomposition. The endothermic event was perhaps so broad due to the overlapping temperature range of all of these events. Despite the large mass loss evident by TGA between ~650-900°C for residue A5, peaks observed by XRD corresponding to $CaCO_3$ were of a low intensity (Table 4.3). This perhaps indicated the significant mass loss was a result of volatisation of other compounds such as the Cl. A5 contained a much greater Cl content relative to the other residues, as shown by the release during BS EN 12457-2 (Table 4.1). As a result, the $CaCO_3$ content of A5 could not be quantified by TGA because it could not be distinguished from the mass loss associated with the volatisation of other compounds (Figure 4.2).

Despite showing a relatively large weight loss (2.4%) across the range corresponding to $Ca(OH)_2$ and CaClOH decomposition by TGA (Figure 4.2), residue A4 showed very little DTA response (Figure 4.1). Weight loss from A5 for example was 1.6% and this residue showed a much more significant DTA response. This discrepancy in the behaviour of A4 resulted in what is believed to be an overestimation of the CaClOH content. This belief is based on the Cl release observed during BS EN 12457-2 (Table 4.1) and the quantity of NaCl and KCl observed in this residue according to XRD analysis (Table 4.3). If all of the 112,600mg/kg Cl release from A4 occurred from CaClOH, NaCl and KCl, according to the ratios observed by XRD the CaClOH content would be ~12.2%w/w_{dry}. Any soluble Cl contributed from other compounds would reduce this percentage. Potentially the DTA response was affected by an alternate influence. Particle size may affect DTA response [144] although treatment of the samples with a pestle and mortar should have prevented this. A4 showed several overlapping peaks on the DTA trace in the temperature range ~360-525℃ which may have been a result of varying crystallinity/crystal size of the compounds and affected the DTA response. Such variation would also affect the semi-quantitative interpretation of the XRD patterns by the RIR methods. Back calculation assuming 12.2% CaClOH indicated 5% $Ca(OH)_2$ but such values can only be considered very approximate.

In pure systems the $Ca(OH)_2$ content may be predicted according to pH buffering above pH~12. However, the buffering observed (Figure 4.7) appeared to indicate a greater $Ca(OH)_2$ content than was observed by STA analysis, particularly for residue A5. This suggests additional alkaline buffers were present in the APC residues, such as CaClOH. The extent of the plateaus at pH~12 were however loosely correlated with the observed $Ca(OH)_2$ content of the residues, suggesting this to be the primary buffer at high pH and residue A4 to contain slightly more $Ca(OH)_2$ than residue A3.

Consistent with other work [69, 82, 104], along with the plateau at pH~12 the ANC titration showed buffering at pH~4.5-7. The extent of the plateaus at pH~4.5-7 increased with greater $CaCO_3$ concentration, consistent with the

behaviour of APC residue before and after treatment by accelerated carbonation [74, 82]. ANC to pH 4.5 of 8-16mEq/g has been reported for several APC residues [20, 59, 69, 82, 83] in agreement with the capacity observed for the MSW residues analysed here. Alkalinity of the clinical waste residue was considerably higher as a result of the significantly greater $Ca(OH)_2$ concentration observed by thermal analysis (Table 4.1). Generally higher levels of PVC in clinical waste than MSW are expected (~4.4%w/w compared to ~0.7%w/w respectively) [61]. Chlorine released from PVC and organic compounds during incineration tends to enter the gas phase as HCl [61]. Clinical incinerator flue gases are therefore expected to consist of higher HCl concentration and as such greater quantities of scrubber may be used. Additionally, to ensure emissions limits were complied with, the scrubber in the incinerator from which A1 was derived was not recirculated. The resultant excess $Ca(OH)_2$ has implications not only for the ANC of the residue but also for its potential treatment in pozzolanic systems. Such excess reduces or even removes the need for lime addition as a reagent. Although Bacciochi *et al* [74] also observed a large excess of $Ca(OH)_2$ in an APC residue collected from a hospital waste incinerator, high excess of $Ca(OH)_2$ does not appear to be necessarily associated with clinical or hospital waste incineration. Little excess $Ca(OH)_2$ has been observed in hospital waste APC residues studied previously [24, 37] and occasionally considerable excess is observed in MSW APC residues [24, 104].

All of the residues would be classed as corrosive due to the high pH resulting from BS EN 12457-2 Table 4.1 [84] and the alkalinity (Table 4.1). The pH of the leachate produced could be primarily attributed to $Ca(OH)_2$ content (Figure 4.1 and Figure 4.4), and is consistent with previous work [20, 51, 67, 76]. The pH in such leachates would however be a very complicated result of the concentration, and interactions between all of the ions solubilised from the crystalline compounds and the amorphous phase [20, 76]. As such, variations from that expected based on $Ca(OH)_2$ concentration may occur [76]. Lower pH was observed for A5 than the other residues for example, despite the higher $Ca(OH)_2$ content than A3 or A4. This was perhaps a result of the greater concentration of Cl ions in the leachate interacting with the

alkali and alkali earth metals which would form bases. The complexity of the systems is highlighted by the greater buffering at pH~12 (Figure 4.7) despite the lower natural pH (12.2) of A5 determined according to BS EN 12457-2 (Table 4.1). Variation in pH during BS EN 12457-2 was very low, as reported previously [51, 67, 76]. Standard deviation of all pH values observed in this study and the referenced literature was just 0.2 pH units with a mean of 12.5 and all values fell within the 11.6-12.8 range reported in [67]. The pH would therefore appear to be reasonably predictable and the influence on leaching would be fairly consistent.

Consistent with previous work [51, 62, 67, 76] the residues contained a large soluble fraction, observed as TDS during BS EN 12457-2. A considerable proportion was due to the soluble Cl and SO_4 salts (Table 4.1) identified by STA and XRD (Figure 4.1 and Figure 4.4). The dissolution of CaClOH and NaCl during BS EN 12457-2 was confirmed by XRD analysis of A1 following leaching and vacuum drying (Figure 4.6) and [66]. Following leaching, residue A1 appeared as slighlty carbonated $Ca(OH)_2$ when analysed by XRD. The removal of CaClOH caused a loss of intensity in the peak at ~47°2Θ which in the as-received residue comprised of the (012) $Ca(OH)_2$ reflection and the (110) CaClOH reflection. In the leached residue this peak appeared to be broad relative to other $Ca(OH)_2$ peaks (Figure 4.6). Broadening of peaks may result from a reduction in the crystal size because the angles at which the reflections from consecutive planes are perfectly out of phase occurs at greater deviation from the ideal Bragg conditions in smaller crystals. This is demonstrated by equation 4.4 [333].

Equation 4.4 $\delta\Theta = \lambda / 2t \cos\Theta$

In which $\delta\Theta$= the deviation from the ideal Bragg angle,
λ= the X-ray wavelength,
Θ= the Bragg angle,
t= the thickness of the crystal= md in which d=the inter plane distance of the lattice and m= the number of lattice planes.

It is evident from Figure 4.6 that the (012) $Ca(OH)_2$ reflection has broadened to a greater extent than other peaks. This would suggest the $Ca(OH)_2$ crystal dimensions normal to the (012) plane to be smaller than along other axis and therefore suggets crystal anisotropy. Broadening of XRD reflections may also result from instrumental factors and microstrain as well as solid solution states which effectively result in a number of reflections across a small range of angles. The latter factor is unlikley in the sample analysed here and crystal anisotropy is considered to be the most probable explanation for the anisotropic peak broadening. Crystal sizes were not calculated however since the instrumental broadening was not determined.

The residues showed a considerable variation in TDS, Cl and SO_4 release during BS EN 12457-2, with a range of 128,300mg/kg for Cl release and a standard deviation of 51,805mg/kg. The Cl release from A5 was significantly greater than the mean value for the five wastes, suggesting the chloride content of this residue was unusually high. Such behaviour was consistent with the observation of $CaCl_2{\cdot}2H_2O$ as well as CaClOH and would support the idea that this residue had been recirculated. Results presented throughout the literature obtained with similar test procedures also showed significant variability [51, 67, 75, 76, 82] ranging from 96,300mg/kg [51] to 237,690mg/kg [82]. Despite the expected higher HCl concentration in the flue gases expected from clinical waste the Cl release from residue A1 was very close to the mean observed for residues examined here and throughout the literature because CaClOH was not the only contributor to water soluble Cl and XRD analysis of A1 showed less evidence of the alkali chlorides associated with the fly ash.

Residues examined in this study showed a range for SO_4 release of 8800mg/kg with a standard deviation of 3810mg/kg. Results presented throughout the literature [51, 67, 82] ranged from 7000mg/kg [67] 20,490mg/kg [51]. SO_4 release from A1 was considerably below the mean result observed for the residues studied here and lower than the range observed in the literature. Lower SO_4 release may be a result of slight waste composition differences between MSW and clinical waste, or simply a

reflection of the inherent variability of the residues. A5 also showed low SO_4 release during BS EN 12457-2 for example. An absence of crystalline sulphates was also observed in hospital waste residues studied by Bodenan and Deniard [24], but $CaSO_4$ was present in the residue studied by Kougemitrou *et al* [37].

Such significant variability in the residue quality has implications when trying to design a suitable treatment process. It suggests modifications to the treatment may be required in order to handle a specific residue. This could increase associated costs and difficulty due to the assessment and alterations required.

The storage conditions of the samples between production and arrival at the university also had a significant impact on the mineralogy. Although CO_2 may be present in the gas stream at concentrations up to ~10% volume [24], greater $CaCO_3$ concentration in several of the residues (in particular A3) was attributed primarily to carbonation of the excess $CaO/Ca(OH)_2$ during storage and transport. A consequence of the formation of $CaCO_3$ and corresponding reduction in $Ca(OH)_2$ and CaO concentration of the residue is an implied reduction in the reactivity of the residue in pozzolanic systems. Unless additional $Ca(OH)_2$ was to be added to the system, it would be crucial to treat the residues before carbonation if pozzolanic reactivity was the primary mechanism of s/s. $KCaCl_3$ was also present in residue A3 (Figure 4.4) which has previously been observed as a carbonation product [128]. $KCaCl_3$ is perhaps a result of carbonation of CaClOH in the presence of KCl. Despite showing a significant DTA peak in the range associated with CaClOH (Figure 4.1) and corresponding weight loss (Figure 4.2), very little CaClOH was apparent by XRD (Figure 4.4). Carbonation may have continued during XRD sample preparation and analysis. The degree of carbonation witnessed did not significantly affect the initial pH, i.e when exposed to de-ionised water (Table 4.1). Carbonation was reflected in the acid neutralisation behaviour, causing a shift in the pH buffering plateau (Figure 4.7). This would significantly alter the leaching behaviour due to pH variations if exposed to acidic solutions.

The majority of the work here reported was performed on residue A1 since it was available from the start of the project whilst other residues were later acquired. A1 was therefore subject to additional examination. Elemental composition of A1 was determined by acid digestion and ICP OES analysis at an industrial laboratory. Full WAC analysis was also performed according to BS EN 12457-2. Some difference in the trace elements present A1 would be expected owing to the fact that this residue resulted from clinical waste incineration. Clinical waste is defined as:

"(i) any waste which consists wholly or partly of human or animal tissue, blood or other body fluids, excretions, drugs or other pharmaceutical products, swabs or dressings, or syringes, needles or other sharp instruments, being waste which unless rendered safe may prove hazardous to any person coming into contact with it; and

(ii) any other waste arising from medical, nursing, dental, veterinary, pharmaceutical or similar practice, investigation, treatment, care, teaching or research, or the collection of blood for transfusion, being waste which may cause infection to any person coming into contact with it" [383].

In practice much of the waste composition is composed of plastics, paper and cardboard resulting from packaging and disposable equipment used in medical practices and laboratories. Idris *et al* [39] suggested 80% of hospital wastes to be comparable to domestic solid waste. Only a small proportion of hospital wastes may actually pose a risk of infection but large amounts of more general refuse items are disposed in the same way [384, 385]. Delay *et al* [71] reported clinical waste composition as approximately 35% plastic, 23% paper, 8% food, 5% metals, 4% glass and 2% cardboard amongst other fractions. The composition of municipal waste has been reported as approximately 10% plastic, 23% paper/cardboard, 18% food, 4% metal, 6% glass [386]. Key differences appear to be greater plastic content in clinical waste and greater food content in municipal waste. A fraction of the MSW would be recycled or sorted for other purposes such as composting. It is difficult to obtain data on the composition of waste incinerated. Recycling and

sorting of clinical waste would be less prominent due to perceived risks of infection when handling the waste.

Table 4.2 shows that, consistent with previous literature [63, 67, 76, 79, 86-88, 90], in addition to the soluble phases identified by STA and XRD, other metals and oxyanions present in A1 were water soluble during BS EN 12457-2. Untreated A1 would exceed SNR WAC for Hg, Pb, Se, Cl and TDS (highlighted in Table 4.2) and hazardous WAC for Hg, Pb, Cl and TDS. Pb release from APC residues has frequently been reported as problematic [51, 59, 67, 73, 75, 76, 81, 82, 88]. This is a result of the Pb concentration in the residues along with the high pH (Table 4.1) which allows dissolution of Pb as $Pb(OH)_3$ or $Pb(OH)_4$ [69, 76] and possibly the presence of soluble lead chlorides in APC residues [73, 82, 88, 387]. Similar to Pb, Zn shows amphoteric behaviour [112, 157] but leaching from APC residues is rarely observed above hazardous WAC thresholds despite its relatively high availability [63, 88]. Several other elements were present in high enough concentrations in the residue to exceed WAC but are sparingly soluble due to the alkaline conditions of the leach test and their speciation [69, 387].

Although Pb, Zn and Cd are associated with PVC [61, 71], a greater concentration of which is expected in clinical waste [61], the concentrations of Pb, Zn and Cd observed in the residues was low in comparison to the ranges presented in previous literature [20, 67]. This was perhaps an effect of the greater scrubber injection, and lack of recirculation, which could in effect dilute the metal concentration in the residues. It has however previously been reported that emissions of Pb, Cd, As and Cr are lower from medical waste (which comprises a large fraction of clinical waste) than MSW [388].

Hg release from APC residues has been observed to exceed relevant regulatory limits [77], but is often not observed to be problematic from MSW APC residues [73, 86]. Certain dental wastes (dental amalgam [383]) can be significant sources of Hg. However, the incineration of such waste is discouraged [383]. Se release from APC residues is very rarely reported. The

availability of Hg and Se observed in A1 both fell within the limits presented previously for MSW APC residue [20, 67]. The leachable Se at l/s=10 was within the limits presented by Lampris *et al* [67] although 2.3mg/kg Hg release was greater than the 0.5mg/kg upper limit. Hg and Se availability in the hospital wastes studied by Kougemtirou *et al*, [37] were not as significant as those present in A1 (0.32mg/kg and 2mg/kg respectively) and also fell within the limits suggested for MSW residues [20, 67]. Although some difference in the concentration of trace elements in APC residues resulting from clinical and MSW EfW incineration would be expected, clear trends are difficult to identify throughout the literature and there appears to be significant overlap between the composition of both types of residue. Certainly the crystalline phases identified in clinical waste, hospital waste and MSW residues analysed here and throughout the literature (e.g. [24, 37]) appear similar.

SEM images presented in Figure 4.8 of A1 showed various size agglomerations of crystals resulting in very high surface area particles which results in increased rate of solubilisation [20] and contributes to the high water demand observed when including APC residues in s/s systems [67, 166, 241]. Such observations are consistent with those reported in previous work [51, 66, 67, 74, 77, 81] although slightly larger spherical agglomerations have also been observed [66, 67]. Carbon deposits could also be seen (top left corner of Figure 4.8). Unusually the agglomeration in Figure 4.8 showed evidence of bright specks, indicating a high average atomic number and therefore discreet heavy metal particles when viewing BSE (Figure 4.8 (a)). EDX analysis of this agglomeration showed trace evidence of Pb, Zn as well as Cu.

4.1.2 Conclusions for as received APC residue characterisation

- APC residues examined here showed similar elemental, mineralogical and morphological composition to those which had been studied elsewhere in the literature.
- All APC residues had a significant water soluble chloride content, and a lower soluble sulphate content. The variability in this content was considerable, residues tested in the current study showed a range for Cl of 128,300mg/kg and standard deviation of 51,805mg/kg, and a range for SO_4 of 8800mg/kg and standard deviation of 3810mg/kg.
- This variability in the leachable anion concentration would have significant implications for treatments applied to different residues. Requiring modification to the treatment depending on the residue composition.
- The crystalline compounds identified in APC residues resulting from the incineration of clinical waste are largely the same as those identified from MSW residues although some difference in the relative concentrations may occur.
- Due to a generally higher PVC content in clinical waste, clinical waste incinerators may use a greater concentration of, and not recirculate, the scrubber. This resulted in a higher $Ca(OH)_2$ and CaClOH concentration in the APC residue which resulted in a much more alkaline residue. This excess scrubber would also be beneficial for treating the waste in a pozzolanic s/s matrix, precluding the need for additional $Ca(OH)_2$.
- Some difference in the concentration of trace elements in clinical waste and MSW APC residues would be expected. However, since the concentration of trace elements in the wastes is inherently so variable, and there is significant overlap between the composition of residues resulting from clinical and MSW incineration, it is difficult to identify clear trends. A more comprehensive study would be required, preferably also monitoring the composition of waste entering the furnace.

4.2 Characterisation of as received PFA

A PFA resulting from the co-firing in a power station with coal and biomass (palm kernel expeller) was studied in this work. Co-combustion of pulverised coal with biomass is performed due to environmental [389, 390] and economic advantages [391]. The economic advantages are complicated, depending on a number of variables however advantages may be found due to gaining ROCs, the lower price of biomass and energy crops than coal, and reduced costs associated with greenhouse gas emissions [391]. The source of the biomass is also a large factor in both the economic and environmental costs [390, 391]. However, it has been suggested that 'Importing waste / co-product biomass is unlikely to have significant negative environmental impacts. GHG (greenhouse gas) emissions associated with bulk transport by sea are low in relation to the GHG benefits from avoided fossil fuel combustion.' [390].

Co combustion affects the composition of the flue gases and the resultant PFA and therefore has implications for the possible uses for this material. End of waste criteria for PFA as a cement replacement material involves restrictions on the use of co-combustion PFA. ASTM C618 does not allow for co-combustion PFA in cement or concrete. EN 450 dictates coal must constitute a minimum of 80% dry weight of the combustion materials. Additional criteria set out in EN 450 for the use of PFA as a cement replacement material (for use in structural concrete according to BS EN 206 and 8500) includes but is not limited to

- LOI< 7% mass
- SO_3< 3% mass
- Fineness (45µm sieve retention) < 45% mass
- Water requirement-95% of cement alone
- $SiO2+Al_2O_3+Fe_2O_3$>70% mass

Table 4.4 includes the elemental composition of the co-fired PFA utilised in the present study (as oxides) as determined by XRF analysis after pressing

into a pellet with a cellulose binder. The PFA did not meet the standards set out in BS EN 450 for use in construction applications, exceeding the limits for SO_3 equivalent and loss on ignition (LOI).

Element	Ca	Si	Al	Fe	Na	K	Mg	Zn	S	LOI
%weight	4.3	51.5	19.3	5.5	1.1	2.3	1.7	0.3	9.4	10.4

Table 4.4 Elemental composition (as oxides) of co-fired PFA

The high LOI could be attributed to significant levels of unburnt carbon which were present in the PFA, identified as large vesicular particles [392, 393] by ESEM analysis (Figure 4.9). Such a high content of unburnt carbon has been shown to have several implications when utilising the fly ash in cementitious materials including increasing the water demand [394]. The role of organic matter in an s/s matrix is difficult to assess. High organic carbon content in s/s systems may be beneficial, offering sorption sites for certain contaminants [150, 250, 387]. However, degradation of organic matter can produce acids which may have deleterious influence on the matrix and the matrix pH [155] and there are WAC limits for dissolved organic carbon (granular SNR=800mg/kg, granular hazardous WAC limit=1000mg/kg). Additionally oxidation of organic matter may cause a reducing environment [169]. This has perceived benefits for mobility of oxyanion species such as Cr and Se [111]. Some studies on s/s of wastes using PFA which exceeded the LOI limits established in EN 450 [226, 250-252, 270, 395] have shown good reactivity, compressive strength development, porosity, hydraulic conductivity, and improved leaching behaviour for certain pollutants. Poon *et al* [251] examined s/s of a synthetic heavy metal sludge containing Pb, Zn, and Cu in a pozzolanic system using a high carbon, non-EN 450 PFA. The immobilisation potential was observed to be equal or superior to that obtained by a finer fly ash after 56 days' curing.

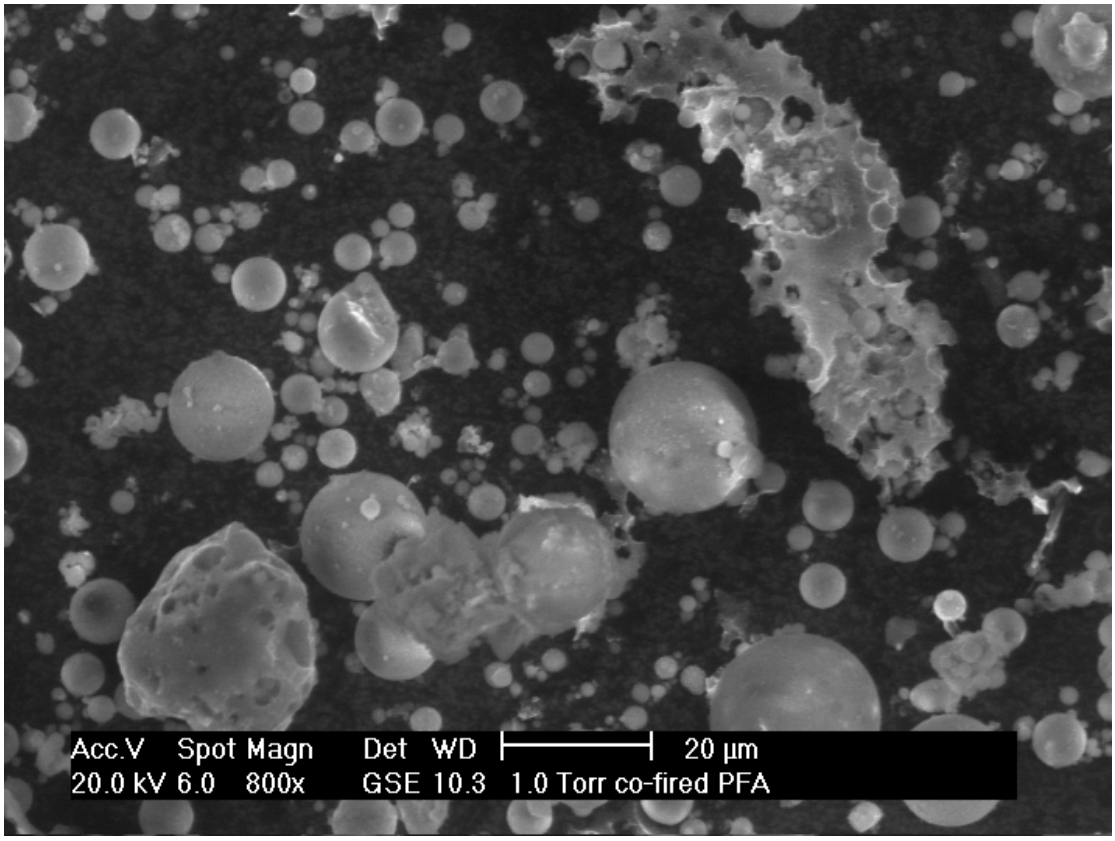

(a)

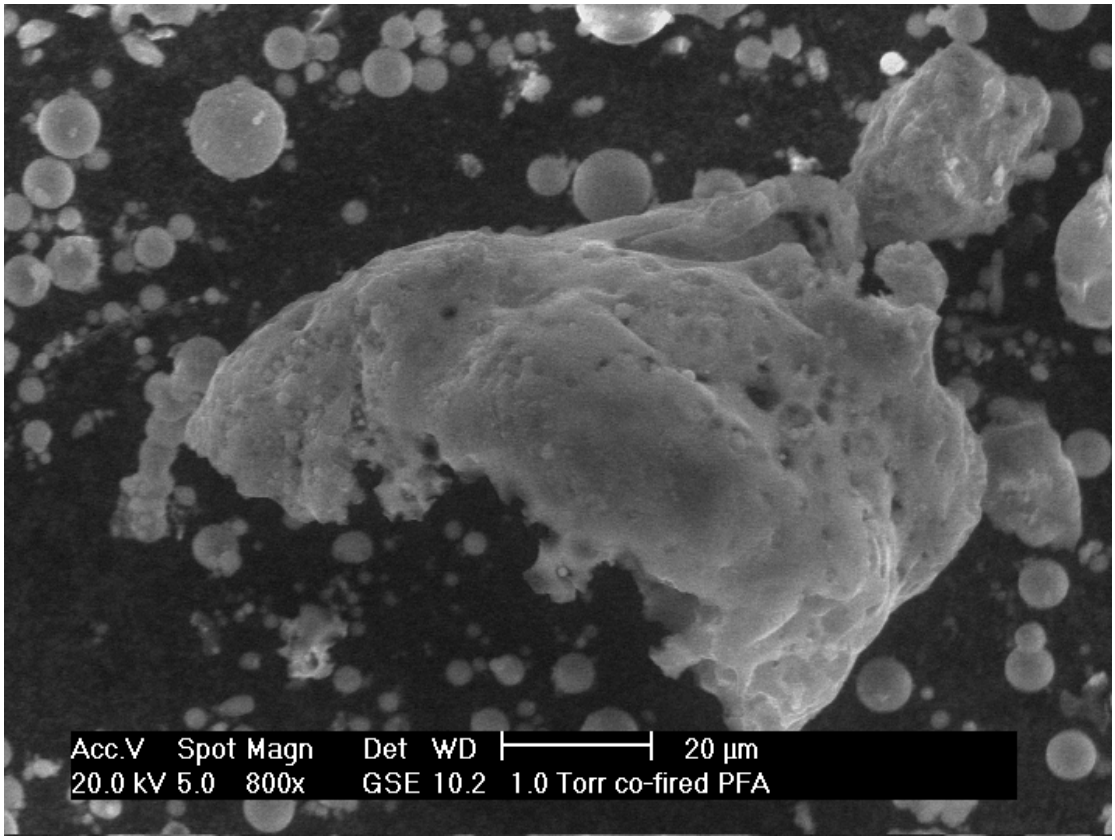

(b)

Figure 4.9 GSE ESEM images of co-fired PFA

High LOI and such particle morphology has been previously identified in co-fired PFAs [396, 397]. No correlation between biomass content as a weight of the combustion materials and LOI of the resultant PFA has been noticed however [398, 399]. Similarly no correlation between biomass content and SO_3 concentration in the resultant PFA is apparent [398, 399]. Despite the substantial sulphur content identified by XRF in the co-fired PFA, no evidence of sulphates was detected by XRD analysis (Figure 4.10) except for perhaps very weak evidence for trace amounts of K_2SO_4. This suggested the sulphur to be present in the amorphous fraction of the PFA. The high unburnt carbon content of this ash indicated incomplete combustion which may suggest the sulphur remained present as reduced or intermediate forms, possibly in the organic fraction [400]. Such speciation of sulphur meant that despite the relatively high content only 2800mg/kg sulphate was water soluble during BS EN 12457-2.

The elemental composition of the material (Table 4.4) showed high concentrations of Si, Al and Fe. SiO_2+Al_2O_3+Fe_2O_3 was greater than the 70% mass required by BS EN 450. Such composition is important from the perspective of utilising the PFA as a pozzolanic reactant or indeed to produce zeolites [266, 287]. The reactivity of the PFA is also dependant on the mineralogy however. Primarily the amorphous content is soluble in alkaline conditions and therefore involved in reactions [266, 287, 401]. The presence of a siliceous glass matrix in the PFA was confirmed by XRD analysis which showed a large amorphous hump with a maxima ~23-27°2θ (Figure 4.10) [337]. In addition crystalline compounds including quartz, mullite and iron oxide ($Fe_{21.34}O_{32}$ ICDD PDF- 83-0112) were present which are all typical of conventional coal combustion PFA [266, 287, 337, 394, 401]. Such mineralogy has been observed in co-combustion PFA containing different forms of biomass [396, 398, 399, 402]. As such the potential for significant strength development and mechanical performance across a range of properties has been demonstrated by substitution of cement with co-fired PFA [399, 402].

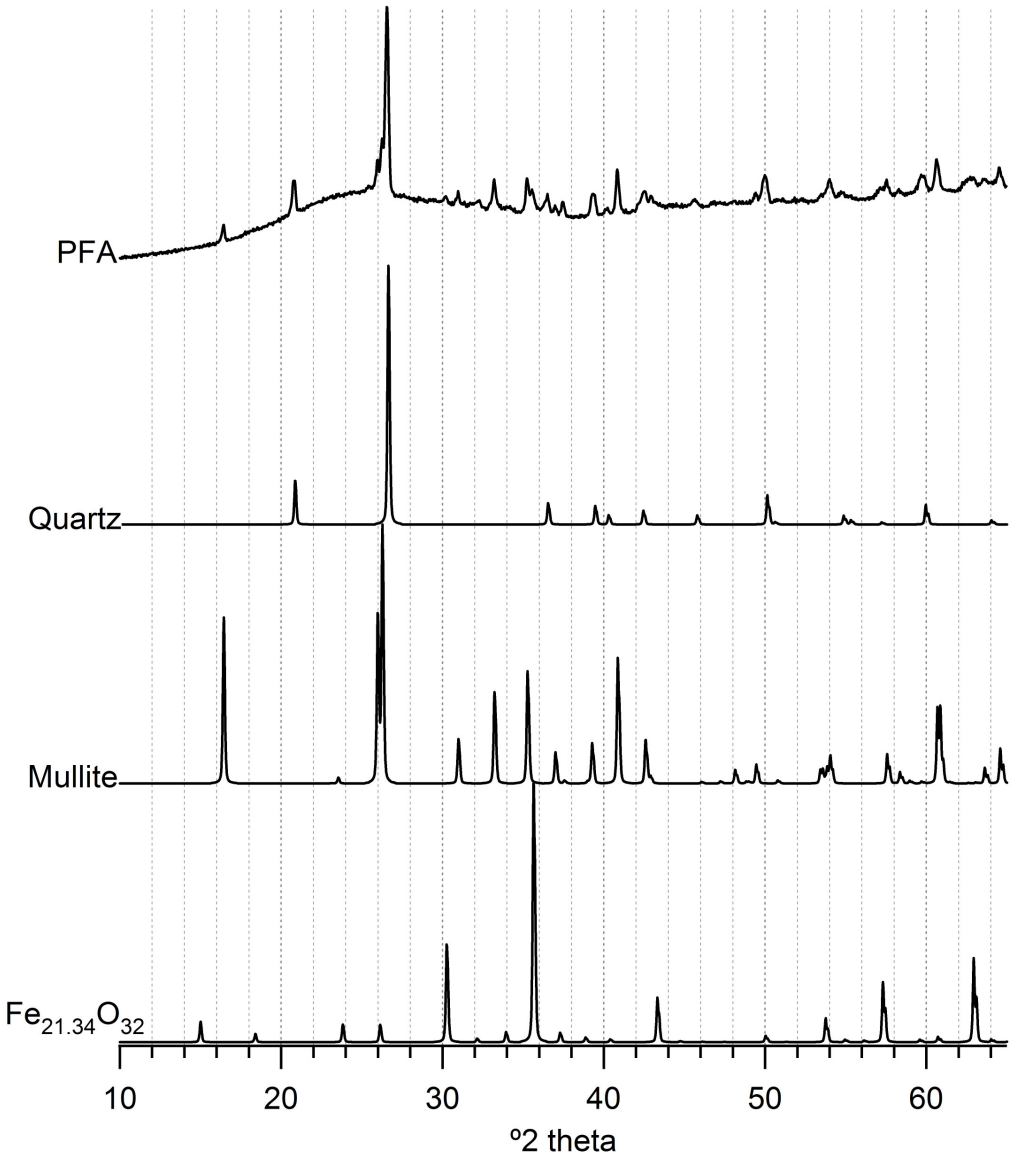

Figure 4.10 XRD pattern for as-received co-fired PFA and matched phases.

A large part of the co-fired PFA studied here was composed of spherical cenospheres and plerospheres (Figure 4.9) which are typical of conventional coal PFAs and are composed of the silicon and aluminium rich glass matrix which may contain mullite and quartz crystals, or may be iron rich [393, 394]. The spherical nature of the particles presents a low specific surface area which lowers water demand for a given workability [330]. The workability is also influenced by the size distribution of the spheres, a coarser particle size distribution resulting in a higher water demand [394]. A very large particle size distribution was evident from ESEM analysis (Figure 4.9). Spherical particles were observed from an undetermined minimum diameter up to

~20µm. In Figure 4.9 (b) it can be seen that some of the unburnt carbon particles greatly exceeded this limit across several dimensions. Particle size distribution of the PFA was determined using a Malvern mastersizer 2000, measuring laser diffraction. Results showed 45µm sieve retention would be 33.7% mass which was acceptable regarding the limits established by BE EN 450 however amongst the coarsest of a range of coal combustion fly ashes previously studied [394]. Such coarse particle size distribution not only affects the workability of blends produced, but also the reaction kinetics. Finer particle size distributions result in increased reaction rate and development of hydration products and therefore particle size distribution affects the rate of strength and microstructure development [394, 401].

4.3 Characterisation of Waste Caustic Solution

The waste caustic solution resulted from the cleaning of aluminium extrusion dyes. The solution was considered promising for use as an activator for pozzolanic systems due to the alkalinity and the soluble aluminium content which would be contained. Typically a small proportion of this highly alkaline cleaning residue is used to neutralise highly acidic waste waters which are generated from the anodising process [403]. However a significant amount remains. In Europe it was estimated that ~14,000m^3 of such waste was produced in 2001 [404]. Methods of valorising this waste stream have previously been studied. Tansens *et al* [405] suggested precipitation of the aluminium as aluminium hydroxide followed by washing to increase purity and enable sale of the material, coupled with recirculation of the remaining NaOH solution into the cleaning bath. Iglesia *et al* [404] examined the potential use of such waste for production of zeolites, concluding zeolites suitable for use in detergents could be synthesised when the waste was blended with silica sources. In order to reduce the impurities in the caustic solution, which included 0.6mg/g Mg, 0.3mg/g F, 0.1mg/g K and Fe as well as a range of other impurities in lower concentrations, the waste was centrifuged prior to use.

The waste caustic solution examined by Iglesia *et al* [404] contained 259,200mg/l $NaAlO_2$ (3.16M) and 129,000mg/l NaOH (3.23M). The waste studied by Tansens *et al* [405] contained 808,000mg/l Na and 199,000mg/l Al. Tansens *et al* [405] discuss the high viscocity of the effluent. This is in contrast to the solution which was utilised during the current project which appeared to have a very low viscosity, similar to water.

XRF analysis was performed on the waste caustic (WC) solution after evaporating the solution to dryness which showed TDS of 238,700mg/kg (267,800mg/l). Analysis of the dry material showed the presence of Na and Al. Along with trace contaminants including Si, S at concentrations <1200mg/l. Analysis of the WC solution by ion chromatography suggested 1831mg/l (1506mg/kg) SO_4 contamination, in close agreement with the 1626mg/kg suggested by XRF analysis after conversion of S to SO_4. A sodium concentration of 96,794mg/l would correspond to a NaOH concentration of 4.2M, however not all of the Na would be present as NaOH. A proportion would be present as $NaAlO_2$ [404] and it is highly likely Na_2CO_3 would also be present due to atmospheric exposure. If carbonation and trace impurities are not considered, and elemental concentrations determined by XRF are applied, assuming all the Al is initially present as $NaAlO_2$, and the remaining Na is present as NaOH, concentrations for $NaAlO_2$ and NaOH are 1.2M and 3M respectively.

pH	**Density (kg/l)**	**TDS (mg/l)**	**Na (mg/l)[a]**	**Al (mg/l)[a]**	**NaOH (M)[a]**	**$NaAlO_2$ (M)[a]**
13.6	1.216	267,800	96,794	32,224	3	1.2

Table 4.5 Characteristics of the WC solution. [a] calculated based on XRF analysis

Solution concentrations were checked by titration with HCl. If the solution had undergone partial carbonation, several reactions would occur during the titration as shown in equations 4.5-4.8. Such reactions would result in three distinct plateaus [406-408]. Quantification of the acid required to reach the first inflection point provides quantification of the NaOH [406-408], signalling completion of equation 4.5. The sodium aluminate and carbonate cannot be

quantified however because equations 4.6 and 4.8, and 4.7 and 4.9 occur in similar pH ranges [406, 407]. In order to quantify the aluminate and the carbonate several methods are possible. These may include precipitation of $Al(OH)_3$ according to equation 4.6 followed by complexation with KF [404, 406], or addition of $BaCl_2$, resulting in precipitation of $BaCO_3$ according to equation 4.10, which results in a distinguishable plateau from those associated with equations 4.6 and 4.7 [407]. The latter method was employed in this study, following the procedure described by Kowalski *et al* [407]. The titration was repeated with different volumes of solution in order to ensure accuracy. Dilution was undertaken prior to titration to reduce the ionic strength to within the range observed to give repeatable results [407], and also to allow submersion of the pH electrode without requiring very large volumes of HCl. Saturated $BaCl_2{\cdot}2H_2O$ solution was injected into the WC solution in high enough volumes to guarantee complete reaction of Na_2CO_3. Following injection of the $BaCl_2$, the solution turned slightly cloudy indicating precipitation. The titration curve obtained is presented in Figure 4.11.

Equation 4.5 $NaOH + HCl \rightarrow NaCl + H_2O$

Equation 4.6 $NaAlO_2 + HCl + H_2O \rightarrow Al(OH)_3 + NaCl$

Equation 4.7 $Al(OH)_3 + 3HCl \rightarrow AlCl_3 + 3H_2O$

Equation 4.8 $Na_2CO_3 + HCl \rightarrow NaCl + NaHCO_3$

Equation 4.9 $NaHCO_3 + HCl \rightarrow NaCl + CO_2 + H_2O$

Equation 4.10 $Na_2CO_3 + BaCl_2 \rightarrow 2NaCl + BaCO_3$

Despite the visible precipitation, no distinguishable plateau occurred which may indicate the low concentration of the Na_2CO_3 present in the solution. The precipitate observed may have been $BaSO_4$. The low concentration of Na_2CO_3 was also supported by the lack of gas evolution observed whilst titrating in the range of the third plateau (Figure 4.11) which would correspond to the reaction shown in equation 4.9 and produce CO_2. Quantification of the titration curve for NaOH and $NaAlO_2$ according to the first and second inflections evident from the derivative and equations 4.5 and 4.6 indicated concentrations of 4.4M NaOH and 0.78M $NaAlO_2$ i.e. 119,140mg/l Na and 21,060mg/l Al. There is clearly discrepancy between the

results observed by XRF and titration. However, it can be said that the solution contained 3-5M NaOH and ~1M $NaAlO_2$.

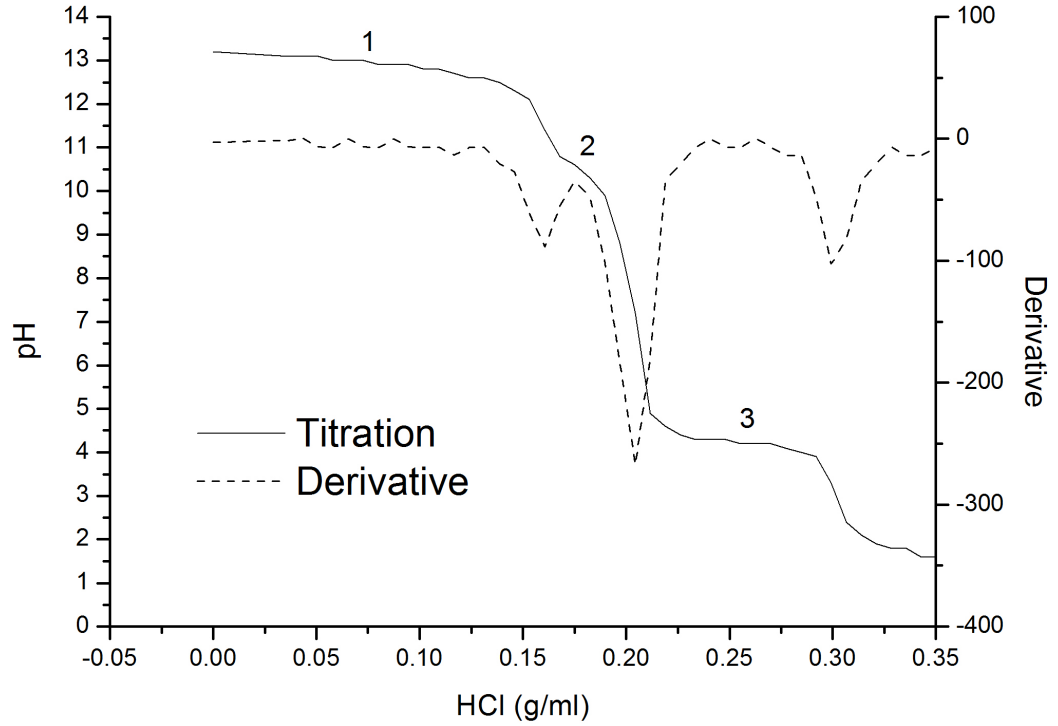

Figure 4.11 Titration and derivative of WC solution after injection of $BaCl_2$

5 Results and Discussion- Characterisation of Products

Within this chapter characterisation of reaction products produced when blending the materials characterised in chapter 4 is discussed. Residue A1 was used for this work. Characterisation was undertaken using XRD, STA, and SEM techniques. Such analysis is important when demonstrating that treatment induces physico-chemical changes in the waste and does not simply cause dilution. This is crucial for satisfying the landfill redulations [14].

Several variables were studied including

- Waste:binder ratio- higher waste incorporation provides a more economical and resource efficient treatment. Waste content is often limited by consequences for the performance of the s/s product.
- Curing temperature- increased curing temperatures can accelerate setting and strength development, offering benefits for reactions with slow kinetics. Temperature variation can also alter the observed

mineralogy. Curing at higher temperatures would be economically feasible for an on-site treatment option, utilising the heat produced at the incinerator.

- Activator type (WC solution or de-ionised water)- Use of the WC solution has benefits since it is valorising the waste and may increase otherwise slow reaction kinetics. However, characterisation of an equivalent blend using de-ionised water was undertaken to assess its effects on the mineralogy of the samples. Additionally considering the availability of the WC solution compared to that of APC residue it is clear that insufficient WC solution would be available for treatment of all APC residue.
- Sample age- most samples were studied after 28 days curing, however selected samples were also studied after 28 days curing at 38°C followed by storage in sealed plastic bags up to ages of 18-20months in order to assess development over longer periods of time.

Sample nomenclature	APC (g)	PFA (g)	WC (g)	DIW (g)	l/s (w/w)	Curing Temp (^{o}C)
1:4	10	40	50		1	38
2:3 (23)	20	30	50		1	23
2:3	20	30	50		1	38
2:3 DIW	20	30		41.1[a]	0.82[a]	38
2:3 (80)	20	30	50		1	80
3:2	30	20	50		1	40

Table 5.1 Mix proportions, curing temperature and nomenclature. APC=A1, PFA=Co-fired PFA, WC=Waste caustic solution, DIW=de-ionised water. [a]DIW content was calculated as the same volume as the WC solution

Samples were generally cured at 38°C using the waste caustic solution as an activator. Table 5.1 indicates the mix proportions used in the current chapter. Curing temperatures were indicated in brackets whilst the use of de-ionised water was indicated by the initials DIW. Mix designs were centred around the mix 2:3 cured at 38°C which preliminary tests suggested to be close to the

optimum ratios for compressive strength development and workability (~175mm flow table spread [157]). In an attempt to avoid excessive workability due to the density difference between the WC solution and DIW, the DIW mix was designed with a l/s similar to that of the WC blends working on a v/w basis. In addition, selected samples were characterised before and after regulatory granular leach testing (BS EN 12457-2) in order to examine phase stability during such a procedure.

Table 5.2 includes a key for peak labels used throughout this chapter, including corresponding chemical formula, mineral names and inorganic crystal structure database (ICDD PDF) reference numbers.

Peak Label	**Chemical Formula**	**Mineral Name**	**ICDD PDF Ref**
P	$Ca(OH)_2$	Portlandite	84-1264
Cl	CaClOH		36-0983
H	NaCl	Halite	05-0628
C	$CaCO_3$	Calcite	72-1652
V	$CaCO_3$	Vaterite	74-1867
M	$Al_{4.75}Si_{1.25}O_{9.63}$	Mullite	79-1454
Q	SiO_2	Quartz	46-1045
Fe	$Fe_{21.34}O_{32}$		83-0112
Al	$AlCl_3 \cdot 6H_2O$		77-1884
F (monoclinic)	$Ca_2Al(OH)_6Cl \cdot 2(H_2O)$	Friedel's salt	78-1219
F (rhombohedral)	$Ca_2Al(OH)_6Cl \cdot 2(H_2O)$	Friedel's salt	35-0105
Z_{P1}	$Na_6Al_6Si_{10}O_{32} \cdot 12H_2O$	Na-P1 Zeolite	71-0962
K	$Ca_{2.93}Al_{1.97}Si_{0.64}O_{2.56}(OH)_{9.44}$	Katoite	84-0917
C_l	$CaO \cdot SiO_2 \cdot H_2O$	C-S-H (I)	34-0002
V_s	$Na_8Al_6Si_6O_{24}(SO_4) \cdot 2H_2O$	Vishnevite	46-1333
X	$Na_8Al_6Si_6O_{24}Cl_2$	Sodalite	82-0517

Table 5.2 Peak labels for XRD patterns with corresponding chemical formula, mineral names and ICDD PDF reference numbers

5.1 Effects of variation in waste:binder ratio

Figure 5.1 shows the concentration of $Ca(OH)_2$ determined by TGA, present in samples prepared with varying waste:binder ratios over the first 28 days curing at 38℃. By monitoring the sample weights, concentrations were normalised to a %weight of the fresh mix. Samples were kept in sealed containers and bags in order to avoid carbonation, leading to erroneous results. Negligible difference in $CaCO_3$ content was observed over the 28 days. Evident from the results was the consumption of $Ca(OH)_2$, and the presence of residual $Ca(OH)_2$ in the samples after 28 days curing.

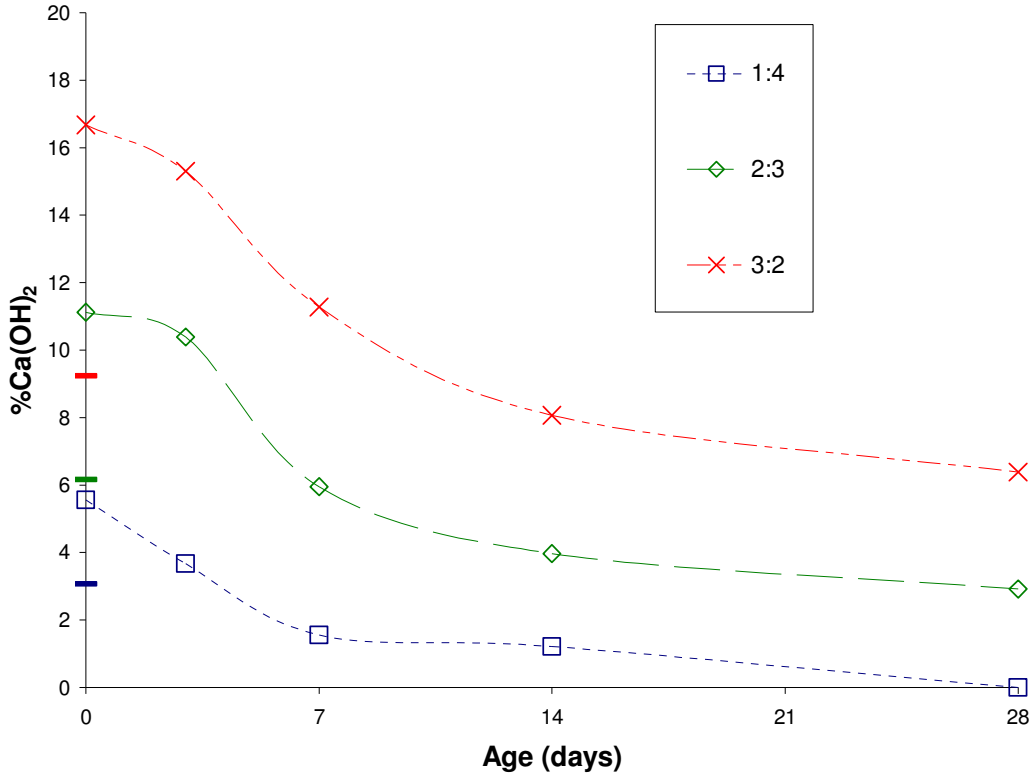

Figure 5.1 $Ca(OH)_2$ concentration (%weight, normalised as weight of fresh mix) over 28 days of curing at 38°C, samples prepared with varying APC residue:PFA ratio, l/s=1

Samples with greater APC residue:PFA ratios retained a higher concentration of $Ca(OH)_2$ because the APC residue was the source of $Ca(OH)_2$. Consumption appeared to occur slightly quicker in samples at a lower APC residue:PFA ratio, particularly at early ages (0-3days). After 7 days the rate of consumption slowed significantly as $Ca(OH)_2$ became depleted. It was noticed that all samples showed an increase in $Ca(OH)_2$

content compared to that calculated from analysis of the as-received materials and dilution. The expected concentration of $Ca(OH)_2$ calculated from the raw material composition is shown by dashes on the y axis in Figure 5.1 (3:2>2:3>1:4). Such an increase was the result of the CaClOH reacting with the NaOH in the WC solution according to equation 5.1. This reaction has previously been proposed by Zheng *et al* [79] based on XRD observations. To confirm and quantify this, residue A1 was blended with a laboratory NaOH solution (3g A1+5ml 3.5M NaOH) and dried in a vacuum desiccator before analysis by XRD and STA. The XRD pattern for the reacted residue is shown in Figure 5.2. Quantification of the TGA curve for the resultant residue showed a $Ca(OH)_2$ concentration of 50.9% weight, a $CaCO_3$ concentration of 10.9%weight and no CaClOH. The increased carbonate content was likely a result of carbonation during drying and preparation for STA. These empirically determined values were in good agreement with calculated values based on complete conversion of the CaClOH in the as-received material, determined in chapter 4.1, which would result in 52.4% weight $Ca(OH)_2$. These values were used to calculate the initial $Ca(OH)_2$ concentration of the residues as shown in Figure 5.1.

Equation 5.1. $CaClOH + NaOH \rightarrow NaCl + Ca(OH)_2$

Also presented in Figure 5.2 is the XRD pattern for residue A1 after blending with the WC solution and vacuum drying. The reaction shown in equation 5.1 has occurred and in addition there was production of aluminate phases including Friedel's salt. Such mineral formation highlights an advantage of valorising the WC solution for this type of application, contributing reactive aluminium to the matrix, increasing the potential for immobilisation of anions within sparingly soluble minerals.

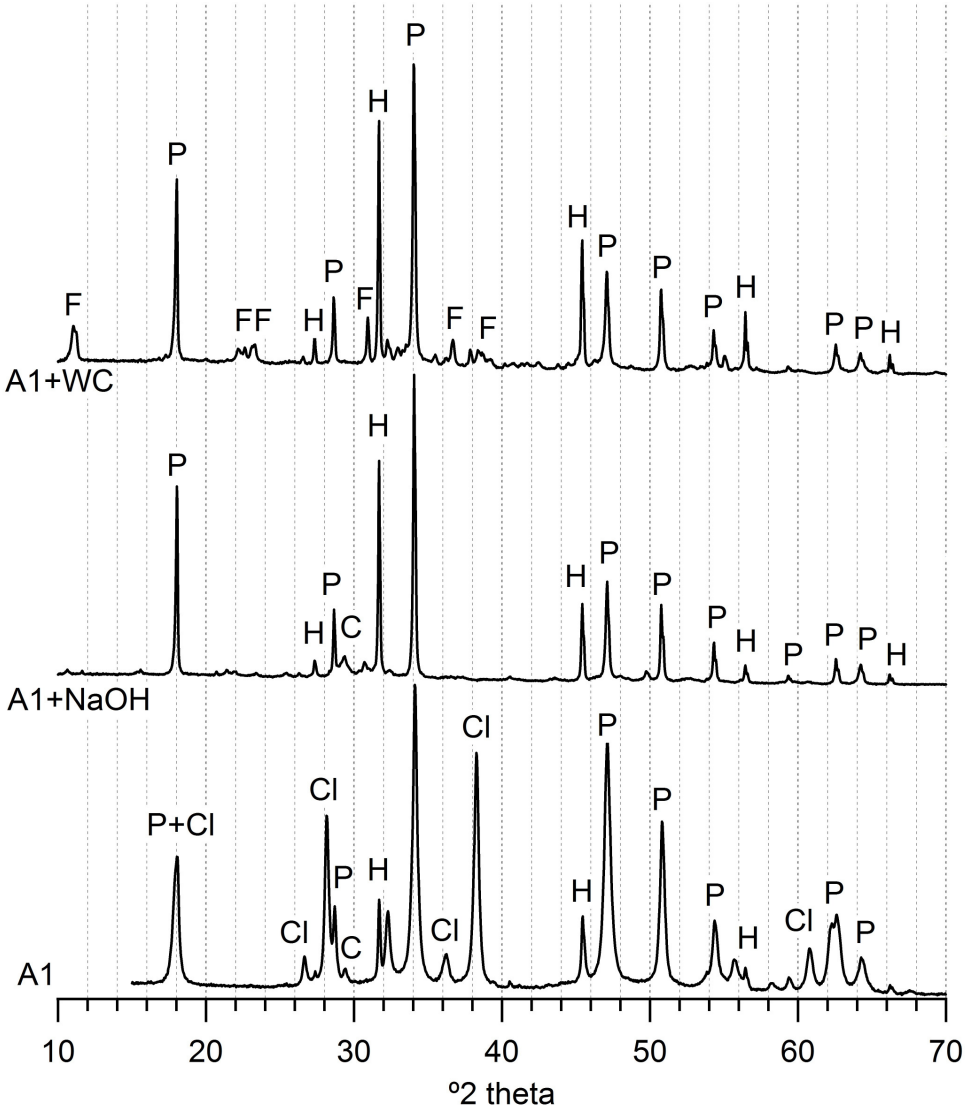

Figure 5.2 XRD patterns (y axis range not normalised) for APC residue A1 before and after blending with NaOH and the WC solution and vacuum drying.

Figure 5.3 and Figure 5.4 show the XRD patterns and DTA traces respectively for samples prepared with varying APC residue:PFA ratios. Due to the highly polycrystalline nature of the samples there were many overlapping peaks causing apparent broadening or discrepancies in peak intensities compared to the reference patterns. In order to demonstrate this, patterns for samples 1:4 and 3:2 are shown alongside the reference patterns for the primary phases present in Figure 5.5 and Figure 5.6 respectively. Patterns in have been corrected using the X'pert HighScore software to display intensities as collected by fixed divergence slits in order that intensities may be compared with reference patterns.

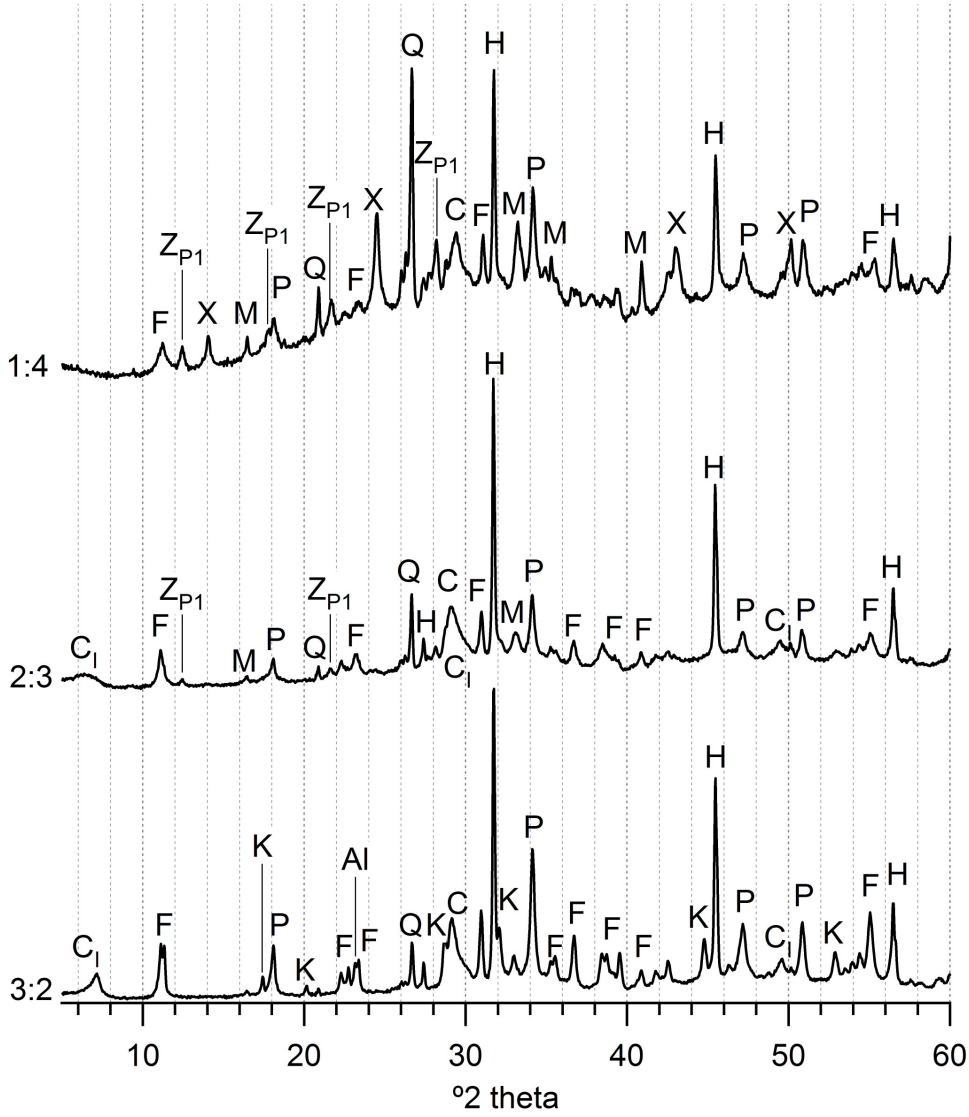

Figure 5.3 XRD diffraction patterns (y axis range not normalised), for samples prepared at varying APC residue:PFA ratios, l/s=1, cured at 38°C for 28 days

Several phases were found in every sample, such as the unreacted quartz and mullite from the PFA, and $Ca(OH)_2$ and $CaCO_3$ from the APC residue, with the latter two also identified by DTA endotherms at ~450 and ~700°C respectively. The considerable presence of NaCl can be explained by the reaction between the CaClOH and NaOH plus the initial presence of NaCl in the APC residue.

Reaction products also included Friedel's salt, formed from the high content of soluble calcium, aluminates and chlorides. Friedel's salt was evidenced by XRD and DTA via an endothermic peak at ~320℃ and ~120℃ as interlayer water is lost, thus reducing the crystallinity of the structure [210]. The initial

endotherm relating to Friedel's salt has been seen as late as 160-180℃ [216, 312] corresponding with the peak seen in samples 2:3 and 3:2. Friedel's salt recrystallises exothermically at ~670℃ [210]. Such a peak was not clear in the plots shown in Figure 5.4, but was evident in other samples analysed, obscuring the endothermic peak associated with $CaCO_3$. XRD analysis showed Friedel's salt to be present in both monoclinic and rhombohedral forms. This reversible phase transition occurs above 30℃ [409, 410] although the transition temperature may change as Cl is substituted by OH [198]. The presence of both phases may be explained by the curing and storage regime.

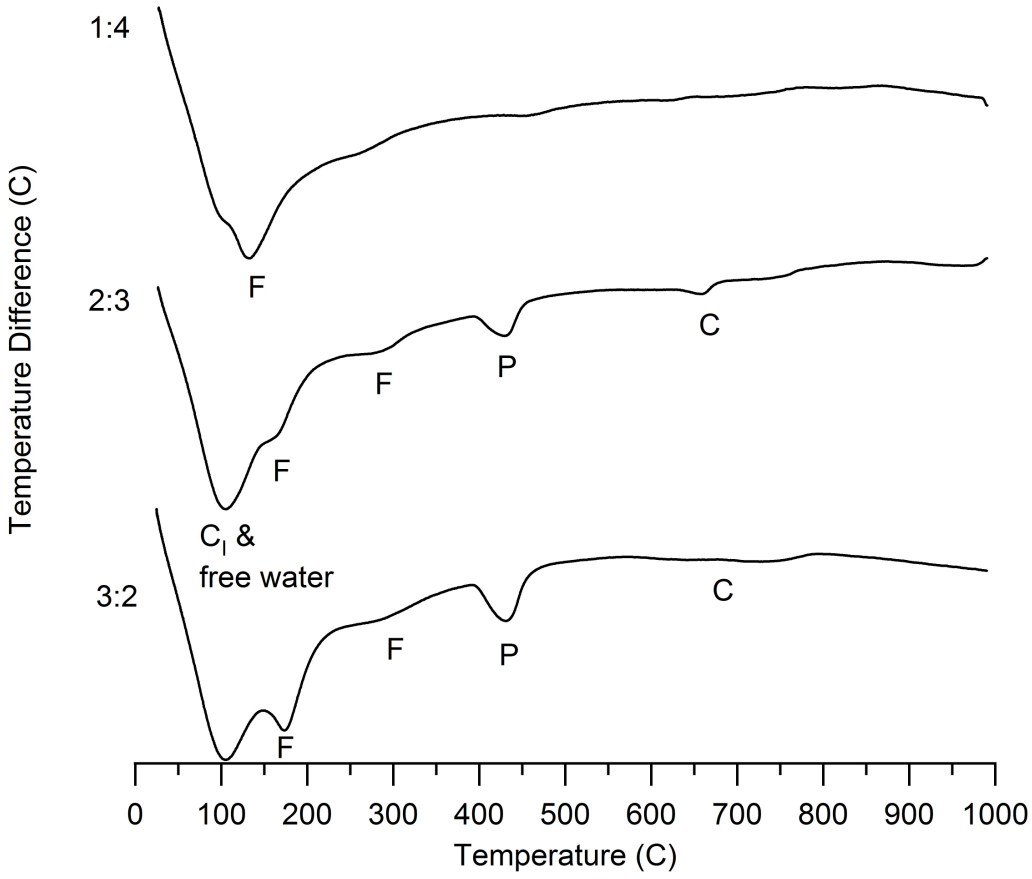

Figure 5.4 DTA patterns (y axis range normalised) for samples prepared with varying APC residue:PFA ratios, l/s=1, cured at 38°C for 28 days

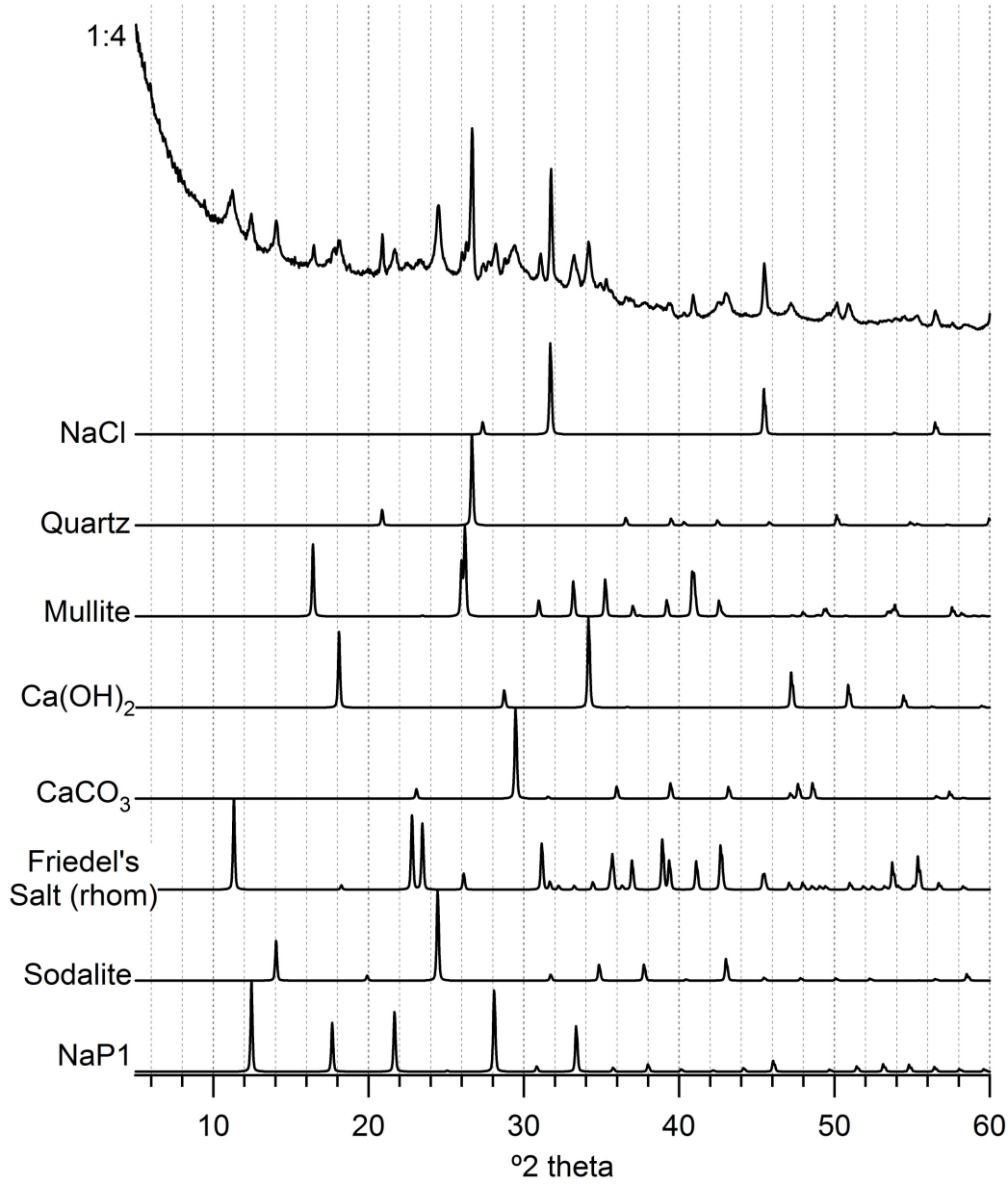

Figure 5.5 XRD pattern for sample 1:4 corrected to fixed divergence slits, and reference patterns for principal crystalline phases present.

Diffraction patterns also showed semi-crystalline C-S-H (I) (C_I in Figure 5.3) which gives an endothermic DTA peak around 90-110℃ and was observed in NaOH activated ggbs by Wang and Scrivener [279], and KOH activated ggbs by Richardson *et al* [277]. This phase became more prominent as the APC residue content increased, probably due to the greater Ca availability. As well as more prominent C-S-H (I) reflections, sample 3:2 showed the presence of katoite which was less prominent in 2:3 and not evident in 1:4. This suggests the Na/Ca ratio was crucial in determining katoite formation, consistent with observations by La Rosa *et al* [298], who saw katoite

formation when activating PFA:cement with NaOH at a PFA:cement ratio of 1:4 but not 4:1, i.e. katoite formed with a lower Na/Ca. Dehydration of katoite has been shown to occur at 250-350°C [411] and therefore the DTA endotherm corresponding to this event would overlap with that of Friedel's salt. The production of katoite, C-S-H (I) and Friedel's salt would explain the consumption of $Ca(OH)_2$ observed by STA.

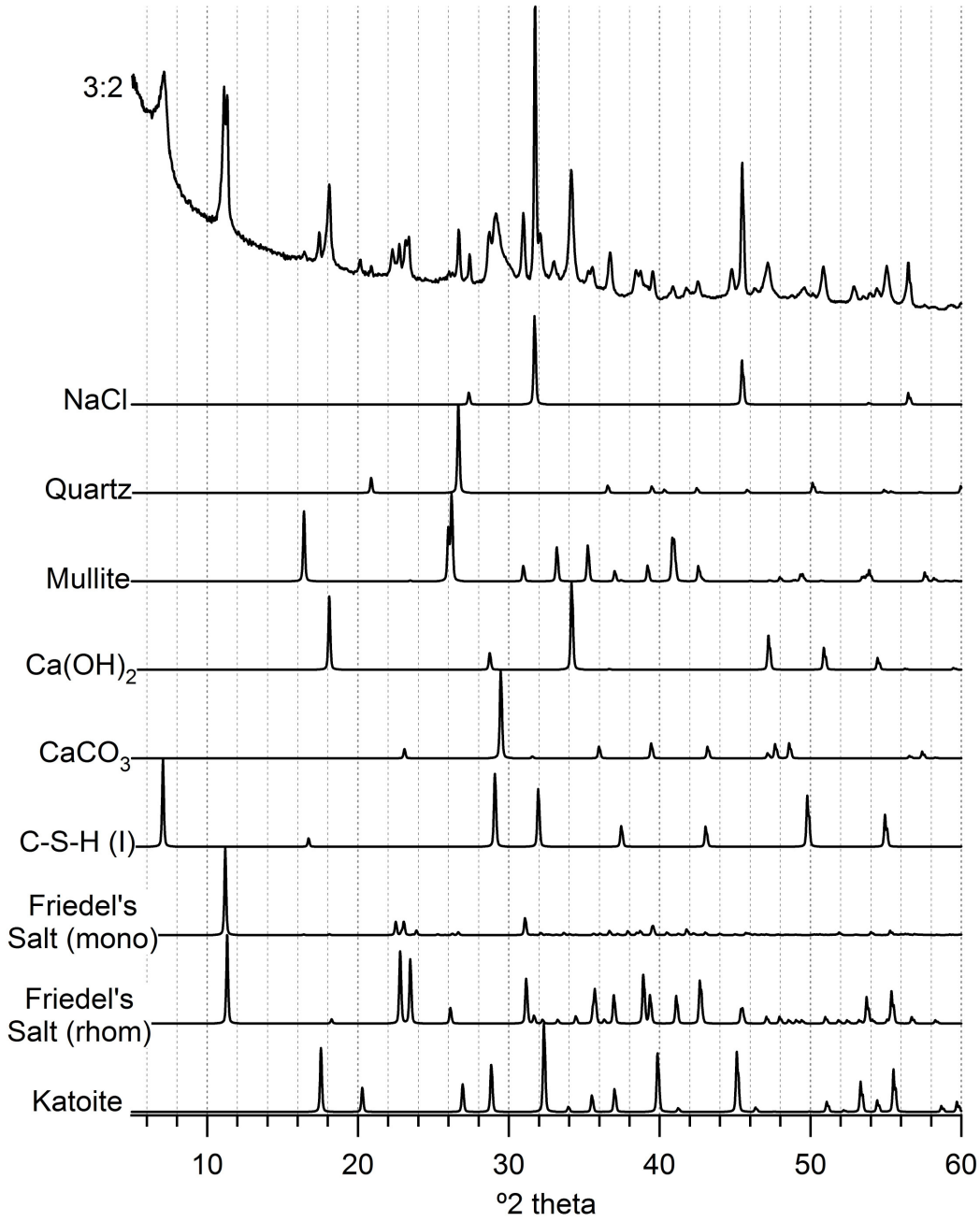

Figure 5.6 XRD pattern for sample 3:2 corrected to fixed divergence slits, and reference patterns for principal crystalline phase present.

Analysis of samples prepared at 1:4 and 2:3 by XRD showed evidence of the zeolite Na-P1 (Figure 5.3). This zeolite has been found when activating PFA

with NaOH solutions [287, 412], and may also occur in the presence of cements [295, 298, 302]. Na-P1 has a high cation exchange capacity and large internal cavities allowing adsorption of pollutants [287, 295]. As such the zeolite has potential for hazardous waste treatment [287, 295, 297] although the efficiency is reduced in alkaline media such as that which would be present in the pores and leachates of the samples studied here [295]. Na-P1 was not present in the 3:2 samples; possibly due to the reduced Na/Ca. Lower availability of Ca appeared to allow formation and stability of this zeolitic phase up to 28 days. Where excess $Ca(OH)_2$ is present zeolites such as Na-P1 may be consumed in pozzolanic reactions [295, 300, 301]. This may explain the lower quantities of this phase in later age samples. Analysis of 2:3 after 20 months showed very weak peaks for this phase and increased intensity of peaks due to C-S-H (I) (Figure 5.7).

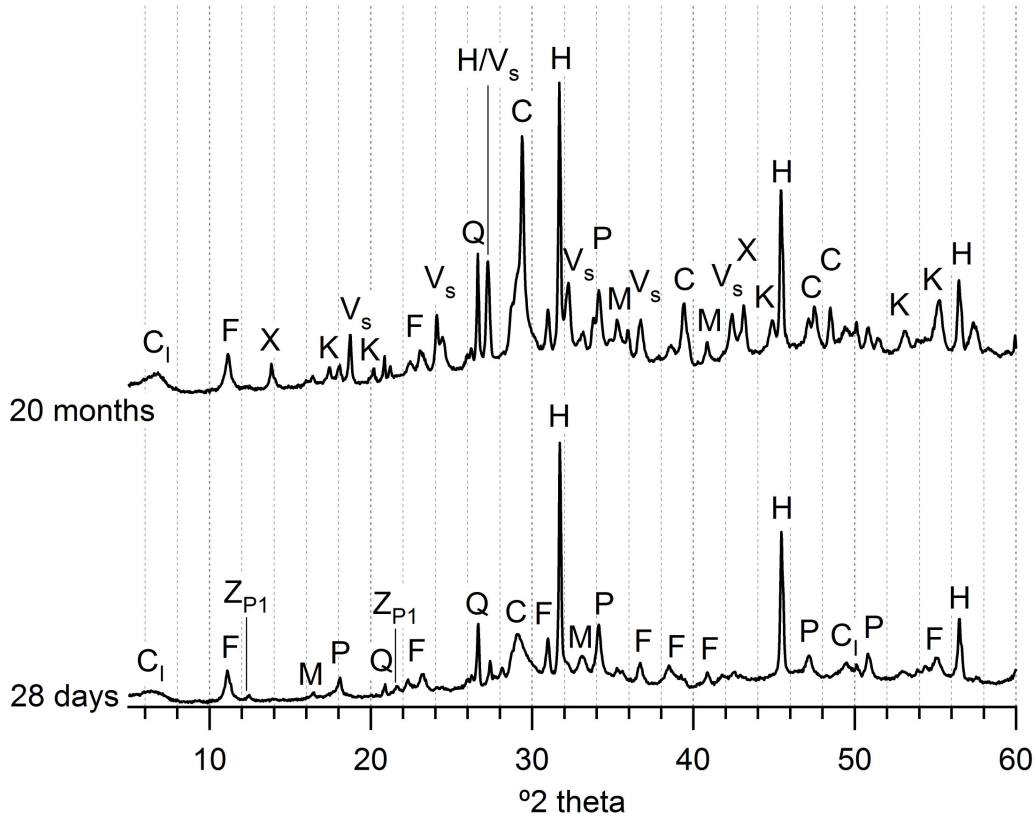

Figure 5.7 XRD patterns (normalised y axis range) for sample 2:3 after curing for 28 days and 20 months

At 28 days, sample 1:4 also showed peaks corresponding to sodalite. Sodalite is also a zeolitic phase but with smaller cavities and lower cation exchange capacity than Na-P1 [287]. Sodalite may include Cl within its

structure although has generally been observed as hydroxy-sodalite [273, 287, 413] or ‘basic sodalite’ [303] in which the anion space is occupied by hydroxyl ions. XRD patterns for sodalite and hydroxy-sodalite are practically indistinguishable. The high Cl concentration in the samples studied here may encourage inclusion of Cl within the sodalite structure. Whilst at 28 days sodalite peaks were only detected in sample 1:4, after curing for 20 months they were also clear in 2:3 (Figure 5.7). This indicated the slow reaction kinetics involve in the production of sodalite at 38°C. Production was perhaps faster in sample 1:4 due to the greater quantity of PFA, and the lower availability of CaClOH which would neutralise the NaOH according to Equation 5.1, causing reduced dissolution of the PFA [261]. More rapid concentration increase of Si and Al in solution would therefore occur in samples prepared with lower waste:binder ratios. Accelerated reaction with lower waste:binder ratios was confirmed by monitoring the heat evolution of the samples by calorimetry as later reported (chapter 6.2) and was also consistent with the increased rate of $Ca(OH)_2$ consumption in the initial 3 days of curing (Figure 5.1). The presence of sodalite alongside C-S-H (I), in samples 2:3 after longer periods of curing, which showed evidence of unreacted $Ca(OH)_2$ by TGA, also suggested that this phase is more stable than the Na-P1 zeolite in such environments, and not consumed in pozzolanic reactions.

In 28 day samples, sulphate bearing reaction products could not be identified. Analysis of sample 2:3 cured for longer periods of time, showed clear evidence of vishnevite-$Na_8Al_6Si_6O_{24}(SO_4)\cdot 2H_2O$ (ICDD PDF: 46-1333) (Figure 5.7). It is noted that vishnevite is a hydrated, sulphate containing analogue of sodalite. The production of the sulphate containing analogue would suggest a change in the ratio of the anions $OH/Cl/SO_4$ over time. This may have occurred due to oxidation of the sulphur present in the PFA as a result of the high pH and exposure to atmospheric O_2 [155, 414].

XRD analysis of sample 1:4 showed a much more significant amorphous hump than other samples (Figure 5.3). This hump was due to unreacted PFA which was corroborated by the observation of a significant quantity of

unreacted, spherical PFA particles when viewing fracture surfaces by ESEM (Figure 5.8). Far fewer unreacted fly ash particles were evident in analysis of sample 3:2 corresponding to a much lower amorphous content visible by XRD. Fracture surface imaging showed distinctly different morphologies in samples 1:4 (Figure 5.8 and Figure 5.9) and 3:2 (Figure 5.11 and Figure 5.12) which is as would be expected based on the phase identification by XRD. Consistent with the XRD analysis the samples appeared highly heterogeneous showing a broad range of morphologies, corresponding to a wide range of reaction products. Fernandez Jimenez *et al* [415] discussed microstructural development in alkali activated fly ash pastes, stating that several morphologies may coexist in the same paste owing to variations in factors such as particle size distribution and local chemistry (e.g. pH) throughout the paste. Varied conditions were also evident from the coexistence of Na-P1 and sodalite as observed by XRD analysis. The different zeolites may form from the same fly ash depending on the reaction conditions [287]. Figure 5.10 shows a fly ash particle which has been attacked at a discreet point which has then expanded into a larger hole. This is consistent with the mechanism described by Fernandez Jimenez *et al* [415] and allows alkali attack to occur from the inside of the cenosphere out, or, allows access to the smaller particles contained in the case of a plerosphere. Reaction products can be seen to have precipitated within the initially dissolved area of the fly ash particle. Additionally there was evidence of ‘crust’ formation around some of the particles, (Figure 5.13) due to rapid precipitation of hydration products of low permeability. Such formation delays further reaction of the fly ash particles since it must occur by a diffusive mechanism [415].

Precise identification of reaction products by SEM was difficult and avoided due to the heterogeneity of the matrix. The morphology presented in Figure 5.12 was not evident in sample 1:4, and bears a striking resemblance to the ‘crumpled foil like morphology’ described for low Ca/Si C-S-H and observed previously with synthesised C-S-H (I) [416]. This would be consistent with analysis by XRD which showed C-S-H (I) in sample 3:2 but not sample 1:4 (Figure 5.3).

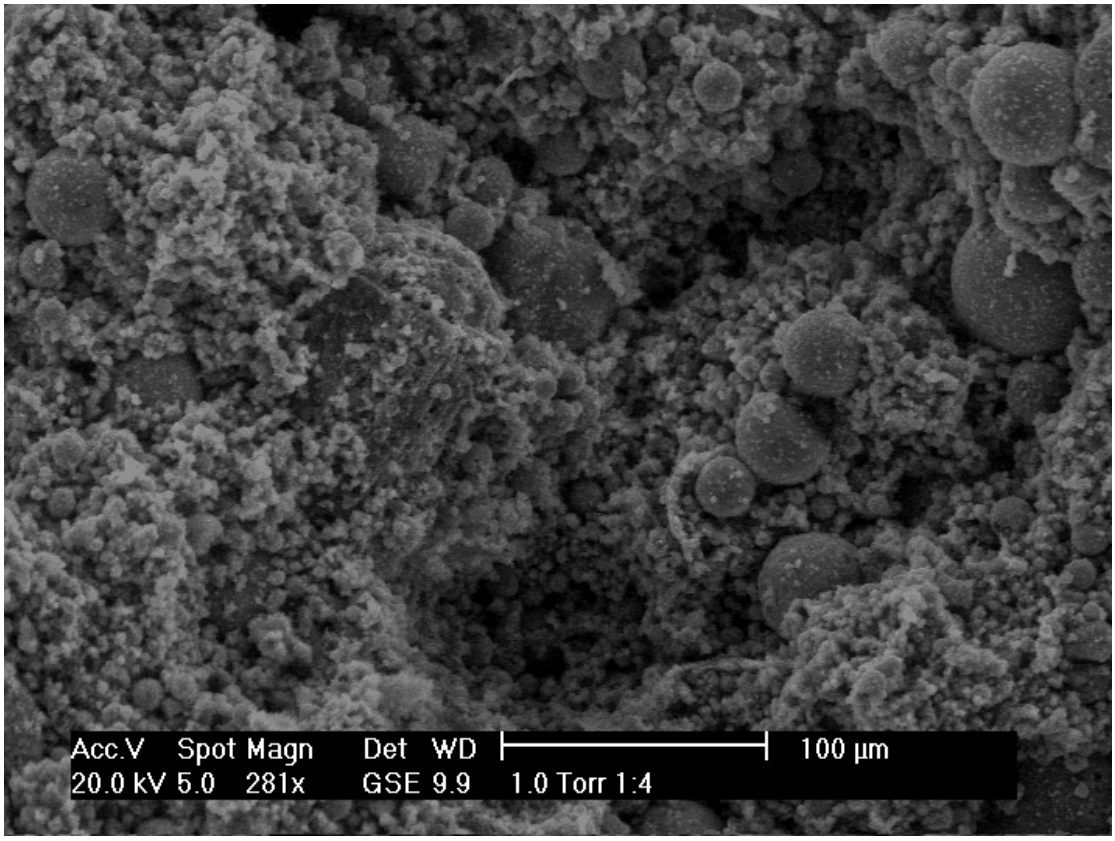

Figure 5.8 Fracture surface of sample 1:4 cured for 28 days, viewed by GSE SEM

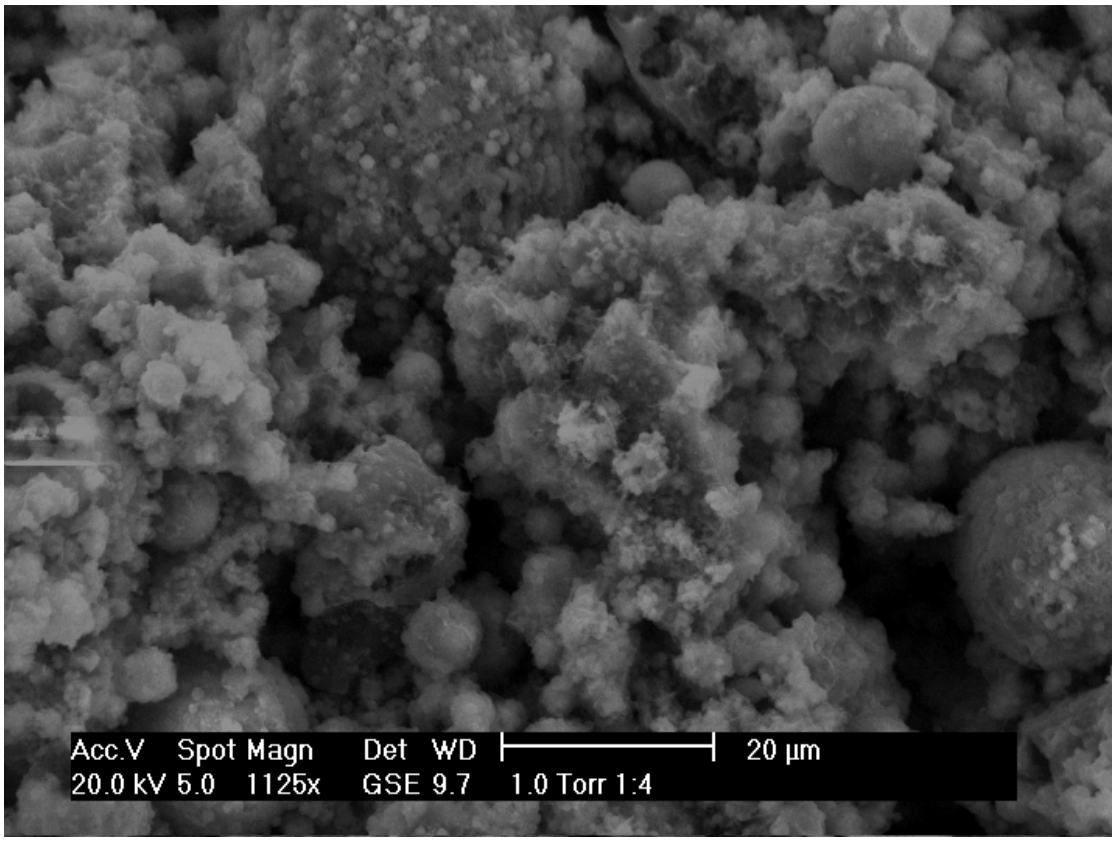

Figure 5.9 Fracture surface of sample 1:4 cured for 28 days, viewed by GSE SEM

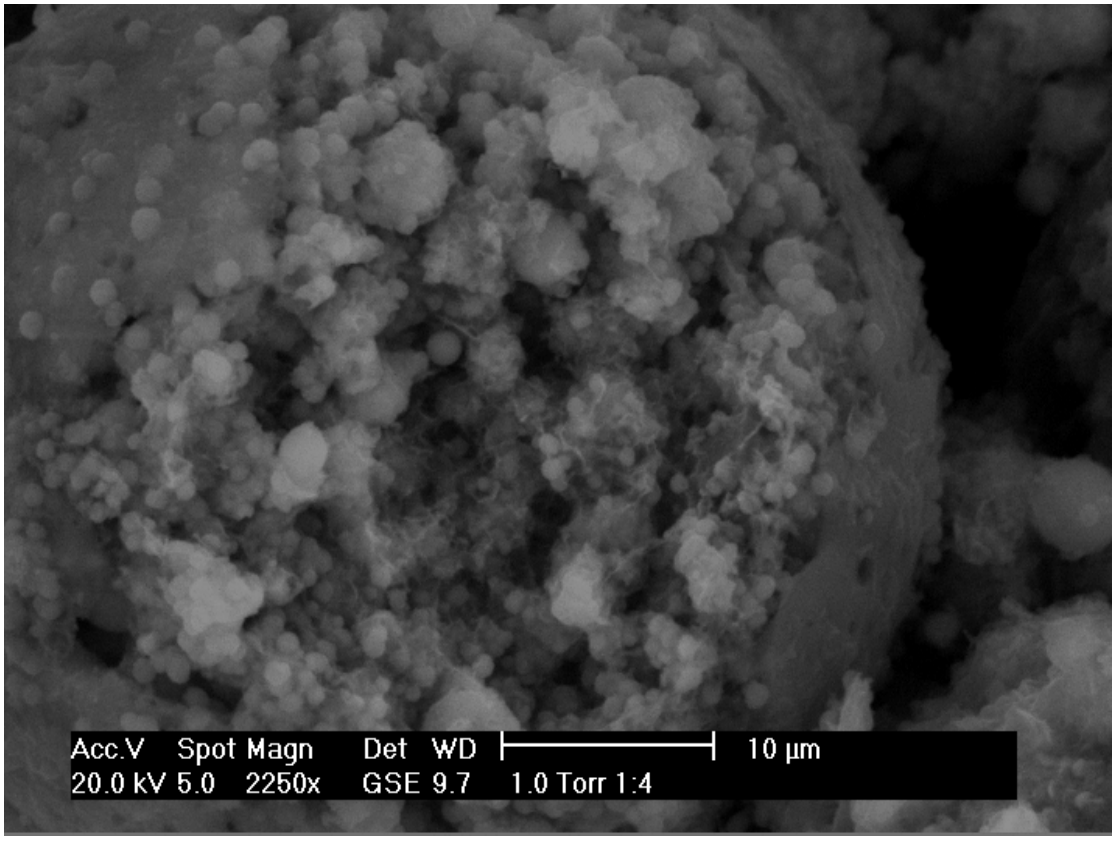

Figure 5.10 Partially reacted fly ash particle viewed by GSE SEM analysis of a fracture surface of sample 1:4 cured for 28 days

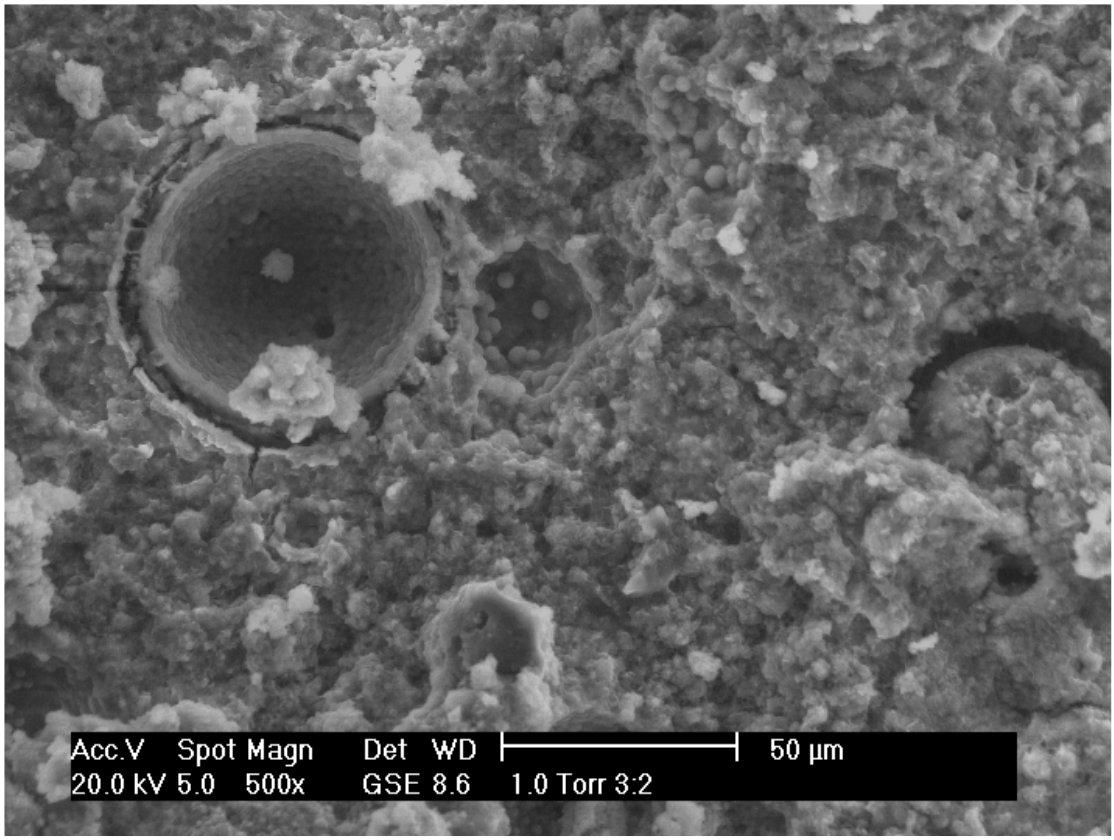

Figure 5.11 Fracture surface of sample 3:2 cured for 28 days, viewed by GSE SEM

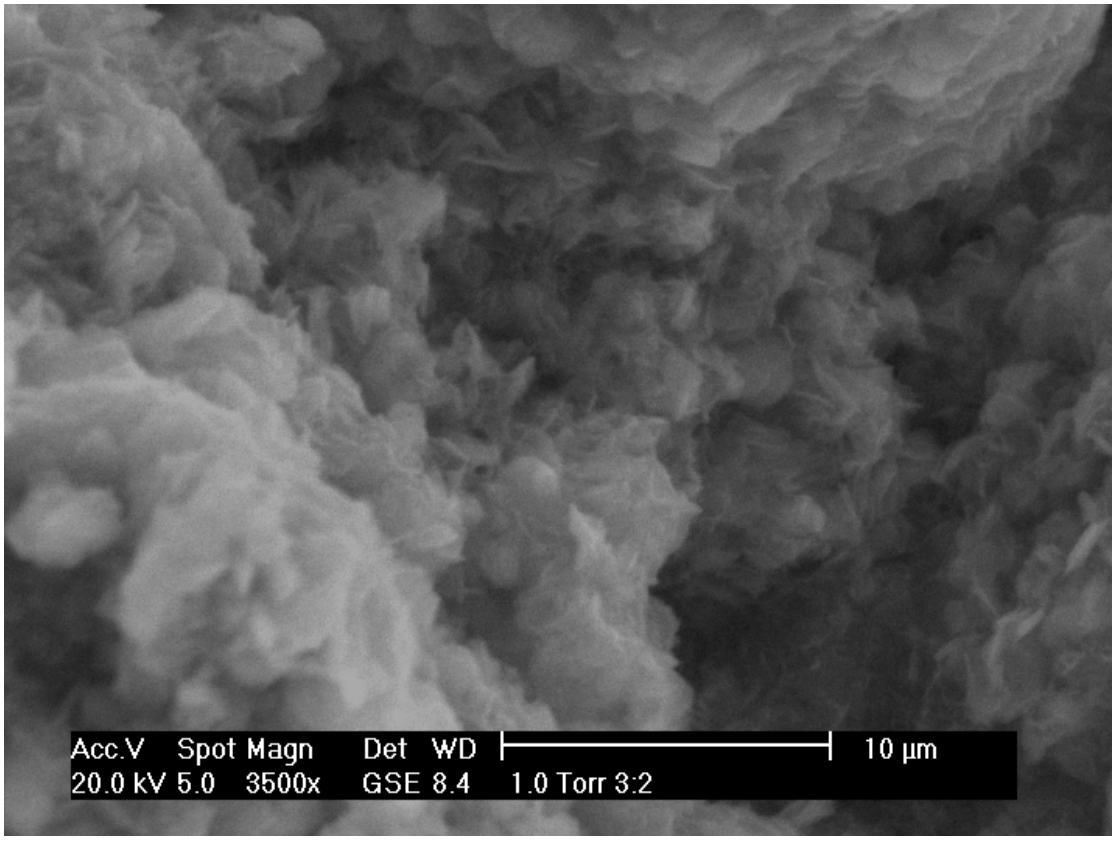

Figure 5.12 Fracture surface of sample 3:2 cured for 28 days, viewed by GSE SEM

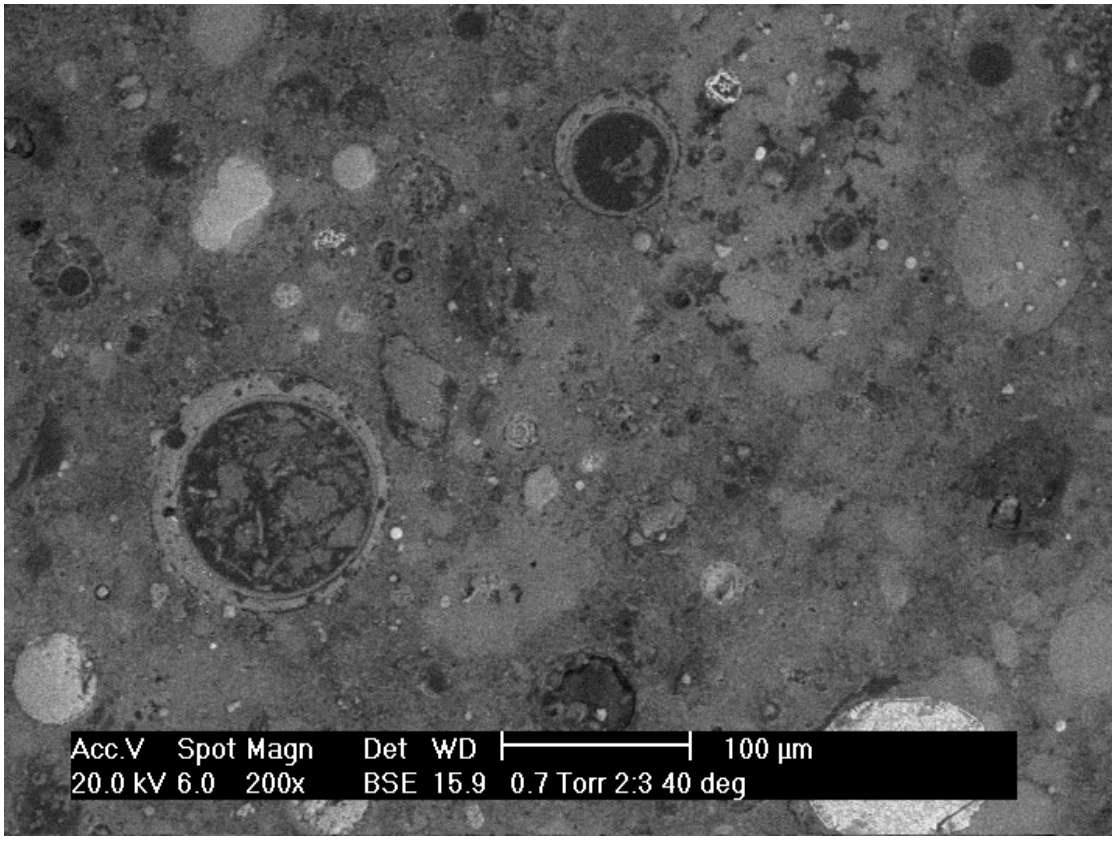

Figure 5.13 Resin impregnated and polished section of sample 2:3 cured for 28 days, viewed by BSE SEM

5.2 Effects of variation in curing temperature

Figure 5.14 shows the change in $Ca(OH)_2$ concentration over the first 28 days of curing in sample 2:3 cured at 38℃ and 80℃. Consumption of $Ca(OH)_2$ was much greater at 80℃. Such behaviour was consistent with the literature. Higher curing temperatures introduce more energy into the system, increasing the rate of fly ash dissolution and reaction kinetics [261, 274, 288, 290, 417] and therefore $Ca(OH)_2$ consumption. The rate of $Ca(OH)_2$ consumption appeared higher over the first three days, after which it was slower than the lower temperature sample. This was consistent with results presented by Shi and Day [290] and was likely a result of the initially rapid formation of hydration products forming largely impermeable 'crusts' around the PFA particles [415].

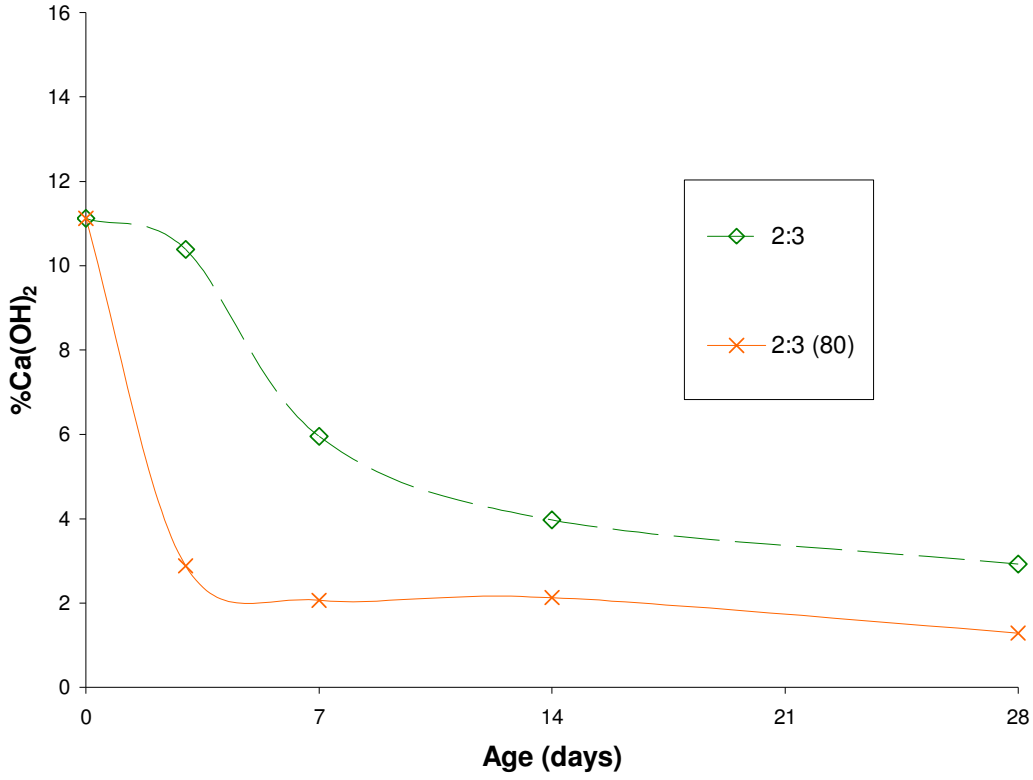

Figure 5.14 $Ca(OH)_2$ concentration (%weight, normalised as weight of fresh mix) in sample 2:3 and sample 2:3 (80) cast with l/s=1 over the first 28 days of curing

Figure 5.15 shows diffraction patterns for sample 2:3 cured at 38℃ and 80℃. Wang and Scrivener [279] reported more crystalline C-S-H (I) when curing at 80℃. The intensity of the peaks corresponding to C-S-H (I) were

not observed to be much greater in the samples analysed here. The clearest reflection was at ~7°2θ since other reflections tended to consist of overlapping peaks e.g. calcite, portlandite and katoite peaks overlapped the peak at ~29°2θ. Although the peak intensity was not noticeably greater, the peak was better defined suggesting greater crystallinity. Additionally there appeared to be a slight shift in the peak to a higher °2θ when curing at 80°C. This peak shift could be associated with loss of water from the C-S-H (I) [418] due to the higher curing temperature.

Samples analysed in this study showed formation of zeolite Na-P1 at 38°C and sodalite at 80°C. Na-P1 was not present in the samples cured at 80°C. Initially this was believed to be a result of the increased rate of pozzolanic reaction and therefore increased rate of consumption of the Na-P1. However, samples analysed after 1 day showed no Na-P1, suggesting the phase did not form. This could perhaps be an implication of rapid hardening and spatial constraints, preventing the crystallisation of Na-P1. The absence of Na-P1 in samples cured at 80°C appeared to contradict previous results [287, 298, 412, 413]. In the literature Na-P1 is still seen to form in samples cured at temperatures up to 200°C. Previous work has shown blends of NaOH and fly ash cured at 38°C and 80°C for less than a week led to faujisite formation at 38°C and Zeolite P at 80°C [412]. Querol *et al* [287] discussed the effects of temperature and concentration of alkali activator on the type of zeolite formed. Higher activator concentration and temperature were suggested to produce low cation exchange capacity (CEC) zeolites such as hydroxy-sodalite, with low temperature and activator concentration resulting in high CEC zeolites such as Na-P1. Whilst the zeolite phases seen in this study occurred in generally lower temperature ranges to those reported previously, the trend of sodalite as opposed to Na-P1 formation at higher temperatures appeared to hold true. A number of factors may have influenced the curing temperature range at which the different phases formed. Samples analysed here had been cured for 28 days as opposed to generally less than 7 in the literature which could have compensated for slower kinetics. Additionally the lower l/s applied to the samples studied here, as opposed to those typically applied when synthesising zeolites (l/s=1-20ml/g) [287] may alter the

temperature range in which phases form due to the quicker concentration increase in the solution. Characteristics of the raw material such as particle size distribution and glass phase composition could also result in changes in reaction products [287] and certainly the high concentration of chloride salts in the APC residue could have an influence.

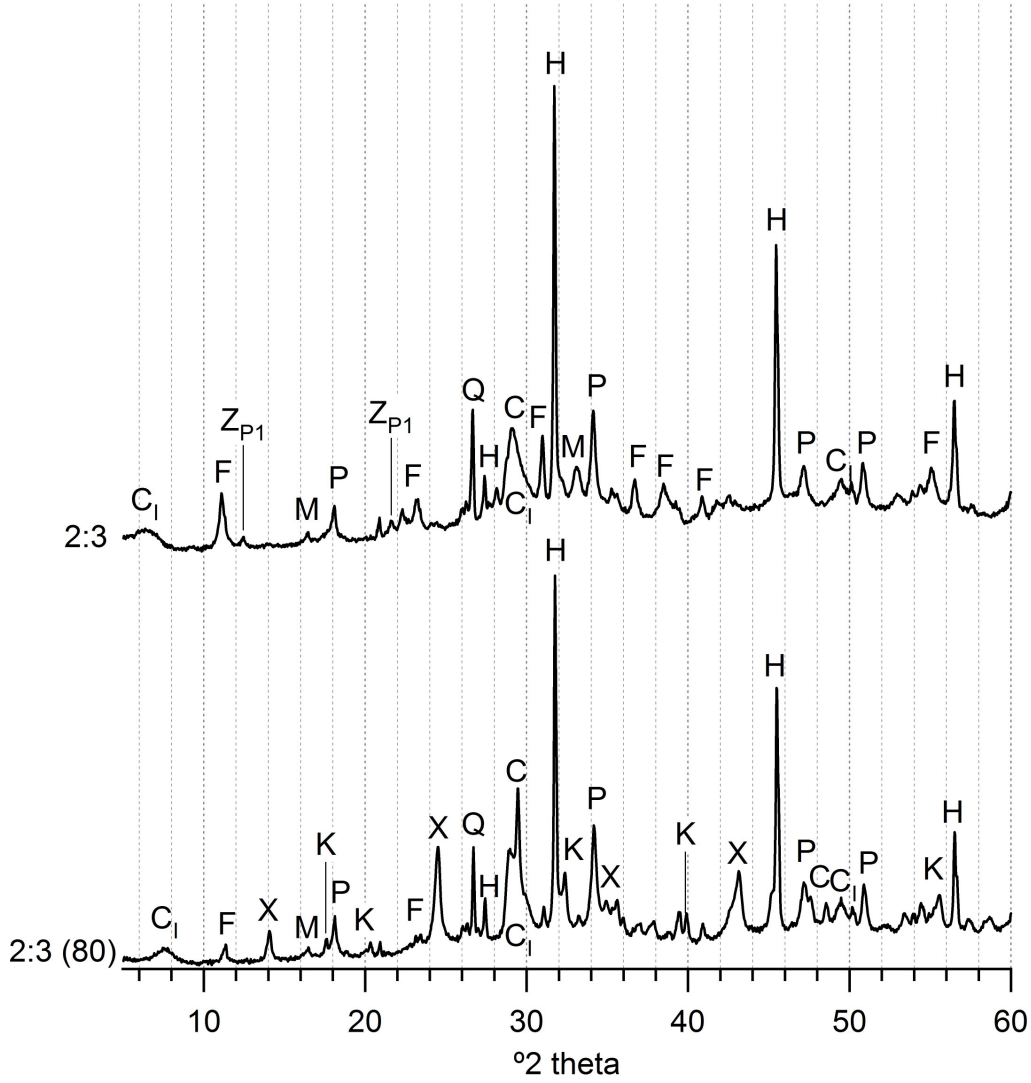

Figure 5.15 XRD patterns (normalised y axis range) for sample 2:3 and 2:3 (80), prepared with l/s=1, cured for 28 days

Working with lower l/s ratios than those typically used for zeolite synthesis, sodalite has been observed to form as a result of several curing regimes. Basic sodalite was observed alongside C-S-H (I) when activating pre-treated fly ash with NaOH at 90°C for 24 hours [303]. Dombrowski *et al* [419], observed sodalite in 28 day old $Ca(OH)_2$/fly ash blends activated with 8M NaOH and cured at 40°C for the initial 3 days whilst Alonso and Palomo

[273] identified hydroxy-sodalite in blends of metakaolin and $Ca(OH)_2$ after curing at 45℃ for 24 hours when activating with a NaOH solution of concentration greater than 5M.

It is noticed that the sample cured at 38℃ showed sodalite and vishnevite formation after 20 months curing (Figure 5.7). Curing at 80℃ accelerated the formation of sodalite such that it was present in 28 day samples (Figure 5.15). However, no vishnevite was evident in the sample cured at 80℃ for 28 days suggesting the same acceleratory effect was not present. Additionally no other crystalline sulphates were clearly evident at 28 days. This is perhaps indication that the formation of vishnevite is dependent on oxidation of some of the sulphur in the PFA.

Increased curing temperature also showed increased prevalence of katoite, in agreement with previously discussed results, which suggest this phase to form in conditions which allow for rapid reaction. Peaks for Friedel's salt were also much less intense when curing at higher temperature, consistent with previously reported results concerning the stability of Friedel's salt with temperature [420].

5.3 Effects of alkali activation

Figure 5.16 shows the DTA plots for samples with APC residue:PFA ratio=2:3 activated by deionised water whilst XRD patterns are presented in Figure 5.17. Although characterisation of the alkali activated blends showed good repeatability, indicating a homogeneous matrix with regard to the quantities used for analysis by STA and XRD, immediately apparent in the DIW blends was the heterogeneity of the samples. At 28 days the DTA plot showed no evidence of CaClOH whilst the XRD pattern was dominated by peaks for this phase. XRD patterns for DIW samples showed a consistently greater amorphous content which can be attributed to the slower rate of PFA dissolution and reaction product formation [266, 274]. The slower rate of reaction was also apparent from the setting time of the water activated samples as discussed later.

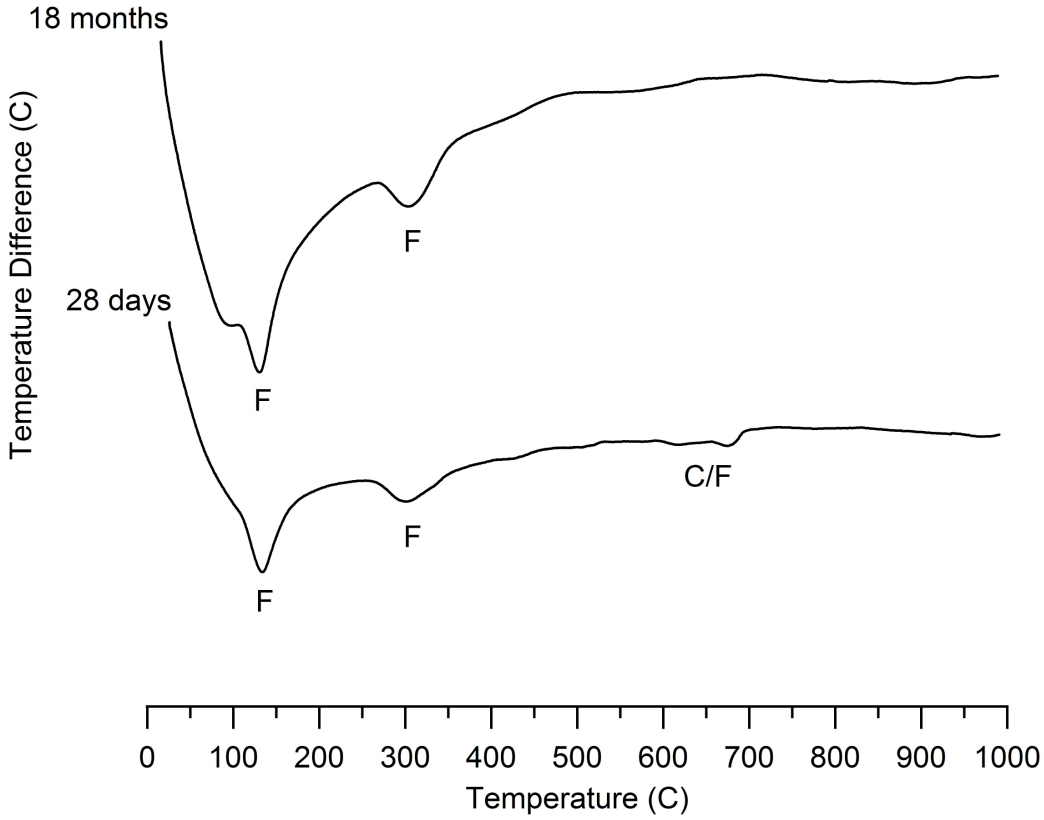

Figure 5.16 DTA plots (y axis range normalised) for sample 2:3 DIW cured for 28 days and 18 months

Changes in phase composition when activating with water as opposed to the WC solution were also apparent. Both NaCl and $Ca(OH)_2$ levels were lower since the absence of NaOH prevented its reaction with CaClOH. NaCl was present in low concentrations owing to its presence in the APC residue. CaClOH was still present in the DIW samples at 28 days (Figure 5.17), and was also observed to remain present in samples cast with high waste:binder ratios, when utilising CEM I as the binder [243]. After curing for 18 months CaClOH was no longer evident in the samples analysed, whilst Friedel's salt appeared more so, suggesting that some of the Cl was now bound within this phase.

The absence of $Ca(OH)_2$ after 18 months in the sample analysed by XRD (Figure 5.17) appeared largely due to carbonation. $CaCO_3$ was present in the DIW samples as calcite and vaterite, but only as calcite in the WC samples. Vaterite is rarely observed as a carbonation product but has been seen to form on $Ca(OH)_2$ intermixed with Ca-rich C-S-H when exposed to ambient air

[421]. Vaterite perhaps did not form in the WC activated blends because alkali activated systems tend to produce C-S-H with low Ca/Si [254, 277, 279].

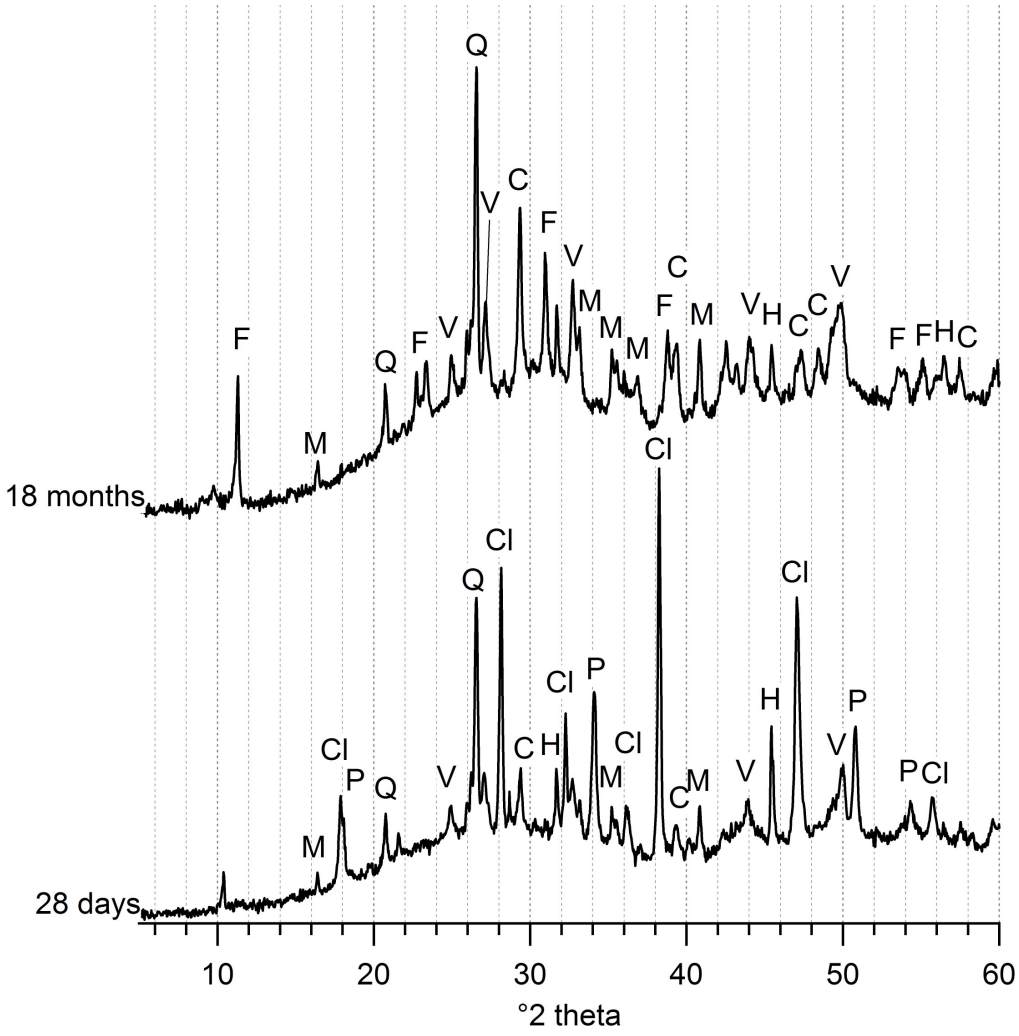

Figure 5.17 XRD patterns (y axis range not normalised) for sample 2:3 DIW cured for 28 days and 18 months

The absence of additional NaOH led to the DIW samples containing no zeolitic phases. Furthermore, no evidence of C-S-H (I) or katoite was observed, consistent with the findings of LaRosa *et al* [298]. Katoite appeared to be produced in highly alkaline, high Ca systems. High alkalinity may assist katoite formation by increasing the solubility of Al and the reaction kinetics.

5.4 Effects of regulatory leach testing (BS EN 12457-2)

Characterisation of selected s/s products before and after leaching was undertaken in order to provide useful information on water soluble phase composition and to explain leach performance examined later (chapter 6). Examination of the XRD patterns before and after leaching (according to BS EN 12457-2) (Figure 5.18 and Figure 5.19) showed the removal of halite and Na-P1. Conversely, there was a large increase in the intensity of the peaks due to quartz, which can be explained by the large TDS which occurred during leaching (2:3=148,500mg kg^{-1}, 2:3(80)=122,500mg kg^{-1}) leading to enrichment of phases of low solubility. The same mechanism can explain the increase in intensity of the peaks associated with Friedel's salt, C-S-H (I), katoite and mullite. It is unclear why sodalite and vishnevite appeared after leaching. Such conditions were not typical of those used for synthesising zeolites, which generally involve higher temperatures to encourage dissolution of the fly ash [287]. Additionally leachate pH values observed during BS EN 12457-2 were ~12.5, occasionally increasing to ~12.7. Such pH values are lower than those typically associated with zeolite production [287]. Zeolite yield is known to be higher at higher l/s however. Such conditions encourage greater dissolution of the fly ash matrix, and provide space for crystallisation of zeolites [287]. It is perceivable that such an effect was responsible for zeolite production during the process of leach testing. Potentially the process of the leach test sped up the oxidation of the sulphates, increasing surface area due to particle size reduction and atmospheric exposure whilst in an aqueous alkaline environment which enabled vishnevite formation. After leaching an exothermic event ~900°C was apparent by DTA which may be associated with spinel transformation of the zeolites (Figure 5.20) [413].

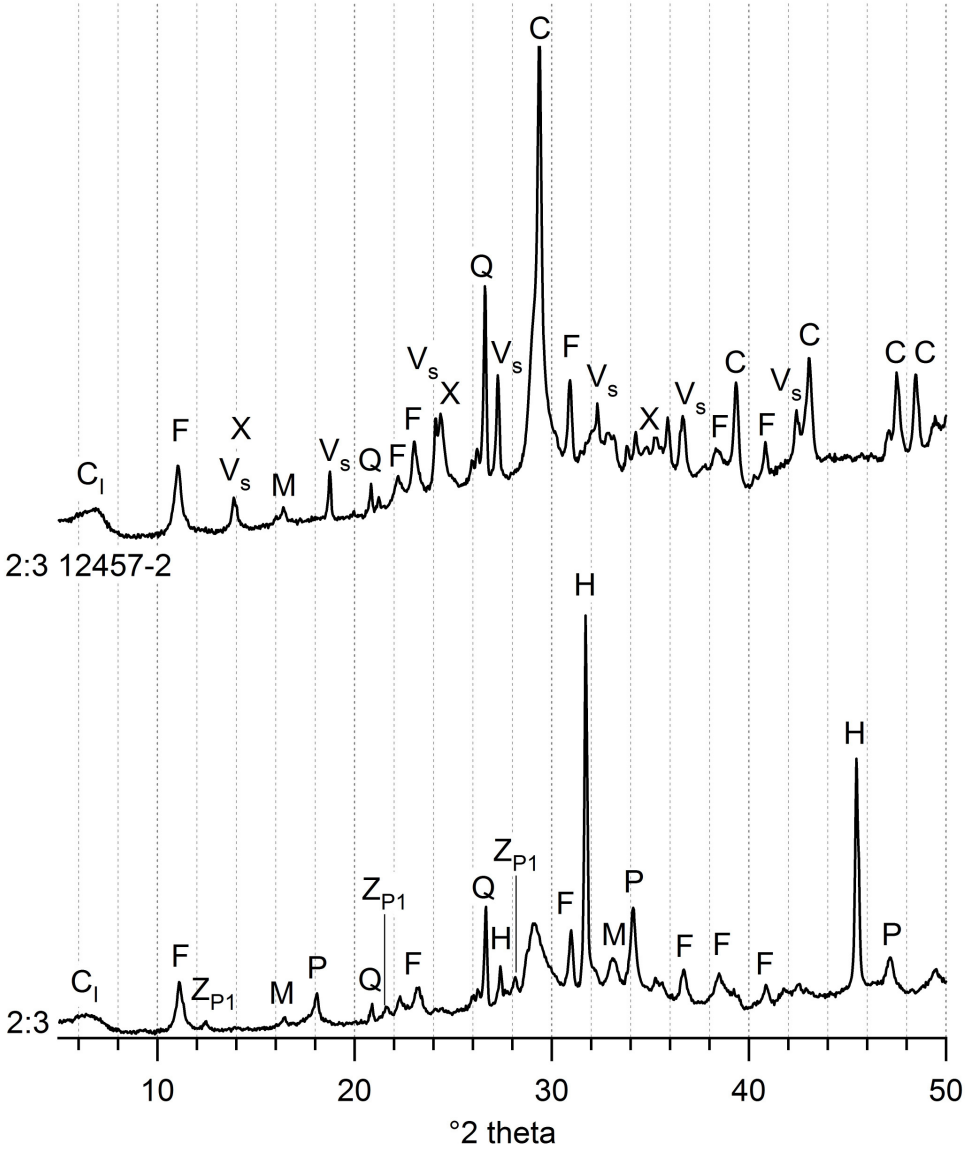

Figure 5.18 XRD patterns (y axis range normalised) for sample 2:3 before and after leach testing according to BS EN 12457-2

Leached samples also showed significant carbonation when analysed by XRD, resulting in a greater calcite peak and removal of the $Ca(OH)_2$ peak. The extent of carbonation was not as apparent by STA analysis, carbonation could have occurred during sample preparation for XRD however it is likely that some $Ca(OH)_2$ was also removed by the leaching procedure, particularly considering the high ionic strength of the solution due to the NaCl release [236]. Leaching of $Ca(OH)_2$ was confirmed by TGA analysis of the sample before and after BS EN 12457-2. No $Ca(OH)_2$ was apparent after leach

testing and the mass of $CaCO_3$ observed was insufficient to explain the decrease in $Ca(OH)_2$.

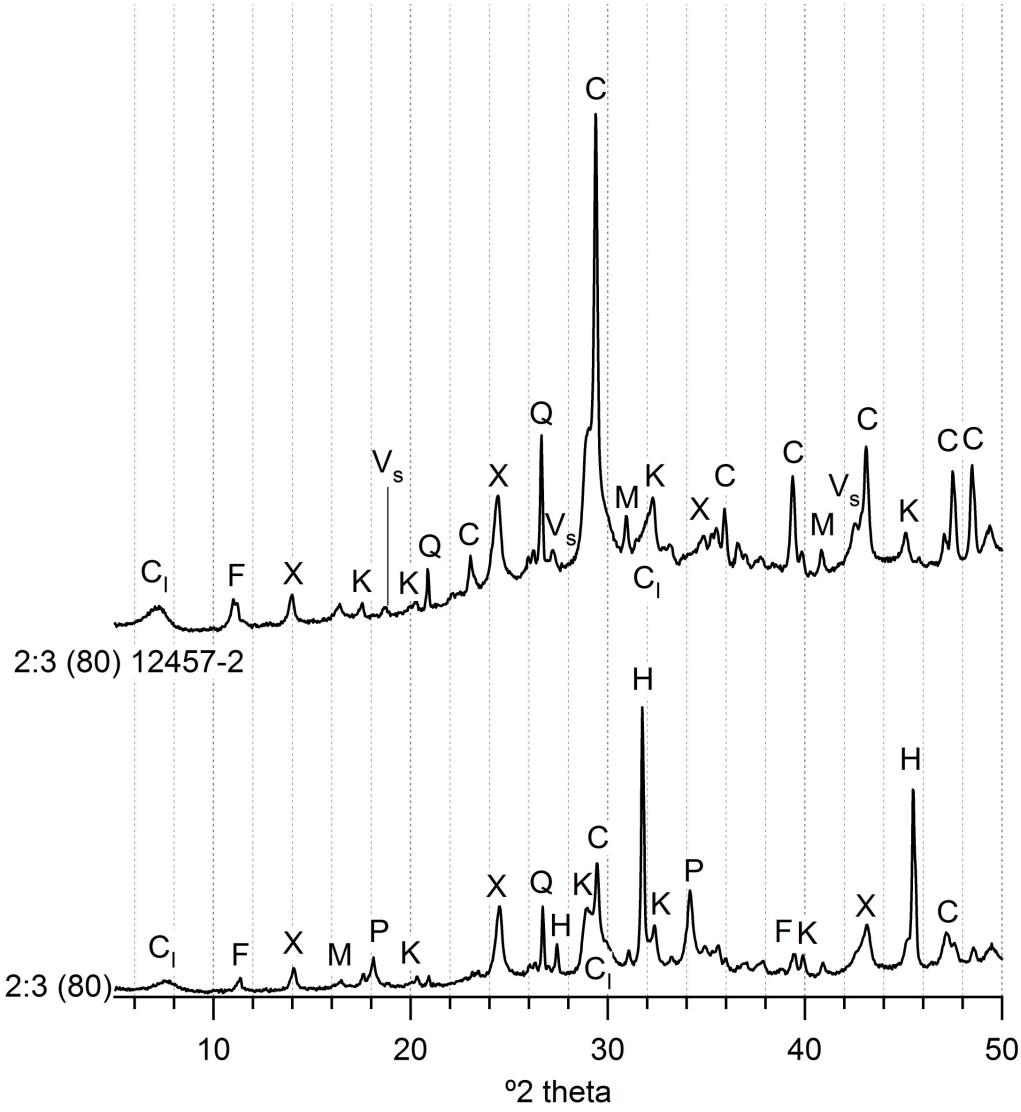

Figure 5.19 XRD patterns (y axis range normalised) for sample 2:3 (80) before and after leach testing according to BS EN 12457-2

Chlorides were retained as Friedel's salt and sodalite during BS EN 12457-2, showing the potential for immobilisation of chlorides within these minerals (Figure 5.19). However, the anion occupies a very low molecular weight fraction within sodalite (Table 5.2) therefore the phase has little potential for immobilising the levels of chlorides present in APC residues. Additionally the predominant chloride phase was NaCl which was removed by leach testing suggesting a high chloride release.

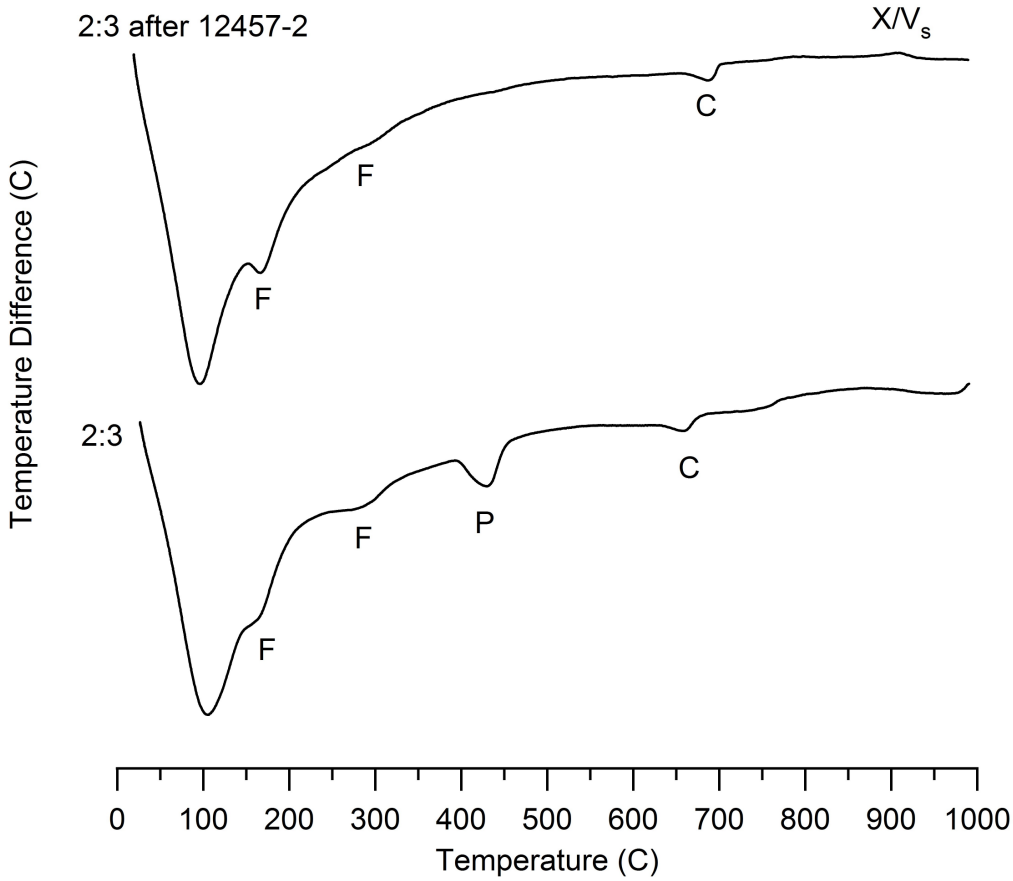

Figure 5.20 DTA analysis of 2:3 before and after granular leach testing according to BS EN 12457-2

5.5 Summary of sample characterisation

- Reactions between APC residue and PFA when activated with water are very slow and large quantities of the PFA remain unreacted. Activation of such blends with an alkali metal solution drastically increases the rate of hydration products formed and also alters their nature.
- The reaction products formed when alkali activating are dependent on a number of factors including the APC residue:PFA ratio, curing temperature and curing time.
- Adjustments in the APC residue:PFA ratio causes a significant difference in crystalline reaction products from primarily Na based zeolitic products such as Na-P1 and sodalite with a low APC residue content, to primarily Ca based products such as C-S-H (I), $Ca(OH)_2$,

Friedel's salt and katoite with high APC residue contents. Higher waste:binder ratios are desirable for industrial application of s/s, reducing the amount of binder necessary and the increase in volume of the waste. As such the Ca rich reaction products would be more likely in an industrially attractive treatment.

- Lower APC residue:PFA ratios may result in high amounts of unreacted PFA owing to both greater availability, and the lower availability of Ca+Na with which to precipitate reaction products.
- Friedel's salt was present at all APC residue:PFA ratios but increased with increasing APC residue input, a consequence of the greater Ca and Cl availability.
- Over time the reaction products develop. Na-P1 may be consumed whilst sodalite and vishnevite are formed along with continued C-S-H formation.
- Curing at higher temperatures rapidly accelerated the rate of reaction. $Ca(OH)_2$ consumption was particularly accelerated over the first 3 days of curing at 80°C. Sodalite formation was also accelerated however vishnevite was still not present in samples cured at 80°C for 28 days. Vishnevite formation is believed to be dependent on the oxidation of the sulphur present in the PFA.
- The formation of Friedel's salt offered a method of Cl retention during regulatory leach testing. Small amounts of Cl may also be retained in sodalite but not to any real consequence. Due to the reaction of the CaClOH phase in the APC residue with NaOH, a significant proportion of the chloride was present as highly soluble NaCl suggesting high release during leach testing.
- Leach testing also resulted in formation of sodalite and vishnevite for reasons which are not known.

6 Results and Discussion-Performance Testing

In this chapter results and discussion of performance testing conducted on the samples characterised in chapter 5 is presented. Testing was performed in order to optimise and examine the suitability of the treatment. Results were assessed against the waste acceptance criteria for stable non-reactive (SNR) and hazardous waste cells [92], and the criteria detailed by Stegemann and Zhou [157].

In addition to the variables examined in chapter 5, namely, waste:binder ratio, curing temperature, and the use of the WC solution or de-ionised water as the liquid phase, performance of blends with varied l/s was examined. Samples were also examined using CEM I and de-ionised water as reagents in order to compare the merits of the different treatment options.

Table 6.1 shows the proportions used for the blends studied in this work. Residue A1 was again used throughout this chapter. Mix designs for samples also examined in chapter 5 are repeated for the readers' convenience. Nomenclature, consistent with chapter 5, indicated waste:binder ratio followed by an indication of deviations from the standard conditions i.e.

- use of the WC solution as an activator,
- curing temperature of 38℃
- use of the co-fired PFA as a reagent,
- l/s=1

Curing temperatures were indicated in brackets whilst reagents and activators were indicated by initials, CEM=CEM I, DIW=de-ionised water.

Sample nomenclature	APC (g)	PFA (g)	CEM (g)	WC (g)	DIW (g)	l/s (w/w)	Curing Temp (°C)
1:4 l/s=0.55	12.9	51.6		35.5		0.55	38
1:4 l/s=0.75	11.4	45.6		43		0.75	38
1:4	10	40		50		1	38
2:3 (23)	20	30		50		1	23
2:3	20	30		50		1	38
2:3 DIW	20	30			41.1[a]	0.82[a]	38
2:3 (80)	20	30		50		1	80
3:2	30	20		50		1	40
2:3 CEM l/s=0.5	26.7		40		33.3	0.5	23
2:3 CEM l/s=0.6	25		37.5		37.5	0.6	23

Table 6.1 Mix proportions, curing temperature and nomenclature. APC=A1, PFA=Co-fired PFA, CEM= CEM I 42.5, WC=Waste caustic solution, DIW=de-ionised water. [a]DIW content was calculated as the same volume as the WC solution

6.1 Effects of l/s ratio variation

Increasing the l/s resulted in greater workability (Table 6.2), due to a reduction in the volume fraction of solids in the paste [330]. With an APC residue:PFA ratio of 1:4, flow criteria of >~175mm suggested by Stegemann and Zhou [157] was met with l/s≥0.75. With l/s=0.75, flow was well in excess of 175mm however, suggesting further reductions in l/s would be possible whilst still satisfying the criteria although a ratio of 0.55 was too low.

Consistent with previous work [67, 241], setting times increased with increasing l/s ratio (Table 6.2). An increase in setting times of cement paste is also typical when increasing the w/c ratio since interparticle spacings are increased, and so a greater degree of hydration may be required to achieve final setting [422]. The final setting time criterion of <~24hours [157] was satisfied with l/s≤0.75 when APC residue:PFA ratio of 1:4 was used and

samples were cured at 38°C. All initial setting times surpassed the 8 hour criteria suggested. Setting times were considerably longer than blends of APC residue with CEM I or ggbs [67, 166, 241]. Shi [271] reported final setting time of 60.05 hours for a lime:fly ash blend (1:4) prepared with l/s=0.35 cured at 23°C. Other work has shown lime:fly ash (3:7) prepared with l/s=0.44, cured at 25°C to produce final setting times of 54 hours [268]. Addition of between 2-6% NaOH or NaCl were observed to reduce the final setting time to ~20 and 43 hours respectively [268]. Such values are of similar order of magnitude to the samples studied here, although some variation would be expected due to factors such as relative fly ash fineness, l/s ratio variations, curing temperature and the inclusion of the APC residue.

Sample	Flow Value (mm)	Final Setting Time (h)	28d UCS (MPa)	UCS (7d sub) (MPa)	Bulk Porosity (%)
1:4 l/s=0.55	145	14.75	13.4 +/- 1.6	12.3	44.9
1:4 l/s=0.75	215	22	10.1 +/-1.4	9.4	52.2
1:4	>	31.75	4.6 +/-1.1	2	60.2

Table 6.2 Workability, final setting time, UCS and bulk porosity results for samples with varying l/s. Prepared with APC residue:PFA=1:4, cured at 38°C. >=greater than testable by flow table

The additional volume contributed by the liquid in the pastes at higher l/s also resulted in greater porosity and consequently lower compressive strength (Table 6.2 and Figure 6.1) [368]. Higher l/s also resulted in a greater proportional loss of compressive strength (from the mean) during submersion in water for 7 days (Table 6.2) as well as during the 64 days of EA NEN 7375 (Table 6.3) due to wash out of solids. Notable strength loss was observed from sample 1:4 as a result of 7 days submersion, due to leaching of solids, whilst strength recorded with l/s=0.55 and 0.75 lay within 1 standard deviation of the mean and may therefore be considered insignificant. Over 64 days submersion significant loss was recorded for samples with l/s=0.75 and

1 whilst sample 1:4 l/s=0.55 showed an increase in compressive strength suggesting continued formation of minerals which contributed to UCS, such as C-S-H, offset the loss due to leaching. All samples met monolithic WAC criteria for compressive strength of >1MPa with and without 7 days submersion as well as following 64 days submersion according to EA NEN 7375. Samples remained cohesive with no signs of deleterious swelling during submersion procedures. Such behaviour confirmed strength development was due to reaction product formation rather than drying [157].

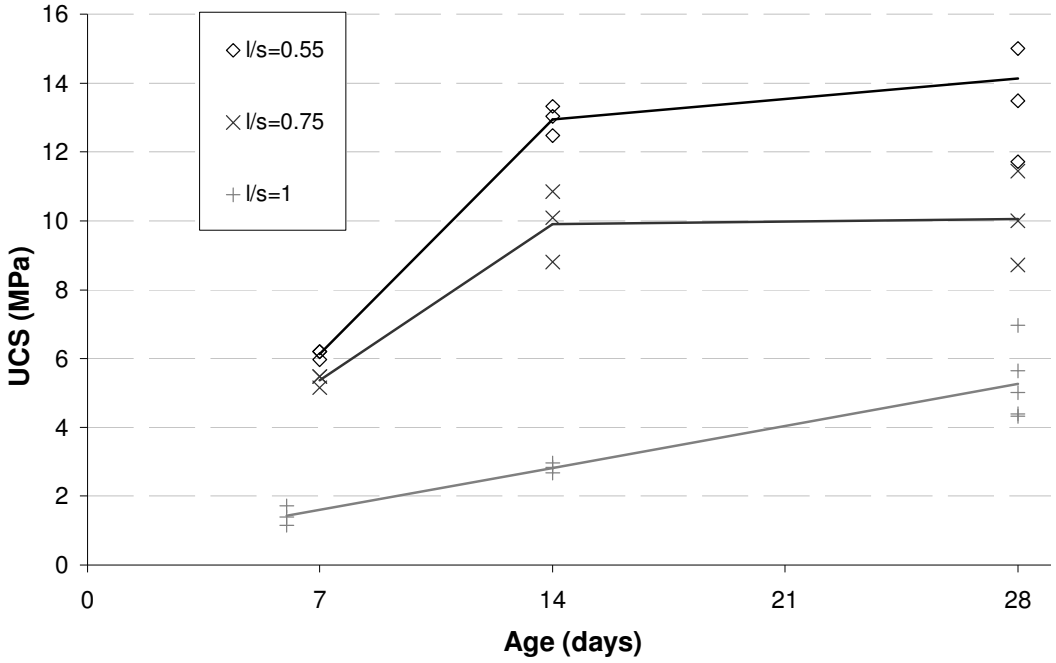

Figure 6.1 Effect of l/s on compressive strength development of samples prepared with APC residue: PFA ratio=1:4, cured at 38°C, over 28 days

Greater strength loss during submersion indicated greater open porosity with higher l/s. This was also reflected in the monolithic leach behaviour. Rapid chloride release from samples prepared at a waste:binder ratio of 1:4 resulted in depletion, as evident from the gradient of the log-log plots (Figure 6.2, Figure 6.3 and Figure 6.4), and prevented calculations of diffusion coefficients. Slower chloride release with reduced l/s could however be seen from the measured cumulative release plots and was reflected in the reduced percentages of Cl released throughout the test (Table 6.4). Release from granular leach tests on the samples following the monolithic test showed little retention of water soluble chlorides in any of the samples. Slightly greater

release from sample 1:4 l/s=0.55 coincided with the lower percentage release calculated during the monolithic test (Table 6.4). Differences in the measured cumulative release (Table 6.4) could be explained in terms of the percentage release and variation in availability. Availability of Cl increased with reduced l/s due to an increased dry fraction and the different degree of compaction the samples underwent when casting. Due to their highly soluble speciation, primarily as NaCl as previously identified, all samples exceeded chloride limits in monolithic SNR and hazardous landfill cell WAC (10,000mg/m^2 and 20,000mg/m^2 respectively).

	UCS before and after EA NEN 7375			
Sample	**Before (MPa)**	**Standard Deviation**	**After (MPa)**	**% loss**
1:4 l/s=0.55	13.4	1.6	16.8	-25.37
1:4 l/s=0.75	10.1	1.4	8.1	19.80
1:4	4.6	1.1	2.1	54.35

Table 6.3 Compressive strength before and after EA NEN 7375. Samples prepared with varying l/s ratios, APC residue:PFA ratio=1:4, cured at 38°C

	Chloride				
Sample	**ε^*_{64} (mg/m^2)**	**pD_e**	**Diffusion controlled increment**	**% release**	**12457-2 after (mg/kg)**
1:4 l/s=0.55	256,500	na	none	67	5480
1:4 l/s=0.75	279,300	na	none	87	380
1:4	234,800	na	none	90	280

Table 6.4 Monolithic leach (EA NEN 7375) chloride results for samples with varying l/s. Prepared with APC residue:PFA ratio=1:4, cured at 38°C. ε^*_{64}=measure cumulative 64 day release. pD_e=-log of effective diffusion coefficient (D_e m^2/s), na=not applicable

The presence of chlorides as primarily NaCl meant the large majority were released during granular leach testing (Table 6.5). This resulted in samples generally exceeding the chloride limits established in the granular WAC for SNR and hazardous cells (15,000mg/kg and 25,000mg/kg respectively).

Release from sample 1:4 l/s=1 was slightly under the hazardous limit but remained very close to the threshold (Table 6.5).

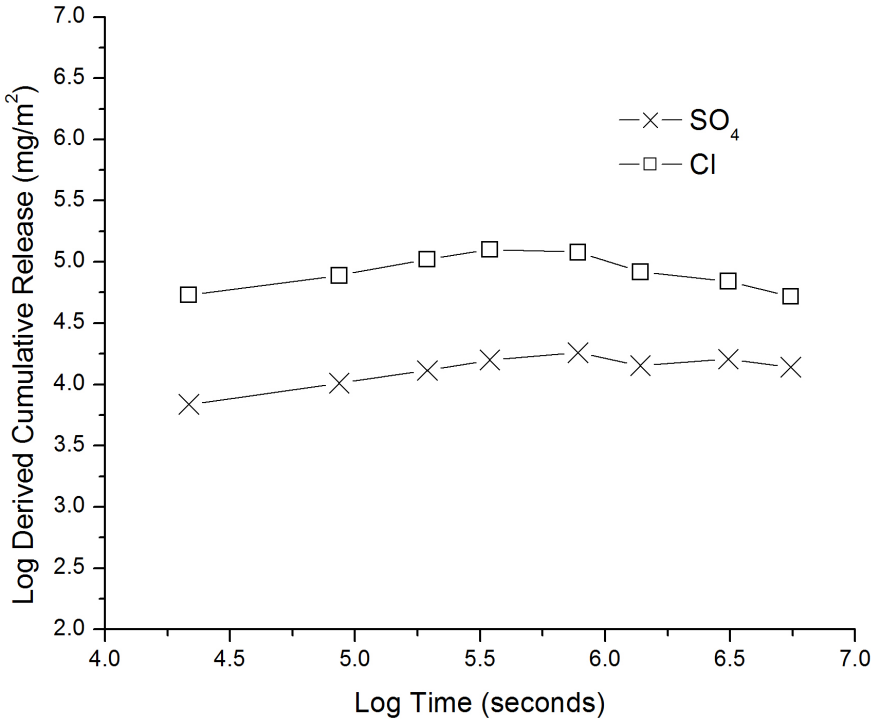

Figure 6.2 Log-log plot for sample 1:4 l/s=0.55, resulting from analysis of EA NEN 7375

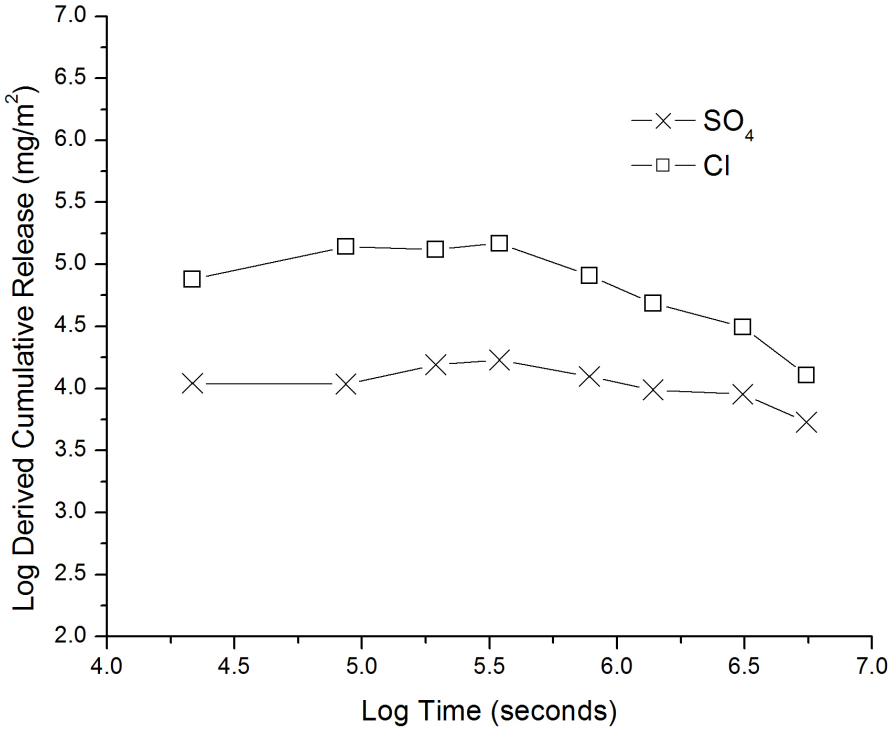

Figure 6.3 Log-log plot for sample 1:4 l/s=0.75, resulting from analysis of EA NEN 7375

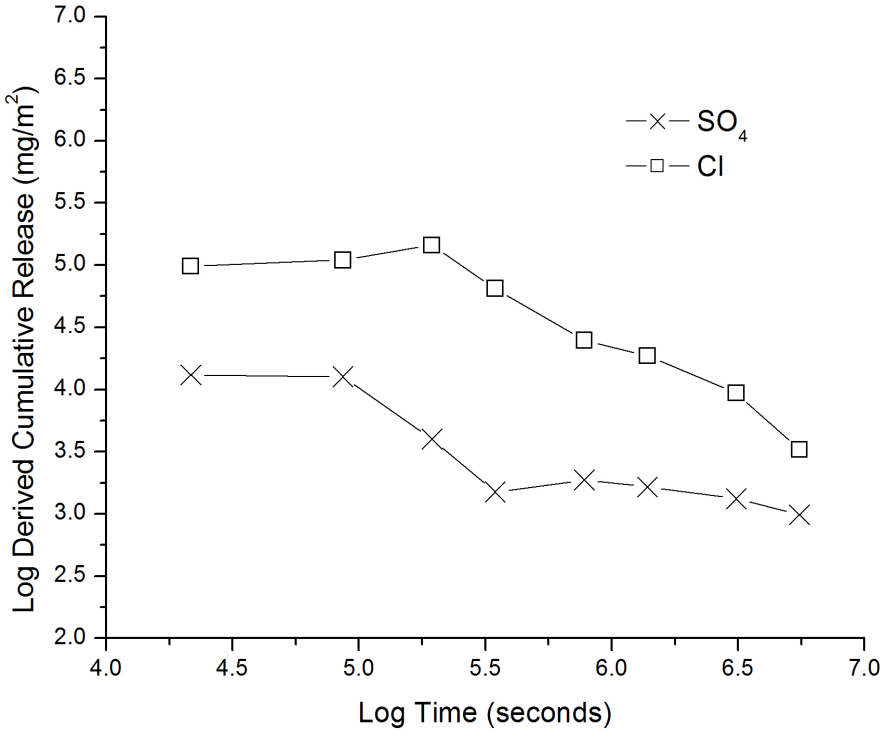

Figure 6.4 Log-log plot of sample 1:4, resulting from analysis of EA NEN 7375

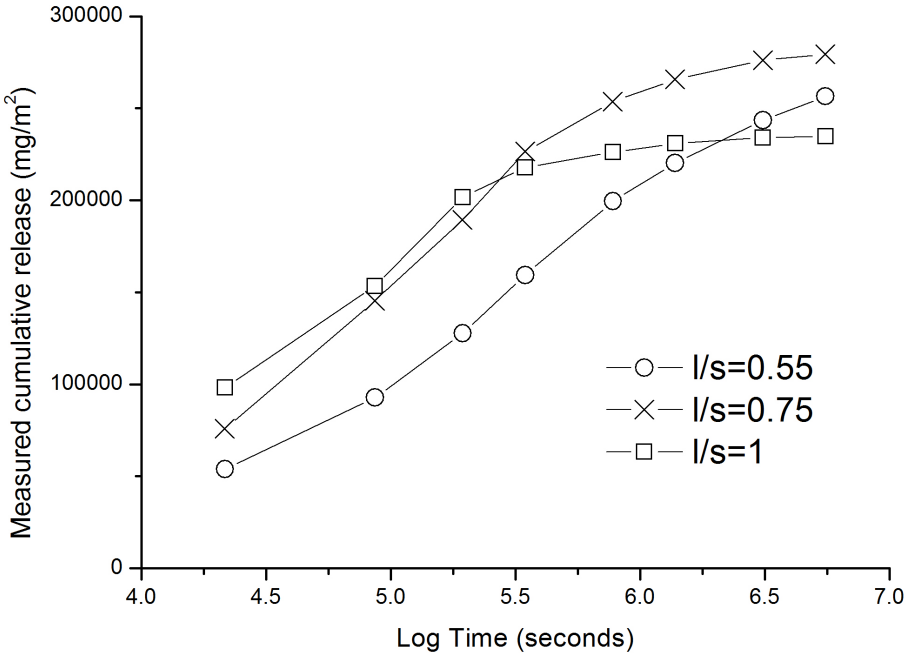

Figure 6.5 Measured cumulative release during EA NEN 7375 from samples prepared with varying l/s, APC residue:PFA=1:4, cured at 38°C for 28 days

	1:4 l/s=0.55	1:4 l/s=0.75	1:4
Cl availability (mg/kg)	35,500	34,700	31,700
Cl 12457-2 (mg/kg)	26,300	27,700	21,200
SO_4 availability (mg/kg)[a]	83,100	81,300	74,400
SO_4 availability (mg/kg)[b]	3341	3536	3526
SO_4 12457-2 (mg/kg)	4900	4350	2850
pH	12.3	12.4	12.3
pH (1mEq/g HNO_3)	11.5	11.7	12
TDS (mg/kg)	175,000	149,500	120,000

Table 6.5 Granular leach (BS EN 12457-2) results for samples with varying l/s. Prepared with APC residue:PFA ratio=1:4, cured at 38°C. [a]availability calculated assuming all S is SO_4 [b]availability calculated based on release from as-received materials according to BS EN 12457-2 and analysis by IC

TDS from all samples also exceeded granular SNR and hazardous WAC (60,000 and 100,000mg/kg respectively) (Table 6.5). Samples prepared at higher l/s bound a greater proportion of water as observed by monitoring the change in dry mass density in the fresh mix and at 28 days. Samples prepared at l/s=0.55, 0.75 and 1 underwent a dry mass increase of 170,000, 272,000 and 330,400mg/kg respectively. This would dilute the soluble fraction which may explain the decreased release of Cl, SO_4 and TDS with increased l/s during granular leach testing.

Sulphate release was constantly below granular SNR WAC limits (20,000mg/kg) and followed the same trend as chloride release, increasing with reduced l/s (Table 6.5). However, despite meeting granular WAC, release exceeded the monolithic limits for both SNR and hazardous sites (10,000mg/m^2 and 20,000mg/m^2 respectively). Conversion of the release during the monolithic test to mg/kg, based on the dry weight of the test piece (50mm cube) at 28 days, revealed the total sulphate release during the

monolithic test to be very similar, or slightly less than that of the granular test. Samples 1:4, 1:4 l/s=0.75 and 1:4 l/s=0.55 released 2763, 3999 and 3620mg/kg respectively during EA NEN 7375. It is noted that sulphate release equal to the SNR granular WAC limit of 10,000mg/kg, occurring from a 50mm^3 test piece with a dry mass of 150g would result in a measured release of 100,000mg/m^2 well above the monolithic hazardous WAC limits. This highlights the extent to which leaching is expected to be reduced from a monolithic product. Such data suggests that similar to chloride release, sulphate release was slowed by physical encapsulation but not sufficiently to meet monolithic WAC. Sulphate release relative to availability calculated assuming all sulphur to be present as sulphate was very low, releasing <6% of available sulphate (Table 6.6 and Table 6.5). This appeared to be primarily a result of the presence of considerable concentration of reduced forms of sulphur in the PFA. When comparing the release relative to availability calculated by performing BS EN 12457-2 on the as-received APC residue and PFA, and analysing the WC solution by ion chromatography, a much greater percentage was released, occasionally greater than 100%. Release greater than 100% would perhaps support the idea of oxidation of the sulphur to increase the sulphate availability.

	Sulphate					
Sample	**ε^*_{64} (mg/m^2)**	**pD_e**	**Diffusion controlled increment**	**% release**		**12457-2 after (mg/kg)**
				a	**b**	
1:4 l/s=0.55	38,700	na	none	3	109	2000
1:4 l/s=0.75	36,800	na	none	3	113	0
1:4	22,900	na	none	2.5	78	0

Table 6.6 Monolithic leach (EA NEN 7375) sulphate results for samples with varying l/s. Prepared with APC residue:PFA ratio=1:4, cured at 38°C. a=availability calculated assuming all S is SO_4, b=availability calculated based on SO_4 release from raw materials according to BS EN 12457-2 and analysis by IC.

Little difference was evident in the pH of the monolithic or granular leachates obtained with varying l/s (Figure 6.6 and Table 6.5 respectively). The NaOH in the WC solution appeared to be neutralised. A significant proportion would

be neutralised by the reaction with the CaClOH. However, considering the mix proportions this could not neutralise all of the NaOH. Other mechanisms of neutralisation may have included carbonation, zeolite formation, charge balancing C-S-H and perhaps Na_2SO_4 production. The pH of the granular leachates slightly exceeded the suggested pH thresholds of ~11.9-12.2 [157] which would have implications for the solubility of amphoteric metals such as Pb and Zn [69, 112]. It may be that the slightly higher pH in the earlier fractions of the monolithic test was related to the greater release of alkalis from the matrix, owing to the greater open porosity, whilst this was reversed in later fractions due to depletion with higher l/s.

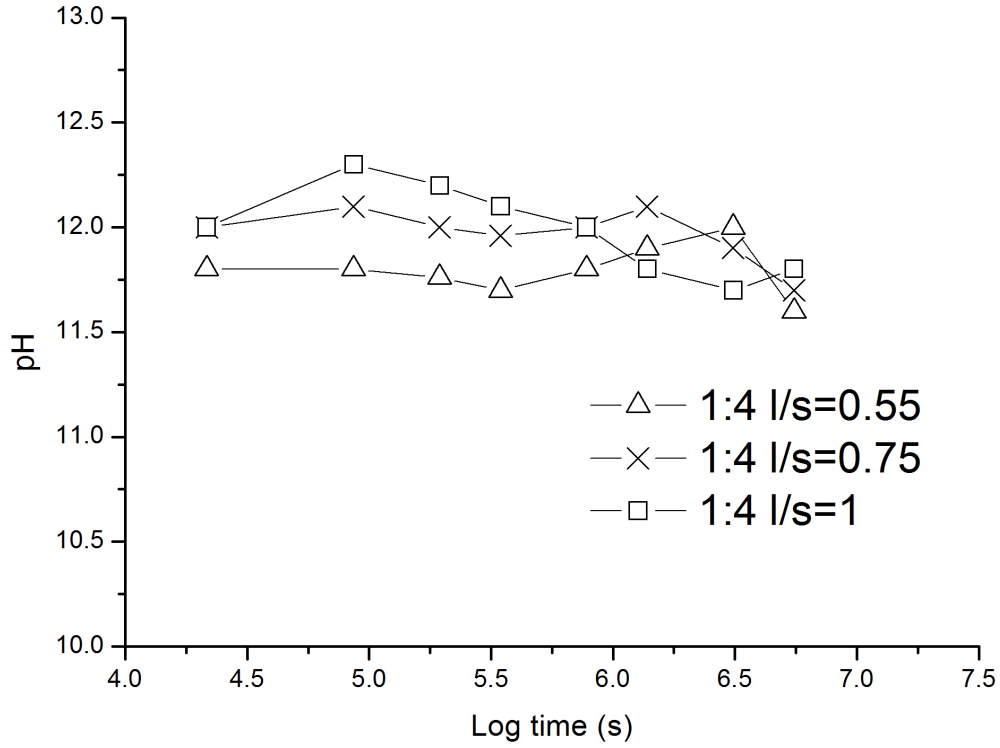

Figure 6.6 Development of leachate pH during EA NEN 7375. Samples with varying l/s ratio prepared with APC residue:PFA=1:4, cured at 38°C

Full ANC curves were not obtained for samples with varying l/s. However, all samples showed ANC>1mEq/g to pH=9 and therefore met the criteria for segregated landfill disposal proposed by Stegemann and Cote [152]. With 1mEq/g addition pH values of 11.5, 11.7 and 12 were observed for l/s=0.55, 0.75 and 1 respectively showing perhaps a slightly greater capacity with higher l/s, coinciding with greater Na concentration. Since Na present as

NaCl would provide no alkaline buffering, the buffering would be attributed to the Na based reaction products formed from the NaOH remaining after complete reaction of the CaClOH.

6.1.1 Summary of the effects of l/s ratio variation

The following conclusions can be drawn on the effects of l/s ratio adjustment

- Increasing l/s causes an increase in workability. Workability criteria of >~175mm flow table spread was exceeded for blends with l/s≥0.75 cast with a waste:binder ratio=1:4. Results suggested criteria would still be met with a slight decrease in l/s.
- Increasing the l/s increased the setting time of the blends. When working with a waste:binder ratio of 1:4 and curing at 38℃, increasing the l/s above 0.75 resulted in final setting times in excess of 24 hours.
- Porosity was increased and compressive strength of the monoliths reduced at all ages between 7 and 28 days due to increased l/s. All samples met 28 day compressive strength of 1MPa as required by the WAC.
- Compressive strength loss (deviation from mean) as a result of 7 days submersion was also greater at higher l/s.
- Increased l/s ratio increased the rate of Cl release during the 64 day monolithic leach test EA NEN 7375.
- Measured chloride release during EA NEN 7375 was a consequence of the rate of release, along with the varied availability. Increasing the l/s ratio decreased the availability in a given volume of sample due to varied dry mass density.
- Variation in the l/s ratio had a minor effect on chloride and SO_4 release during granular leach testing. Samples prepared at higher l/s bound a greater amount of water which resulted in dilution of analytes as a %w/w of dry mass.
- pH of batch extractions of the samples with de-ionised water did not appear to be affected by variations in l/s.

In conclusion when optimising performance of an s/s matrix it is preferential to reduce the l/s ratio as far as possible without making the paste unworkable. This minimises setting time, increases compressive strength and increases physical encapsulation offered by the product. Minimising l/s also appeared to reduce the dilution of contaminants however, resulting in higher availability in a given volume or weight of s/s product.

6.2 Effects of waste:binder ratio variation

As found previously [67, 241] mix workability decreased as APC residue content was increased (Table 6.7). This is due to the hygroscopic nature of the residues owing to a high salt content and specific surface area/irregular morphology of the residue [67]. To meet the flow table spread criterion of >~175mm with an APC residue content >20%w/w, a l/s>1 would be required. This behaviour implies significant l/s would be required to achieve an economic and resource efficient treatment i.e. with a high waste:binder ratio. Increasing the l/s ratio had implications for the structure and durability of the samples as previously discussed (chapter 6.1) and would also have implications for the amount of residue which could be treated with the WC solution.

Sample	Flow Value (mm)	Final Setting Time (h)	28d UCS (MPa)	UCS (7d sub) (MPa)	Bulk Porosity (%)
1:4	>	31.75	4.6 +/-1.1	2	60.2
2:3	180	31.25	8.7 +/-1.5	7.5	55.3
3:2	135	49	6.5 +/-1.6	6.3	56.0

Table 6.7 Workability, final setting time, UCS and bulk porosity results for samples prepared at varying APC residue:PFA ratios, l/s=1, cured at 38°C. >=greater than testable by flowtable

The setting time of the blends was a result of several factors. Workability shows strong positive correlation with the setting time of pastes [67, 241]. Workability is largely a reflection of the interparticle spacings i.e. the volume fraction of solids/liquids [330]. Greater spacing (lower volume fraction of

solids) increases workability and, as previously discussed, also results in a greater degree of hydration necessary for the physical process of setting [422]. Although l/s was equal for the mixes prepared at different waste:binder ratios, the hygroscopic nature of the APC residue appeared to reduce the amount of active water, reducing workability and the interparticle spacing of the solids. Considering only the physical properties of the pastes (indicated by flow table spread), the setting time of the blends with varied APC residue:PFA ratios would be expected as 1:4>2:3>3:2. This wasn't the case, samples 1:4 and 2:3 had very similar setting times, both considerably shorter than sample 3:2 (Table 6.7). The results therefore showed that when working at a constant l/s, increasing the waste:binder ratio (increasing the APC residue weight %) had a retarding influence on setting time which was offset to different extents by the physical properties of the pastes. This was confirmed by monitoring the heat flow from the samples with a calorimeter (Figure 6.7).

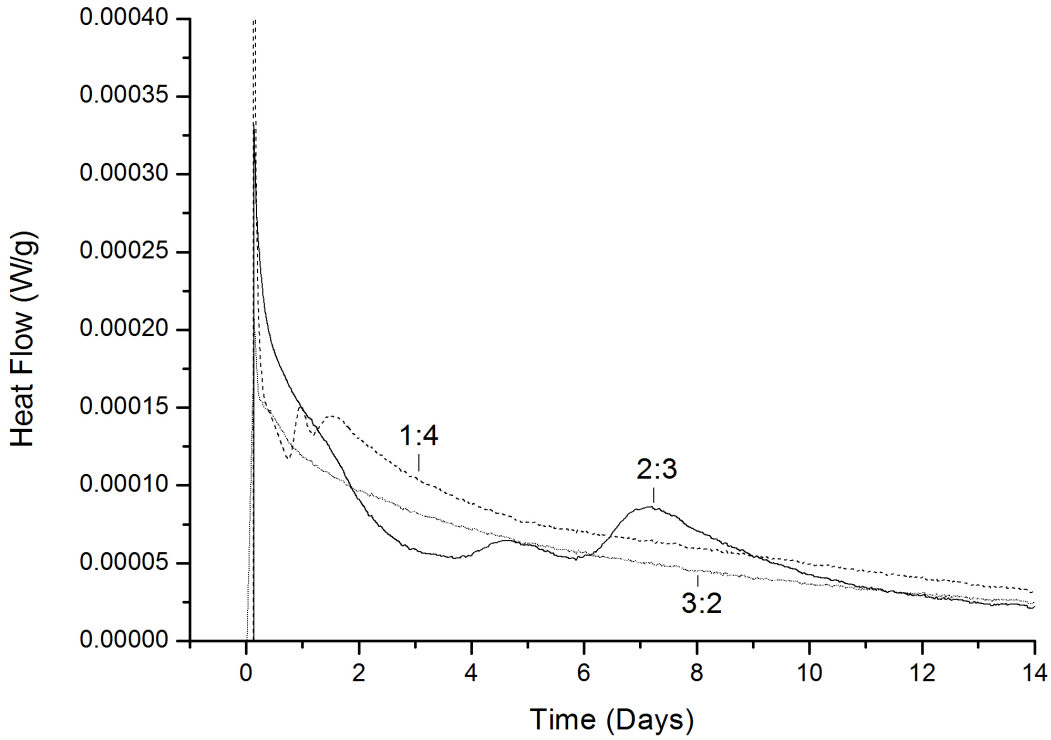

Figure 6.7 Effect of varying APC residue:PFA ratio on heat evolution of samples prepared with l/s=1, cured at 38°C

Samples 1:4 and 2:3 showed similar heat evolution profiles consisting of three distinct peaks. With apparent acceleration as the APC residue content was reduced, highlighting the retarding effect on reaction kinetics of increasing the APC residue:PFA ratio. Sample 3:2 showed a constantly diminishing underlying heat evolution but the later two peaks were not observed despite monitoring the heat evolution for 28 days. In spite of these observations, sample 3:2 developed considerable compressive strength over this time (Table 6.7) and significant formation of reaction products was evident (chapter 5). Setting time could not be predicted from the heat evolution curves, since final set occurred at different positions relative to the peaks in each sample. This confirmed the influence of additional processes (the physical properties of the pastes) on setting, alongside the chemical reactions which can be monitored by calorimetry. Setting time of cement pastes may also vary in relation to heat evolution peaks depending on the w/c ratio [422], similarly showing the dependence on both the physical properties and chemical reactions.

The retarding effect on the chemical reactions could perhaps be attributed to the variation in the mass ratio of CaClOH to NaOH. Increasing the APC residue content resulted in greater conversion of NaOH to NaCl and $Ca(OH)_2$. Unlike NaOH, NaCl has little effect on accelerating setting time or strength development of lime/fly ash matrices [268, 272]. This is due to the greater effect NaOH would have on the dissolution of the glass matrix of the PFA owing to the higher pH [261]. Dissolution of the glass matrix is observed as the first, sharp exothermic peak evident when monitoring the heat flow over time (Figure 6.7) [267, 273]. Due to the delay between addition of the liquid phase and beginning calorimetry measurements (time for mixing, weighing and loading of sample<10 minutes+time for calorimeter to equilibrate after the drop in temperature due to opening and addition of materials ~20 minutes), a proportion of this peak was missed. However, the magnitude of the observed proportion of this peak was greatly increased with lower waste:binder ratio. This can be attributed to the greater NaOH content remaining after reaction with CaClOH as well as greater PFA content. To assist in clarity, the y axis of Figure 6.7 was limited to $4*10^{-4}$ W/g, however,

the height of the initial peaks for 1:4, 2:3 and 3:2 were ~$8.9*10^{-4}$, $3.7*10^{-4}$ and $2.1*10^{-4}$ W/g respectively. If the heat evolved was simply an effect of dilution then the peak height of sample 3:2 may have been expected to be approximately half of that observed for sample 1:4. It was considerably less, showing proportionally less dissolution of PFA, attributable to NaOH conversion to NaCl. In order to better study this peak, an attachment may be used to mix the samples within the calorimeter. Acceleration of the fly ash dissolution was consistent with the observed increase in the rate of $Ca(OH)_2$ consumption at early ages, and of sodalite formation in sample 1:4 than 2:3 reported in chapter 5.1. The initial peak appeared to occur at the same time for all of the samples and consisted of a shoulder, indicating it was composed of multiple peaks. Such behaviour has previously been observed [267] and attributed to the rapid precipitation of reaction products which depend on the solution composition but may include calcium silicate and aluminate hydrates, or $CaCO_3$ when Na_2CO_3 is introduced to the solution [267]. In the current samples, the formation of $Ca(OH)_2$ as the NaOH solution reacts with the CaClOH phase in the APC residue may contribute although it is assumed this reaction would occur rapidly i.e. before or at the same time as dissolution of the glassy PFA matrix. Friedel's salt was observed to be present in sample 2:3 after 3 days curing (Figure 6.8) suggesting the formation of this phase may contribute. Rapid formation of Friedel's salt may be assisted by the aluminium already solubilised in the WC solution which was observed to form Friedel's salt upon blending with the APC residue (chapter 5.1).

The cause of the heat production for the latter two peaks was less clear. Analysis by XRD on the sample 2:3 after 3 and 6 days curing (corresponding to either side of the second well defined peak observed by calorimetry) showed no new crystalline hydration products, (Figure 6.8) this peak may therefore be associated with formation of an amorphous product. This could include an amorphous zeolite precursor or calcium silico-aluminate [273]. The sample increased in crystallinity over time as evident from the increased intensity of the peaks including the quartz and mullite peaks. This indicated consumption of the amorphous glassy fraction of the PFA. Additionally, consistent with the TGA data previously reported (Figure 5.1), $Ca(OH)_2$ was

consumed. This was apparent by the loss of portlandite peak intensity relative to the quartz peak. The peaks associated with C-S-H (I) were also observed to be more prominent at later ages, particularly after 6 days (Figure 6.8). This may suggest the third peak was largely associated with C-S-H (I) formation.

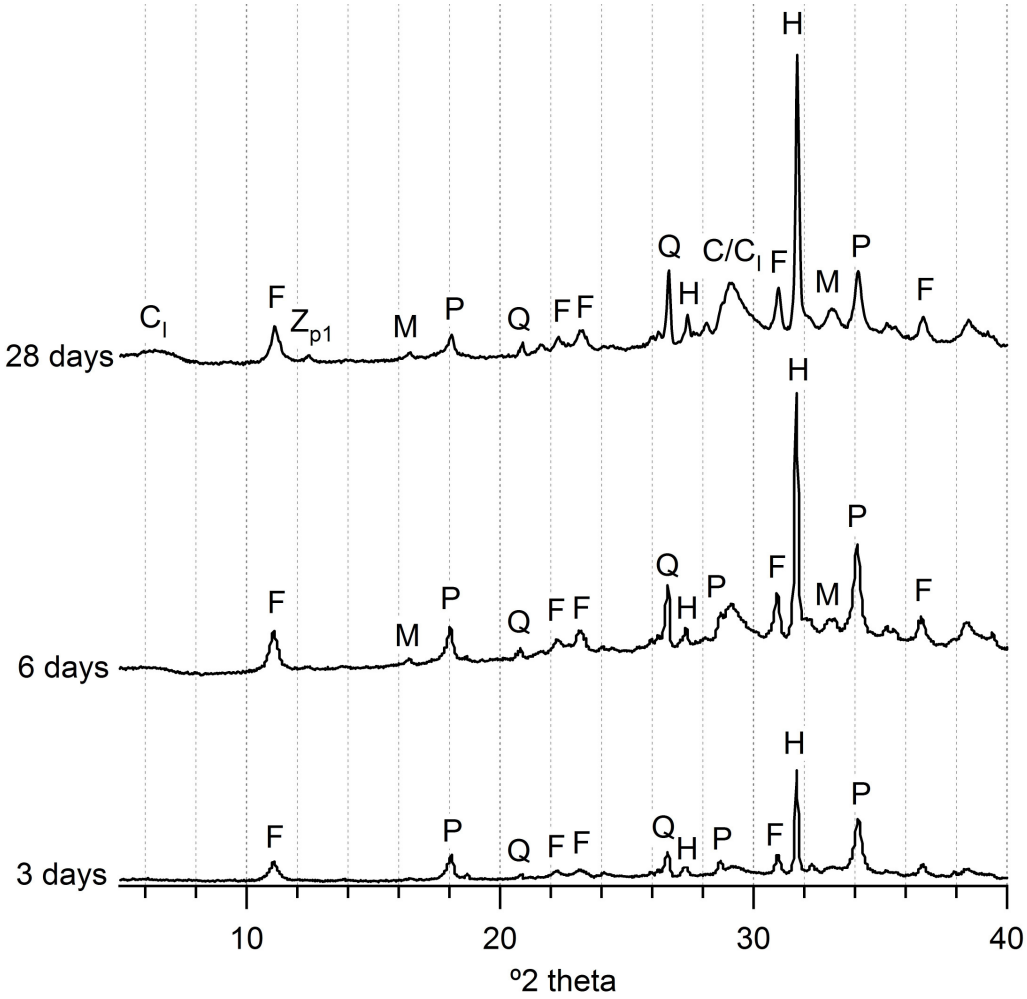

Figure 6.8 XRD patterns (y axis range normalised) for sample 2:3 cured for 3, 6 and 28 days at 38°C. F=Friedel's salt, M=mullite, P=portlandite, Q=quartz, H=halite, Z_{p1}=Na-P1

Figure 6.9 shows the effect of varying the APC residue:PFA ratio on compressive strength development of mixes with l/s=1. Since strength development was primarily due to pozzolanic reactions, then the variation in Ca/Al+Si as the APC residue:PFA ratio was changed, and the change in the nature of the reaction products can be assumed to have significantly impacted the UCS. Cumulative heat evolution over 28 days was greater with lower waste:binder ratios (Figure 6.10). However, this did not correspond to

increased compressive strength or reduced porosity since sample 1:4 displayed lower strength and higher porosity than samples 2:3 and 3:2 (Figure 6.9 and Table 6.7).

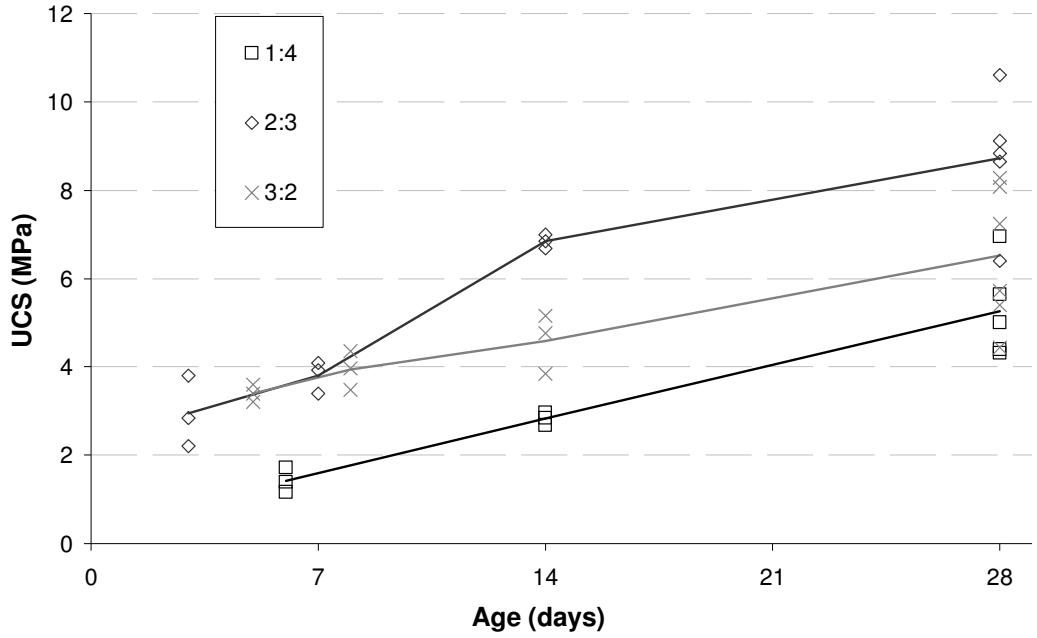

Figure 6.9 Effect of APC residue:PFA ratio on compressive strength development of samples prepared with l/s=1, cured at 38°C, over 28 days

The variations in plastic behaviour of the mixes, and therefore the degree of compaction achieved also played a considerable role in structural development. Freshly compacted samples showed densities of 1580, 1625, and 1660kg/m^3 for samples 1:4, 2:3 and 3:2 respectively. This degree of compaction achieved, coupled with the chemical reactions resulted in the observed porosities and compressive strengths. Sample 2:3 showed the highest strengths as well as the lowest porosity (Table 6.7).

All samples surpassed monolithic WAC criteria for compressive strength before and after submersion procedures. Strength loss upon 7 days submersion was far greater from sample 1:4 than samples 2:3 and 3:2 (Table 6.7), indicating strength loss during this procedure was mostly associated with the porosity rather than the soluble fraction present, which was observed by granular leach testing to be higher with increased waste:binder ratio (Table 6.8). Despite sample 3:2 having similar bulk porosity to 2:3, strength loss compared to the mean during 7 days submersion was lower, and a lower

effective diffusion coefficient was observed for chloride release during EA NEN 7375 (Table 6.9).

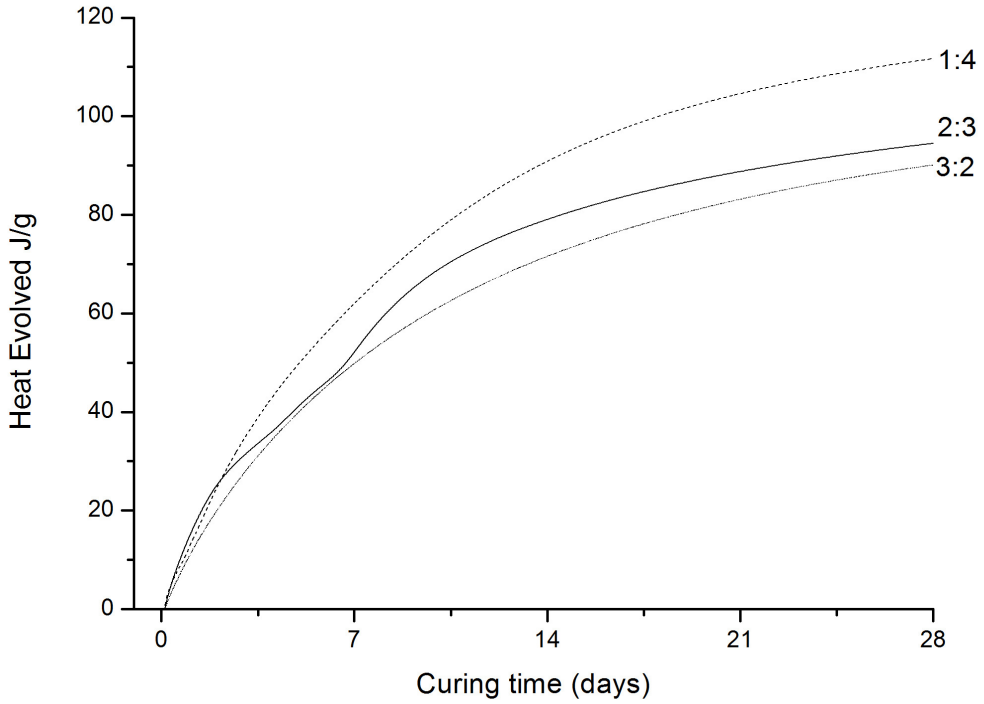

Figure 6.10 Cumulative heat evolution over the initial 28 days curing of samples prepared at l/s=1, cured at 38°C

	1:4	**2:3**	**3:2**
Cl availability (mg/kg)	31,700	62,400	97,800
Cl 12457-2 (mg/kg)	21,200	45,900	70,900
SO_4 availability (mg/kg)[a]	74,400	58,700	45,700
SO_4 availability (mg/kg)[b]	3526	3580	3816
SO_4 12457-2 (mg/kg)	2850	2259	5420
pH	12.3	12.5	12.5
pH (1mEq/g HNO_3)	12	12.3	12.5
TDS (mg/kg)	120,000	148,500	159,500

Table 6.8 Granular leach (BS EN 12457-2) results for samples prepared with varying APC residue:PFA ratios, l/s=1, cured at 38°C. [a]availability calculated assuming all S is SO_4 [b]availability calculated based on release from as-received materials according to BS EN 12457-2 and IC

	Chloride					
Sample	**ε^*_{64} (mg/m^2)**	**pD_e**	**ε_{64}**	**Diffusion controlled increment**	**% release**	**12457-2 after (mg/kg)**
1:4	234,800	na	na	none	90	280
2:3	298,500	10.7	746,400	1-4	55	13,170
3:2	466,300	11.5	434,300	2-7	55	22,660

Table 6.9 Monolithic leach (EA NEN 7375) chloride results for samples prepared with varying APC residue:PFA ratios, l/s=1, cured at 38°C. ε^*_{64}=measure cumulative 64 day release. pD_e=-log of effective diffusion coefficient (D_e m^2/s), ε_{64}=derived cumulative 64 day release (mg/m^2), na=not applicable

Considering the similar mineralogy of the chlorides in both samples, and low immobilisation observed by granular leach testing, these results appeared to indicate lower permeability. The permeability of samples 1:4, 2:3 and 3:2 was assessed at 28 days with and without 7 days prior submersion in de-ionised water and the results are presented in Figure 6.11. As discussed in chapter 3.3.9.1, due to the drying method employed such results should be viewed qualitatively. A permeability ranking of 1:4>2:3>3:2 positively correlated to the rate of chloride release, evidenced by effective diffusion coefficients for 2:3 and 3:2 and the rapid release precluding the calculation of a coefficient for 1:4. These results therefore suggested permeability of the monoliths to be responsible for the relative rates of diffusion observed. Considering the bulk porosity results this would indicate greater closed porosity in sample 3:2.

Despite the qualitative nature of the permeability results, the increase in permeability upon 7 days submersion in de-ionised water showed good correlation with compressive strength loss (deviation from mean) upon the same procedure (Figure 6.12) indicating that the same mechanism may be responsible for both. Absolute values were plotted because proportional values were influenced by the initial permeability for which several orders of magnitude difference may apply. Absolute values were also considered more accurate because removal of 1g of NaCl from one sample would increase porosity by approximately the same absolute volume as removal from another, however the proportional effect may be very different.

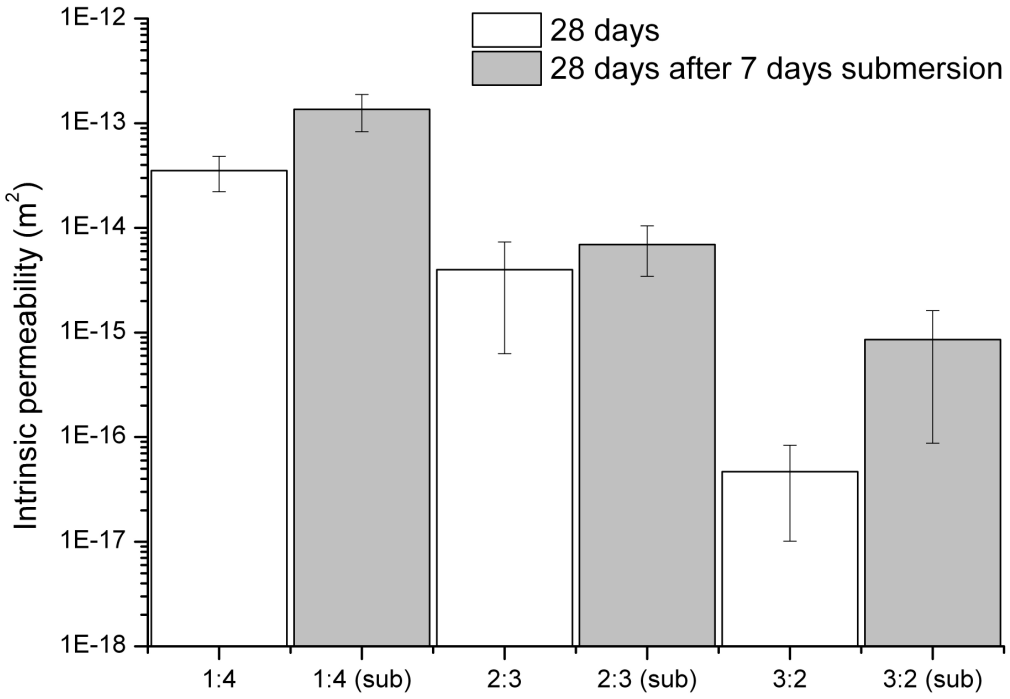

Figure 6.11 Intrinsic permeability of samples measured using N_2 with an absolute inlet pressure of 2bar, with and without 7 days submersion in de-ionised water. Samples prepared with varying APC residue:PFA ratios, l/s=1, cured at 38°C. Error bars indicate standard devation. Y scale is logarithmic.

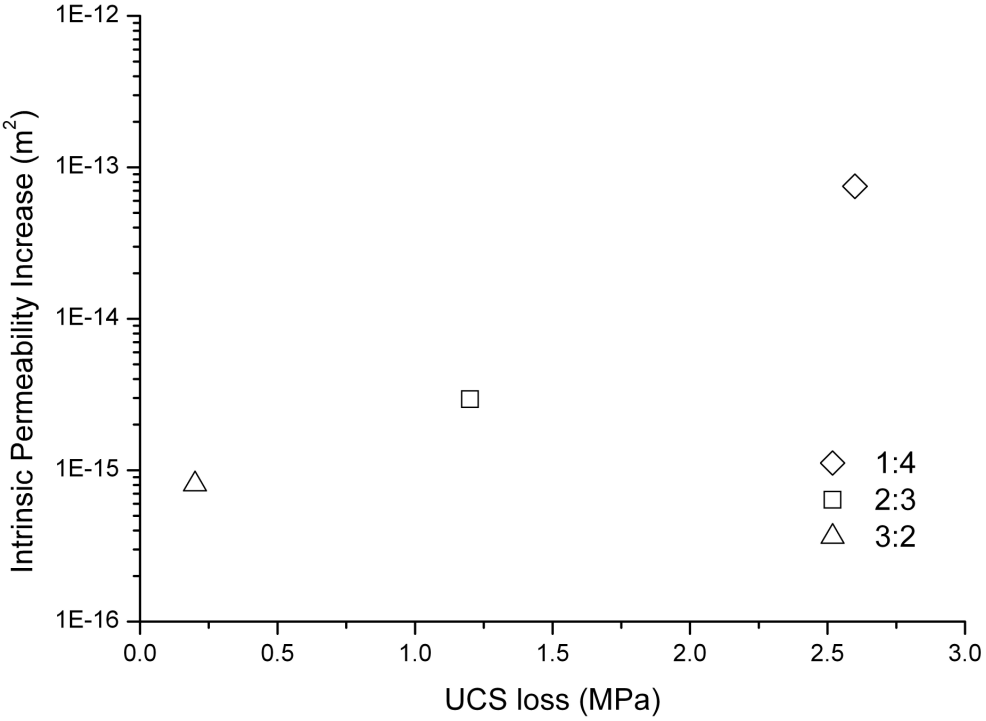

Figure 6.12 Relationship between absolute UCS loss and absolute permeability increase during 7 days submersion in de-ionised water

All samples showed an increase in permeability as a result of the submersion procedure. Such behaviour is important since the low permeability of s/s products is one of the key properties which prevent contaminant release, limiting the contact with water. As such an increase in the permeability may have significant consequences for the long term performance of an s/s product, reducing physical encapsulation of pollutants. These results also have implications for the suitability of prediction of long term release from similar s/s matrices based on diffusion coefficients obtained during EA NEN 7375 since such calculations assume a constant permeability which is evidently not the case. Effective diffusion coefficients may therefore only be observed as relative indexes [20].

The change in permeability after submersion for longer periods was not measured, however, samples 2:3 and 3:2 appeared to gain strength after longer periods of submersion (Table 6.10). This was perhaps a result of the longer submersion time allowing pozzolanic reactions to continue sufficiently to compensate for the loss of solids by leaching. If permeability fluctuations positively correlated with strength development over longer periods, the permeability of these pozzolanic matrices may be expected to fluctuate, suffering an initial increase as soluble salts are removed, but then decreasing as pozzolanic reactions progress over longer periods. As was discussed in chapter 3.3.9.1 samples could not be dried to a constant weight without suffering cracking due to drying shrinkage. This highlighted a concern for the treatment. Any s/s product should be able to withstand wetting and drying cycles without degradation in order to maintain long term performance in the field [152].

	UCS before and after EA NEN 7375			
Sample	**Before (MPa)**	**Standard Deviation**	**After (MPa)**	**% loss**
1:4	4.6	1.1	2.1	54.35
2:3	8.7	1.5	13.6	-56.32
3:2	6.5	1.6	8.4	-29.23

Table 6.10 Compressive strength before and after EA NEN 7375. Samples prepared with varying APC residue:PFA ratios, l/s=1, cured at 38°C

Despite the slower rate of release owing to the reduced permeability at higher APC residue:PFA ratios, the measured chloride release was positively correlated with availability for both granular (Table 6.8) and monolithic (Table 6.9) tests and both granular and monolithic hazardous WAC limits were exceeded (or close to the limit in the case of sample 1:4). Such behaviour was consistent with the previously reported characterisation of the samples after leaching, showing removal of large quantities of NaCl.

As observed for samples with different l/s ratios, sulphate release met SNR granular WAC limits but exceeded hazardous monolithic limits. Sulphate release was highest from sample 3:2 in both granular and monolithic tests (Table 6.8 and Table 6.11 respectively). Leach testing of the raw materials revealed SO_4 release of 3500mg/kg from the APC residue, 2800mg/kg from the PFA and 1506mg/kg in the WC solution. If these values were maintained when blended the APC residue would be the most significant contributor to soluble SO_4, in which case sulphate release from sample 3:2 would be expected to be the highest. Sulphate release from sample 3:2 exceeded that calculated as available based on release from the as-received PFA and APC residue according to BS EN 12457-2, and the concentration in the WC solution determined by IC. However, due to the high pH environment and atmospheric exposure, the reduced sulphur in the PFA would be expected to gradually oxidise [155, 414], supplying more SO_4. This was evidenced by production of vishnevite over extended curing periods (chapter 5). The availability in sample 1:4 could therefore potentially increase beyond that of sample 3:2. The sustained high chloride release from sample 3:2 could also play a role in sulphate solubilisation. Sulphates are known to be more soluble in NaCl solutions due to solute-solvent ion interactions which reduce the activity of the sulphate ions therefore demanding greater solubilisation to maintain equilibrium [323, 423]. The same process increases the solubility of $Ca(OH)_2$ and C-S-H in NaCl solutions [236]. This effect is concentration dependant, Duchesne and Reardon [424] showed changes to be most prominent in concentrations up to ~1M NaCl. Previous work has generally presented data in relation to equilibrium conditions. Monolithic leach tests are designed to avoid equilibrium conditions since the concentration gradient is

the driving force for diffusion which is the property being studied. However, if the same process also increases the rate of dissolution it may explain the often observed similarity between the log-log plots for the chlorides and sulphates. Fractions which demonstrated high chloride release also generally showed high sulphate release as evident from the log derived cumulative release-log time plots (e.g. Figure 6.13 and Figure 6.14). Such behaviour may also explain the greater percentage release of SO_4 from sample 3:2 during EA NEN 7375 (Table 6.11).

Sample 3:2 showed a surface wash off during the monolithic test, which was evident from the shape of the log derived cumulative release-log time plot (Figure 6.14). Such an event was consistent with the observation of a 'fluffy' white efflorescence which XRD analysis revealed to be NaCl (Figure 6.15). A surface wash off may occur due to a soluble surface coating resulting from process conditions or a condensation process [20]. In this case, the high levels of NaCl present in the sample, coupled with the relatively low porosity, and transport of the chlorides as the sample dried appeared to form the efflorescence. The surface wash off explained the equal percentage chloride release observed from 2:3 and 3:2 (Table 6.9) despite the slower diffusion behaviour.

	Sulphate						
Sample	**ε^*_{64} (mg/m^2)**	**pD_e**	**ε_{64}**	**Diffusion controlled increment**	**% release**		**12457-2 after (mg/kg)**
					a	**b**	
1:4	22,900	na	na	none	2.5	78	0
2:3	21,200	11.2	48,700	1-4	2.5	68	1700
3:2	28,900	11.5	34,700	2-7	4.5	88	1660

Table 6.11 Monolithic leach (EA NEN 7375) sulphate results for samples prepared with varying APC residue:PFA ratios, l/s=1, cured at 38°C. a= availability calculated assuming all S is SO_4, b=availability calculated based on release from as-received materials during BS EN 12457-2 and IC

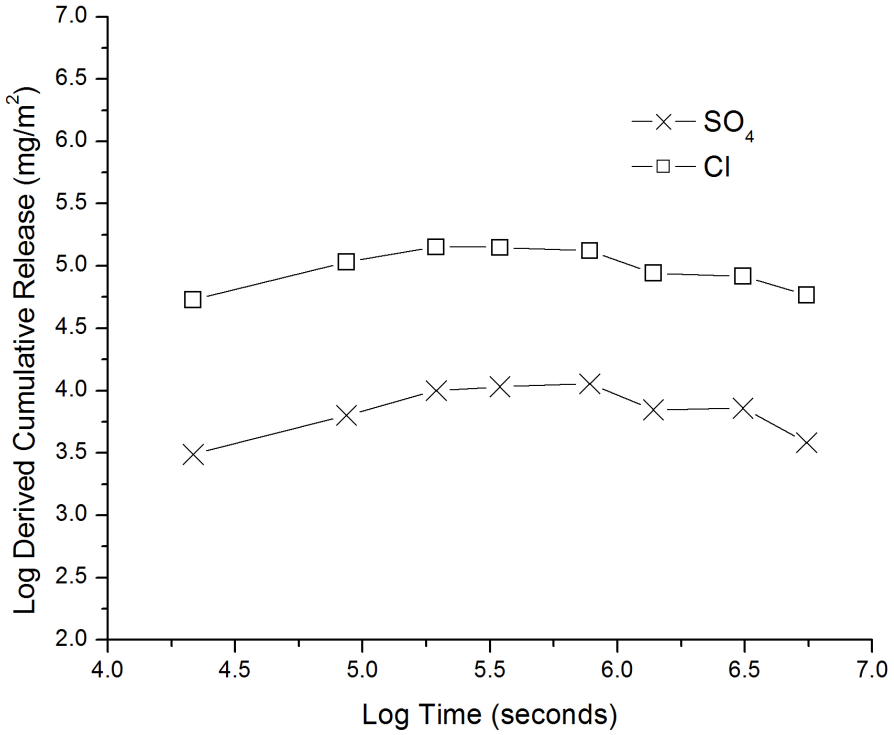

Figure 6.13 Log-log plot for sample 2:3, resulting from analysis of EA NEN 7375

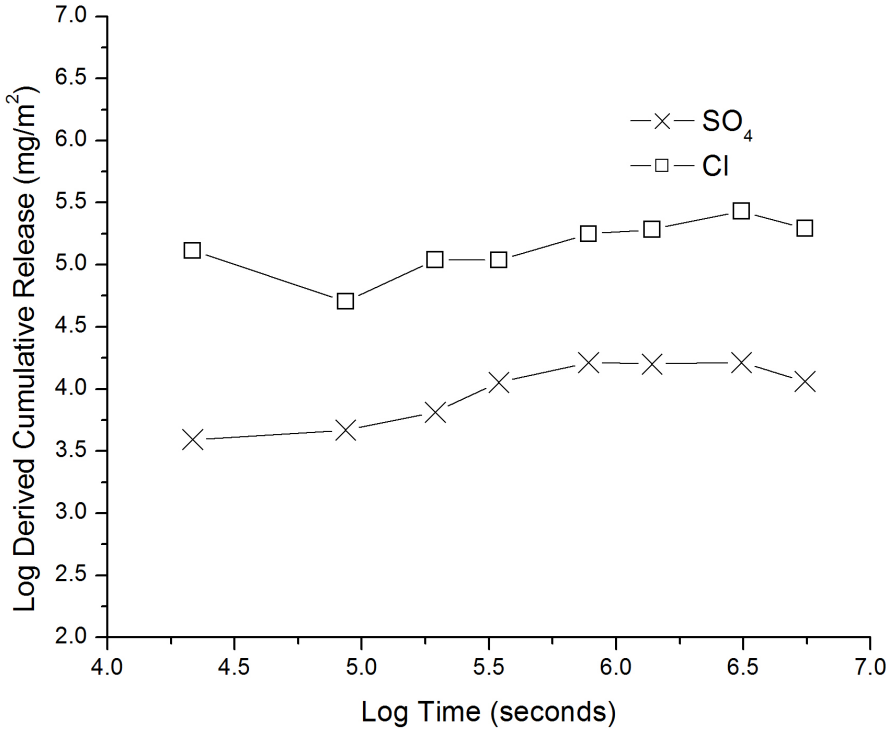

Figure 6.14 Log-log plot for sample 3:2, resulting from analysis of EA NEN 7375

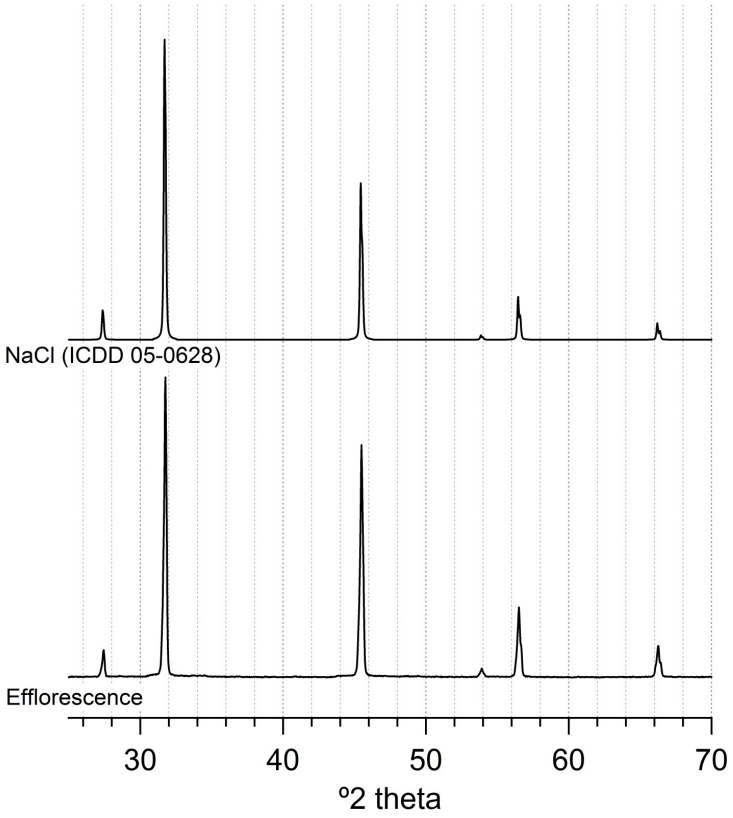

Figure 6.15 XRD pattern for NaCl efflorescence of sample 3:2

The pH observed during BS EN 12457-2 varied very little with waste:binder ratio (Table 6.8) and consistently exceeded the suggested upper limit of 12.2 [157]. Based on the pH values (~12.5) $Ca(OH)_2$ appeared to be the controlling factor, which was identified in the samples by XRD and STA (chapter 5). $Ca(OH)_2$ was likely to have leached in significant quantities, perhaps aided by the high Cl concentration in the early fractions of the test [236, 424]. Such behaviour, coupled with the availability of $Ca(OH)_2$ in the samples (1:4<2:3<3:2 see Figure 5.1) resulted in significant variation in pH during the later fractions of the monolithic test (Figure 6.16). It was likely that following EA NEN 7375 $Ca(OH)_2$ was no longer present in sample 1:4 and whilst some remnant was observed in sample 2:3 (results not presented), and would also be expected in sample 3:2. The pH of ~11.8 over the later fractions of EA NEN 7375 of sample 1:4 may be regarded as a result of buffering by some of the less soluble compounds present in the matrix. Sample 1:4 showed the lowest compressive strength and highest porosity but importantly did maintain cohesion and a UCS greater than 1MPa after EA NEN 7375 suggesting some stable hydration products were retained.

Leaching of synthetic C-S-H samples showed a pH of 11.8 to correspond to a Ca/Si ratio of 1.21 [173].

In addition to maintaining a higher pH during the monolithic test, the greater alkalinity of samples prepared with higher waste:binder ratios was reflected in the ANC (Figure 6.17). All samples showed ANC to pH 9 >1mEq/g, satisfying minimum suggested criteria [152]. As would be expected from the STA analysis of the samples shown previously (chapter 5), i.e. $Ca(OH)_2$ concentrations in the order 3:2>2:3>1:4, ANC was greater with higher waste:binder ratios. $Ca(OH)_2$ was not the only buffer present in the samples however. Buffering also occurred due to the C-S-H and other reaction products [164, 165].

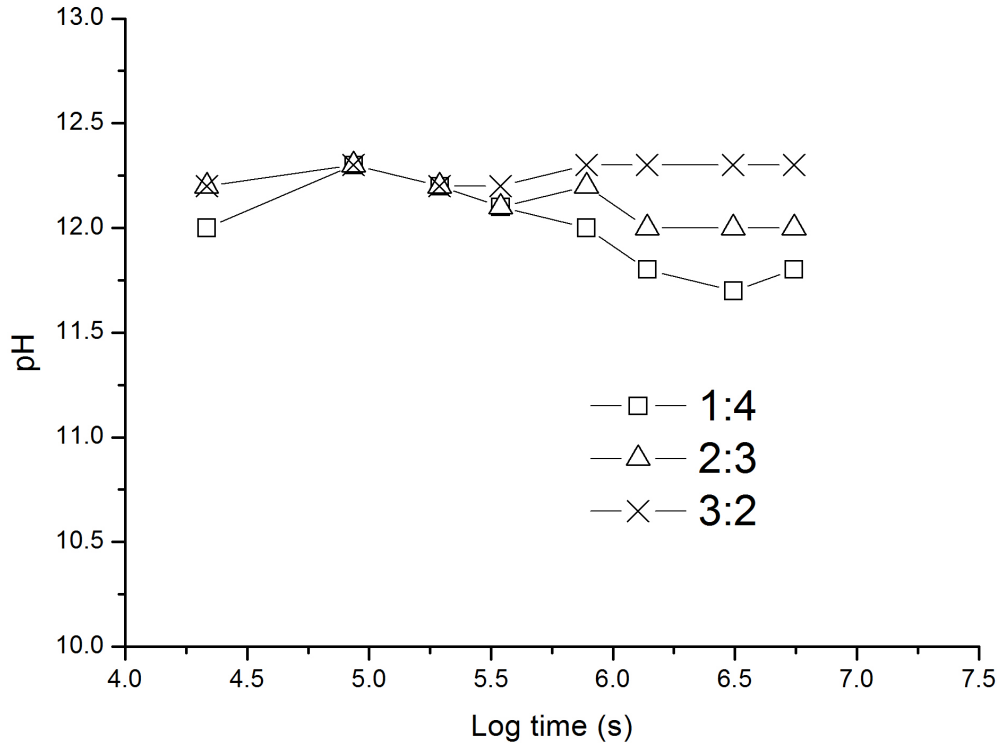

Figure 6.16 Development of leachate pH throughout EA NEN 7375. Samples with varying APC residue:PFA ratio, prepared with l/s=1, cured at 38°C

In purer systems it may be possible to distinguish inflexions and assign buffering plateaus to reaction products. This was difficult with the samples studied here due to the great diversity of reaction products present. In an attempt to further characterise the materials and understand the nature of the

acid buffering, batch extractions were performed with different levels of acid addition. After reaching equilibrium, the extractions were filtered and rinsed with de-ionised water before submersion in IPA and vacuum drying. Once dried the samples were analysed by XRD. Samples 1:4 and 3:2 were analysed since they contained the greatest variation in reaction products and ANC.

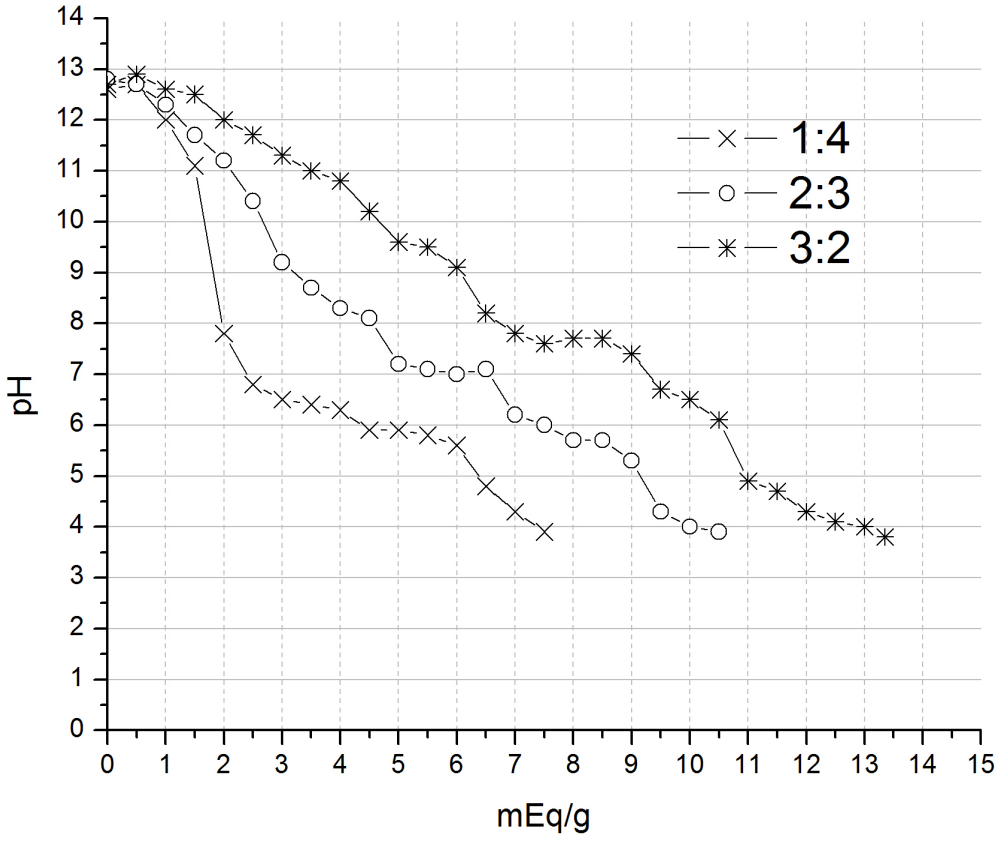

Figure 6.17 ANC titration curves. Samples with varying APC residue:PFA ratio, prepared with l/s=1, cured at 38°C

Based on the ANC titration curves obtained, batch extractions were performed at l/s=10 with 0, 2 and 6.5mEq/g HNO_3 (corresponding to inflexions identified by the derivative). pH values obtained for the batch extractions were up to 2.1 pH units higher than observed for the titration curves. The discrepancies between pH values observed by titration and batch extractions were considered to be the result of atmospheric CO_2 exposure due to the longer time period associated with the ANC titrations and repeated opening of the containers in order to measure and titrate samples. Batch extractions of sample 1:4 with HNO_3 addition of 2.5 and

6.5mEq/g showed pH values of 8.9 and 5.4 respectively. Extractions for sample 3:2 with HNO_3 additions of 2.5 and 6.5mEq/g showed pH values of 11.7 and 10.1 respectively. The samples were additionally analysed by XRD after a batch extraction with 8.5mEq/g HNO_3, resulting in pH values of 3.6 and 9.1 for sample 1:4 and 3:2 respectively. The XRD patterns obtained are presented in Figure 6.18 and Figure 6.19 for samples 1:4 and 3:2 respectively.

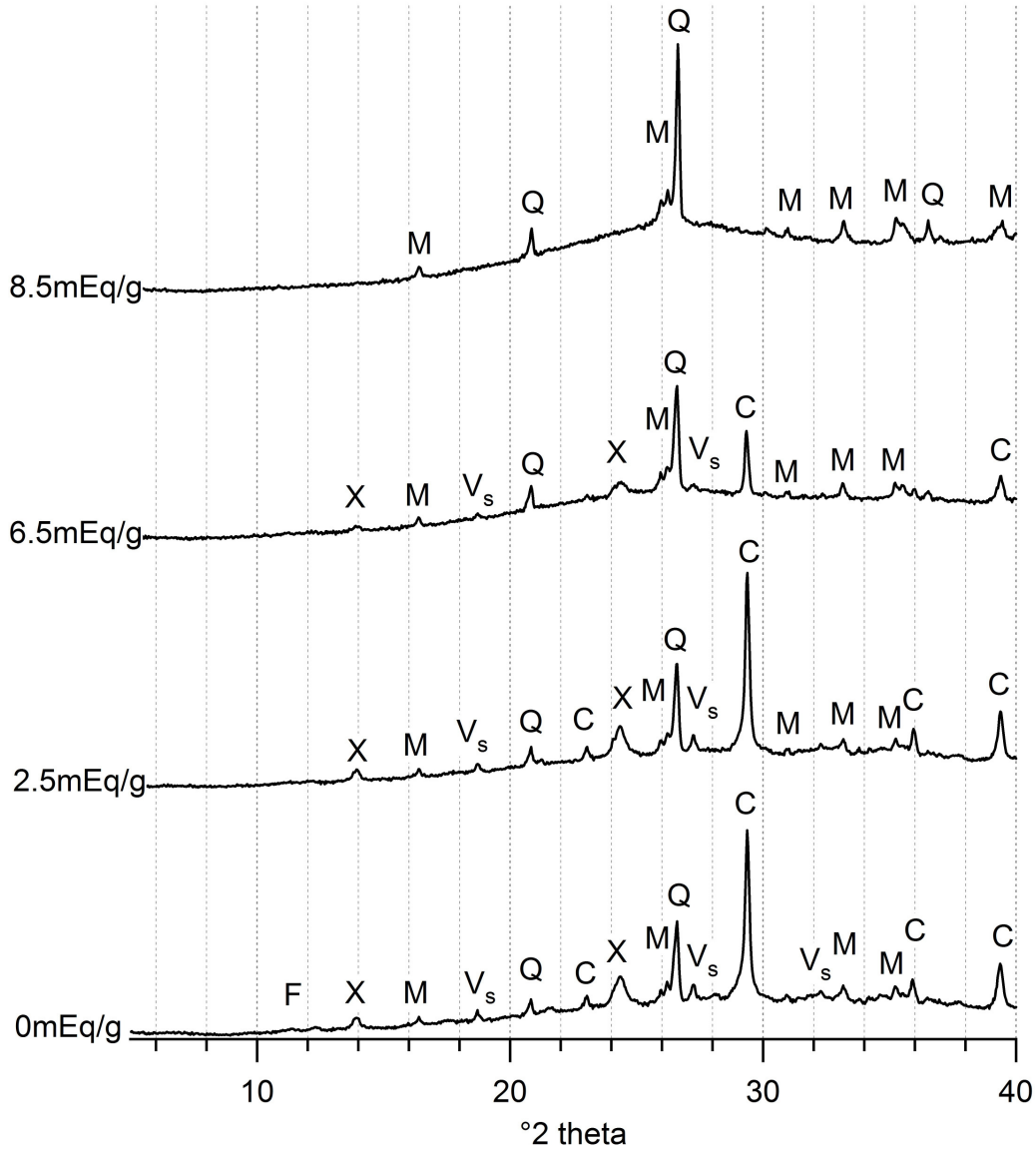

Figure 6.18 XRD patterns (y axis range normalised) for samples following batch extractions in different concentration HNO_3 solutions. Samples with APC residue:PFA=1:4, l/s=1, cured at 38°C. F=Friedel's salt, X=Sodalite, M=Mullite, V_s=Vishnevite, Q=Quartz, C=Calcite

The samples without HNO_3 addition had still been exposed to de-ionised water at l/s=10 explaining the removal of readily soluble phases such as

NaCl. However the patterns do not precisely correspond to testing according to BS EN 12457-2 because all samples were left in solution until the last sample had reached equilibrium (this was always the sample with the highest acid addition), in order to avoid differences due to exposure time.

Regarding sample 1:4, it was not possible to determine a precise order for dissolution. Only trace evidence of Friedel's salt was observed after extraction in de-ionised water and no evidence remained with 2.5mEq/g HNO_3 addition. Vishnevite, sodalite, calcite, quartz and mullite remained evident with up to 6.5mEq/g HNO_3 addition. The amorphous fraction of the sample became noticeably more significant as the acid concentration increased, eventually leaving just quartz, mullite and a very large amorphous hump centred~27°2θ indicating a siliceous glass structure [337]. In agreement with the pH titration curves presented in Figure 6.17, the ANC of sample 3:2 was evidently greater than that of sample 1:4, retaining several crystalline compounds and notably C-S-H (I) even with 8.5mEq/g HNO_3 addition. The remaining presence of C-S-H (I) suggests that pH equilibrium had not yet been achieved, despite being observed as stable for 4 days, since even with a very low Ca/Si the pH of C-S-H would be ~9.9 [175]. Additionally ettringite was present in sample 3:2 after 8.5mEq/g HNO_3 addition (resulting in a pH of 9.1) but has been shown by Gabrisova *et al* [206] to convert to gypsum and aluminium sulphate below pH 10.

$Ca(OH)_2$ was the first compound to react with the HNO_3 providing the initial buffering plateau. All samples were susceptible to carbonation as a result of drying, storage and sample preparation for XRD which would reduce the $Ca(OH)_2$ concentration. However, all samples underwent the same procedure and $Ca(OH)_2$ was only present in the sample without HNO_3 addition. Additionally peaks corresponding to $CaCO_3$ were weak in all the acidified samples indicating that carbonation was only slight and $Ca(OH)_2$ was removed due to HNO_3 addition.

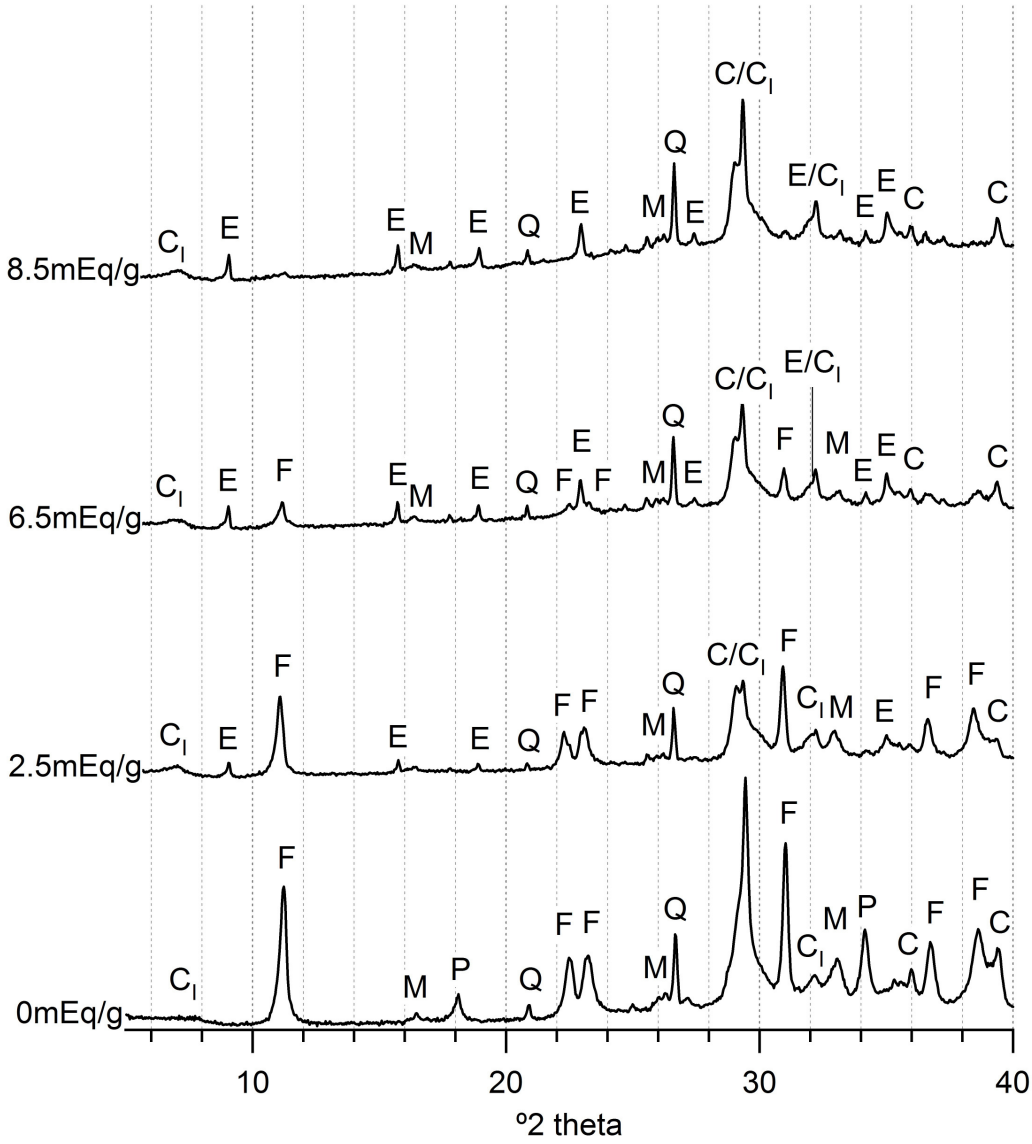

Figure 6.19 XRD patterns (y axis range normalised) for samples following batch extractions in different concentration HNO_3 solutions. Samples prepared with APC residue:PFA ratio=3:2, l/s=1, cured at 38°C. C_I=C-S-H (I), E=Ettringite, F=Friedel's salt, M=Mullite, P=Portlandite, Q=Quartz, C=Calcite

Friedel's salt was again removed relatively quickly from the sample as acid addition was increased. Owing to both the greater initial concentration of Friedel's salt, and the greater buffering capacity prior to Friedel's salt consumption, Friedel's salt remained present in sample 3:2 with up to 6.5mEq/g, compared to removal from sample 1:4 with 2.5mEq/g. As Friedel's salt was removed from sample 3:2, there was a notable increase in the presence of ettringite. Ettringite was not present in the sample before leaching and was not present without HNO_3 addition. The results were repeated and confirmed. No contamination with sulphates was possible due

to the use of 18MΩ de-ionised water and high purity HNO_3. The ettringite production was clearly an effect of the HNO_3 exposure. Peak intensity increased as the acid concentration increased. Such production of ettringite could be associated with a reduction in the pH of the system to within the range of ettringite stability or greater crystallinity of ettringite [207, 425]. The pH recorded for the batch extraction performed with 0mEq/g HNO_3 addition was 12.9, notably higher than that observed during BS EN 12457-2 and close to the upper limit of ettringite stability previously reported [205, 207]. Additionally HNO_3 is a strong oxidising agent which may have resulted in an adjustment to the Cl/SO_4 balance in the system, oxidising some of the reduced and intermediate forms of sulphur in the PFA. Cl concentration would certainly still be greater than SO_4 concentration in the 3:2 system, however, sulphate uptake may occur preferentially to chloride uptake [166, 215, 216]. Although results are not presented, exposure of samples to a high concentration sulphate solution was observed to similarly encourage ettringite formation at the expense of Friedel's salt. If oxidation of the sulphur was occurring, a similar process would have been expected in sample 1:4. Sample 1:4 showed no evidence of ettringite production but did show vishnevite. Ettringite production in sample 1:4 perhaps did not occur due to the low availability of Ca. Additionally the rapid pH reduction of sample 1:4 may have hindered observation of the reaction products, encouraging their dissolution. With continued acid addition ettringite formed in sample 3:2 would be dissolved.

The implications of such variation in the mineralogy on the leaching behaviour are not fully understood. Ettringite production has immediate negative implications for chloride binding and may cause expansive stresses resulting in loss of physical encapsulation. However, due to the high levels of ion substitution possible in ettringite, its production may improve the leaching behaviour of several contaminants [192, 201].

6.2.1 Summary of the effects of APC residue:PFA ratio variation

The following conclusions can be drawn on the effects of variation in APC residue:PFA ratio.

- Increasing the APC residue:PFA ratio reduced the workability of the blend when working at constant l/s. A consequence of the high water demand of the APC residue.
- Increasing the APC residue:PFA ratio delayed the chemical reactions responsible for setting, neutralising the NaOH and thereby slowing fly ash dissolution.
- Setting was also affected by the physical properties of the paste which as indicated by the workability, varied with waste:binder ratio. As such a reduction in the reaction kinetics as the waste:binder ratio was increased, may be partially or completely offset by the physical property adjustment when working at a constant l/s ratio.
- Optimum 28 day compressive strengths were obtained with an APC residue:PFA ratio close to 2:3 when working at l/s=1. This was a consequence of the variations in the chemistry of the mix design and the physical properties of the blends in their plastic state.
- Permeability of the matrices was reduced as the APC residue:PFA ratio was increased. This was attributed to the increased dry mass density achievable when compacting the fresh mix.
- Permeability increased after 7 days submersion in deionised water. This would have negative implications for maintained physical encapsulation of the monoliths and also highlights the lack of accuracy in predicting long term leaching based on effective diffusion coefficients calculated from monolithic leach testing.
- Permeability increase and compressive strength decrease was higher at lower waste:binder ratios. This was a result of the initial permeability variations allowing rapid dissolution of a significant proportion of the matrix.
- Primarily due to permeability variations, chloride and sulphate diffusion from the matrices was slower at higher waste:binder ratios.

- Little chemical immobilisation of the chlorides meant release from granular tests was availability driven. As such increased waste:binder ratio increased the concentration leached. WAC for chloride release could only be met by dilution with the binder, increasing the cost and efficiency of the treatment.
- The pHs of leachates obtained by one step batch extractions (BS EN 12457-2) were similar with all waste:binder ratios. However, owing to the high alkalinity of the APC residues, increasing the waste:binder ratio increased the ANC and maintained higher pHs over longer term leach tests (EA NEN 7375).
- Exposure to nitric acid not only caused dissolution of crystalline phases in the matrices but also changes in mineralogy, notably causing ettringite production. This was considered to be a result of matrix pH reduction and possible oxidation of the sulphur in the PFA.

6.3 Effects of variation in curing temperature

Consistent with previous work, increasing the curing temperature drastically reduced the setting time of the blends [255]. This is associated with the greater energy in the system and the increased rate of dissolution of the fly ash [261]. The reduction in setting time observed when curing at 80℃ bought it well within the suggested 24 hour upper limit [157]. Initial setting time of the sample cured at 80℃ was ~2 hours, very close to the lower limit suggested to facilitate handling [157]. Concern relating to rapid setting and therefore handling difficulties were not an issue however since setting was not accelerated until exposure to higher temperatures which occurred after casting. Setting times observed when curing at room temperature showed the treatment to be unfeasible on an industrial scale due to the significant storage time which would be necessary before the monoliths could be handled.

Sample	Flow Value (mm)	Final Setting Time (h)	28d UCS (MPa)	UCS (7d sub) (MPa)	Bulk Porosity (%)
2:3 (23)	180	120.75	3 +/-0.07	5.4	57.9
2:3	180	31.25	8.7 +/-1.5	7.5	55.3
2:3 (80)	180	5.75	7.9 +/- 0.18	4.2	58.5

Table 6.12 Workability, final setting time, compressive strength and bulk porosity results for samples cured at various temperature, prepared with APC residue:PFA ratio=2:3 and l/s=1

Accelerated compressive strength development was also observed with increased temperatures. Figure 6.20 shows the significant effect of curing temperature on the strength development of mixes prepared with a waste:binder ratio of 2:3, over 28 days. At 23°C strength gain was both slight and slow, with samples remaining malleable and therefore not suffering acceptable failure according to BS EN 12390-3 at 7 days. With an increase in curing temperature to 38°C there was more pronounced strength development, including at early age (3 days). This pattern was consistent with previous work showing moderately elevated temperatures to drastically increase pozzolanic activity and therefore the rate of strength development [254-256]. As the curing temperature was raised to 80°C, early-age strength was much greater, consistent with the increased rate of $Ca(OH)_2$ consumption over 28 days as was presented in chapter 5.2. $Ca(OH)_2$ consumption was very rapid over the first three days, after which it slowed considerably. This was also reflected in the compressive strength development. At 80°C 80-90% of the maximum strength was developed during the first 24 hours and little development was observed between 7 and 28 days. Such behaviour is similar to that previously observed, for example Shi and Day [255] showed strength development of a pozzolanic system not to increase significantly after 10 days when curing at 65°C and 75 days when curing at 23°C.

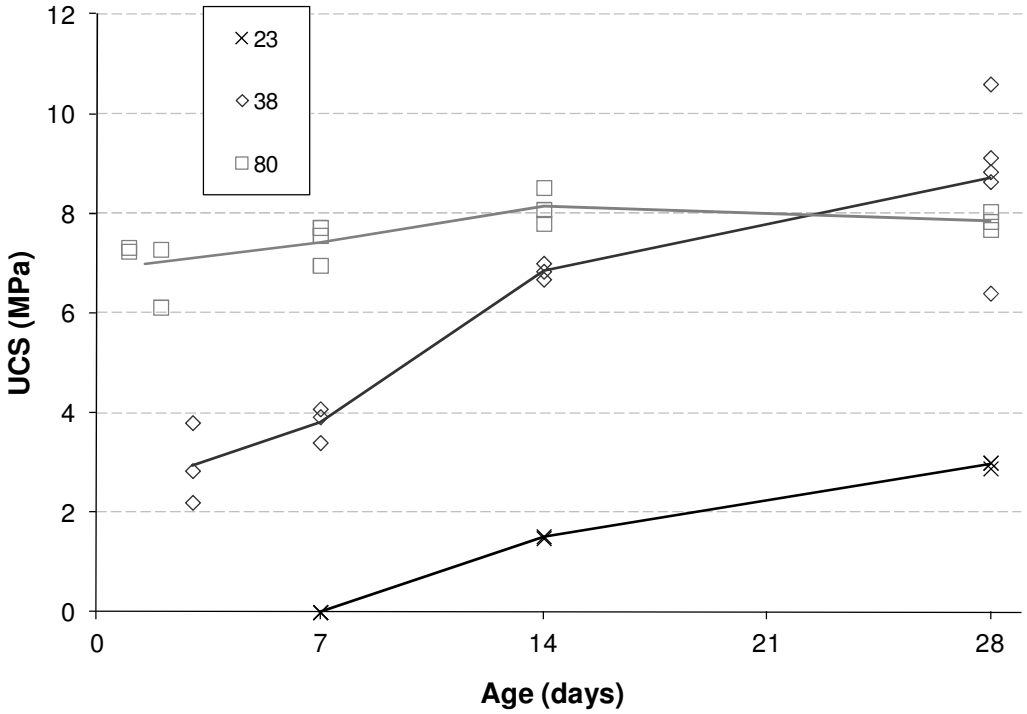

Figure 6.20 Effect of curing temperature on compressive strength development of samples prepared with APC residue:PFA ratio of 2:3 and l/s=1, over 28 days

After 28 days the strength of the samples cured at 80°C and 38°C were very similar with the 38°C samples perhaps showing slightly greater UCS (Figure 6.20). Such behaviour is not unknown in cement science, where high curing temperatures induce more rapid hydration, and therefore higher early age strength, but result in uneven distribution of hydration products and possible resistance to complete hydration. Such conditions result in a more open microstructure and therefore lower later-age strength [255, 257, 258, 417]. This effect can also be seen by the increase in bulk porosity of the sample cured at 80°C (Table 6.12). The effects of temperature on pozzolanic systems can vary and as such the age at which temperature is detrimental to UCS may vary considerably. According to Ezziane *et al* [417] 'the activation energy defines the temperature sensitivity of a mixture.' The age at which compressive strengths overlapped in the current study was much later than reported by Puertas *et al* [254] or Wang *et al* [256] when studying NaOH activated blends of PFA/GGBS or PFA/CKD respectively; perhaps showing a lower initial reactivity i.e. higher activation energy of the materials used here. The mathematical relationship between compressive strength, curing

temperature and age derived by Shi and Day [255] for a water activated lime/pozzolan blend, showed compressive strengths obtained when curing at 23℃ and 35℃ to exceed those achieved when curing at 65℃ after 36 and 15 days respectively. The overlap was delayed substantially when 4% $CaCl_2 \cdot 2H_2O$ was added, seemingly increasing the activation energy [255]. The overlap close to 28 days observed for the current samples may therefore also reflect the Cl concentration present.

Samples cured at room temperature showed an increase in strength after submersion, despite considerable TDS. This suggested production of minerals with significant contribution to UCS between 21 and 28 days, such as C-S-H, overwhelmed the strength loss due to TDS. This was perhaps due to the extent of the reaction which had occurred prior to submersion, and the reaction kinetics at the time of submersion. For example, sample 2:3 (80) was no longer developing compressive strength at 21 days (Figure 6.20), and suffered significant compressive strength loss as a result of submersion for 7 days (Table 6.12) and 64 days (Table 6.13).

	UCS before and after EA NEN 7375			
Sample	**Before (MPa)**	**Standard Deviation**	**After (MPa)**	**% loss**
2:3 (23)	3.0	0.069	9.6	-220.00
2:3	8.7	1.5	13.6	-56.32
2:3 (80)	7.9	0.18	3.6	54.43

Table 6.13 Compressive strength development during EA NEN 7375. Samples cured at various temperatures, prepared with APC residue:PFA ratio=2:3 and l/s=1

Sample 2:3 (80) showed very rapid release of chlorides during EA NEN 7375 as evident from the log-log plot and high % release (Table 6.14 and Figure 6.21). Several samples cured at 80℃ showed cracking due to drying shrinkage, an example of which is shown in Figure 6.22. Such cracking would have been responsible for the rapid ingress of water and chloride leaching observed by EA NEN 7375. This rendered such curing unsuitable as the physical encapsulation provided by the s/s product was greatly reduced.

Such problems could be avoided by curing for shorter times at high temperatures.

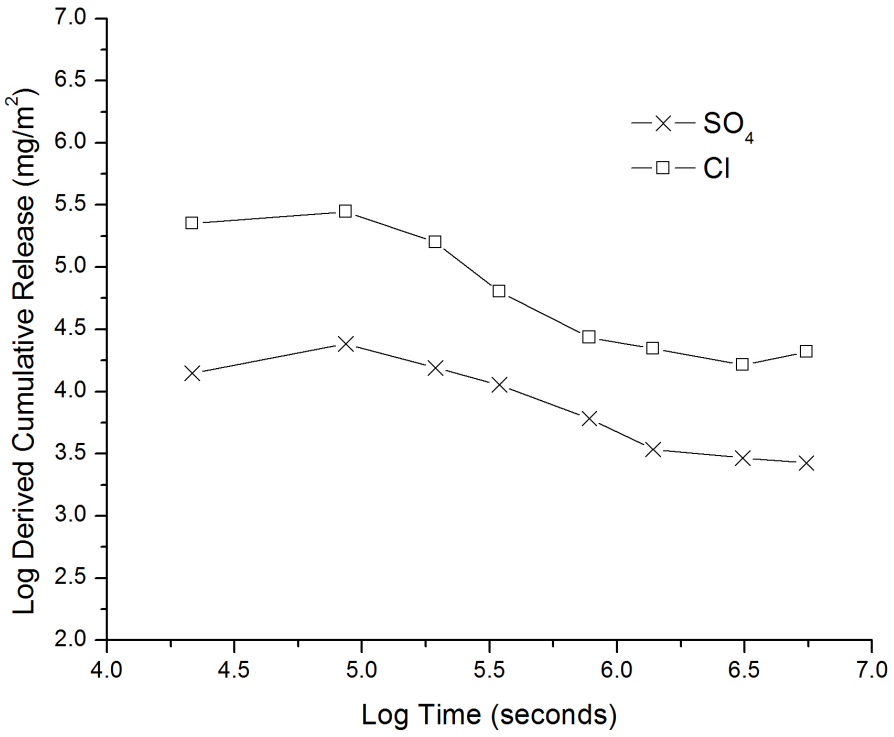

Figure 6.21 Log-log plot for sample 2:3(80) resulting from analysis of EA NEN 7375

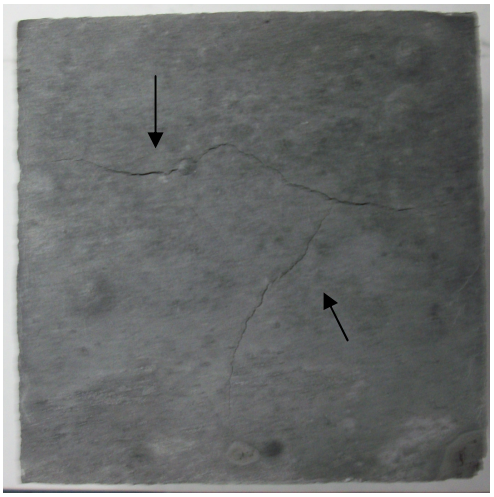

Figure 6.22 Drying shrinkage cracking of sample 2:3 (80), cracks highlighted by arrows

	Chloride					
Sample	**ε^*_{64} (mg/m^2)**	**pD_e**	**ε_{64}**	**Diffusion controlled increment**	**% release**	**12457-2 after (mg/kg)**
2:3 (23)	340,600	na	na	none	63	9690
2:3	298,500	10.7	746,400	1-4	55	13,170
2:3 (80)	460,800	na	na	none	85	460

Table 6.14 Monolithic leach (EA NEN 7375) chloride results for samples cured at various temperatures, prepared with APC residue:PFA ratio=2:3 and l/s=1. ε^*_{64}=measure cumulative 64 day release. pD_e=-log of effective diffusion coefficient (D_e m^2/s), ε_{64}=derived cumulative 64 day release, na=not applicable

Despite the sample cured at 23℃ not showing a diffusion controlled increment for chlorides (Table 6.14 and Figure 6.23), an increment could be identified for sulphates (Table 6.15 and Figure 6.23). Comparison of the log-log plots for chloride release from samples cured at 23℃ and 38℃ is shown in Figure 6.24. It is clear that very fine margins distinguish between whether or not a sample shows diffusion controlled release according to EA NEN 7375. Despite the gradient of 2:3 (23) falling just below that required for calculation of a diffusion coefficient (increment 1-4 showed a gradient of 0.33), depletion was not rapid. The ultimate percentage of chlorides released was only 63%, slightly higher than that from the sample cured at 38℃. This was reflected in the release from the subsequent granular leach test (Table 6.14).

	Sulphate						
Sample	**ε^*_{64} (mg/m^2)**	**pD_e**	**ε_{64}**	**Diffusion controlled increment**	**% release**		**12457-2 after (mg/kg)**
					a	**b**	
2:3 (23)	30,300	11.2	45,500	2-5	4	98	2240
2:3	21,200	11.2	48,700	1-4	2.5	68	1700
2:3 (80)	38,700	na	na	none	5	124	0

Table 6.15 Monolithic leach (EA NEN 7375) sulphate results for samples cured at various temperatures, prepared with APC residue:PFA ratio=2:3 and l/s=1. a=availability calculated assuming all S is SO_4, b=availability calculated based on release from as-received materials according to BS EN 12457-2 and analysis by IC

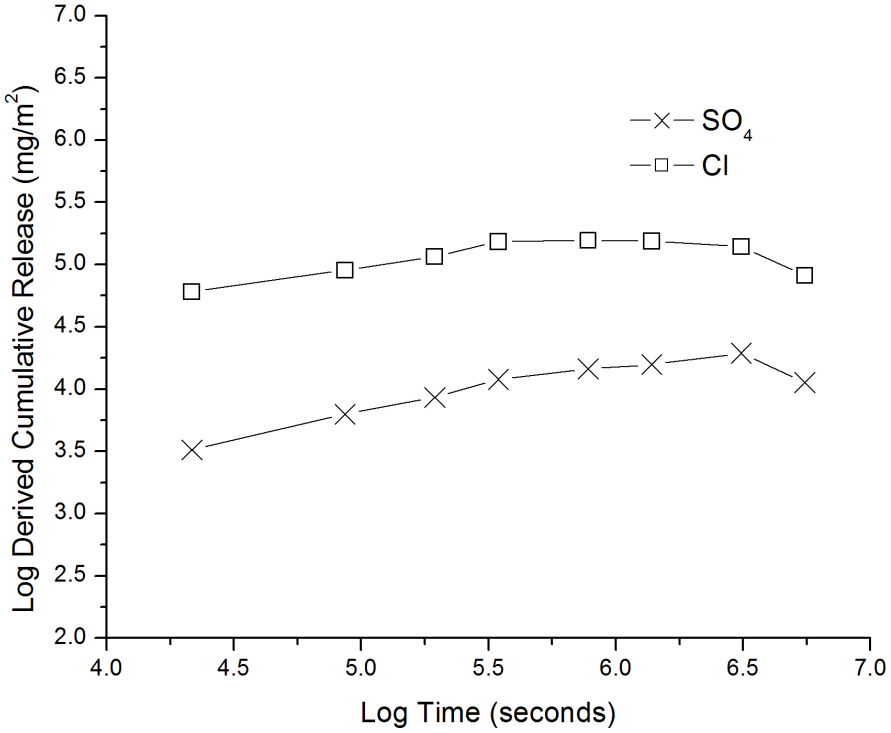

Figure 6.23 Log-log plot for sample 2:3 (23) resulting from analysis of EA NEN 7375

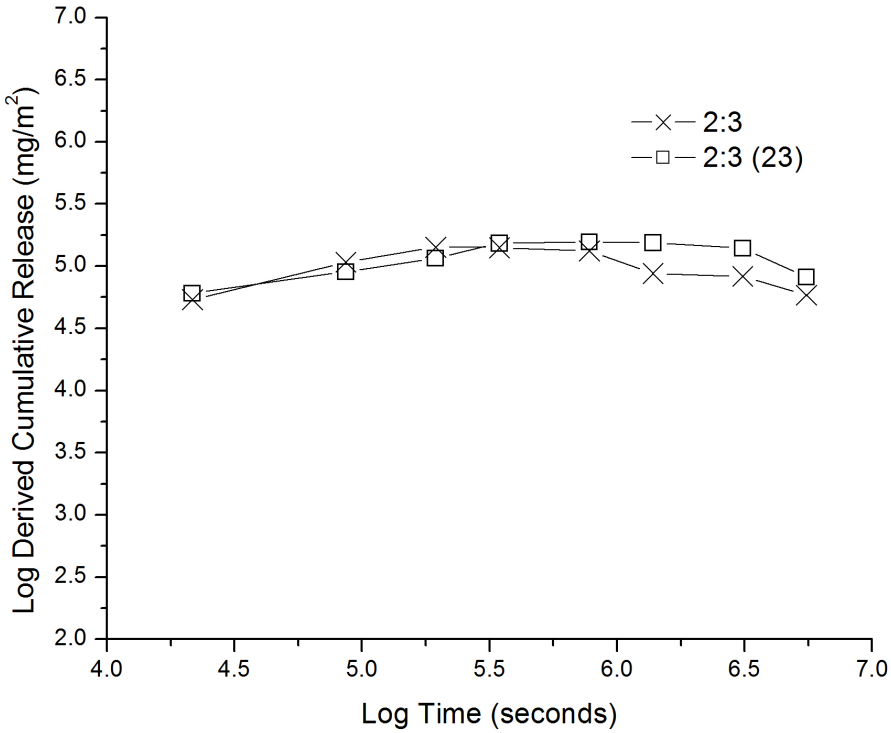

Figure 6.24 Comparison of log-log plots for Cl release from sample 2:3 and 2:3 (23) resulting from analysis of EA NEN 7375

Samples cured at all temperatures exceeded hazardous granular (Table 6.16) and monolithic (Table 6.14) WAC for chlorides. Hazardous monolithic WAC for sulphates was exceeded (Table 6.15) despite meeting SNR granular WAC (Table 6.16). Curing at 38℃ gave the greatest extent of encapsulation which was attributed to the greater degree of curing at 38℃ compared to 23℃, and the absence of the cracking seen at 80℃.

Leachate pH obtained during BS EN 12457-2 was again observed to be at a level which suggested $Ca(OH)_2$ to be the controlling factor (Table 6.16). pH of the leachate from 2:3 (23) was slightly higher at 12.7. This perhaps indicated hydrolysis of alkali metal hydroxides which may have been a result of the slower reaction kinetics, binding a smaller proportion of the Na. Based on a 4.4M NaOH concentration in the WC solution (determined by titration chapter 4.3) and a CaClOH concentration of 15.3% weight in A1 (chapter 4.1), a slight excess of NaOH would be present after the reaction to produce NaCl and $Ca(OH)_2$. Previously discussed results suggested slight variation in mineralogy of the samples as curing temperature varied. Zeolitic phases were more evident when higher curing temperatures were employed (chapter 5) which would remove the strong alkali Na from solution. Full ANC curves were not obtained for samples cured at varying temperature. However, batch extractions showed all samples to exceed the suggested minimum capacity of 1mEq/g to pH 9 [152] and extractions with 2mEq/g for samples 2:3 and 2:3 (80) showed pH of 11.7 and 10.1 respectively. This was in agreement with an expected lower $Ca(OH)_2$ plateau when curing at higher temperatures due to the greater rate of $Ca(OH)_2$ consumption as previously shown (chapter 5.2). The sample cured at 80℃ showed a higher pH in the first leachate fraction of EA NEN 7375 but pH fell as the test progressed and the final fractions showed lower pH than samples cured at lower temperatures (Figure 6.25). This was perhaps due to the rapid solubilisation of the alkaline solids in the early fractions owing to the poor encapsulation, and depletion in latter fractions. The sample cured at 23℃ maintained a slightly higher pH throughout most of the test which was perhaps a result of the greater $Ca(OH)_2$ content due to the lower degree of pozzolanic activity reflected in the compressive strength development.

	2:3 (23)	2:3	2:3 (80)
Cl availability (mg/kg)	65,400	62,400	64,700
Cl 12457-2 (mg/kg)	49.500	45,900	43,700
SO_4 availability (mg/kg)[a]	61,500	58,700	60,800
SO_4 availability (mg/kg)[b]	3750	3580	3712
SO_4 12457-2 (mg/kg)	4900	2259	2163
pH	12.7	12.5	12.5
pH (1mEq/g HNO_3)	12.3	12.3	12
TDS (mg/kg)	133,500	148,500	122,500

Table 6.16 Granular leach (BS EN 12457-2) results for samples cured at various temperatures, prepared with APC residue:PFA ratio=2:3 and l/s=1. [a]availability calculated assuming all S is SO_4 [b]availability calculated based on release from as-received materials according to BS EN 12457-2 and IC

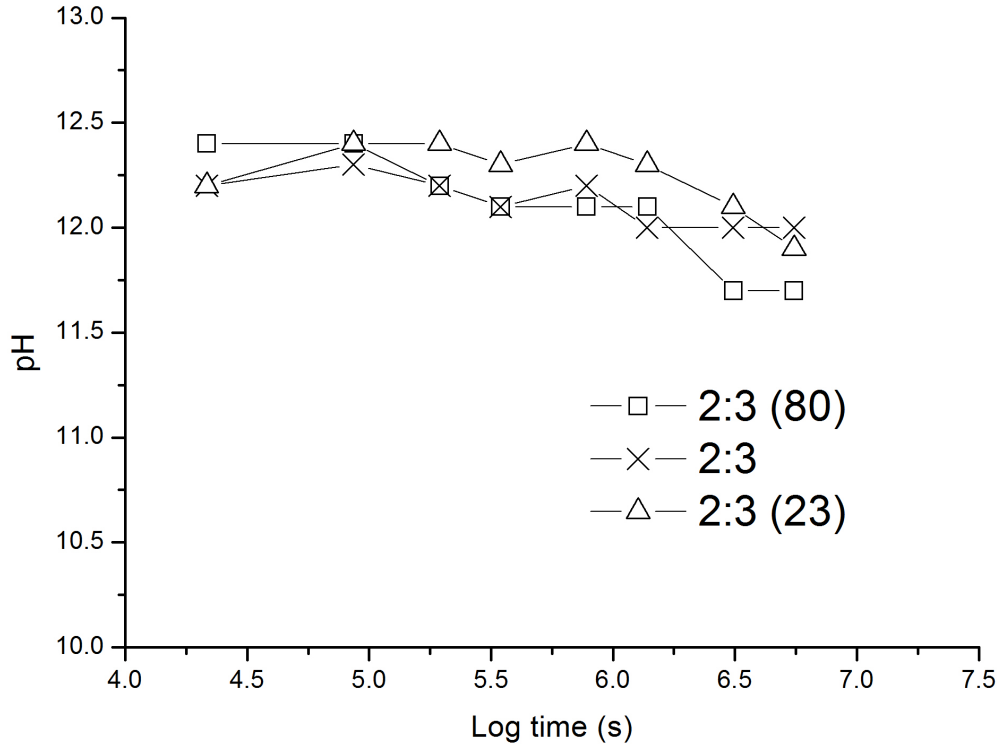

Figure 6.25 Development of leachate pH throughout EA NEN 7375. Samples cured at varying temperatures. Prepared with APC residue:PFA ratio=2:3 and l/s=1

6.3.1 Samples cured at 80℃ for 24 hours

To avoid the shrinkage cracking observed at later ages when curing at 80℃, and because a quicker curing period would be more attractive industrially. It was considered of interest to examine the performance of the samples after just 24 hours curing at 80℃ followed by storage at room temperature in a sealed container. These samples were assigned the nomenclature x:y (80 1d+n) in which x:y was the waste:binder ratio and n was the number of days stored at room temperature. Samples were tested for compressive strength (singular result), and monolithic leach performance as well as being analysed by XRD.

The compressive strength of sample 2:3 (80 1d+27) (7.9MPa) was the same as observed when curing at 80℃ for 28 days (Table 6.12 and Table 6.13). Compressive strength of 7.2MPa was observed when curing for 24 hours at 80℃ and storage for a further 24 hours. This was considerably higher than the compressive strengths achieved for equivalent samples cured at 23℃ or 38℃ after the same curing time (Figure 6.20). Consistent with the development curve observed for compressive strength at 80℃ (Figure 6.20), strength was developed very rapidly. Very little additional compressive strength was then developed during the 27 days storage. The compressive strength gain and setting time of sample 3:2 were accelerated significantly compared to those observed at 38℃. Curing at 38℃ sample 3:2 had not met final set until 49 hours (Table 6.7). Final setting time of 3:2 was reduced to 6.6 hours when curing at 80℃ and a compressive strength of 3.1MPa was achieved after 1 day curing at 80℃ and 1 day storage at room temperature. Consistent with behaviour observed at 38℃ (Figure 6.9), the sample prepared with APC residue:PFA=3:2 resulted in lower compressive strength than that prepared at 2:3.

In contrast to the sample cured at 80℃ for 28 days, the samples cured for just 24 hours at 80℃ showed an increase in compressive strength following the EA NEN 7375 monolithic leach procedure (Table 6.17). This increase coincided with a much lower release of solids during the test as evidenced by

considerably lower chloride and sulphate release (Table 6.18 and Table 6.19).

	UCS (MPa)	
Sample	**Before 7375**	**After 7375**
2:3 (80 1d+1)	7.3	8.8
2:3 (80 1d+6)	nd.	9.32
2:3 (80 1d+27)	7.9	10.0
3:2 (80 1d+1)	3.1	5.3

Table 6.17 Compressive strength development during EA NEN 7375 of samples cured at 80°C for 24 hours

Chloride release from samples 2:3 (80 1d+n) did not exceed 27.7% of that calculated as available and release from sample 3:2 (80 1d+1) was just 34% (Table 6.18). This was significantly lower than the release observed when curing samples 2:3 and 3:2 at 38℃ (both 55%), sample 2:3 at 23℃ (63%), or sample 2:3 at 80℃ for 28 days (85%). Sample 3:2 (80 1d+6) released only slightly more Cl (287,100mg/m^2) than samples prepared with APC residue:PFA=1:4 cured at 38℃ (234,800-279,300mg/m^2) despite initially having approximately 3 times the available chloride content. The lower release was however not due to chemical fixation of the chlorides. BS EN 12457-2 performed on 2:3 (80 1d+27) showed chloride and sulphate release of a similar order to that observed from sample 2:3, 2:3 (23) and 2:3 (80) (Table 6.20). Additionally the chlorides retained were solubilised during the granular leach test performed following EA NEN 7375 (Table 6.18), further proving a lack of chemical immobilisation. This was also corroborated by characterisation of the samples which showed significant NaCl presence, similar to that observed in previous samples (Figure 6.26).

It was therefore believed that the reduced chloride leaching was due to improved physical encapsulation. The bulk porosity of sample 2:3 (80 1d+27) was determined as 57.8%, very close to the equivalent samples cured at 23, 38 and 80℃ for 28 days (57.9, 55.3 and 58.5% respectively). However, the sample was certainly not consistent throughout, a clear discrepancy between the moisture content around the edge and centre of the sample was evident

by visual examination after testing compressive strength, the centre of the sample retained much more moisture. The permeability of high temperature samples was not measured because evaporation of the mould oil whilst curing prevented demoulding of the samples without damage (permeability samples were cast in moulds requiring high pressure air to remove samples).

	Chloride				
Sample	**ε^*_{64} (mg/m^2)**	**ε_{64} (mg/m^2)**	**Diffusion increment**	**% release**	**12457-2 after**
2:3 (80 1d+1)	121,400	na	none	22.5	36,240
2:3 (80 1d+6)	150,400	367,000	1-4	27.7	33,450
2:3 (80 1d+27)	119,100	209,000	1-4	21.9	31,080
3:2 (80 1d+1)	287,100	na	none	34	38,090

Table 6.18 EA NEN 7375, chloride leach results for samples cured at 80°C for 24 hours

	Sulphate					
Sample	**ε^*_{64} (mg/m^2)**	**ε_{64} (mg/m^2)**	**Diffusion increment**	**% release**		**12457-2 after**
				a	**b**	
2:3 (80 1d+1)	8300	4300	5-8	1.6	27	5070
2:3 (80 1d+6)	8700	na	none	1.7	28	4230
2:3 (80 1d+27)	8400	13,500	2-5	1.7	27	4440
3:2 (80 1d+1)	14,900	8200	5-8	3.8	48	3840

Table 6.19 EA NEN 7375, sulphate leach results for sample cured at 80°C for 24 hours. a=availability calculated assuming all S to be SO_4. b=availability calculated based on release during BS EN 12457-2 from as received materials and analysis by IC.

BS EN 12457-2			
Cl (mg/kg)	**SO_4 (mg/kg)**	**TDS (mg/kg)**	**pH**
40,500	4900	137,700	12.7

Table 6.20 BS EN 12457-2 results for sample 2:3 (80 1d+27)

Despite similar measured release of chlorides and sulphates during EA NEN 7375 from samples with comparable APC residue:PFA ratios cured at 80°C

for 24 hours, some showed diffusion controlled increments and others did not (Table 6.18 and Table 6.19). This highlights the fine margins between the mechanisms controlling release according to EA NEN 7375. Apparent depletion of chlorides following fraction 1-4 despite the low percentage released could be indicative of a change in chemical form i.e. a change in the solubility controlling phase [20]. However, there was no evidence for such behaviour by XRD analysis (Figure 6.26) and the chlorides were known to be retained as a soluble compound by the granular leach results (Table 6.18 and Table 6.20).

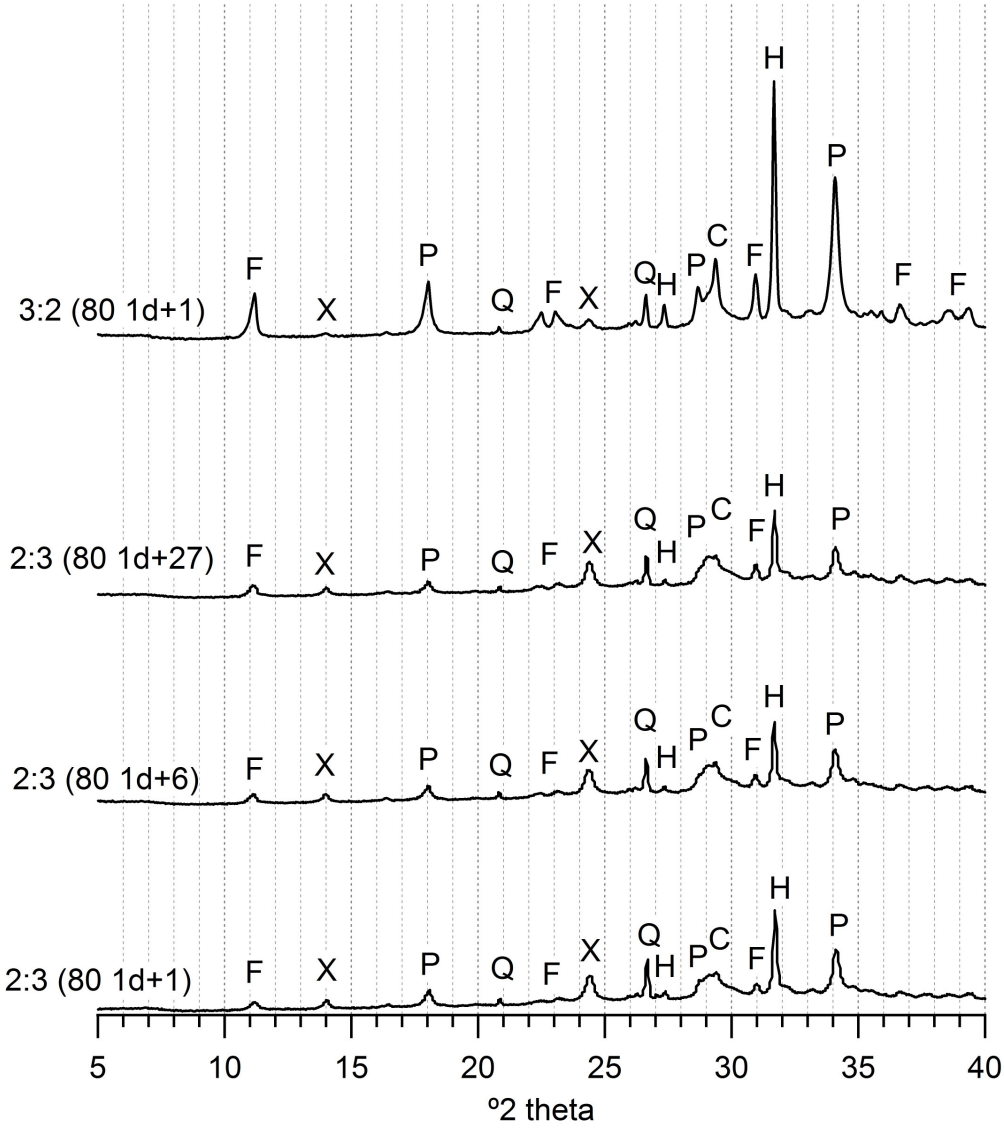

Figure 6.26 XRD patterns (y axis range normalised) for samples cast with varying APC residue:PFA ratios, cured for 24 hours at 80°C followed by storage at room temperature. F=Friedel's salt, X=Sodalite, P=Portlandite, Q=Quartz, H=Halite, C=Calcite

The apparent depletion of chlorides, and the delayed diffusion observed for sulphate release, indicated by a diffusion controlled increment in fraction 5-8 of the test (Table 6.19), may perceivably have been due to different conditions throughout the sample owing to the short term exposure to 80℃ and evidenced by the clear moisture gradient by visual inspection. This could perhaps have resulted in a 'shell' formed around a less reacted centre of the cube and therefore, rather than a change in chemical retardation to analyte diffusion, a change in the physical retardation. Such an effect would be expected to become more prevalent if sample sizes were scaled up to sizes attractive for industrial application. Further work would be necessary to fully understand the behaviour observed for the samples cured at 80℃ for 24 hours. The most appropriate method to study the pore structure would perhaps be through slicing the samples in order to give sub samples representative of the structure at depths relative to the sample surface, and examination of polished cross sections by microscopy or fracture pieces by gas adsorption.

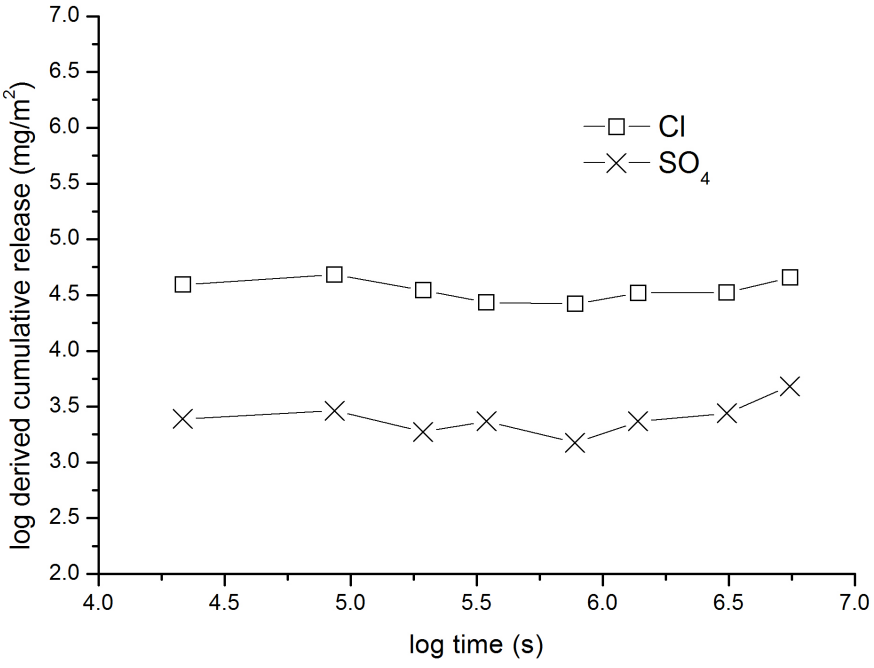

Figure 6.27 Log-log plot corresponding to sample 2:3 (80 1d+1), resulting from analysis according to EA NEN 7375

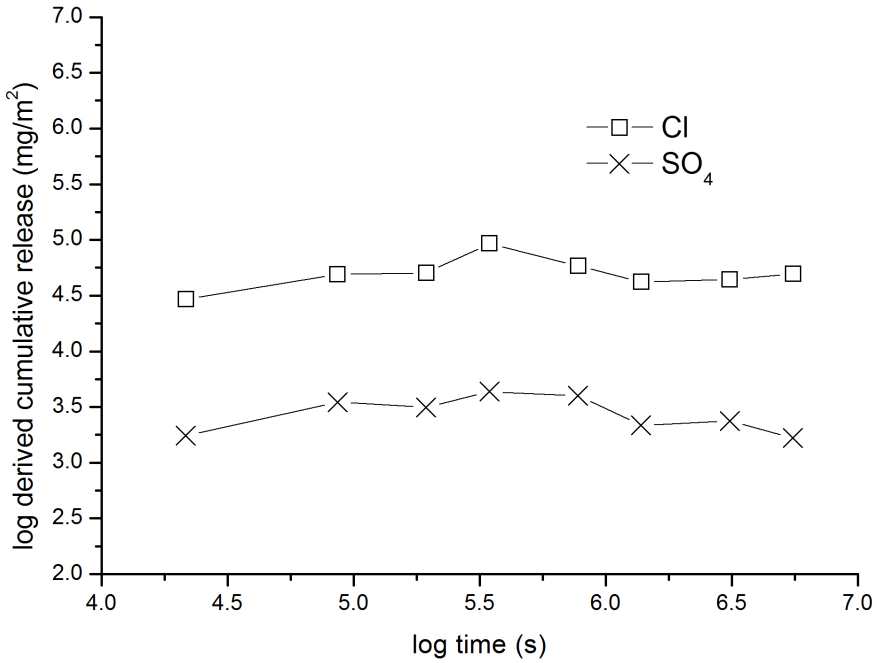

Figure 6.28 Log log plot corresponding to sample 2:3 (80 1d+6), resulting from analysis according to EA NEN 7375

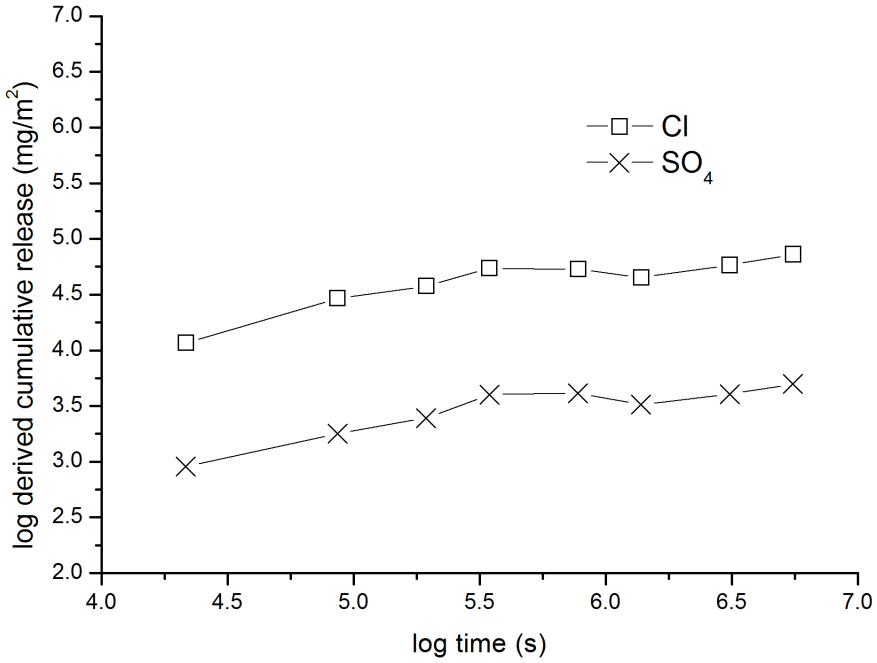

Figure 6.29 Log log plots corresponding to sample 2:3 (80 1d+27), resulting from analysis according to EA NEN 7375

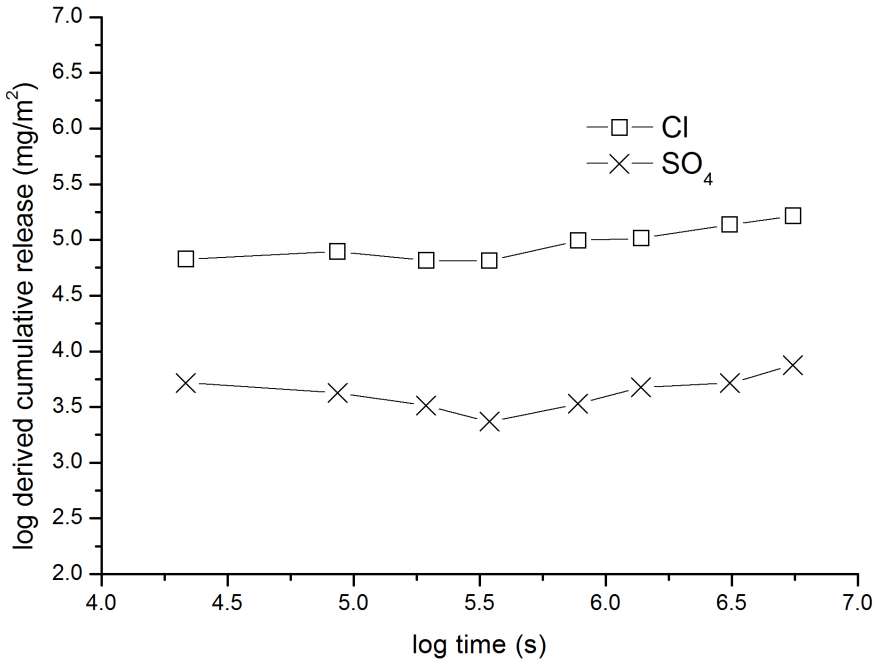

Figure 6.30 Log-log plot corresponding to samples 3:2 (80 1d+1), resulting from analysis according to EA NEN 7375

Importantly, despite the large improvement in chloride immobilisation upon short term, high temperature curing, chloride release was still well above hazardous monolithic WAC limits. Sulphate immobilisation was also improved, this reduction caused sulphate release below SNR WAC limits for samples prepared with APC residue:PFA=2:3. Samples prepared with APC residue:PFA=3:2 exceeded SNR WAC limits but hazardous limits were met. The pH of the leachates fluctuated slightly throughout EA NEN 7375 but all fractions for all samples remained within pH boundaries of 11.6-12.3 (Figure 6.31). The pH was generally slightly lower than that observed for samples cured at 23 or 38℃, or those cured at 80℃ for longer time periods. This was likely a result of the lower release of the alkaline solids.

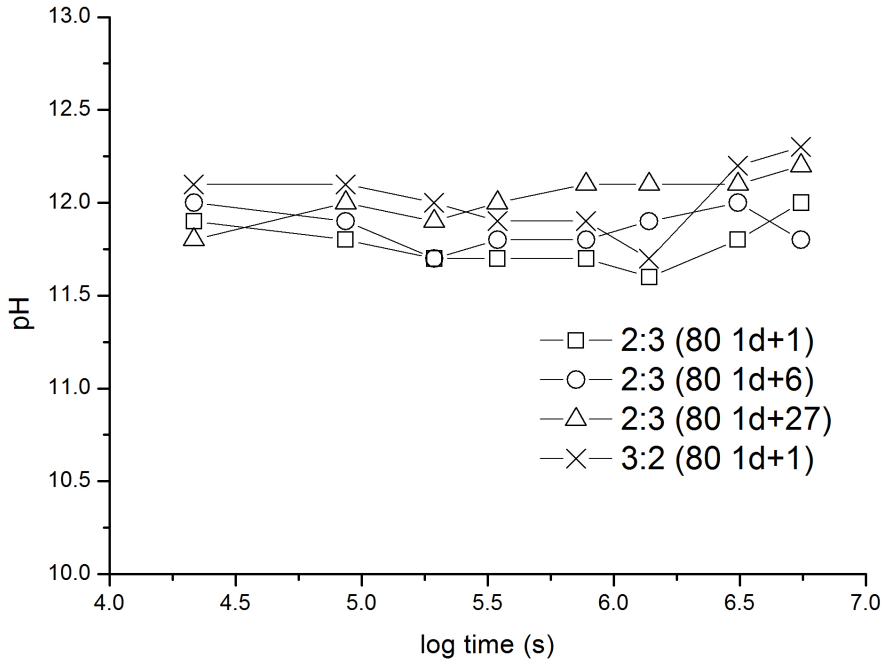

Figure 6.31 pH development during EA NEN 7375 of samples prepared with varying APC residue:PFA ratios cured at 80°C for 24 hours before storage at room temperature

6.3.2 Summary of the effects of curing temperature

The following conclusions could be drawn on the influence of curing temperature on the s/s products.

- Increasing the curing temperature between 23℃ and 80℃ dramatically reduced the setting time of the samples, from 120.8 to 5.8 hours. Compressive strength development was also rapidly increased.
- At 28 days sample cured at 38℃ showed slightly higher compressive strengths than those cured at 80℃. The small difference indicated the high activation energy required for the APC residue:co-fired PFA blend.
- Curing at 23℃ would be unfeasible for industrial application due to prolonged setting times and curing time required to develop compressive strengths and improve leach performance.
- Although curing at 80℃ resulted in shorter setting times and rapid compressive strength development, cracking induced by drying

shrinkage over longer times, and the more open microstructure, drastically reduced physical encapsulation of soluble salts.

- Curing at 80℃ for 24 hours followed by storage at room temperature resulted in much greater immobilisation of chlorides than any of the other samples analysed according to the monolithic leaching procedure, although hazardous WAC was still exceeded. Large quantities of NaCl were still evident by XRD analysis and granular leaching remained high. This suggested the immobilisation was physical rather than chemical and therefore a result of the pore structure achieved by this curing regime. However, further work would be required to characterise the pore structure and confirm this.
- pH obtained in short term batch extractions may be similar at different curing temperatures. More rapid consumption of $Ca(OH)_2$ at higher temperatures may result in a reduced initial buffering plateau when testing ANC.

6.4 Effects of alkali activation

There was a significant density difference between water and the waste caustic solution (1.216 kg/L) which affected the volume of liquid used when working on a w/w basis. Equivalent weight mixes were considerably more workable when mixed with water. Sample 2:3 DIW was cast with an equivalent volume of water and still showed a much greater workability than the WC mix, being too great to test by flow table. This suggested volume was not the only factor, perhaps the difference was due to the viscosity of the WC solution owing to the considerable TDS (267,800mg/l). This was not tested and no significant variability from that of water was noticeable by visual examination. However, the TDS present in the WC solution would effectively lower the l/s (v/w) of the blends.

The final setting time of sample 2:3 DIW exceeded 62 hours when curing at 38℃. DIW activated samples also demonstrated notable shrinkage and cracking and rarely surpassed WAC criteria of 1MPa compressive strength at 28 days. As a result of these observations DIW activated samples were not

subjected to monolithic leach testing. Release of chlorides during granular testing was 45,200mg/kg suggesting very little chemical immobilisation, similar to the WC caustic samples (45,900mg/kg) despite the different speciation of the chlorides. No sulphate release was observed from the water activated samples. The WC solution contained 1506mg/kg SO_4 but removal of this SO_4 contribution would not have accounted for reducing release below detection limits. Perhaps alkali activation encouraged formation of more soluble sulphates such as Na_2SO_4 as was observed by Wang *et al* [256]. Leachate pH was 11.4, reflecting the lack of $Ca(OH)_2$ observed in the samples at 28 days by STA (chapter 5). Sample heterogeneity is reiterated however since $Ca(OH)_2$ was evident in the XRD pattern obtained for the same sample. The ANC of sample 2:3 DIW was considerably lower than the equivalent sample cast with the WC solution (Figure 6.32). This was perhaps a result of both the production of $Ca(OH)_2$ and the alkalis contributed by the WC solution. Minimum criteria of 1mEq/g to pH 9 [152] was still achieved with the DIW sample.

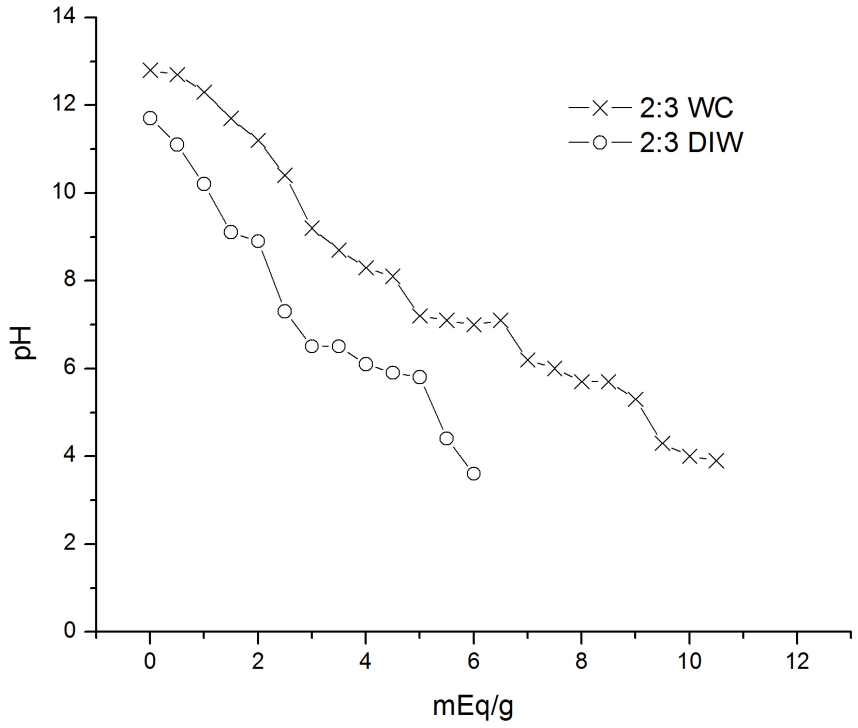

Figure 6.32 ANC titration curves for samples prepared with waste:binder=2:3, cured at 38°C for 28 days, activated with DIW or WC

6.5 Comparison with other binders

Throughout this chapter a comparison of the s/s systems produced using the co-fired PFA and WC solution as reagents, was made with a more common CEM I/de-ionised water s/s system. The use of CEM I for s/s of APC residues had already been examined by Lampris *et al* [67] as discussed in the literature review. However, in order to eliminate the effect of varying the APC residue, and waste:binder ratio employed, blends were studied using residue A1 mixed with CEM I and de-ionised water at l/s ratios of 0.5 and 0.6, satisfying flow criteria [157].

The co-fired PFA/WC blends studied here required much higher l/s ratios than equivalent blends with CEM I (Table 6.21) [67]. The water demand also appeared to be greater than that required for ggbs blends [241]. Despite the high LOI and 45µm sieve retention of the co-fired PFA, it has been shown to improve workability in cement/PFA/DIW pastes [426]. The greater l/s required by the APC residue/PFA/WC solution blends can therefore be primarily attributed to the use of the WC solution.

Mix	Flow Value (mm)	Final Setting Time (h)	28d UCS (MPa)	UCS (7d sub) (MPa)	Bulk Porosity (%)
2:3	180	31.25	8.7 +/-1.5	7.5	55.3
3:2	135	49	6.5 +/-1.6	6.3	56.0
2:3 CEM l/s=0.5	190	0.67	10.2 +/-2.3	11.3	45.4
2:3 CEM l/s=0.6	230	nd	7.3 +/-0.17	12.7	46.4.

Table 6.21 Comparison of workability, final setting time, compressive strength and bulk porosity data for samples cast with PFA/WC or CEM I/DIW. 2:3 and 3:2 cast with co-fired PFA and WC solution, l/s=1, cured at 38°C. 2:3 CEM samples cast using CEM I and DIW, cured at 23°C. nd=not determined, na=not available

Setting times of the PFA blends were considerably longer than setting times observed when blending APC residue with cement (Table 6.21). This was the

case even when curing the PFA blends at 80℃ (final setting time of 2:3 (80)= 5.75 hours). Initial setting time of the cement matrices were below 0.42 hours (25mins), less than the recommended minimum criteria of 2 hours to ensure ease of handling [157] whilst initial setting time of the PFA blends exceeded the 8 hour upper limit unless cured at 80℃ (initial setting time ~2 hours). The slower reaction kinetics of pozzolanic reactions when compared to cement hydration is well documented, delaying the setting time and strength development as a greater fraction of cement is replaced by PFA [427]. Longer setting times were also observed for APC residue/PFA/WC solution blends studied here than ggbs blends previously studied with a waste:binder ratio of 1:1 [263]. Both the PFA and ggbs blends were dependant on pozzolanic reactions. Setting times of ggbs/CEM blends may be shorter than setting times for PFA/CEM blends [427] but considering the increased temperatures and activator used in the current study the longer setting times were surprising.

Working with a similar workability and waste:binder ratio, slightly higher 28 day compressive strengths and lower bulk porosities were observed when using CEM I as the reagent [67, 263](Table 6.21). Due to the increased reaction kinetics 28 day strengths would be expected to be higher for CEM I blends as well as shorter setting times. Higher ultimate compressive strengths are also generally achieved for cement than lime/pozzolan blends. Lime/pozzolan blends may only develop strengths of 10-20MPa even after curing for greater than 90 days [255, 290, 325]. Higher compressive strengths were also achieved with APC residue/ggbs blends prepared with waste:binder of 1:1 [241]. The reactivity of the ggbs used by Lampris *et al* [241] appears to have been significantly higher than that of the co-fired PFA studied here, yielding shorter setting times and higher 28 day compressive strengths despite a lower curing temperature and the absence of a NaOH activator. Zheng *et al* [79] observed compressive strengths close to 15MPa for an APC residue activated by 10M NaOH solution and 0.8M Na_2SiO_3. The slightly higher strengths than those observed for the samples examined in the current study were likely a result of the sample preparation methods. 2.5ml activator solution was blended with 12g APC residue which was then

compressed under a uniaxial load of 6MPa i.e. the mixture was not flowable. This type of preparation would increase dry mass density resulting in reduced porosity and increased compressive strengths.

Generally differences in compressive strength after 7 days submersion in water were of low statistical significance, lying within 1 standard deviation of the mean. Interestingly sample 2:3 CEM l/s=0.6 showed an increase in compressive strength (Table 6.21). This was perhaps a result of continued hydration of the cement when submerged in de-ionised water which offset the strength lost by the leaching of soluble solids. Pozzolanic reactions would also be expected to continue during the submersion process. This would explain the strength increase observed for several of the PFA blends as a result of the 64 day monolithic leaching procedure. Due to the slower kinetics, pozzolanic reactions may not offset the loss resulting from leaching over 7 days. This was perhaps supported by testing the gas permeability of the samples before and after submersion. Figure 6.33 shows the permeability of 2:3 CEM l/s=0.6 and samples 2:3 and 3:2 cast with the co-fired PFA and WC solution. Noticeably the change in the permeability of the cement blend was negligible. This was attributed to the expansive cement hydration products filling the pore space left by the leaching of solids. These result suggest that cement based binders may maintain physical encapsulation of contaminants to a greater degree than pozzolanic blends when exposed to short term leaching. However, longer term performance is not known and certainly variable results would be expected based on factors such as the reaction kinetics, the degree of cement hydration prior to leaching, and the initial pore structure of the monoliths which would affect both the loss of soluble material and the ingress of water required to hydrate the unreacted cement or facilitate pozzolanic reactions.

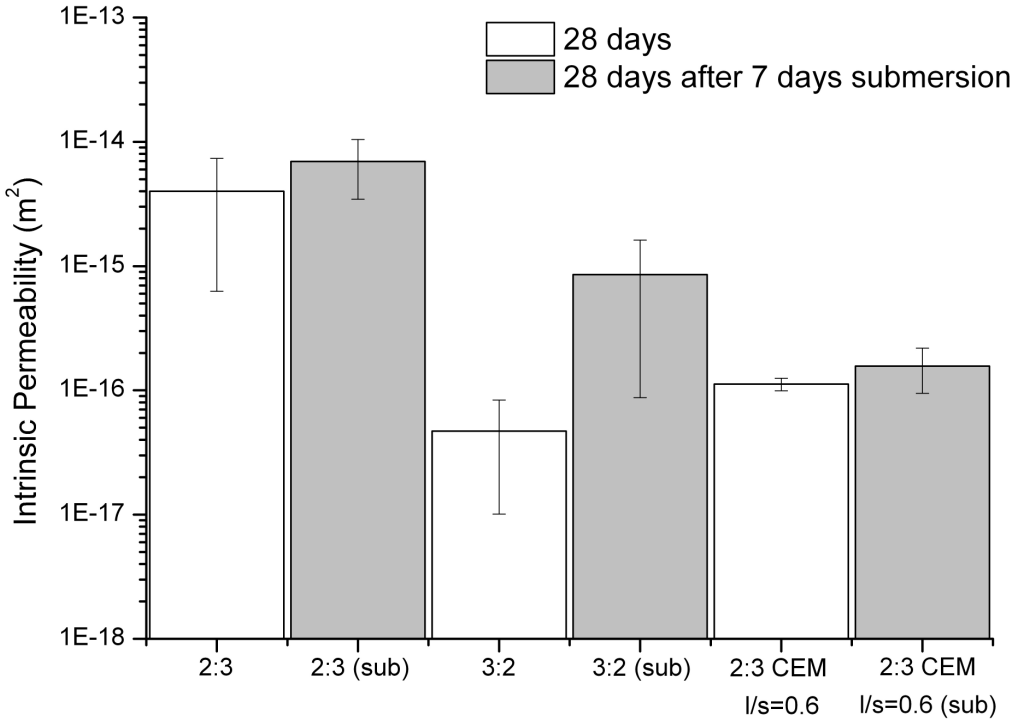

Figure 6.33 Intrinsic permeability of samples prepared with PFA/WC or CEM I/DIW, measured with N_2 at an absolute inlet pressure of 2bar. Samples 2:3 and 3:2 prepared with co-fired PFA and WC solution at l/s=1, cured at 38°C. 2:3 CEM prepared with CEM I, cured at 23°C. Error bars show standard deviation. Logarithmic Y scale.

Lower measured cumulative release (ε^*_{64}) and lower percentage chloride release were observed from the PFA blends than the cement blends during EA NEN 7375. Greater measured release was observed from sample 2:3 CEM l/s=0.6 (538,200mg/m^2) than sample 3:2 (466,300mg/m^2) despite the lower availability (per cube, given in mg in Table 6.22) and an initial surface wash off from sample 3:2. In addition slower diffusion of chlorides was observed by the effective diffusion coefficients (pD_e) and derived 64 day release (ε_{64}) (Table 6.22). Determination of diffusion appeared to be highly variable regarding the current samples however. Although the cement sample cast with l/s=0.6 showed a diffusion controlled increment, according to EA NEN 7375 no increment could be identified from the sample cast with l/s=0.5. This was counter-intuitive since reducing the l/s ratio should reduce the permeability of the sample [368] slowing the diffusion process.

	Chloride						
Sample	**Available (mg)**	**ε^*_{64} (mg/m^2)**	**ε_{64} (mg/m^2)**	**Inc.**	**pD_e**	**%**	**12457-2 after (mg/kg)**
2:3	8160	298,500	746,400	1-4	10.7	55	13,170
3:2	12,620	466,300	434,300	2-7	11.5	55	22,660
2:3 CEM l/s=0.5	nd	583,200	na	none	na	nd	3390
2:3 CEM l/s=0.6	11,170	538,200	1,272,100	1-4	10.3	95	3350

Table 6.22 Comparison of monolithic leach (EA NEN 7375) results for samples prepared with PFA/WC or CEM I/DIW. ε^*_{64}=measured cumulative 64 day release. Inc.=diffusion controlled increment. ε_{64}=derived 64 day release, pD_e=-log of the effective diffusion coefficient (D_e m^2/s) nd=not determined, na=not applicable

Permeability results showed sample 2:3 (cast with PFA/WC) to be more permeable than sample 2:3 CEM l/s=0.6, suggesting lower physical immobilisation. Although sample 3:2 showed initially lower permeability, it appeared as though this would rapidly change during the leaching procedure, resulting in greater permeability than sample 2:3 CEM l/s=0.6 (Figure 6.33). These results suggest lower physical immobilisation in the PFA blends. The reduced chloride leaching from PFA blends was therefore perhaps a result of the greater aluminium availability, contributed by the PFA and WC solution, allowing greater production of Friedel's salt and therefore greater chemical immobilisation of the chlorides. Thomas *et al* [212] showed the use of high aluminium materials such as PFA in cement to improve the chloride binding capacity. Such interpretation was corroborated by XRD observations which showed peaks of much stronger intensity for Friedel's salt in the blends cast with the PFA (Figure 6.34) (although it is appreciated that without refinement and correction for the amorphous content of the samples this is a poor indication of concentration). Such observations were consistent with XRD patterns reported by Lampris *et al* who observed stronger peaks corresponding to Friedel's salt in ggbs samples than CEM I samples [243] and slower chloride diffusion [67, 241]. However, considering the large difference in monolithic leach performance it was surprising that release of

chlorides during granular leach tests was so similar (Table 6.23). Additionally, the results of the granular leach test following the monolithic test suggested a greater amount of soluble chlorides were retained in the PFA monoliths. The greater release observed from the PFA samples following the monolithic leach test may have been a result of greater release of solids other than chlorides during EA NEN 7375 from the PFA samples. This would be expected based on the TDS observed during the granular tests (Table 6.23) and would increase the weight fraction that retained soluble chlorides would occupy. The release observed in subsequent granular tests gives an indication of water soluble chlorides retained, but due to changes in the sample during the leach test, including removal of solids and binding of water as pozzolanic reactions or cement hydration progress, is difficult to precisely relate to release during BS EN 12457-2 before the monolithic test or availability. Alternatively a greater retention of soluble chlorides may suggest the permeability results are not indicative of the relative permeability of the samples throughout the monolithic test, as the pore structure may continue to develop. Whilst the permeability results revealed some interesting qualitative information regarding the ranking of sample permeability and confirmed changes to the pore structure as a result of leaching, the method does test a modified pore structure due to the need for drying. The method is also severely limited with regards to the current materials due to the inability to dry the samples to a constant weight without inducing cracking. As such, flow through the samples would be inconsistent across the radius, preferentially flowing around a core which may have retained moisture. Certainly the test method would have to be further developed or alternative methods used to provide a more accurate idea of the influence of leaching on permeability of such products.

Ultimately release of chlorides from all binders was well in excess of both granular and monolithic hazardous WAC. Chloride release from geopolymeric matrices has not been reported. However, considering large amounts of NaCl were evidenced by XRD analysis [79], it is expected that release from a geopolymeric matrix would also surpass WAC limits.

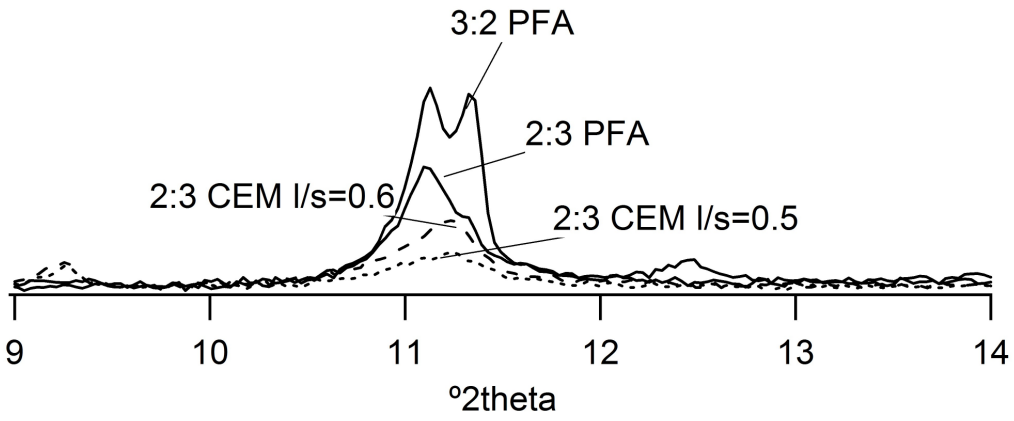

Figure 6.34 Comparison of most intense Friedel's salt peaks (monoclinic hkl=002, rhombohedral hkl=006) in XRD patterns of PFA and CEM samples. Normalised y axis range. Monoclinic and rhombohedral Friedel's salt is evident for PFA blends.

	2:3	**3:2**	**2:3 CEM l/s=0.6**	**2:3 CEM l/s=0.5**
Cl availability (mg/kg)	62,400	97,800	70,200	nd
Cl 12457-2 (mg/kg)	45,900	70,900	48,500	43,900
SO_4 availability (mg/kg)[a]	3580	3816	1228[b]	nd
SO_4 12457-2 (mg/kg)	2259	5420	0	0
pH	12.5	12.5	12.4	12.6
TDS (mg/kg)	148,500	159,500	124,300	119,400

Table 6.23 BS EN 12457-2 results for samples prepared with PFA/WC or CEM I/DIW binders. a=calculated based on release from as-received materials according to BS EN 12457-2 and IC. b=SO_4 in CEM I not considered. nd=not determined

No sulphate release was observed from the cement samples cast in this study. This appeared to be a consequence of the binding of sulphate within AFt, which was detected by XRD and may be prevented in alkali activated blends [207, 425]. The soluble sulphates contributed by the co-fired PFA and

WC solution would also have been removed. There would be sulphates present in the cement (typically <4% as SO_3 [98]) but the composition of the CEM I used was not determined and would likely not be detectable by leach testing because it would react with the tricalcium aluminates and remain insoluble. Sulphate release was not observed from PFA samples cast with DIW. As such sulphate release may be associated with the use of the WC solution. It would be of interest to see if sulphate release occurred from cement samples if activated by NaOH or the WC solution.

The pH of all leachates obtained from BS EN 12457-2 was similar, and suggested $Ca(OH)_2$ to be the pH determining species. Leachate fractions of the monolithic leach test performed on cement samples showed increasing pH whilst a reduction or steady pH was observed for the PFA samples (Figure 6.35). This was due to the production of $Ca(OH)_2$ as the cement hydrated, as shown by the increase in compressive strength upon immersion, compared with depletion of the $Ca(OH)_2$ as the pozzolanic reactions progressed and as $Ca(OH)_2$ and alkalis were leached. The end pH for the cement samples indicated a saturated $Ca(OH)_2$ solution which was verified by the observation of a white precipitate in the leachates of the later fractions of EA NEN 7375. This precipitate was collected after filtration and STA showed it to be $CaCO_3$. This was considered to be $Ca(OH)_2$ which had carbonated during filtration and loading into the STA. The production of $Ca(OH)_2$ as the cement hydrated also had significant influence on the ANC of the cement samples which was consequently significantly higher than the PFA blends (Figure 6.36).

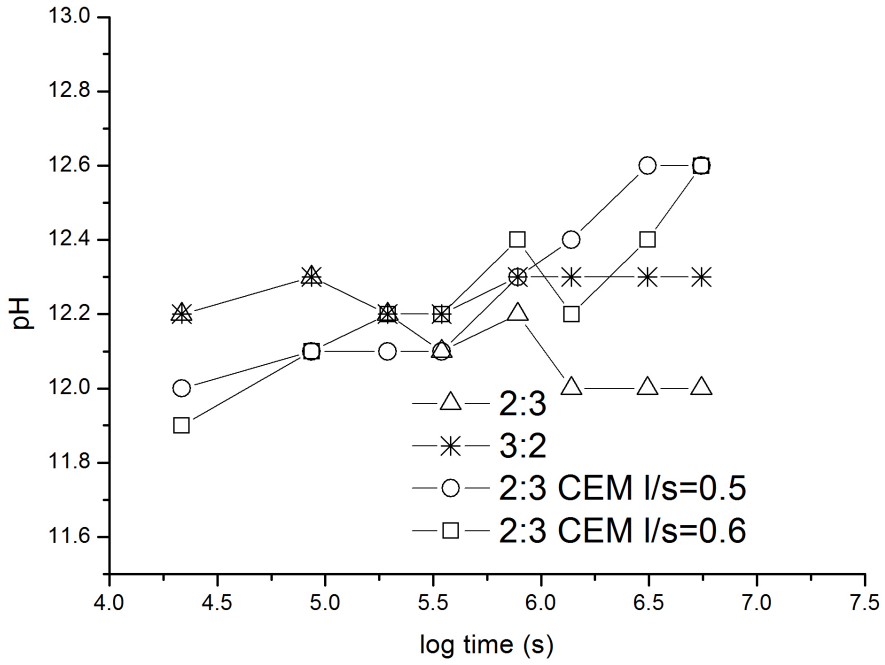

Figure 6.35 pH development during EA NEN 7375, comparison of samples prepared with PFA/WC or CEM I/DIW

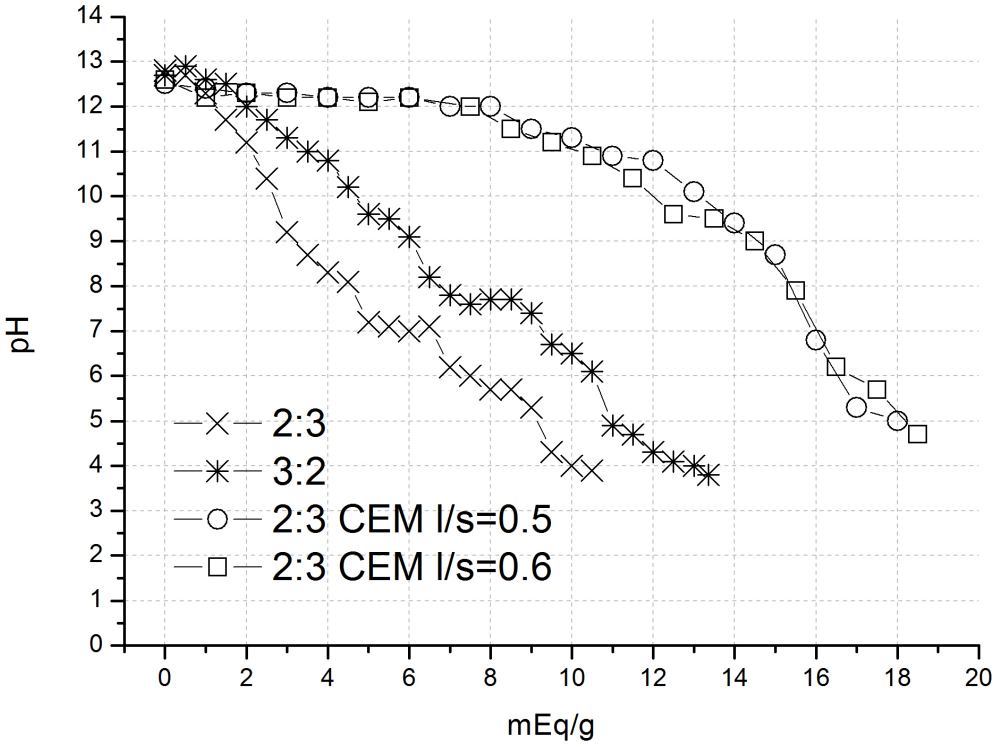

Figure 6.36 ANC titration curves. Comparison of PFA/WC and CEM I/DIW samples.

6.5.1 Summary of binder comparison

Although the use of pozzolanic binders appears to offer greater retention of chlorides during monolithic leach testing, no binders either studied here or throughout the literature have displayed the potential to immobilise the high amounts of chlorides which are present in APC residues by s/s treatment.

Compared to more traditional CEM I s/s matrices, many disadvantage were observed when using PFA and the WC solution as reagents. These included higher l/s demand, prolonged setting times, lower compressive strengths up to 28 days when working with similar waste:binder ratios and consistence, an increase in permeability as a result of 7 days submersion in water, and lower ANC. The increased l/s required was not of particular concern considering the liquid fraction was a valorised waste material. However, excessively high demand would further limit the quantities of waste which could be treated due to limited WC solution supply. If the WC solution supplies were consumed, replacement with a non-waste caustic solution would increase the cost of the treatment, particularly with high demand. The lower compressive strengths were also not of great concern since WAC criteria were met by all samples. The increase in permeability as a result of 7 days submersion in de-ionised water was a particular concern for the durability of the products since physical encapsulation of contaminants would be drastically reduced. Although the PFA blends showed lower ANC, the capacity was still sufficient according to recommended criteria [152]. Sulphate release was also greater from the PFA/WC samples. This appeared to be a result of the immobilisation of sulphates as ettringite in the CEM I matrices.

6.6 Summary of Performance Testing

Considering the results observed for performance testing it is clear that s/s of air pollution control residues using the reagents studied is not a feasible waste management option. The mass of APC residue which could be treated would be limited due to the high l/s (w/w) ratio required at economically attractive waste:binder ratios, owing to the high water demand of the APC

residue and the implications of the TDS in the WC solution, and the limited quantities of WC solution available.

Setting times were also prohibitive and typically longer than those which are judged to be industrially attractive. Setting times were a result of the reaction kinetics and physical properties of the pastes. Although reaction kinetics were significantly accelerated by alkali activation, neutralisation of the NaOH by the CaClOH present in the APC residue significantly reduced this effect at higher waste:binder ratios. Setting times could however be substantially accelerated by curing at elevated temperatures.

Although the reagents were shown to be reactive by development of matrices of substantial compressive strength, greater than that required by WAC, and remained cohesive during 64 days submersion in water, durability was also a concern. Low resistance to wetting and drying cycles was observed which would risk cracking of the monolithic product, drastically reducing physical encapsulation of contaminants and durability. Additionally, due to the high water soluble proportion of the matrices, the pore structure was observed to alter significantly due to short term leaching. This process not only has implications for the maintained physical encapsulation offered by the monolithic product, but also highlights the lack of accuracy in predicting the long term leaching of contaminants from similar matrices based on effective diffusion coefficients calculated from the regulatory monolithic leaching procedure EA NEN 7375. The effect of leaching on matrices prepared with different binders may not be consistent. For example, although the pozzolanic matrices studied showed an increase in permeability as a result of short term leaching, cement based matrices showed no increase. This was considered to be a result of the different reaction kinetics of the binders during the leaching procedure and therefore the amount of expansive reaction products produced which may compensate for the leaching of water soluble solids.

The significant proportion of the matrices which remained water soluble meant hazardous WAC for TDS was frequently exceeded. Primarily this was

owing to the high water soluble chloride salt content. Despite the relatively high availability of aluminium in the matrices, and observed production and retention of chlorides as Friedel's salt during granular leach testing, the majority of the chlorides remained present as highly soluble NaCl and therefore release was essentially availability controlled and only slowed by physical encapsulation which was insufficient to meet hazardous WAC limits. In addition the alkali activated PFA matrices showed less potential for immobilisation of sulphates than cement based matrices.

The pH obtained from the matrices during batch extraction tests in de-ionised water was also excessively high with implications for the solubility of amphoteric metals such as lead and zinc. The pH of the matrices appeared to be predominantly determined by $Ca(OH)_2$. As such the pH observed during monolithic leaching of the pozzolanic matrices decreased over time as $Ca(OH)_2$ was consumed or leached, whilst the pH of the cement based samples steadily increased to that of a saturated $Ca(OH)_2$ solution as cement hydration continued. The $Ca(OH)_2$ concentration of the matrices also appeared to have a dominant influence on the ANC observed and therefore lower ANC was observed for the pozzolanic than the cement based samples. All samples met the minimum recommended ANC to pH 9 of >1mEq/g however.

7 Results and Discussion- Effects of variability in APC residue composition

It is evident from the results presented in chapter 4.1, and from the literature that the composition of APC residues can vary considerably. Such variation may have implications for the application of treatment processes. In order to examine these implications, treatment by s/s using the WC solution and co-fired PFA was attempted on different residues. Figure 7.1 shows an example of a monolith resulting from blending a different APC residue with the co-fired PFA and WC solution. Such treatment resulted in gas production and as such a highly porous monolith. Exposure of residues A2-A5 to a 3.5M NaOH solution resulted in similar gas production but gas was not produced when

blending the residues with PFA and DIW. This gas was collected by water displacement and exposed to a glowing/lighted splint. Such analysis revealed the gas was not hydrogen, oxygen or carbon dioxide. The precise nature of the gas is not known, considering the STA, XRD and elemental compositions of the residues there were no clear differences which would suggest gas production from residues A2-A5.

Figure 7.1 Example of a porous monolith typical of those produced when alkali activating PFA/APC residue blends which include residues other than A1. Porous structure results from gas produced when blending APC residue with NaOH.

A possible explanation could be the use of nitrogenous compounds to control NO_x emissions in all of the gas streams except for that from which A1 was collected. Excess injected ammonia may combine with HCl in the gas stream to produce NH_4Cl [20]. Ammonium chloride may then react with NaOH to produce ammonia gas as equation 7.1

Equation 7.1 $NH_4Cl + NaOH \rightarrow NaCl + H_2O + NH_3$

Several observations make such an explanation unlikely however. The gas produced did not have the odour associated with ammonia. No water solubility was observed (gas immediately displaced the water), and the pH of the water bath containing the displaced water remained neutral, whilst with dissolved ammonia would cause the pH to rise. The nature of the gas therefore remained undetermined. Collection and mass spectrometry would seem appropriate to assist in identification.

Such gas production meant alkali activation was unsuitable for most APC residues. Interestingly no gas production was noted for the residues blended with NaOH and Na_2SiO_3 by Zheng *et al* [79]. This residue was referred to as MSWI fly ash by Zheng *et al* however was collected from the fabric filter and contained significant amounts of CaClOH suggesting the scrubber had been injected and therefore the residue should be referred to as APC residue according to the definitions suggested by Chandler *et al* [20]. Luna Galliano *et al* [304] examined geopolymerisation of MSWI fly ash with NaOH and Na_2SiO_3 and did not mention gas production whilst Lancellotti *et al* [305] examined geopolymerisation with a NaOH/Na_2SiO_3 solution, of MSWI fly ash and scrubber residue collected separately. Gas production was not eluded to however images presented showed very large pores which may have been the result of gas production in the samples containing MSWI fly ash. Similar morphology was not apparent in the samples prepared with the scrubber residue. Bacciochi *et al* [74, 82] also added NaOH to a hospital waste incinerator APC residue and did not report gas production

In order to examine the influence of APC variability on the performance of s/s matrices, blends were cast utilising CEM I and de-ionised water. In this way all the residues could be treated by the same process. A waste:binder ratio of 2:3 was used. A l/s ratio of 0.5 was employed for all samples based on preliminary testing which showed this l/s was the most appropriate for keeping workability within sensible boundaries for all residues. Nomenclature used throughout this chapter refers to the waste:binder ratio and the residue used (A1-A5 corresponding with that used in chapter 4.1).

The variability in water demand of the different residues was clearly evident, giving a large range of flow table spreads (Table 7.1). This demand appeared in part to be a result of the salt concentration in the residue. For example residue A5 gave the lowest flow table spread and was observed by performing BS EN 12457-2 to contain the highest concentration of soluble chlorides (chapter 4.1). The residues containing lower concentrations of chloride salts had much higher flow table spreads. Other factors must have had influence as well however. Residue A3 had a higher salt concentration

than A2 or A4 yet the viscosity of this blend was too low to test by flow table. It is likely that the lower water demand for the blend containing A3 was also a result of the carbonation this residue had undergone. Wang *et al* [128] showed the specific surface area of APC residues to reduce from 0.938 to 0.34m^2/g after natural carbonation in ambient conditions for 4 days. This decrease in specific surface area would reduce the water demand [330]. The sample prepared with a waste:binder ratio=2:3 incorporating residues A1-A4 all met the >175mm flow table spread criteria, residue A3 was excessively workable and a reduction in the l/s ratio would be recommended. Sample 2:3 A5 fell short of the 175mm flow criteria.

Setting times also varied substantially (Table 7.1). Only samples cast with residues A3 and A4 met the minimum time for initial set recommended to facilitate handling, of ~2 hours [157]. All samples met final set within the recommended 24 hours [157]. Several factors would interact with regards to the setting time. Depending on the concentration, the chlorides may accelerate the set [67, 166, 229, 242] whilst the metals such as Pb would act as retarders [220, 228]. Hydration of $CaSO_4$ to produce gypsum, and interlocking of gypsum crystals can cause false set i.e. stiffening occurs but the paste regains plasticity on further mixing [144]. Such phenomenon was not apparent in the current mixes.

Sample	**Flow Value (mm)**	**Setting Time (h)**		**28d UCS (MPa)**	**UCS (7d sub) (MPa)**	**Bulk Porosity (%)**
		In.	**Fin.**			
2:3 A1	190	0.3	0.7	10.2 +/-2.3	11.3	45.4
2:3 A2	205	1.7	3.5	10.5 +/- 0.5	15.2	44.2
2:3 A3	>	5.5	5.9	10.2 +/-0.9	14.4	47.2
2:3 A4	195	5.2	5.5	10.2 +/-0.2	10.7	45.6
2:3 A5	145	0.1	0.2	11.3 +/-0.2	9.0	40.3

Table 7.1 Workability, Setting time (in=initial, Fin=final), compressive strength and bulk porosity results for samples prepared with different APC residues, APC residue:CEM I=2:3, l/s=0.5, cured at 23°C. >=greater than testable

Residues A2, A3 and A4 showed the longest setting times and contained the lowest concentration of chlorides (chapter 4.1) suggesting chloride concentration may be an important influence, accelerating the setting time. However, it is also noted that the setting time was typically correlated with the flow table spread. The physical properties of the pastes may be considered to have had significant influence on the setting times [422]. This influence is why the standard methods (BS EN 480-2 or BS EN 196-3) require standard consistence which was deviated from in the current work.

Bulk porosity and compressive strength after 28 days appeared similar for all blends (Table 7.1) and compressive strength surpassed minimum WAC limits. Sample 2:3 A5 showed a slightly higher compressive strength and lower bulk porosity, which was perhaps an effect of the dry mass density achieved when compacting the blend, owing to the absorption of the water by the APC residue and therefore higher volume fraction of solids (indicated by the workability-flow table spread Table 7.1). In general the blends showed slightly higher compressive strengths following 7 days submersion in de-ionised, indicating further hydration of the cement. Sample A5 showed a slight decrease in strength. Loss of strength from the blend containing this residue may have been a result of the higher soluble fraction of A5 (chapter 4.1) which was reflected in the TDS from sample 2:3 A5 by the granular leach test (Table 7.2). The greater TDS was primarily due to the higher chloride release.

Significantly higher chloride release was also observed from 2:3 A5 over the 64 days monolithic leach test (Table 7.3). The samples were ranked in the same order (A5>A1>A3>A4>A2) for chloride release from untreated and cement stabilised residues, in both granular and monolithic tests. This highlighted the minimal fixation of chlorides in the s/s products, and as such availability controlled release of the chlorides. Minimal immobilisation of chlorides was confirmed by performing the granular test on the sample after monolithic leaching (Table 7.3). TDS was also ranked in the same order for cement solidified samples and untreated residues, highlighting the importance of the chlorides to TDS.

Mix	Cl 12457-2 (mg/kg)	TDS 12457-2 (mg/kg)	pH
2:3 A1	43,900	119,400	12.6
2:3 A2	30,400	88,000	12.6
2:3 A3	43,300	102,000	12.6
2:3 A4	32,500	95,100	12.6
2:3 A5	63,900	163,700	12.5

Table 7.2 Granular leach results (BS EN 12457-2) for samples prepared with different APC residues, APC residue:CEM I=2:3, l/s=0.5, cured at 23°C

Mix	ε^*_{64} (mg/m^2)	Diffusion controlled increment	12457-2 after (mg/kg)	UCS before (MPa)	UCS after (MPa)
2:3 A1	583,200	none	3390	10.2 +/-2.3	12.8
2:3 A2	369,300	none	1710	10.5 +/- 0.5	12.6
2:3 A3	460,400	none	2060	10.2 +/-0.9	18.2
2:3 A4	392,100	none	1730	10.2 +/-0.2	17.1
2:3 A5	859,300	none	3480	11.3 +/-0.2	9.2

Table 7.3 Monolithic leach results (EA NEN 7375) for samples prepared with different APC residues, APC residue:CEM I=2:3, l/s=0.5, cured at 23°C

Despite showing significantly different measured release of chlorides, the mechanisms controlling release were similar for all samples as was evident from the similarity of the log-log plots (Figure 7.2). All samples showed depletion controlled release. Gradients for fractions 1-4 of all tests were ~0.30-0.33, just short of the 0.35 required by EA NEN 7375 to class behaviour as diffusion controlled. This similarity again highlights the lack of chemical immobilisation or physical encapsulation provided by the samples. All samples exceeded hazardous WAC limits for chloride release in granular and monolithic tests. Hazardous WAC limits for TDS were exceeded by all samples except those made with residues A2 and A4 which fell just below the 100,000mg/kg limit. No sulphate release was detected from any of the samples with a detection limit of 20mg/kg (after dilution); indicating SNR granular WAC limits were met. This was despite the relatively high SO_4

concentration in some of the residues, but SO_4 was observed to be bound as ettringite by XRD (Figure 7.3).

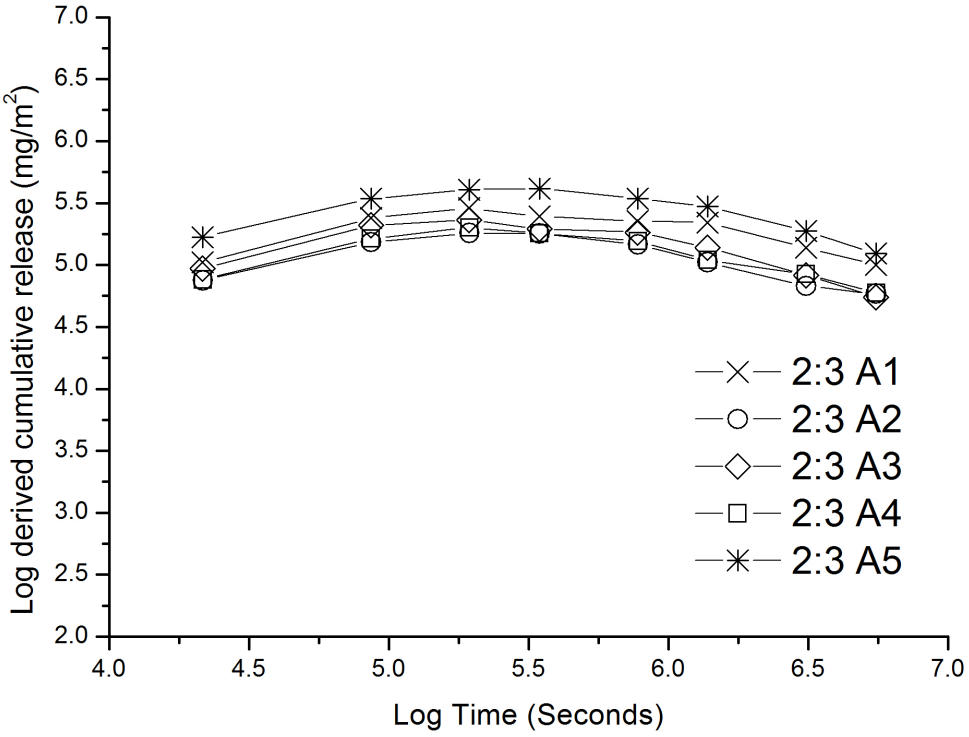

Figure 7.2 Log-log plots resulting from analysis of EA NEN 7375 results for samples prepared with different APC residues, APC residue:CEM I=2:3, l/s=0.5, cured at 23°C.

The pH of the granular test leachates were all very close to one another and reflected the $Ca(OH)_2$ content of the samples (Table 7.2). Slight differences were observed in the pH of the early fractions of the monolithic leach tests, which corresponded to the pH obtained for the granular leachates produced by the untreated residues (chapter 4.1) i.e. residue A5 produced the lowest granular leachate pH and the lowest pH in the initial fractions of the monolithic test (Figure 7.4). As such the pH in the early fractions of EA NEN 7375 reflected the pH of the individual APC residues. In later fractions the pH values converged and all reflected saturation with $Ca(OH)_2$. As was previously discussed a $Ca(OH)_2$ precipitate was evident in the leachates of the later fractions of EA NEN 7375 (chapter 6.5).

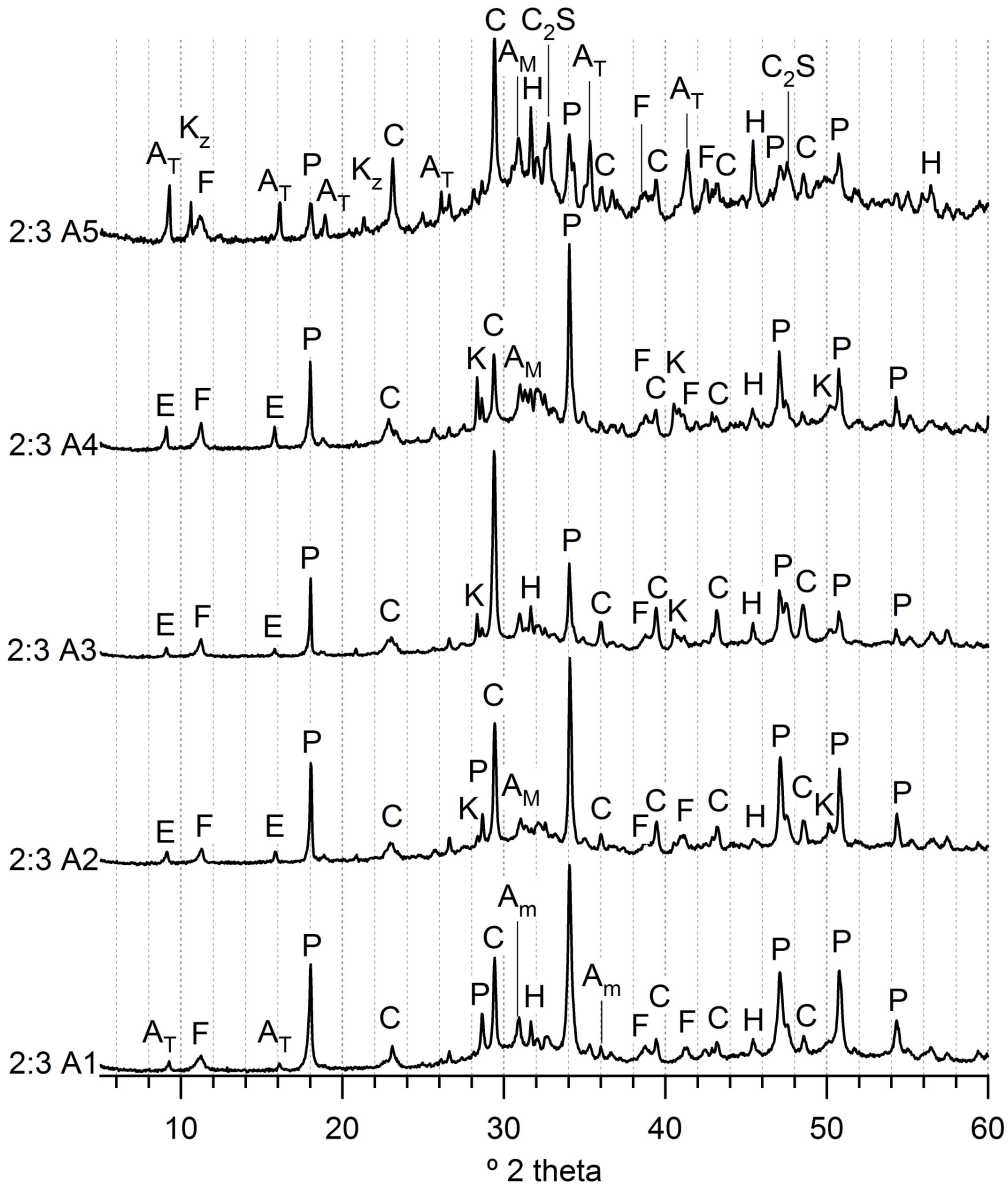

Figure 7.3 XRD patterns (y axis range not normalised) for samples prepared with different APC residues, APC residue:CEM I=2:3, l/s=0.5, cured at 23°C for 28 days. Samples taken from cube centers. P=$Ca(OH)_2$, C=$CaCO_3$, H=NaCl, K=KCl, F=Friedel's salt, E=ettringite (ICDD PDF=72-0646), A_T=Substituted AFt, see text, A_m=$Ca_2Al(OH)_7{\cdot}3H_2O$ (ICDD PDF=33-0255), K_z=Kuzel's salt (ICDD PDF=19-0203)

After 28 days' curing considerable differences in the quantity of $Ca(OH)_2$ and $CaCO_3$ were present in the cement treated residues (Table 7.4). Such concentrations largely correlated with the contribution made by the initial residue (chapter 4.1). Residue A1 contained the greatest amount of $Ca(OH)_2$ and sample 2:3 A1 also contained the highest concentration. Similarly residue A3 contained the highest amount of $CaCO_3$ which was reflected in the concentration in 2:3 A3 after 28 days. The $Ca(OH)_2$ present would also

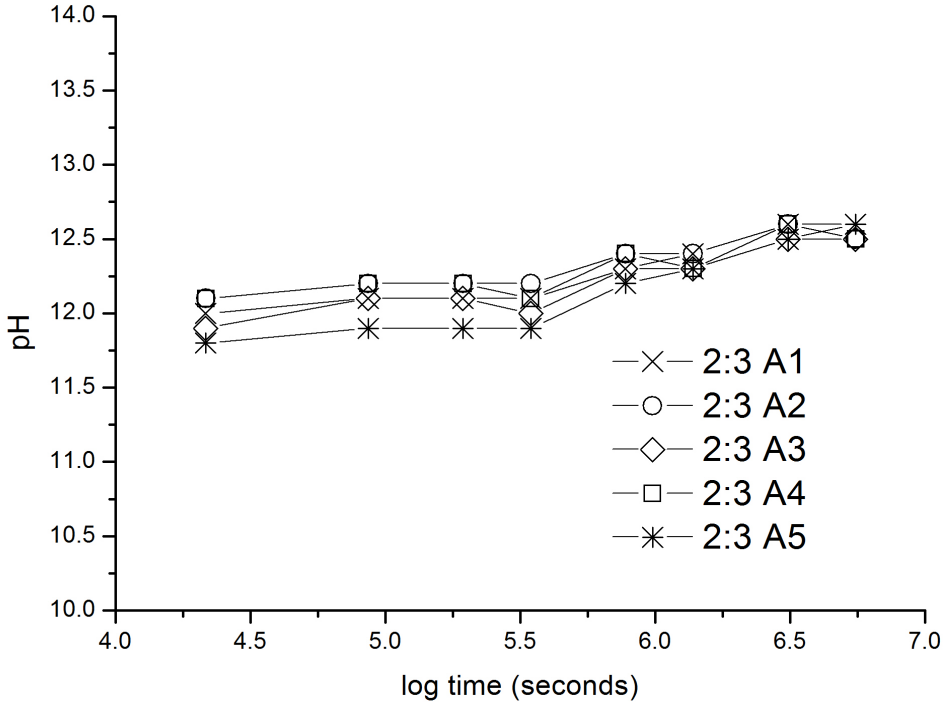

Figure 7.4 pH development during EA NEN 7375 for samples prepared with different APC residues, APC residue:CEM I=2:3, l/s=0.5, cured at 23°C

	2:3 A1	2:3 A2	2:3 A3	2:3 A4	2:3 A5
%$Ca(OH)_2$	20.6	11.8	8.7	9.3	7.2
%$CaCO_3$	8.8	10.8	18.8	5.2	10.8

Table 7.4 $Ca(OH)_2$ and $CaCO_3$ content in samples prepared with different APC residues, APC residue:CEM I=2:3, l/s=0.5, cured at 23°C for 28 days. Samples taken from centre of cubes. Concentrations presented as % of dry weight

have been contributed to by the cement hydration which may have occurred at different rates in the different samples owing to the type and level of contaminants present. Despite residue A5 containing a higher concentration of $Ca(OH)_2$ than residue A3 (Table 4.1), sample 2:3 A5 contained a lower $Ca(OH)_2$ concentration than 2:3 A3. This may suggest a greater extent of cement hydration had occurred in sample 2:3 A3 than 2:3 A5. However, the density of the fresh mixes was not determined therefore it was not possible to quantify the $Ca(OH)_2$ concentration supplied by the residue or produced by cement hydration. Effects of carbonation on the concentration of $Ca(OH)_2$ and $CaCO_3$ observed after 28 days curing were considered to be negligable

due to curing in sealed plastic bags and taking samples from the centre of the cubes.

The effects of the different $Ca(OH)_2$ and $CaCO_3$ concentrations were apparent in the ANC behaviour of the samples (Figure 7.5). Sample 2:3 A1 showed a greater initial buffering plateau consistent with the greater $Ca(OH)_2$ concentration. Sample 2:3 A3 showed a slightly greater carbonate plateau (pH~6-4) [82]. Considering the ANC curves for cement, it seems likely that a true equilibrium would not be met for a very long time because the cement would continue to hydrate, producing $Ca(OH)_2$ and C-S-H and therefore providing additional buffering capacity. Perhaps a true equilibrium could only be met once complete reaction of the cement clinker phases had occurred. It is known this had not occurred by 28 days in the current samples due to the continued strength development of the samples as a result of submersion, and because reflections associated with unreacted belite (~32-33°2θ) were observed in all samples by XRD (Figure 7.3).

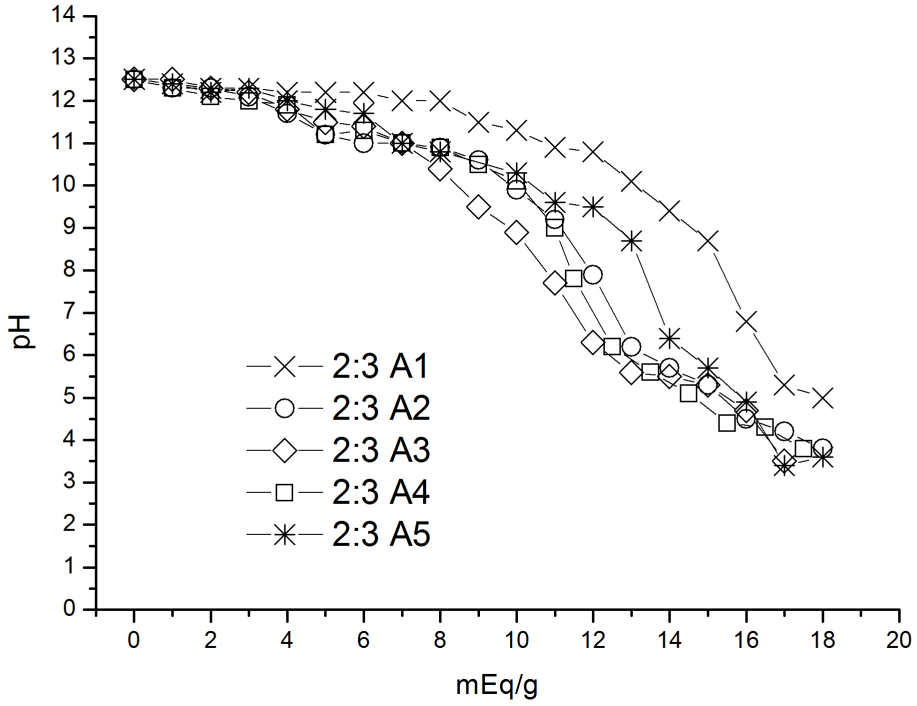

Figure 7.5 ANC titration curves for samples prepared with APC residue:CEM I=2:3 and l/s=0.5 cured for 28 days at 23°C using different APC residues

STA and XRD showed no CaClOH to remain present in the samples. This is consistent with previous work working at similar waste:binder ratios [243], and the behaviour of the WC/PFA matrices. XRD analysis provided patterns very similar to those obtained in previous literature [243]. Predominant peaks belonged to $Ca(OH)_2$ and $CaCO_3$. Retention of NaCl and KCl from the original residues was also evident. Consistent with the diffraction patterns obtained for the as received residues, no KCl was evident in samples containing A1 or A5. Friedel's salt was produced through the reaction with the calcium aluminate clinker phases (tri-calcium aluminate and tetra-caclium aluminoferrite) and was evident in all samples, however a number of other peaks corresponding to the hydration of these phases were also evident. Peaks corresponding to $Ca_2Al(OH)_7{\cdot}3H_2O$ ($0.5(4CaO{\cdot}Al_2O_3{\cdot}13H_2O$) (ICDD PDF=33-0255) were evident in all samples as also identified by Lampris *et al* [243] and previous studies utilising washed residues [239].

Other peaks were evidenced corresponding to AFt phases. For samples containing residues A2-A4, peaks were identified as ettringite, as previously observed when blending MSWI fly ash with calcium aluminate cements [215] and APC residues with CEM I [166, 239]. The peaks for samples prepared with residues A1 and A5 were shifted to a slightly higher °2θ (Figure 7.6). Notably, A1 and A5 were the residues with the lowest sulphate concentrations, as evidenced by leaching tests (chapter 4.1). This change in the concentration of anions present in the systems could alter the composition of the AFt minerals produced. Peaks in the samples prepared with residues A1 and A5 showed a good match for the AFt mineral $3CaO{\cdot}Al_2O_3{\cdot}3Ca(OH)_2{\cdot}32H_2O$ (ICDD PDF=41-0216) i.e. complete OH substitution of SO_4 in ettringite, but this mineral is readily carbonated [144] and therefore unlikley to be present. It seems likely that partial replacement of SO_4 with OH or CO_3 has occurred, resulting in the peak shift [428]. This would be a consequence of the reduced SO_4 concentration of the residues. Cl substituted ettringite is reportedly unstable above 0°C [144] and therefore was unlikely to be present.

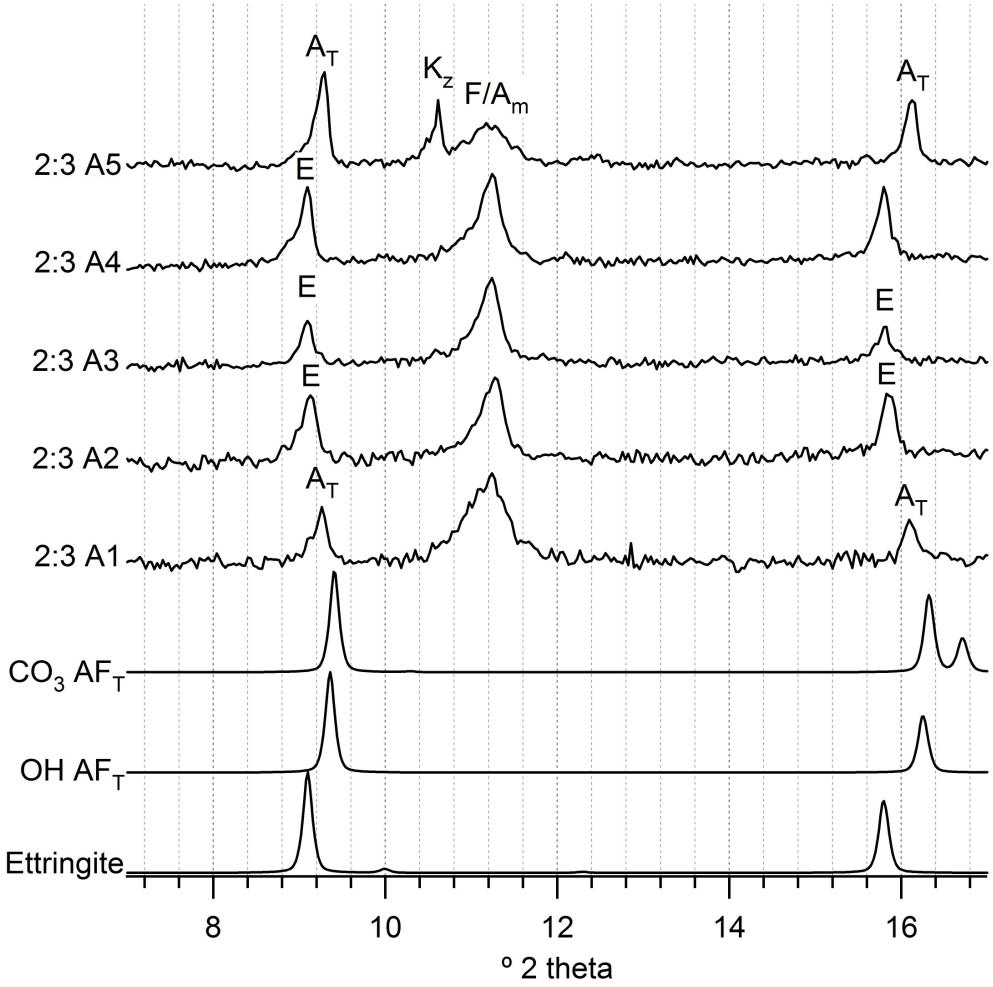

Figure 7.6 XRD patterns for samples prepared with different APC residues, APC residue:CEM I=2:3, l/s=0.5, cured for 28 days at 23°C. (Y axis range not normalised but adjusted for clarity). CO_3 AF_T=$3CaO{\cdot}Al_2O_3{\cdot}3CaCO_3{\cdot}32H_2O$ (ICDD PDF=41-0215), OH AF_T=$3CaO{\cdot}Al_2O_3{\cdot}3Ca(OH)_2{\cdot}32H_2O$ (ICDD PDF=41-0216), Ettringite=$3CaO{\cdot}Al_2O_3{\cdot}3CaSO_4{\cdot}32H_2O$ (ICDD PDF=72-0646)

A solid solution would also be expected amongst the AFm phases which are readily substituted depending on the local chemical environment [198, 214]. Such minerals are readily altered to the extent that changes such as carbonation or dehydration may also occur during XRD analysis [214]. No solid solution occurs between Friedel's salt and monosulphoaluminate [198] however an intermediate phase 'Kuzel's salt' may occur ($3CaO{\cdot}Al_2O_3{\cdot}0.5CaCl_2{\cdot}0.5CaSO_4{\cdot}10H_2O$) [198, 214]. Such a phase was identified in the diffraction pattern of sample 2:3 A5 (Figure 7.3 and Figure 7.6). The tetra-calcium aluminoferrite phase may hydrate to produce an iron containing analogue of Friedel's salt which may form a solid solution state with Friedel's salt [144, 211, 213] or, in the presence of $CaSO_4$, as would be

the case when blending the cement with APC residue, it has been reported that the tetra-calcium aluminoferrite phase hydrates to produce ettringite and an amorphous iron rich gel phase [144].

XRD data were not quantified due to the difficulties of quantifying such complex patterns and the lack of RIR ratios for several of the matched patterns. Similar to the PFA blends, the matrices were very polycrystalline and therefore several overlapping reflections were observed as demonstrated in Figure 7.7. Patterns for samples 2:3 A2 and 2:3 A4 are included as examples in Figure 7.7, after correction to present data as collected with fixed divergence slits, for comparison of intensities with references patterns.

Considering the chloride concentration in the APC residue, and the amount of tricalcium aluminate and tetracalcium aluminoferrite which would be present in the CEM I (~19.9% weight [204] or 10-25% weight [144]), together with the fact that these phases hydrated to form a range of SO_4, Cl, CO_3 and OH containing AFm and AFt phases. It is clear that only a small proportion of the chlorides could have been immobilised as Friedel's salt. Other chloride containing phases included NaCl and KCl. However, considering the peak intensities of the phases and the limited availability of Na and K in the mix, together with the chloride concentration known to be present in water soluble form by the release observed from leaching tests, it is likely that a large proportion of the chlorides were associated with the x-ray amorphous phases. Large amorphous contents were evident in all of the samples from the XRD baselines (Figure 7.3), the amorphous fraction would be expected to consist of C-S-H and perhaps residual amorphous fraction of the APC residue. It seems likely that the chloride is associated with the C-S-H [198, 199]. Since the vast majority of chlorides associated with C-S-H are readily leachable by water [199] and NaCl and KCl are highly soluble, very little chemical immobilisation of chlorides occurs in these systems as was observed by the leach test results.

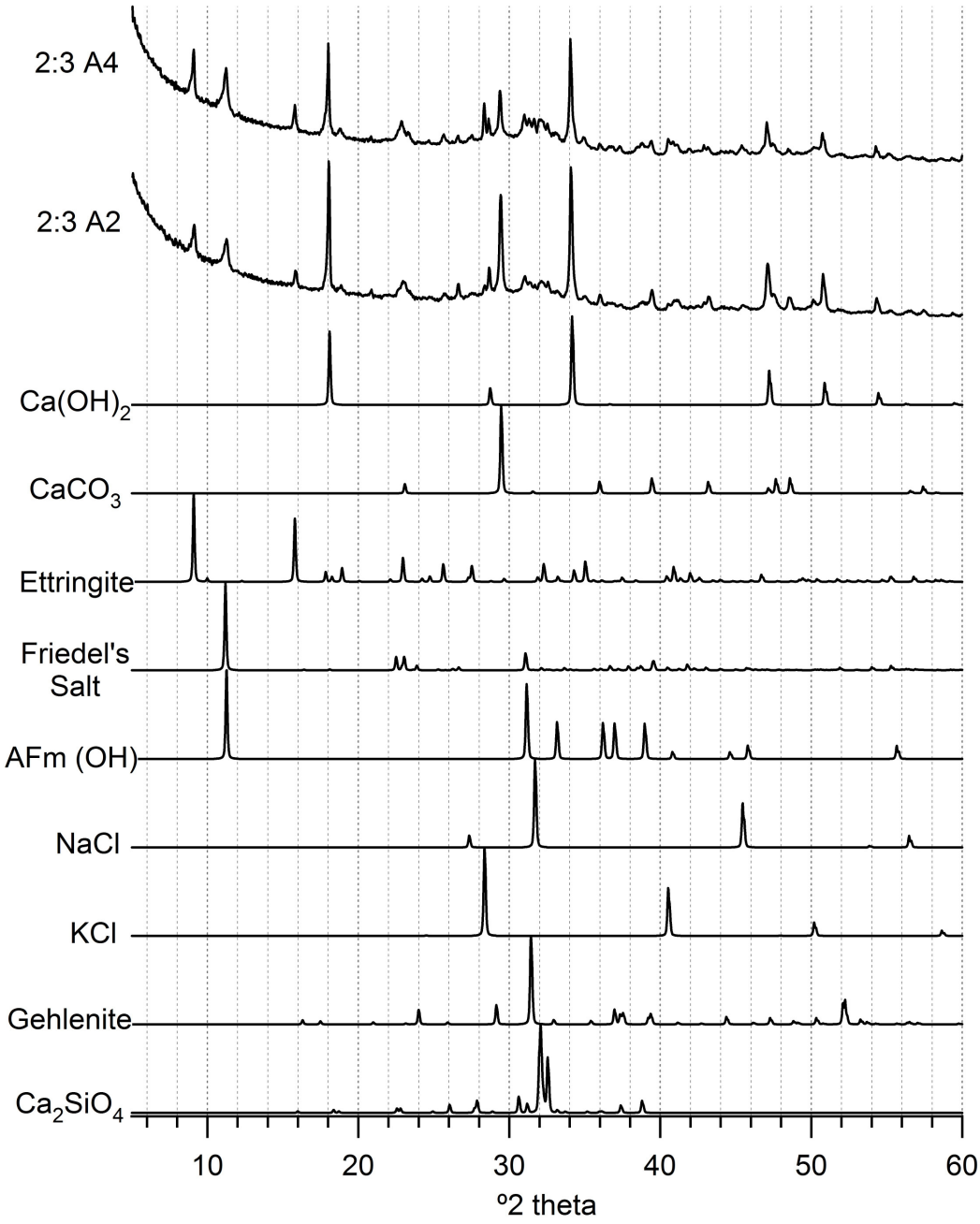

Figure 7.7 XRD patterns for samples 2:3 A2 and 2:3 A4 corrected to fixed divergence slits, and reference patterns for principal crystalline phases present.

7.1 Summary of APC residue variability effects

The majority of APC residues (4 out of 5 examined in this study) produced a gas when contact with NaOH was made. The nature of this gas remains unknown. Such behaviour precludes the use of alkali activated solidification/stabilisation treatments for APC residue since gas evolution

during mixing could be dangerous depending on the gas evolved, and resulted in a highly porous monolithic product.

The variability in APC residue composition has implications for the performance of applied s/s treatment. Most notably the variability in the hygroscopic nature of the residues appeared to affect the water demand of the s/s blends. When working at a constant l/s and waste:binder ratio the workability may vary considerably, flow table spread for equivalent samples examined in the current study ranged from 145mm to a value which could not be determined by flow table due to excessively low viscosity. This variability also had small implications for the compressive strength and porosity of the resultant monoliths, and more significant implications for the setting times. Initial setting times observed ranged from 0.1-5.5 hours and final setting times from 0.2-5.9 hours. In addition to the implications of the physical properties of the pastes, setting times of APC residue/cement samples are also affected by the mineralogy of the residue, specifically the concentration of chloride salts which would determine the effect on cement setting.

The variation in the concentration of chloride and sulphate salts in the residues also affected the mineralogy of the resultant samples, most notably varying the formation of AFt and AFm minerals. Such variation had little consequence regarding regulatory limits for the leaching of chloride and sulphate however. The magnitude of chloride release was highly variable but always exceeded hazardous WAC limits and occurred by a similar mechanism from all samples due to limited chemical or physical immobilisation. Sulphates were in contrast always below SNR WAC limits despite the considerable variability in the availability, due to binding in AFt minerals. Variability in the calcium salt availability in the residues was observed to significantly affect the ANC. Residues with a greater concentration of $Ca(OH)_2$ owing to excess scrubber result in more alkaline s/s matrices when blending with CEM I.

8 Conclusions

The study examined the possibility of treating hazardous air pollution control residues created during solid waste incineration in a modern energy from waste facility with other waste materials by solidification/stabilisation. The aim was to minimise the environmental impact of the hazardous waste whilst valorising other waste materials through their use as reagents. Such a treatment would offer an economical and resource efficient solution to hazardous waste management.

Based on the characteristics of the air pollution control residues, two waste materials were identified which may be valorised as reagents. These were a pozzolanic pulverised fuel ash, classed as unsuitable for construction applications primarily due to an excessively high organic carbon and sulphur content, and a waste caustic solution, resulting from cleaning of aluminium dyes. The use of such materials was considered to offer the potential for development of a relatively high compressive strength, low porosity matrix via pozzolanic reactions with the excess lime present in the air pollution control residues. Additionally the high aluminium content in the pulverised fuel ash, coupled with that present in the caustic solution and the calcium in the air pollution control residue, were believed to be potentially beneficial for the production of large amounts of Friedel's salt and therefore for chemically immobilising the high concentrations of chlorides present in the air pollution control residues. Chlorides have been shown to remain problematic when using other, more traditional binders such as cement. The use of the caustic solution was also considered to offer additional benefits including increasing the rate of the typically slow pozzolanic reactions, thereby reducing setting times and accelerating the rate of strength development to commercially attractive levels. Alkali activation has also shown potential for the production of zeolitic minerals which may have high cation exchange capacity and therefore offer benefits for immobilisation of the pollutant metal cation present in air pollution control residues.

Alkali activation was observed to reduce the setting time and increase strength development of the air pollution control residue/pulverised fuel ash blends. However, increased curing temperatures were also required to achieve commercially suitable setting times. Due to the calcium chloride hydroxide present in air pollution control residues, increasing the waste content also resulted in reduced reaction kinetics due to neutralisation of the alkali metal hydroxides present in the activator. Blends were observed to produce monolithic products which exceeded minimum regulatory compressive strength limits and remained cohesive when exposed to water for 64 days during regulatory monolithic testing. Such development was primarily a result of pozzolanic activity, producing calcium silicate hydrates similar to those responsible for the physical properties of hydrated cement. Crystalline zeolitic minerals were also observed. Zeolites were more prominent when working at low waste:binder ratios which are less attractive commercially due to cost implications. Due to the high concentration of calcium hydroxide and calcium chloride hydroxide in the air pollution control residues, increasing the waste:binder ratio resulted in more calcium rich hydration products such as calcium silicate hydrates and Friedel's salt. Increasing the waste:binder ratio also resulted in excess unreacted calcium hydroxide and largely as a result of this, the acid neutralisation capacity of the samples was increased. A proportion of the chlorides were observed to be retained as Friedel's salt and sodalite during granular leach testing. However, the majority of the chlorides were present as highly soluble sodium chloride, and, as such, chloride release remained high and essentially availability controlled. Waste acceptance criteria could only be met by means of dilution with reagents. Significant levels of dilution would be required which rendered the treatment unsuitable for immobilisation of air pollution control residues.

Compared to more traditional cement based solidification/stabilisation treatment several disadvantages were observed including prolonged setting times, reduced workability and lower compressive strengths. Additionally sulphate release was higher from the alkali activated pulverised fuel ash matrices than the cement samples. Sulphates were predominantly retained

as ettringite in the cement samples. Ettringite was not evident in the pulverised fuel ash samples but sulphates were identified as vishnevite at later ages and after granular leach testing. The co-fired pulverised fuel ash had a very high sulphur concentration but did not appear to be the primary contributor to sulphate release because most of the sulphur appeared to be present in reduced or intermediate forms, possibly due to incomplete combustion which was also evidence by the high organic carbon content of the ash.

The pozzolanic pulverised fuel ash matrices suffered an increase in permeability due to submersion in de-ionised water for 7 days. No permeability increase was observed for cement based matrices and an increase in compressive strength was apparent. This highlighted important differences between the types of matrices with regard to maintained physical encapsulation of contaminants. Additionally, because the samples did not maintain constant permeability during leaching, which is one of the boundary conditions for the use of the regulatory monolithic leach test employed for assessment against waste acceptance criteria, prediction of long term leaching based on diffusion coefficients calculated from monolithic leach testing should not be undertaken.

Four of the five air pollution control residues examined produced an unidentified gas upon mixing with a sodium hydroxide solution. This gas was believed to be associated with the use of nitrogenous compounds to control nitrous oxide emissions because the only residue not to produce the gas resulted from an incinerator where such compounds were not employed. Gas production on exposure to sodium hydroxide solutions was therefore considered typical of air pollution control residues and as such alkali activated solidification/stabilisation treatment options were considered unsuitable.

Despite the unsuitability of the treatment for application to air pollution control residues, the mineralogy and physical performance of the resultant products showed potential and the reagents could perhaps be applied to alternative

waste streams. Without the excess lime in the air pollution control residues, additional reagents including lime or cement would be necessary. Several factors may limit such application with lime addition. These factors included prolonged setting times. Setting time could be reduced by increased curing temperature or reduced l/s ratio. Reducing the l/s ratio also reduced the workability of the blended waste and therefore, to ensure ease of handling, this would require balancing with setting time. Increasing the curing temperature was observed to reduce ultimate compressive strength and prolonged exposure to increased temperatures resulted in cracking due to drying shrinkage, drastically reducing physical encapsulation. Curing at 80℃ for 24 hours before allowing to cure at room temperature showed particular promise however, resulting in vastly improved retention of chloride and sulphate salts due to physical encapsulation during monolithic leach testing (although waste acceptance criteria limits were still exceeded) as well as reducing setting times and increasing the rate of compressive strength development. The durability of the products, including resistance to wetting and drying cycles and permeability variations as a result of leaching were also observed to be concerns. Durability of the pulverised fuel ash samples could perhaps be improved by the use of additional reagents, such as the replacement of a proportion of the pulverised fuel ash with cement.

Air pollution control residues were observed to have significant variability in composition. Since the implications of this variability on the performance of a solidification/stabilisation treatment could not be fully studied by the alkali activated treatment option due to gas production, the implications were studied by solidification/stabilisation with cement and de-ionised water. Very variable workability and setting times were observed as well as highly variable chloride and total solids release during regulatory leach tests. This behaviour was consistent with highly variable qualities observed in the as-received residues. Such behaviour suggested treatment options for air pollution control residues may require modifications, increasing difficulty and cost of operation unless residues were blended and homogenised before treatment. Solidified/stabilised products for all residues consistently exceed regulatory leach limits for chlorides. The inability of treatment by

solidification/stabilisation to immobilise the high levels of chlorides present in air pollution control residues at economical and resource efficient waste:binder ratios has been consistently demonstrated for a range of binders in this work and other literature. For this reason, solidification/stabilisation as a waste management option for air pollution control residues is considered unsuitable. Chlorides may be washed from the residues prior to treatment, however this adds expense to the treatment process, increasing water use and resulting in a secondary waste stream.

9 Recommendations for further work

Although not suitable for solidification/stabilisation of air pollution control residues, use of the co-fired pulverised fuel ash and the waste caustic solution as reagents for solidification/stabilisation showed some promise and could feasibly find application for treatment of other waste materials. Further work may include examining their suitability for use alongside cement or lime for immobilisation of waste materials with lower soluble salt contents, containing metals or other inorganic contaminants. The reaction products produced suggested potential for chemical immobilisation of such contaminants, and promising physical properties such as reasonable compressive strength development as well as low porosity and permeability were apparent when curing conditions and mix designs were correctly applied. Laboratory work may include examining the matrices potential for metal immobilisation via doping.

Further durability studies and improvements would also be required to ensure physical integrity is maintained during such as wetting and drying and freeze thaw cycles. Additionally it would be of interest to further examine the implications of leaching on the pore structure of solidification/stabilisation products. Such work may examine variations over different periods of time than the 7 days examined in the current work. One possibility may be to subject samples to the monolithic leach test EA NEN 7375 and examine the pore structure after each leachant renewal by methods such as permeability testing, gas adsorption, mercury intrusion porosimetry and microscopy.

Analysis of leachate fractions would also provide information on the solids leached during the procedure which would help interpret the changes in pore structure observed.

The bulk of the work focused on the very novel system combining the air pollution control residue, co-fired pulverised fuel ash, and waste caustic solution. With hindsight it is felt that the work would have been better conducted by starting with a more typical pulverised fuel ash and an uncontaminated NaOH solution of the same concentration as the waste caustic solution. The waste materials could then have been substituted into the blends individually and together which would have given a better indication of the implications of each waste material.

Along with the effects of pulverised fuel ash variability, and the contaminants present in the waste caustic solution on the workability, setting time, compressive strength and mineralogy of the resultant product, the implications of the high sulphur content in the co-fired pulverised fuel ash may be further studied. Leach testing of equivalent blends containing the co-fired ash and a lower sulphur ash meeting EN 450 criteria would better inform on the contribution made by the co-fired ash to sulphate release. The potential for oxidation of the sulphur and the implications this would have on the matrix chemistry, leaching and physical integrity is also of particular interest. Similarly, considering the organic carbon and reduced sulphur present, the implications of the co-fired pulverised fuel ash, compared to an ash with lower organic carbon and sulphur content, suitable for construction purposes, on the redox potential of matrices and the implications of this for the mobility of certain contaminants such as the oxyanions would be of interest. Results appeared to suggest that alkali activation may be detrimental for sulphate immobilisation, this can be further studied by granular leach testing of equivalent blends containing sulphate contamination cast with and without activation with an alkali metal solution.

The interaction between chloride and sulphate leaching could also merit further work. Although it is known that sulphate salt solubility may be

increased in solutions of increased ionic strength, it would be of interest to determine the extent of this influence in the non-equilibrium conditions encountered in monolithic leach tests. It is thought an appropriate method for examining this interaction would be to perform a monolithic leach test on samples containing sulphate salts in varying concentration chloride solutions.

Other more specific areas which would have been of interest to examine include the variability in the pore structure of the samples cured at high temperature for 24 hours as a function of the depth from the sample surface. It is thought that this would provide a better understanding of the leach performance observed for these samples. Likewise the calorimetry curves obtained may have been better understood by a more in depth study of the reaction product development over the time periods in which the main heat evolution peaks were observed. This study may have required characterisation of the amorphous portion of the samples utilising techniques such as infrared spectroscopy and nuclear magnetic resonance.

A more detailed examination of the acid neutralisation capacity of samples containing similar reaction products would also be of interest, examining sample composition after more regular, and a greater range of acid addition intervals. This work would perhaps be better performed on ‘simplified’ samples, composed of less complicated mineralogy which would allow better identification of buffering plateaus associated with the individual minerals. Additionally comparison of the development of sample prepared with different binders and exposed to different acids would be of interest.

Appendix A. Hydration Stopping Techniques

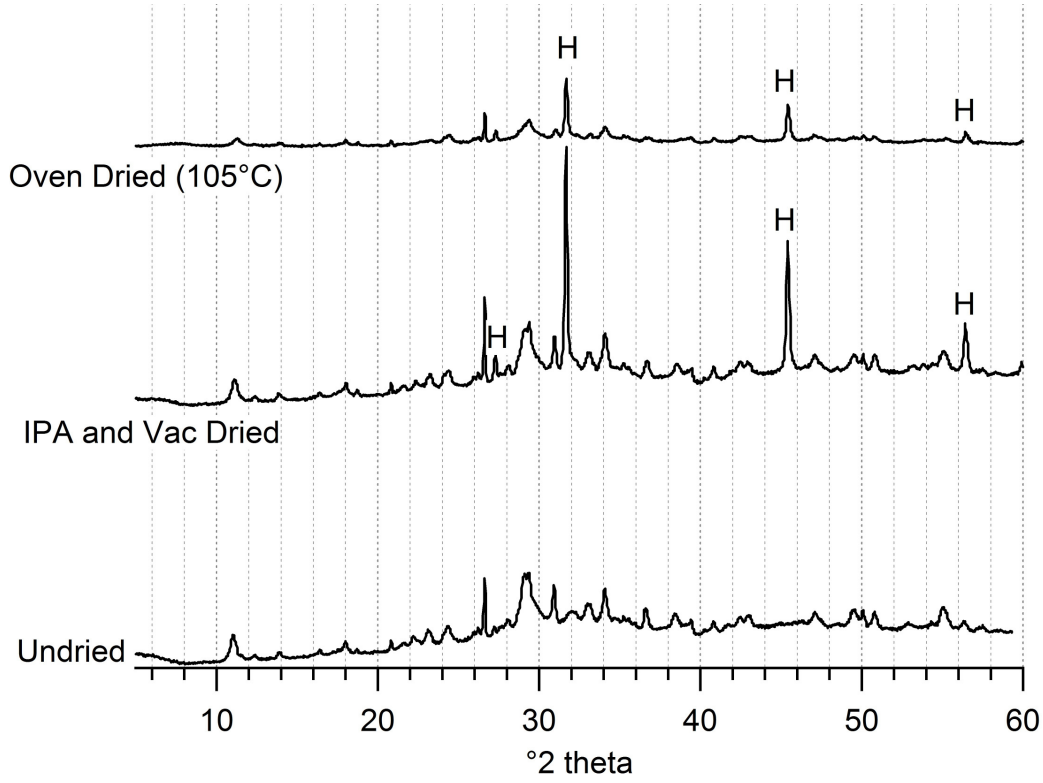

Figure A.1. Comparison of XRD patterns (y axis range normalised) for the same sample undried and after different hydration stopping techniques. H=NaCl.

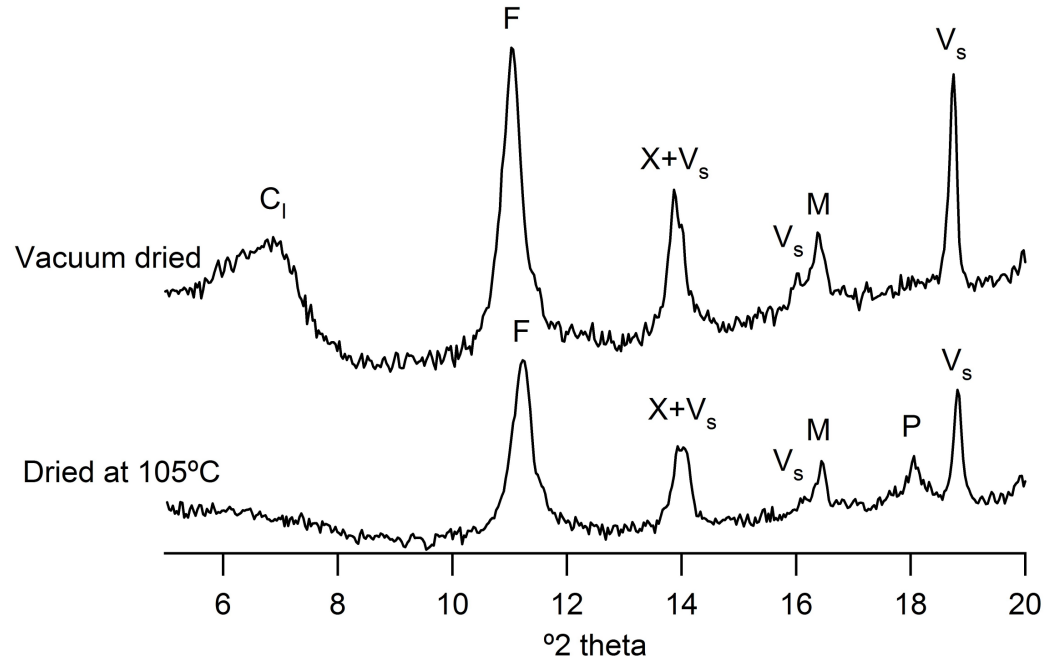

Figure A.2. XRD patterns (y axis range normalised) showing reduction in peak corresponding to C-S-H I due to oven drying at 105°C. C_I=C-S-H I, F=Friedel's salt, X=sodalite, V_s=vishnevite, M= mullite, P=portlandite

Without drying peaks corresponding to NaCl were not visible (Figure A.1). This appeared to be due to the NaCl being solubilised. The sample analysed in Figure A.1 had a moisture content of 28.5%, enough to solubilise ≤10.17% NaCl (taking solubility of NaCl as 357g/l [209]) which was greater than the NaCl concentration in any of the samples studied.

Oven drying is a simple and effective way to remove water from a sample however reactions continue during this drying process which may be accelerated by the increased temperatures. Drying at elevated temperatures may also remove chemically bound water from minerals such as gypsum and ettringite as well as removing interlayer water from C-S-H [144, 318, 319]. Unless CO_2 is excluded, oven drying also leaves the sample exposed to carbonation and therefore mineralogical changes. Figure A.1 and Figure A.2 show the effects of oven drying at 105℃ on XRD analysis of typical samples studied in this work, reduction in the presence of peaks corresponding to C-S-H (I) is apparent (Figure A.2) as is a reduction in the background intensity and intensity of all other peaks. Due to the significant variation imparted by the oven drying method it was not considered suitable for mineralogical analysis. Loss of the $Ca(OH)_2$ peak when vacuum dried can be seen in the sample analysed in Figure A.2 due to carbonation resulting from the longer drying period necessary. Vacuum drying was therefore also not considered suitable.

Other than the very conspicuous appearance of the NaCl peaks very little deviation from the pattern for the undried pattern was evident in the sample submerged in IPA for 24 hours followed by vacuum drying for a further 24 hours (Figure A.1). This hydration stopping technique was therefore considered suitable for mineralogical analysis of the samples studied within this thesis.

Appendix B. Quantification methods for compounds observed by STA with overlapping weight losses.

Due to the overlapping nature of the weight losses attributed to $Ca(OH)_2$ and CaClOH in the as received APC residues, quantification by drawing tangents to the TGA curves as discussed in chapter 3.2.2.1 was not possible. Several alternative methods were therefore examined in order to quantify the concentrations of these compounds. These methods included

- Differentiation of the TGA curve followed by subtracting a baseline, Gaussian peak fitting using Origin Pro software, and integration undertaken to determine the relative areas of the peaks. The ratio of these areas was then applied to the cumulative mass loss across the temperature range in which the overlapping peaks occurred.
- Peak fitting and integration of the DTA curves. Areas of DTA peaks for dehydration of $Ca(OH)_2$ and CaClOH could not be directly compared for quantification because the extent to which each reaction is exothermic would be different therefore a DTA peak area ratio of 1:1 would not necessarily mean equal water loss from both compounds or a 1:1 weight ratio. However, although there is evidence that a number of factors including particle size and the degree of crystallinity effect the DTA peak area [144, 429], Figure B.1 demonstrates good linearity between DTA peak area and $Ca(OH)_2$ concentrations between 0-50%w/w as determined by TGA for several samples analysed during the present study. Quantification was therefore carried out by first subtracting a baseline, created by drawing a tangent across the overlapping DTA peaks, before fitting Gaussian peaks using Origin Pro software and integrating the peaks. The % weight $Ca(OH)_2$ was then calculated assuming the linear relationship shown in Figure B.1 from which the weight loss due to $Ca(OH)_2$ could be calculated. The rest of the loss occurring within the range of the overlapping peaks was attributed to loss of water from CaClOH.
- Integration of peaks detected by mass spectrometer and application of peak areas to the weight loss.

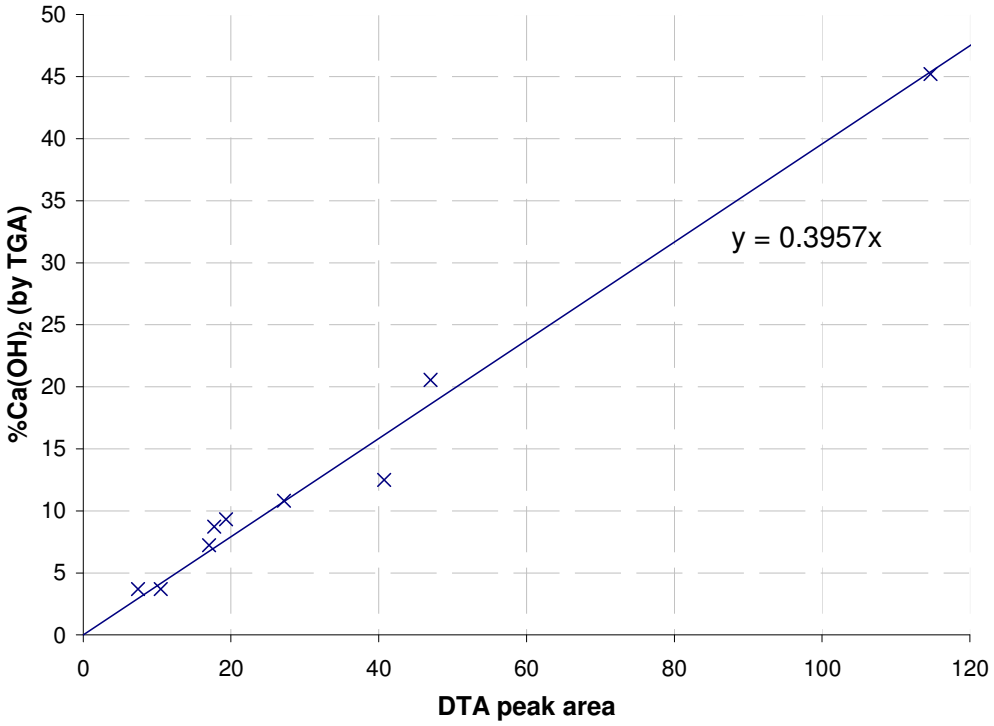

Figure B.1. Response of DTA peak area compared to %w/w $Ca(OH)_2$ determined by analysis of TG curve

Examples of the baselines and peaks fitted when performing the various methods on one of the APC residues examined within this study (A1) are shown in Figures B.2-B.4 with results presented in Table B.1.

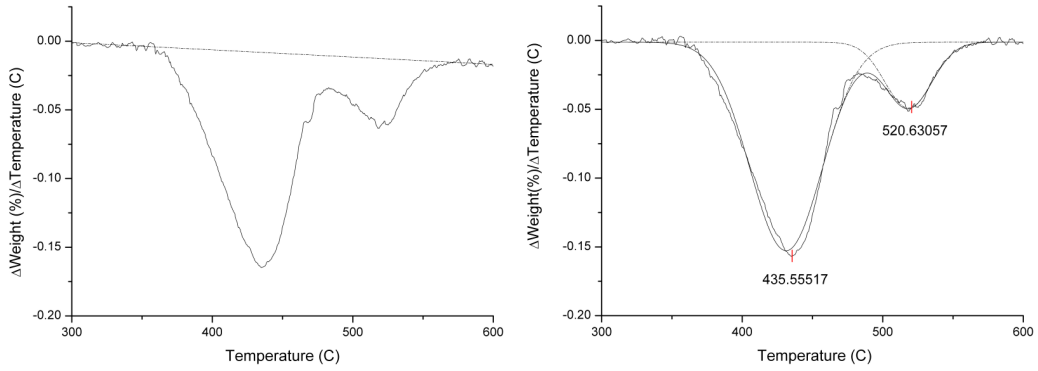

(a) **(b)**

Figure B.2. (a) Baseline fitted and subsequently subtracted from DTG curve. (b) Gaussian peaks fitted to DTG curve using OriginPro 8.1 software.

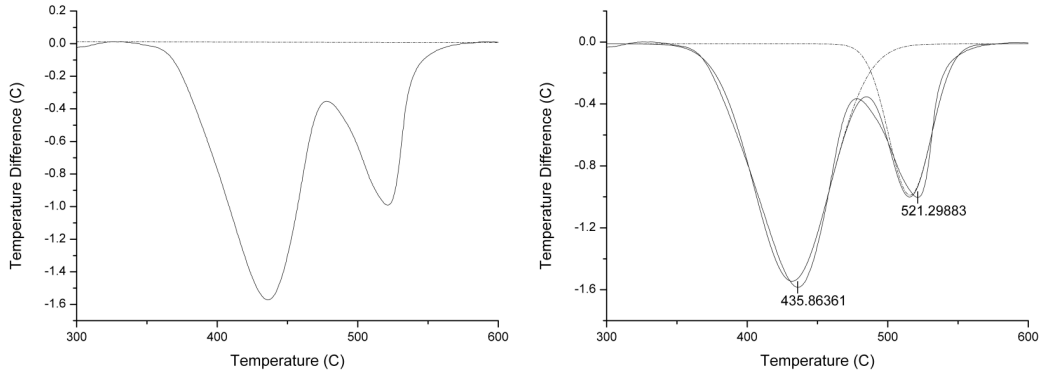

(a) **(b)**

Figure B.3. (a) Baseline fitted and subsequently subtracted from DTA curve. (b) Gaussian peaks fitted using OriginPro 8.1 software

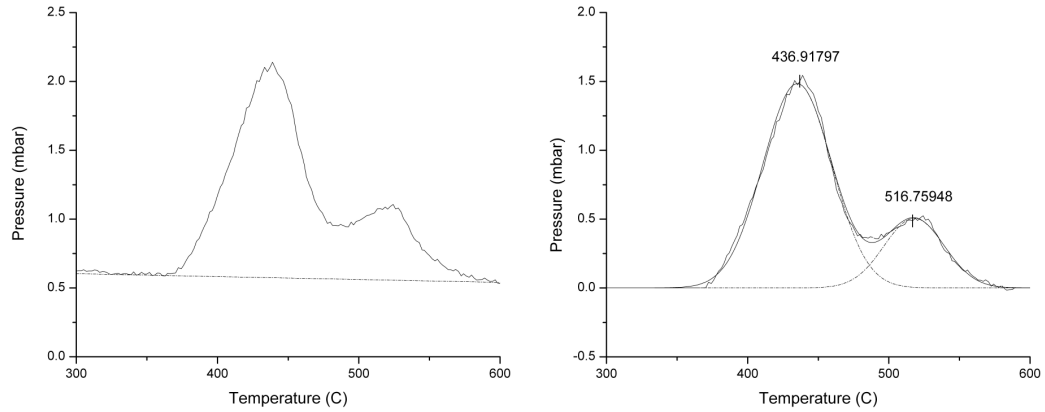

(a) **(b)**

Figure B.4. (a) Baseline fitted and subsequently subtracted from mass spectrometer curve for H_2O. (b) Gaussian peaks fitted using OriginPro 8.1 software

	TGA differentiation +Integration	DTA integration	Mass Spec Integration
%$Ca(OH)_2$	37.8%	39.6%	34.1%
%CaClOH	16%	15.1%	25.3%

Table B.1. Comparison of methods for quantification of $Ca(OH)_2$ and CaClOH concentrations

The method of differentiating the TGA curve proved impossible with some of the residues studied due to the poor resolution of the peaks achieved. The mass spectrometer was unavailable for analysis of several of the residues. The DTA integration method was therefore used because resolution of DTA

peaks for all materials was good enough to reliably fit peaks using Origin pro software. Clearly the methods resulted in significantly different values, particularly for the CaClOH phase due to the large molecular weight of the decomposition product (2CaClOH molecular mass=185) relative to the volatilised fraction (H_2O molecular mass=18). The quantification was therefore only considered suitable for comparison of the relative concentration of compounds within materials to which the same analysis method was applied. This technique was only necessary for analysis of the APC residues as received. Quantification of the TGA curves for other samples could be undertaken by drawing tangents.

References

1. European council, *Council directive 1975/442/EEC of 15 July 1975 on waste.* Official journal of the European union, 1975. L194.
2. European council, *Council directive 2008/98/EC of the European Parliament and of the Council of 19 November 2008 on waste and repealing certain directives.* Official journal of the European union, 2008. L312: p. 3-30.
3. DEFRA, *Waste strategy for England 2007*, 2007.
4. DEFRA, *Government review of waste policy in England 2011.* 2011.
5. *Waste (England and Wales) regulations*, 2011: UK.
6. DEFRA, *The environment in your pocket.* 2009.
7. Metcalfe, A., *Incineration transformation*, in *CIWM The journal for waste and resource management proffesionals*2010.
8. DEFRA, *A stratergy for hazardous waste management in England.* 2010.
9. DEFRA, *Anaerobic digestion strategy and action plan.* 2011.
10. Environment Agency, *Solid residues from municipal waste incinerators in England and Wales*, 2002.
11. Amutha Rani, D., A.R. Boccaccini, D. Deegan, and C.R. Cheeseman, *Air pollution control residues from waste incineration: Current UK situation and assessment of alternative technologies.* Waste Management, 2008. 28(11): p. 2279-2292.
12. European council, *Council directive 2008/1/EC of 15 January 2008 concerning integrated pollution prevention and control.* Official journal of the European union, 2008. L24: p. 8-29.
13. European council, *Council directive 1999/31/EC of 26 April 1999 on the landfill of waste.* Official journal of the European union, 1999. L182: p. 1-19.
14. DEFRA, *Government interpretation of the landfill (England and Wales) regulations 2002 (as amended).* 2005.
15. European council, *Directive 2000/76/EC of 4 December 2000 on the incineration of waste.* Official journal of the European communities, 2000. L332: p. 91-111.
16. European council, *Directive 2001/80/EC of 23 October 2001 on the limitation of emissions of certain pollutants into the air from large combustion plants.* Official journal of the European communities, 2001. L309: p. 1-21.
17. European commission, *Integrated pollution prevention and control, reference document on the best available techniques for waste incineration.* available online at http://eippcb.jrc.es, 2006.
18. European commission, *Integrated pollution prevention and control, reference document on best available techniques for large combustion plants.* available online at http://eippcb.jrc.es, 2006.
19. Frandsen, F.J., K. Laursen, S. Arvelakis, M. Stenseng, T.L. Jørgensen, L. Sørum, M.K. Jensen, R. Backman, A. Zbogar, and K. Dam-Johansen, *Ash chemistry in MSW incineration plants: Advanced characterisation and thermodynamic considerations.* Final Technical Report in EFP Project, J. No. 1373/01-0029 2004.
20. Chandler, A.J., H. Sloot, and I.A.W. Group, *Municipal solid waste incinerator residues,*1997, Amsterdam; New York: Elsevier.

21. Williams, P.T., *Waste Treatment and Disposal*. 2nd ed, 2005, Chichester: Wiley.
22. *The renewable obligations (ammendment) order*, 2011: UK.
23. *Visitors presentation-An introduction to the energy from waste plant*, 2009, Coventry and Solihull waste disposal company.
24. Bodenan, F. and P. Deniard, *Characterization of flue gas cleaning residues from European solid waste incinerators: Assessment of various Ca-based sorbent processes.* Chemosphere, 2003. 51(5): p. 335-347.
25. Jozewicz, W. and B.K. Gullett, *Reaction-mechanisms of dry Ca-based sorbents with gaseous HCl.* Industrial & Engineering Chemistry Research, 1995. 34(2): p. 607-612.
26. Hasselriis, F. and A. Licata, *Analysis of heavy metal emission data from municipal waste combustion.* Journal of Hazardous Materials, 1996. 47(1-3): p. 77-102.
27. Zevenhoven, R. and P. Kilpinen, *Control of pollutants in flue gases and fuel gases,*2002: available online at http://large.stanford.edu/publications/coal/references/leep/docs.
28. Vehlow, J. *Bottom ash and APC residue management*. in *Expert meeting on Power Production from Waste and Biomass - IV* 2002. Hanasaari Cultural Center, Espoo, Finland, : available online at www.seas.columbia.edu/earth/wtert/sofos/res-02-helsinki.pdf.
29. Cheeseman, C.R., S.M. da Rocha, C. Sollars, S. Bethanis, and A.R. Boccaccini, *Ceramic processing of incinerator bottom ash.* Waste Management, 2003. 23(10): p. 907-916.
30. Wei, Y.M., T. Shimaoka, A. Saffarzadeh, and F. Takahashi, *Mineralogical characterization of municipal solid waste incineration bottom ash with an emphasis on heavy metal-bearing phases.* Journal of Hazardous Materials, 2011. 187(1-3): p. 534-543.
31. Bethanis, S., C.R. Cheeseman, and C.J. Sollars, *Effect of sintering temperature on the properties and leaching of incinerator bottom ash.* Waste Management & Research, 2004. 22(4): p. 255-264.
32. Stegemann, J.A., J. Schneider, B.W. Baetz, and K.L. Murphy, *Lysimeter washing of MSW incinerator bottom ash.* Waste Management & Research, 1995. 13(2): p. 149-165.
33. Bethanis, S., C.R. Cheeseman, and C. Sollars, *Properties and microstructure of sintered incinerator bottom ash.* Ceramics International, 2002. 28(8): p. 881-886.
34. Forteza, R., M. Far, C. Segui, and V. Cerda, *Characterization of bottom ash in municipal solid waste incinerators for its use in road base.* Waste Management, 2004. 24(9): p. 899-909.
35. Juric, B., L. Hanzic, R. Ilic, and N. Samec, *Utilization of municipal solid waste bottom ash and recycled aggregate in concrete.* Waste Management, 2006. 26(12): p. 1436-1442.
36. Qian, G.R., Y. Song, C.G. Zhang, Y.Q. Xia, H.H. Zhang, and P.C. Chui, *Diopside-based glass-ceramics from MSW fly ash and bottom ash.* Waste Management, 2006. 26(12): p. 1462-1467.
37. Kougemitrou, I., A. Godelitsas, C. Tsabaris, V. Stathopoulos, A. Papandreou, P. Gamaletsos, G. Economou, and D. Papadopoulos, *Characterisation and management of ash produced in the hospital*

waste incinerator of Athens, Greece. Journal of Hazardous Materials, 2011. 187(1-3): p. 421-432.
38. Ibanez, R., A. Andres, J.R. Viguri, I. Ortiz, and J.A. Irabien, *Characterisation and management of incinerator wastes.* Journal of Hazardous Materials, 2000. 79(3): p. 215-227.
39. Idris, A. and K. Saed, *Characteristics of slag produced from incinerated hospital waste.* Journal of Hazardous Materials, 2002. 93(2): p. 201-208.
40. Whittaker, M., R. Taylor, Q. Li, and L. Black. *The behaviour of finely ground bottom ash in Portland cement*. in *Cement and Concrete Science*. 2009. Leeds.
41. Genazzini, C., G. Giaccio, A. Ronco, and R. Zerbino, *Cement-based materials as containment systems for ash from hospital waste incineration.* Waste Management, 2005. 25(6): p. 649-654.
42. Genazzini, C., R. Zerbino, A. Ronco, O. Batic, and G. Giaccio, *Hospital waste ashes in Portland cement mortars.* Cement and Concrete Research, 2003. 33(10): p. 1643-1650.
43. Environment Agency, *Technical guidance WM2 v2.2 Hazardouus waste, interpretation of the definition and classification of hazardous waste*, 2008.
44. Baun, B.L., B. Kamuk, and P. Avanzi, *Treatment of bottom ash from waste to energy plants: overview and experiences*, in *Sardinia 2007 Eleventh international waste managment and landfill symposium*2007: S. Margherita di Pula, Cagliari, Italy, Gagliari: Environmental Sanitary Engineering Centre (CISA).
45. Sawell, S.E., A.J. Chandler, T.T. Eighmy, J. Hartlen, O. Hjelmar, D. Kosson, H.A. vanderSloot, and J. Vehlow, *An international perspective on the characterisation and management of residues from MSW incinerators.* Biomass & Bioenergy, 1995. 9(1-5): p. 377-386.
46. van der Sloot, H.A., D. Hoede, D.J.F. Cresswell, and J.R. Barton, *Leaching behaviour of synthetic aggregates.* Waste Management, 2001. 21(3): p. 221-228.
47. Wainwright, P.J. and D.J.F. Cresswell, *Synthetic aggregates from combustion ashes using an innovative rotary kiln.* Waste Management, 2001. 21(3): p. 241-246.
48. Pecqueur, G., C. Crignon, and B. Quenee, *Behaviour of cement-treated MSWI bottom ash.* Waste Management, 2001. 21(3): p. 229-233.
49. *Foamed concrete explosion-HSE investigation update.* Health and safety executive, available online at www.hse.gov.uk/construction/liveissues/foamedconcrete.htm, 2010.
50. Shih, H.C. and H.W. Ma, *Life cycle risk assessment of bottom ash reuse.* Journal of Hazardous Materials, 2011. 190(1-3): p. 308-316.
51. Quina, M.J., R.C. Santos, J.C. Bordado, and R.M. Quinta-Ferreira, *Characterization of air pollution control residues produced in a municipal solid waste incinerator in Portugal.* Journal of Hazardous Materials, 2008. 152(2): p. 853-869.
52. Hossain, M.S., A. Santhanam, N.A.N. Norulaini, and A.K.M. Omar, *Clinical solid waste management practices and its impact on human*

health and environment - A review. Waste Management, 2011. 31(4): p. 754-766.
53. Chen, S.J., M.C. Hung, K.L. Huang, and W.I. Hwang, *Emission of heavy metals from animal carcass incinerators in Taiwan.* Chemosphere, 2004. 55(9): p. 1197-1205.
54. Gwyther, C.L., A.P. Williams, P.N. Golyshin, G. Edwards-Jones, and D.L. Jones, *The environmental and biosecurity characteristics of livestock carcass disposal methods: A review.* Waste Management, 2011. 31(4): p. 767-778.
55. Anderson, M., *Encouraging prospects for recycling incinerated sewage sludge ash (ISSA) into clay-based building products.* Journal of Chemical Technology and Biotechnology, 2002. 77(3): p. 352-360.
56. Anderson, M. and R.G. Skerratt, *Variability study of incinerated sewage sludge ash in relation to future use in ceramic brick manufacture.* British Ceramic Transactions, 2003. 102(3): p. 109-113.
57. Donatello, S., A. Freeman-Pask, M. Tyrer, and C.R. Cheeseman, *Effect of milling and acid washing on the pozzolanic activity of incinerator sewage sludge ash.* Cement & Concrete Composites, 2010. 32(1): p. 54-61.
58. Donatello, S., M. Tyrer, and C.R. Cheeseman, *EU landfill waste acceptance criteria and EU Hazardous Waste Directive compliance testing of incinerated sewage sludge ash.* Waste Management, 2010. 30(1): p. 63-71.
59. Geysen, D., C. Vandecasteele, M. Jaspers, E. Brouwers, and G. Wauters, *Effect of improving flue gas cleaning on characteristics and immobilisation of APC residues from MSW incineration.* Journal of Hazardous Materials, 2006. 128(1): p. 27-38.
60. Polettini, A., R. Pomi, P. Sirini, and F. Testa, *Properties of Portland cement - stabilised MSWI fly ashes.* Journal of Hazardous Materials, 2001. 88(1): p. 123-138.
61. Jacquinot, B., O. Hjelmar, and J. Vehlow, *The influence of PVC on the quantity and hazardousness of flue gas residues from incineration.* Bertin technologies report, available online at http://ec.europa.eu/environment/waste/studies/pvc/incineration.pdf, 2000.
62. Abbas, Z., A.P. Moghaddam, and B.M. Steenari, *Release of salts from municipal solid waste combustion residues.* Waste Management, 2003. 23(4): p. 291-305.
63. Astrup, T., H. Mosbaek, and T.H. Christensen, *Assessment of long-term leaching from waste incineration air-pollution-control residues.* Waste Management, 2006. 26(8): p. 803-814.
64. Chiang, K.Y., C.C. Tsai, and K.S. Wang, *Comparison of leaching characteristics of heavy metals in APC residue from an MSW incinerator using various extraction methods.* Waste Management, 2009. 29(1): p. 277-284.
65. Chimenos, J.M., A.I. Fernandez, A. Cervantes, L. Miralles, M.A. Fernandez, and F. Espiell, *Optimizing the APC residue washing process to minimize the release of chloride and heavy metals.* Waste Management, 2005. 25(7): p. 686-693.

66. Dimech, C., C.R. Cheeseman, S. Cook, J. Simon, and A.R. Boccaccini, *Production of sintered materials from air pollution control residues from waste incineration.* Journal of Materials Science, 2008. 43(12): p. 4143-4151.
67. Lampris, C., J.A. Stegemann, and C.R. Cheeseman, *Solidification/stabilisation of air pollution control residues using Portland cement: Physical properties and chloride leaching.* Waste Management, 2009. 29(3): p. 1067-1075.
68. Lundtorp, K., D.L. Jensen, M.A. Sorensen, T.H. Christensen, and E.P.B. Mogensen, *Treatment of waste incinerator air-pollution-control residues with FeSO4: Concept and product characterisation.* Waste Management & Research, 2002. 20(1): p. 69-79.
69. Quina, M.J., J.C.M. Bordado, and R.M. Quinta-Ferreira, *The influence of pH on the leaching behaviour of inorganic components from municipal solid waste APC residues.* Waste Management, 2009. 29(9): p. 2483-2493.
70. Sabbas, T., A. Polettini, R. Pomi, T. Astrup, O. Hjelmar, P. Mostbauer, G. Cappai, G. Magel, S. Salhofer, C. Speiser, S. Heuss-Assbichler, R. Klein, P. Lechner, and H.W.G.M.M.S.W. p, *Management of municipal solid waste incineration residues.* Waste Management, 2003. 23(1): p. 61-88.
71. Delay, I., J. Swithenbank, and B.B. Argent, *Prediction of the distribution of alkali and trace elements between the condensed and gaseous phases generated during clinical waste incineration.* Journal of Alloys and Compounds, 2001. 320(2): p. 282-295.
72. WRAP, *Case study: PVC recycling ltd.* available online at www.wrap.org.uk, 2009.
73. Alba, N., S. Gasso, T. Lacorte, and J.M. Baldasano, *Characterization of municipal solid waste incineration residues from facilities with different air pollution control systems.* Journal of the Air & Waste Management Association, 1997. 47(11): p. 1170-1179.
74. Bacciochi, R., G. Costa, A. Pollettini, R. Pomi, E. Di Bartolomeo, and E. Traversa, *Leaching behaviour and CO_2 sequestration capacity of MSWI APC residues*, in *Sardinia 2007, Eleventh International Waste Management and Landfill Symposium*2007: S. Margherita di Pula, Cagliari, Italy; .
75. Cappai, G., S. Cara, A. Muntoni, and M. Piredda, *Application of accelerated carbonation on MSW combustion APC residues for metal immobilization and CO_2 sequestration.* Journal of Hazardous Materials, in press.
76. Geysen, D., C. Vandecasteele, M. Jaspers, and G. Wauters, *Comparison of immobilisation of air pollution control residues with cement and with silica.* Journal of Hazardous Materials, 2004. 107(3): p. 131-143.
77. He, P.J., Q.K. Cao, L.M. Shao, and D.J. Lee, *Aging of air pollution control residues from municipal solid waste incinerator: Role of water content on metal carbonation.* Science of the Total Environment, 2006. 359(1-3): p. 26-37.

78. Wu, K., H.S. Shi, and X.L. Guo, *Utilization of municipal solid waste incineration fly ash for sulfoaluminate cement clinker production.* Waste Management, 2011. 31(9-10): p. 2001-2008.
79. Zheng, L., C.W. Wang, W. Wang, Y.C. Shi, and X.B. Gao, *Immobilization of MSWI fly ash through geopolymerization: Effects of water-wash.* Waste Management, 2011. 31(2): p. 311-317.
80. Le Forestier, L. and G. Libourel, *Characterization of flue gas residues from municipal solid waste combustors.* Environmental Science & Technology, 1998. 32(15): p. 2250-2256.
81. Fernandez Bertos, M., X. Li, S.J.R. Simons, C.D. Hills, and P.J. Carey, *Investigation of accelerated carbonation for the stabilisation of MSW incinerator ashes and the sequestration of CO_2.* Green Chemistry, 2004. 6(8): p. 428-436.
82. Bacciochi, R., G. Costa, A. Polettini, and R. Pomi, *An insight into the effect of accelerated carbonation on metal release from incinerator ash*, in *Sardinia 2009, Twelfth International Waste Management and Landfill Symposium*2009: S. Margherita di Pula, Cagliari, Italy.
83. Quina, M.J., J.C.M. Bordado, and R.M. Quinta-Ferreira, *Chemical stabilization of air pollution control residues from municipal solid waste incineration.* Journal of Hazardous Materials, 2010. 179(1-3): p. 382-392.
84. Environment Agency, *Technical guidance WM2, Hazardous waste, interpretation of the definition and classification of hazardous waste*, 2011.
85. Fernee, P. *Speaker from Environment Agency*. in *CIWM Futureproofing Thermal Treatment Conference*. 15 November 2011. Austin Court Birmingham.
86. Hyks, J., T. Astrup, and T.H. Christensen, *Long-term leaching from MSWI air-pollution-control residues: Leaching characterization and modeling.* Journal of Hazardous Materials, 2009. 162(1): p. 80-91.
87. Kosson, D.S., H.A. vanderSloot, and T.T. Eighmy, *An approach for estimation of contaminant release during utilization and disposal of municipal waste combustion residues.* Journal of Hazardous Materials, 1996. 47(1-3): p. 43-75.
88. Quina, M.J., J.C.M. Bordado, and R.M. Quinta-Ferreira, *Percolation and batch leaching tests to assess release of inorganic pollutants from municipal solid waste incinerator residues.* Waste Management, 2011. 31(2): p. 236-245.
89. Sawell, S.E., T.R. Bridle, and T.W. Constable, *Heavy-metal leachability from solid-waste incinerator ashes.* Waste Management & Research, 1988. 6(3): p. 227-238.
90. van der Sloot, H.A., D.S. Kosson, and O. Hjelmar, *Characteristics, treatment and utilization of residues from municipal waste incineration.* Waste Management, 2001. 21(8): p. 753-765.
91. Environment Agency, *Assessing the value of groundwater, Science report SC040016/SR1*, in *available online at* http://publications.environment-agency.gov.uk/PDF/SCHO0207BMBD-E-E.pdf2007.
92. *The Landfill (England and Wales) (Amendment) Regulations 2005*, 2005: UK.

93. DEFRA and Environment Agency, *Landfill Directive - Defra/ Environment Agency approach to the use of higher Waste Acceptance Criteria (WAC) limits for hazardous waste version 2* available online at http://archive.defra.gov.uk/environment/waste/topics/documents/wac080723.pdf, 2008.
94. Astrup, T., *Management of APC residues from W-T-E plants, an overview of management options and treatment methods, second edition.* ISWA-WG Thermal treatment of waste, October 2008.
95. Hjelmar, O., *Disposal strategies for municipal solid waste incineration residues.* Journal of Hazardous Materials, 1996. 47(1-3): p. 345-368.
96. Environment Agency, *Hazardous waste management market pressures and opportunities:background paper, R&D technical report P1-484/TR.* available online at www.wbcsdcement.org/pdf/tf2/p1484tr.pdf, 2003.
97. Campbell, P., *Veolia Minosus*, in *CIWM Futureproofing thermal treatment conference*15 November 2011: Austins court, Birmingham.
98. British Standards Institution, *197-1 Cement Part 1: Composition, specifications and conformity criteria for common cements* 2011.
99. Jones, A. *Future Industrial Services ltd*. in *CIWM Futureproofing thermal treatment conference*. 15 November 2011. Austins court Birmingham.
100. Benjamin, M.M., R.S. Sletten, R.P. Bailey, and T. Bennett, *Sorption and filtration of metals using iron-oxide-coated sand.* Water Research, 1996. 30(11): p. 2609-2620.
101. Lundtorp, K., D.L. Jensen, M.A. Sorensen, H. Mosbaek, and T.H. Christensen, *On-site treatment and landfilling of MSWI air pollution control residues.* Journal of Hazardous Materials, 2003. 97(1-3): p. 59-70.
102. Derie, R., *A new way to stabilize fly ash from municipal incinerators.* Waste Management, 1996. 16(8): p. 711-716.
103. Eighmy, T.T., B.S. Crannell, L.G. Butler, F.K. Cartledge, E.F. Emery, D. Oblas, J.E. Krzanowski, J.D. Eusden, E.L. Shaw, and C.A. Francis, *Heavy metal stabilization in municipal solid waste combustion dry scrubber residue using soluble phosphate.* Environmental Science & Technology, 1997. 31(11): p. 3330-3338.
104. Geysen, D., K. Imbrechts, C. Vandecasteele, M. Jaspers, and G. Wauters, *Immobilization of lead and zinc in scrubber residues from MSW combustion using soluble phosphates.* Waste Management, 2004. 24(5): p. 471-481.
105. Nzihou, A. and P. Sharrock, *Calcium phosphate stabilization of fly ash with chloride extraction.* Waste Management, 2002. 22(2): p. 235-239.
106. Quina, M.J., J.C.M. Bordado, and R.M. Quinta-Ferreira, *Environmental impact of APC residues from municipal solid waste incineration: Reuse assessment based on soil and surface water protection criteria.* Waste Management, 2011. 31(9-10): p. 1984-1991.
107. Uchida, T., I. Itoh, and K. Harada, *Immobilization of heavy metals contained in incinerator fly ash by application of soluble phosphate - Treatment and disposal cost reduction by combined use of "high specific surface area lime".* Waste Management, 1996. 16(5-6): p. 475-481.

108. Katsuura, H., T. Inoue, M. Hiraoka, and S. Sakai, *Full-scale plant study on fly ash treatment by the acid extraction process.* Waste Management, 1996. 16(5-6): p. 491-499.
109. Wang, K.S., K.Y. Chiang, K.L. Lin, and C.J. Sun, *Effects of a water-extraction process on heavy metal behavior in municipal solid waste incinerator fly ash.* Hydrometallurgy, 2001. 62(2): p. 73-81.
110. Quina, M.J., J.C. Bordado, and R.M. Quinta-Ferreira, *Treatment and use of air pollution control residues from MSW incineration: An overview.* Waste Management, 2008. 28(11): p. 2097-2121.
111. Cornelis, G., C.A. Johnson, T. Van Gerven, and C. Vandecasteele, *Leaching mechanisms of oxyanionic metalloid and metal species in alkaline solid wastes: A review.* Applied Geochemistry, 2008. 23(5): p. 955-976.
112. van der Sloot, H.A., J.C.L. Meeussen, A. van Zomeren, and D.S. Kosson, *Developments in the characterisation of waste materials for environmental impact assessment purposes.* Journal of Geochemical Exploration, 2006. 88(1-3): p. 72-76.
113. van der Sloot, H.A., A. van Zomeren, J.C.L. Meeussen, P. Seignette, and R. Bleijerveld, *Test method selection, validation against field data, and predictive modelling for impact evaluation of stabilised waste disposal.* Journal of Hazardous Materials, 2007. 141(2): p. 354-369.
114. Nishida, K., Y. Nagayoshi, H. Ota, and H. Nagasawa, *Melting and stone production using MSW incinerated ash.* Waste Management, 2001. 21(5): p. 443-449.
115. Park, Y.J. and J. Heo, *Vitrification of fly ash from municipal solid waste incinerator.* Journal of Hazardous Materials, 2002. 91(1-3): p. 83-93.
116. Romero, M., R.D. Rawlings, and J.M. Rincon, *Development of a new glass-ceramic by means of controlled vitrification and crystallisation of inorganic wastes from urban incineration.* Journal of the European Ceramic Society, 1999. 19(12): p. 2049-2058.
117. Sakai, S. and M. Hiraoka, *Municipal solid waste incinerator residue recycling by thermal processes.* Waste Management, 2000. 20(2-3): p. 249-258.
118. Park, Y.J., *Stabilization of a chlorine-rich fly ash by colloidal silica solution.* Journal of Hazardous Materials, 2009. 162(2-3): p. 819-822.
119. Wu, K., H. Shi, G.D. Schutter, X. Guo, and G. Ye, *Preparation of alinite cement from municipal solid waste incineration fly ash.* Cement and Concrete Composites, 2011. 34(3): p. 322-327.
120. Amutha Rani, D., E. Gomez, A.R. Boccaccini, L. Hao, D. Deegan, and C.R. Cheeseman, *Plasma treatment of air pollution control residues.* Waste Management, 2008. 28(7): p. 1254-1262.
121. Wise, M. *Plasma arc APC treatment*. in *CIWM Futureproofing thermal treatment conference*. 15 November 2011. Austins court, Birmingham.
122. Kourti, I., D.A. Rani, D. Deegan, A.R. Boccaccini, and C.R. Cheeseman, *Production of geopolymers using glass produced from DC plasma treatment of air pollution control (APC) residues.* Journal of Hazardous Materials, 2010. 176(1-3): p. 704-709.
123. Kourti, I., A.R. Devaraj, A.G. Bustos, D. Deegan, A.R. Boccaccini, and C.R. Cheeseman, *Geopolymers prepared from DC plasma treated air pollution control (APC) residues glass: Properties and characterisation*

of the binder phase. Journal of Hazardous Materials, 2011. 196: p. 86-92.
124. Costa, G., R. Baciocchi, A. Polettini, R. Pomi, C.D. Hills, and P.J. Carey, *Current status and perspectives of accelerated carbonation processes on municipal waste combustion residues.* Environmental Monitoring and Assessment, 2007. 135(1-3): p. 55-75.
125. Ferretti, D. and Z.P. Bazant, *Stability of ancient masonry towers: Moisture diffusion, carbonation and size effect.* Cement and Concrete Research, 2006. 36(7): p. 1379-1388.
126. Jianguo, J., M.Z. Chen, Y. Zhang, and X. Xu, *Pb stabilization in fresh fly ash from municipal solid waste incinerator using accelerated carbonation technology.* Journal of Hazardous Materials, 2009. 161(2-3): p. 1046-1051.
127. Todorovic, J. and H. Ecke, *Demobilisation of critical contaminants in four typical waste-to-energy ashes by carbonation.* Waste management (New York, N.Y.), 2006. 26(4): p. 430-41.
128. Wang, L., Y.Y. Jin, and Y.F. Nie, *Investigation of accelerated and natural carbonation of MSWI fly ash with a high content of Ca.* Journal of Hazardous Materials, 2010. 174(1-3): p. 334-343.
129. Miyake, M., S. Komarneni, and R. Roy, *Immobilization of Pb^{2+}, Cd^{2+}, Sr^{2+} and Ba^{2+} ions using calcite and aragonite.* Cement and Concrete Research, 1988. 18(3): p. 485-490.
130. Pickering, W.F., *Extraction of copper, lead, zinc or cadmium ions sorbed on calcium-carbonate.* Water Air and Soil Pollution, 1983. 20(3): p. 299-309.
131. Van Gerven, T., E. Van Keer, S. Arickx, M. Jaspers, G. Wauters, and C. Vandecasteele, *Carbonation of MSWI-bottom ash to decrease heavy metal leaching, in view of recycling.* Waste Management, 2005. 25(3): p. 291-300.
132. Li, X.M., M.F. Bertos, C.D. Hills, P.J. Carey, and S. Simon, *Accelerated carbonation of municipal solid waste incineration fly ashes.* Waste Management, 2007. 27(9): p. 1200-1206.
133. Li, Q., *Unpublished results, carbonation of air pollution control residue*, 2011, University of Leeds.
134. Carey, P.J. *Carbon-8 Accelerated carbonation technology*. in *CIWM Futureproofing thermal treatment*. 15 November 2011. Austin court, Birmingham.
135. Hills, C.D. *Carbon-8, Accelerated carbon technology*. in *Guest lecture*. 2011. University of Leeds.
136. Ecke, H., N. Menad, and A. Lagerkvist, *Carbonation of municipal solid waste incineration fly ash and the impact on metal mobility.* Journal of Environmental Engineering-Asce, 2003. 129(5): p. 435-440.
137. Chandra, S., *Waste materials used in concrete manufacturing,*1996: Noyes Publications.
138. Chang, J., X. Cheng, L. Lu, F.T. Liu, and J.P. Zhu, *Study on the composition and hydration of alinite and calcium chloroaluminate minerals.* Cement and Concrete Research, 2005. 35(2): p. 248-255.
139. Ftikos, C., A. Georgiades, and T. Philippou, *Preparation and hydration study of alinite cement.* Cement and Concrete Research, 1991. 21(6): p. 1129-1136.

140. Ftikos, C., T. Philippou, and J. Marinos, *A study of the effect of some factors influencing alinite clinker formation.* Cement and Concrete Research, 1993. 23(6): p. 1268-1272.
141. Kim, Y.M., S.H. Hong, and H.M. Park, *Isomorphic substitution and the hydration behavior of alinite cement.* Journal of the European Ceramic Society, 2003. 23(12): p. 2067-2073.
142. Neubauer, J. and H. Pollmann, *Alinite-chemical composition, solid-solution and hydration behavior.* Cement and Concrete Research, 1994. 24(8): p. 1413-1422.
143. Singh, M., P.C. Kapur, and Pradip, *Preparation of alinite based cement from incinerator ash.* Waste Management, 2008. 28(8): p. 1310-1316.
144. Taylor, H., *Cement chemistry*. 2nd ed, 1997, London: Thomas Telford.
145. Kacimi, L., A. Simon-Masseron, A. Ghomari, and Z. Derriche, *Reduction of clinkerization temperature by using phosphogypsum.* Journal of Hazardous Materials, 2006. 137(1): p. 129-137.
146. Ftikos, C. and D. Kiatos, *The effect of chlorides on the formation of belite and alinite phase.* Cement and Concrete Research, 1994. 24(1): p. 49-54.
147. Kostogloudis, G.C., D. Kalogridis, C. Ftikos, C. Malami, B. Georgali, and V. Kaloidas, *Comparative investigation of corrosion resistance of steel reinforcement in alinite and Portland cement mortars.* Cement and Concrete Research, 1998. 28(7): p. 995-1010.
148. Pradip, D.V. and P.C. Kapur, *Production and properties of alinite cements from steel plant wastes.* Cement and Concrete Research, 1990. 20(1): p. 15-24.
149. Saikia, N., S. Kato, and T. Kojima, *Production of cement clinkers from municipal solid waste incineration (MSWI) fly ash.* Waste Management, 2007. 27(9): p. 1178-1189.
150. Bone, B.D., L.H. Barnard, D.I. Boardman, P.J. Carey, C.D. Hills, H.M. Jones, M. C.L., and M. Tyrer, *Review of scientific literature on the use of stabilisation/solidification for the treatment of contaminated soil, solid waste and sludges, Science report, SC980003/SR2.* available online at http://publications.environment-agency.gov.uk/PDF/SCHO0904BIFP-E-E.pdf, 2004.
151. Roy, A., H.C. Eaton, F.K. Cartledge, and M.E. Tittlebaum, *Solidification stabilization of hazardous waste-evidence of physical encapsulation.* Environmental Science & Technology, 1992. 26(7): p. 1349-1353.
152. Stegemann, J.A. and P.L. Cote, *A proposed protocol for evaluation of solidified wastes.* Science of the Total Environment, 1996. 178(1-3): p. 103-110.
153. Al-Tabbaa, A. and A.S.R. Perera, *UK stabilization/solidification treatment and remidiation-Part II: Performance, QA/QC and guidance documents.* Land contamination and reclamation, 2006. 14(1): p. 23-41.
154. Chen, Q.Y., M. Tyrer, C.D. Hills, X.M. Yang, and P. Carey, *Immobilisation of heavy metal in cement-based solidification/stabilisation: A review.* Waste Management, 2009. 29(1): p. 390-403.

155. Glasser, F.P., *Fundamental aspects of cement solidification and stabilisation.* Journal of Hazardous Materials, 1997. 52(2-3): p. 151-170.
156. Jantzen, C., A. Johnson, D. Read, and J.A. Stegemann, *Cements in waste management.* Advances in Cement Research, 2010. 22(4): p. 225-231.
157. Stegemann, J.A. and Q. Zhou, *Screening tests for assessing treatability of inorganic industrial wastes by stabilisation/solidification with cement.* Journal of Hazardous Materials, 2009. 161(1): p. 300-306.
158. van der Sloot, H.A., *Characterization of the leaching behaviour of concrete mortars and of cement-stabilized wastes with different waste loading for long term environmental assessment.* Waste Management, 2002. 22(2): p. 181-186.
159. Conner, J.R. and S.L. Hoeffner, *The history of stabilization/solidification technology.* Critical Reviews in Environmental Science and Technology, 1998. 28(4): p. 325-396.
160. Conner, J.R. and S.L. Hoeffner, *A critical review of stabilization/solidification technology.* Critical Reviews in Environmental Science and Technology, 1998. 28(4): p. 397-462.
161. Antemir, A., C.D. Hills, P.J. Carey, K.H. Gardner, E.R. Bates, and A.K. Crumbie, *Long-term performance of aged waste forms treated by stabilization/solidification.* Journal of Hazardous Materials, 2010. 181(1-3): p. 65-73.
162. Fitch, J.R. and C.R. Cheeseman, *Characterisation of environmentally exposed cement-based stabilised/solidified industrial waste.* Journal of Hazardous Materials, 2003. 101(3): p. 239-255.
163. Shi, C. and J.A. Stegemann, *Acid corrosion resistance of different cementing materials.* Cement and Concrete Research, 2000. 30(5): p. 803-808.
164. Stegemann, J.A. and N.R. Buenfeld, *Prediction of leachate pH for cement paste containing pure metal compounds.* Journal of Hazardous Materials, 2002. 90(2): p. 169-188.
165. Stegemann, J.A., A.S.R. Perera, C. Cheeseman, and N.R. Buenfeld, *1/8 factorial study of metal effects on acid neutralization by cement.* Journal of Environmental Engineering-Asce, 2000. 126(10): p. 925-933.
166. Alba, N., E. Vazquez, S. Gasso, and J.M. Baldasano, *Stabilization/solidification of MSW incineration residues from facilities with different air pollution control systems. Durability of matrices versus carbonation.* Waste Management, 2001. 21(4): p. 313-323.
167. Andac, M. and F.P. Glasser, *Long-term leaching mechanisms of Portland cement-stabilized municipal solid waste fly ash in carbonated water.* Cement and Concrete Research, 1999. 29(2): p. 179-186.
168. Bonen, D. and S.L. Sarkar, *The effects of simulated environmental attack on immobilization of heavy-metals doped in cement-based materials.* Journal of Hazardous Materials, 1995. 40(3): p. 321-335.
169. Nelson, D., *Natural variations in the composition of groundwater.* Presented at Groundwater Foundation Annual Meeting, available online at

http://public.health.oregon.gov/HealthyEnvironments/DrinkingWater/SourceWater/Documents/gw/chem.pdf, November 2002.
170. Todorovic, J., H. Ecke, and A. Lagerkvist, *Solidification with water as a treatment method for air pollution control residues.* Waste Management, 2003. 23(7): p. 621-629.
171. Richardson, I.G., *The nature of C-S-H in hardened cements.* Cement and Concrete Research, 1999. 29(8): p. 1131-1147.
172. Richardson, I.G., *The calcium silicate hydrates.* Cement and Concrete Research, 2008. 38(2): p. 137-158.
173. Chen, J.J., J.J. Thomas, H.F.W. Taylor, and H.M. Jennings, *Solubility and structure of calcium silicate hydrate.* Cement and Concrete Research, 2004. 34(9): p. 1499-1519.
174. Richardson, I.G., *Tobermorite/jennite- and tobermorite/calcium hydroxide-based models for the structure of C-S-H: applicability to hardened pastes of tricalcium silicate, beta-dicalcium silicate, Portland cement, and blends of Portland cement with blast-fumace slag, metakaolin, or silica fume.* Cement and Concrete Research, 2004. 34(9): p. 1733-1777.
175. Grutzeck, M., A. Benesi, and B. Fanning, *Silicon-29 magic angle spinning nuclear magnetic-resonance study of calcium silicate hydrates.* Journal of the American Ceramic Society, 1989. 72(4): p. 665-668.
176. Jonsson, B., H. Wennerstrom, A. Nonat, and B. Cabane, *Onset of cohesion in cement paste.* Langmuir, 2004. 20(16): p. 6702-6709.
177. Richardson, I.G. and G.W. Groves, *The incorporation of minor and trace-elements into calcium silicate hydrate (C-S-H) gel in hardened cement pastes.* Cement and Concrete Research, 1993. 23(1): p. 131-138.
178. Ivey, D.G., R.B. Heimann, M. Neuwirth, S. Shumborski, D. Conrad, R.J. Mikula, and W.W. Lam, *Electron-microscopy of heavy-metal waste in cement matrices.* Journal of Materials Science, 1990. 25(12): p. 5055-5062.
179. Lin, C.K., J.N. Chen, and C.C. Lin, *An NMR, XRD and EDS study of solidification/stabilization of chromium with portland cement and C_3S.* Journal of Hazardous Materials, 1997. 56(1-2): p. 21-34.
180. Park, C.K., *Hydration and solidification of hazardous wastes containing heavy metals using modified cementitious materials.* Cement and Concrete Research, 2000. 30(3): p. 429-435.
181. Omotoso, O.E., D.G. Ivey, and R. Mikula, *Containment mechanism of trivalent chromium in tricalcium silicate.* Journal of Hazardous Materials, 1998. 60(1): p. 1-28.
182. Omotoso, O.E., D.G. Ivey, and R. Mikula, *Hexavalent chromium in tricalcium silicate - Part I - Quantitative X-ray diffraction analysis of crystalline hydration products.* Journal of Materials Science, 1998. 33(2): p. 507-513.
183. Omotoso, O.E., D.G. Ivey, and R. Mikula, *Hexavalent chromium in tricalcium silicate - Part II - Effects of Cr-VI on the hydration of tricalcium silicate.* Journal of Materials Science, 1998. 33(2): p. 515-522.

184. Chen, Q.Y., C.D. Hills, M. Tyrer, I. Slipper, H.G. Shen, and A. Brough, *Characterisation of products of tricalcium silicate hydration in the presence of heavy metals.* Journal of Hazardous Materials, 2007. 147(3): p. 817-825.
185. Komarneni, S., E. Breval, D.M. Roy, and R. Roy, *Reactions of some calcium silicates with metals-cations.* Cement and Concrete Research, 1988. 18(2): p. 204-220.
186. Moulin, I., W.E.E. Stone, J. Sanz, J.Y. Bottero, F. Mosnier, and C. Haehnel, *Lead and zinc retention during hydration of tri-calcium silicate: A study by sorption isotherms and (29)Si nuclear magnetic resonance spectroscopy.* Langmuir, 1999. 15(8): p. 2829-2835.
187. Stumm, A., K. Garbev, G. Beuchle, L. Black, P. Stemmermann, and R. Nuesch, *Incorporation of zinc into calcium silicate hydrates, Part I: formation of C-S-H(I) with C/S=2/3 and its isochemical counterpart gyrolite.* Cement and Concrete Research, 2005. 35(9): p. 1665-1675.
188. Ziegler, F., R. Giere, and C.A. Johnson, *Sorption mechanisms of zinc to calcium silicate hydrate: Sorption and microscopic investigations.* Environmental Science & Technology, 2001. 35(22): p. 4556-4561.
189. Ziegler, F., A.M. Scheidegger, C.A. Johnson, R. Dahn, and E. Wieland, *Sorption mechanisms of zinc to calcium silicate hydrate: X-ray absorption fine structure (XAFS) investigation.* Environmental Science & Technology, 2001. 35(7): p. 1550-1555.
190. Thevenin, G. and J. Pera, *Interactions between lead and different binders.* Cement and Concrete Research, 1999. 29(10): p. 1605-1610.
191. Rose, J., I. Moulin, J.L. Hazemann, A. Masion, P.M. Bertsch, J.Y. Bottero, F. Mosnier, and C. Haehnel, *X-ray absorption spectroscopy study of immobilization processes for heavy metals in calcium silicate hydrates: 1. Case of lead.* Langmuir, 2000. 16(25): p. 9900-9906.
192. Gougar, M.L.D., B.E. Scheetz, and D.M. Roy, *Ettringite and C-S-H Portland cement phases for waste ion immobilization: A review.* Waste Management, 1996. 16(4): p. 295-303.
193. Komarneni, S. and D.M. Roy, *New tobermorite cation exchangers.* Journal of Materials Science, 1985. 20(8): p. 2930-2936.
194. Shrivastava, O.P. and F.P. Glasser, *Ion-exchange properties of $Ca_5Si_6O_{18}H_2$-$4H_2O$.* Journal of Materials Science Letters, 1985. 4(9): p. 1122-1124.
195. Akhter, H., L.G. Butler, S. Branz, F.K. Cartledge, and M.E. Tittlebaum, *Immobilization of As, Cd, Cr and Pb-containing soils by using cement or pozzolanic fixing agents.* Journal of Hazardous Materials, 1990. 24(2-3): p. 145-155.
196. Cartledge, F.K., L.G. Butler, D. Chalasani, H.C. Eaton, F.P. Frey, E. Herrera, M.E. Tittlebaum, and S.L. Yang, *Immobilization mechanisms in solidification stabilization of Cd and Pb salts using Portland cement fixing agents.* Environmental Science & Technology, 1990. 24(6): p. 867-873.
197. Li, X.D., C.S. Poon, H. Sun, I.M.C. Lo, and D.W. Kirk, *Heavy metal speciation and leaching behaviors in cement based solidified/stabilized waste materials.* Journal of Hazardous Materials, 2001. 82(3): p. 215-230.

198. Balonis, M., B. Lothenbach, G. Le Saout, and F.P. Glasser, *Impact of chloride on the mineralogy of hydrated Portland cement systems.* Cement and Concrete Research, 2010. 40(7): p. 1009-1022.
199. Beaudoin, J.J., V.S. Ramachandran, and R.F. Feldman, *Interaction of chloride and C-S-H.* Cement and Concrete Research, 1990. 20(6): p. 875-883.
200. Perkins, R.B. and C.D. Palmer, *Solubility of $Ca_6[Al(OH)_6]_2(CrO_4)_3$-$26H_2O$, the chromate analog of ettringite; 5-75 degrees C.* Applied Geochemistry, 2000. 15(8): p. 1203-1218.
201. Chrysochoou, M. and D. Dermatas, *Evaluation of ettringite and hydrocalumite formation for heavy metal immobilization: Literature review and experimental study.* Journal of Hazardous Materials, 2006. 136(1): p. 20-33.
202. Damidot, D., B. Lothenbach, D. Herfort, and F.P. Glasser, *Thermodynamics and cement science.* Cement and Concrete Research, 2011. 41(7): p. 679-695.
203. Illston, J.M. and P.L.J. Domone, *Construction materials: their nature and behaviour,*2001: Spon Press.
204. Neville, A.M. and J.J. Brooks, *Concrete technology*. 2nd (revised) ed, 1994, Harlow: Longman Scientific and Technical.
205. Damidot, D. and F.P. Glasser, *Thermodynamic investigation of the CaO-Al_2O_3-$CaSO_4$-H_2O system at 25 degrees C and the influence of Na_2O.* Cement and Concrete Research, 1993. 23(1): p. 221-238.
206. Gabrisova, A., J. Havlica, and S. Sahu, *Stability of calcium sulfoaluminate hydrates in water solutions with various pH values.* Cement and Concrete Research, 1991. 21(6): p. 1023-1027.
207. Hampson, C.J. and J.E. Bailey, *The microstructure of the hydration products of tri-calcium aluminate in the presence of gypsum.* Journal of Materials Science, 1983. 18(2): p. 402-410.
208. Damidot, D., M. Atkins, A. Kindness, and F.P. Glasser, *Sulfate attack on concrete- limits of the AFt stability domain.* Cement and Concrete Research, 1992. 22(2-3): p. 229-234.
209. Dean, J.A. and N.A. Lange, *Lange's handbook of chemistry,*1999: McGraw-Hill.
210. Birnin-Yauri, U.A. and F.P. Glasser, *Friedel's salt, $Ca_2Al(OH)_6(Cl,OH)$-$2H_2O$: Its solid solutions and their role in chloride binding.* Cement and Concrete Research, 1998. 28(12): p. 1713-1723.
211. Suryavanshi, A.K., J.D. Scantlebury, and S.B. Lyon, *The binding of chloride-ions by sulfate resistant Portland cement.* Cement and Concrete Research, 1995. 25(3): p. 581-592.
212. Thomas, M.D.A., R.D. Hooton, A. Scott, and H. Zibara, *The effect of supplementary cementitious materials on chloride binding in hardened cement paste.* Cement and Concrete Research, 2012. 42(1): p. 1-7.
213. Csizmadia, J., G. Balazs, and F.D. Tamas, *Chloride ion binding capacity of aluminoferrites.* Cement and Concrete Research, 2001. 31(4): p. 577-588.
214. Glasser, F.P., A. Kindness, and S.A. Stronach, *Stability and solubility relationships in AFm phases - Part 1. Chloride, sulfate and hydroxide.* Cement and Concrete Research, 1999. 29(6): p. 861-866.

215. Auer, S., H.J. Kuzel, H. Pollmann, and F. Sorrentino, *Investigation on MSW fly-ash treatment by reactive calcium aluminates and phases formed.* Cement and Concrete Research, 1995. 25(6): p. 1347-1359.
216. Ubbriaco, P., *Hydration behaviour of a lime-pozzolan cement containing MSW incinerator fly ash.* Journal of Thermal Analysis, 1996. 47(1): p. 7-16.
217. Goni, S. and A. Guerrero, *Accelerated carbonation of Friedel's salt in calcium aluminate cement paste.* Cement and Concrete Research, 2003. 33(1): p. 21-26.
218. Suryavanshi, A.K. and R.N. Swamy, *Stability of Friedel's salt in carbonated concrete structural elements.* Cement and Concrete Research, 1996. 26(5): p. 729-741.
219. Alford, N.M., A.A. Rahman, and N. Salih, *The effect of lead nitrate on the physical properties of cement pastes.* Cement and Concrete Research, 1981. 11(2): p. 235-245.
220. Asavapisit, S., G. Fowler, and C.R. Cheeseman, *Solution chemistry during cement hydration in the presence of metal hydroxide wastes.* Cement and Concrete Research, 1997. 27(8): p. 1249-1260.
221. Olmo, I.F., E. Chacon, and A. Irabien, *Influence of lead, zinc, iron (III) and chromium (III) oxides on the setting time and strength development of Portland cement.* Cement and Concrete Research, 2001. 31(8): p. 1213-1219.
222. Qiao, X.C., C.S. Poon, and C.R. Cheeseman, *Investigation into the stabilization/solidification performance of Portland cement through cement clinker phases.* Journal of Hazardous Materials, 2007. 139(2): p. 238-243.
223. Batchelor, B., *Overview of waste stabilization with cement.* Waste Management, 2006. 26(7): p. 689-698.
224. Stegemann, J.A. and N.R. Buenfeld, *Prediction of unconfined compressive strength of cement paste with pure metal compound additions.* Cement and Concrete Research, 2002. 32(6): p. 903-913.
225. Stegemann, J.A. and N.R. Buenfeld, *Prediction of unconfined compressive strength of cement paste containing industrial wastes.* Waste Management, 2003. 23(4): p. 321-332.
226. Leonard, S.A. and J.A. Stegemann, *Stabilization/solidification of petroleum drill cuttings.* Journal of Hazardous Materials, 2010. 174(1-3): p. 463-472.
227. Suryavanshi, A.K., J.D. Scantlebury, and S.B. Lyon, *Pore-size distribution of OPC and SRPC mortars in presence of chlorides.* Cement and Concrete Research, 1995. 25(5): p. 980-988.
228. Cheeseman, C.R. and S. Asavapisit, *Effect of calcium chloride on the hydration and leaching of lead-retarded cement.* Cement and Concrete Research, 1999. 29(6): p. 885-892.
229. Thomas, N.L., *Corrosion problems in reinforced-concrete-why accelerators of cement hydration usually promote corrosion of steel.* Journal of Materials Science, 1987. 22(9): p. 3328-3334.
230. Tashiro, C., J. Oba, and K. Akama, *Effects of several heavy-metal oxides on the formation of ettringite and the microstructure of hardened ettringite.* Cement and Concrete Research, 1979. 9(3): p. 303-308.

231. Palomo, A. and M. Palacios, *Alkali-activated cementitious materials: Alternative matrices for the immobilisation of hazardous wastes - Part II. Stabilisation of chromium and lead.* Cement and Concrete Research, 2003. 33(2): p. 289-295.
232. Gouda, V.K., W.E. Mourad, and R.S. Mikhail, *Additives to cement pastes-simultaneous effects on pore structure and corrosion of steel reinforcement.* Journal of Colloid and Interface Science, 1973. 43(2): p. 294-302.
233. Hansson, C.M., T. Frolund, and J.B. Markussen, *The effect of chloride cation type on the corrosion of steel in concrete by chloride salts.* Cement and Concrete Research, 1985. 15(1): p. 65-73.
234. Skalny, J., I. Odler, and Hagymass.J, *Pore structure of hydrated calcium silicates. 1. Influence of calcium chloride on pore structure of hydrated tricalcium silicate.* Journal of Colloid and Interface Science, 1971. 35(3): p. 434-&.
235. Young, J.F., *Capillary porosity in hydrated tricalcium silicate pastes.* Powder Technology, 1974. 9(4): p. 173-179.
236. Glasser, F.P., J. Pedersen, K. Goldthorpe, and M. Atkins, *Solubility reactions of cement components with NaCl solutions: I. $Ca(OH)_2$ and C-S-H.* Advances in Cement Research, 2005. 17(2): p. 57-64.
237. Andersson, K., B. Allard, M. Bengtsson, and B. Magnusson, *Chemical-composition of cement pore solutions.* Cement and Concrete Research, 1989. 19(3): p. 327-332.
238. Glasser, F.P., K. Luke, and M.J. Angus, *Modification of cement pore fluid compositions by pozzolanic additives.* Cement and Concrete Research, 1988. 18(2): p. 165-178.
239. Baur, I., C. Ludwig, and C.A. Johnson, *The leaching behavior of cement stabilized air pollution control residues: A comparison of field and laboratory investigations.* Environmental Science & Technology, 2001. 35(13): p. 2817-2822.
240. Ludwig, C., C.A. Johnson, M. Kappeli, A. Ulrich, and S. Riediker, *Hydrological and geochemical factors controlling the leaching of cemented MSWI air pollution control residues: A lysimeter field study.* Journal of Contaminant Hydrology, 2000. 42(2-4): p. 253-272.
241. Lampris, C., J.A. Stegemann, and C.R. Cheeseman, *Chloride leaching from air pollution control residues solidified using ground granulated blast furnace slag.* Chemosphere, 2008. 73(9): p. 1544-1549.
242. Zhou, X.S., X. Lin, M.J. Huo, and Y. Zhang, *The hydration of saline oil-well cement.* Cement and Concrete Research, 1996. 26(12): p. 1753-1759.
243. Lampris, C., J.A. Stegemann, M. Pellizon-Birelli, G.D. Fowler, and C.R. Cheeseman, *Metal leaching from monolithic stabilised/solidified air pollution control residues.* Journal of Hazardous Materials, 2011. 185(2-3): p. 1115-1123.
244. Tritthart, J., *Chloride binding in cement. 2. The influence of the hydroxide concentration in the pore solution of hardened cement paste on chloride binding.* Cement and Concrete Research, 1989. 19(5): p. 683-691.

245. Dehwah, H.A.F., *Effect of sulphate contamination on chloride-binding capacity of plain and blended cements.* Advances in Cement Research, 2006. 18(1): p. 7-15.
246. Environmental integrity project, *Toxic waters run deep, coal ash open dumps still open for buissness?* Available online at http://www.environmentalintegrity.org/documents/ToxicWatersRunDeepReport.pdf, 2011.
247. Environmental integrity project, *Out of control: monting damages from coal ash waste sites.* Available online at http://www.environmentalintegrity.org/news_reports/news_02_24_10.php, 2010.
248. Environment Agnecy and WRAP, *Quality protocol, pulverised fuel ash (PFA) end of waste criteria for the production of pulverised fuel ash (PFA) and furnace bottom ash (FBA) for use in bound and grout applications in specified construction and manufacturing uses* Available online at http://www.environment-agency.gov.uk/business/topics/waste/114443.aspx, 2010.
249. British Standards Institution, *BS EN 450-1 Fly ash for concrete- Part 1: Definitions specification and conformity criteria.* 2005.
250. Leonard, S.A. and J.A. Stegemann, *Stabilization/solidification of petroleum drill cuttings: Leaching studies.* Journal of Hazardous Materials, 2010. 174(1-3): p. 484-491.
251. Poon, C.S., *Applications of rejected fly ash in stabilisation and solidification processes*, in *Stabilisation/Solidification treatment and remidiation*, A. Al-Tabbaa and J.A. Stegemann, Editors. 2005, A.A. Balkema Publishers.
252. Poon, C.S., X.C. Qiao, C.R. Cheeseman, and Z.S. Lin, *Feasibility of using reject fly ash in cement-based stabilization/solidification processes.* Environmental Engineering Science, 2006. 23(1): p. 14-23.
253. Qiao, X.C., C.S. Poon, and C. Cheeseman, *Use of flue gas desulphurisation (FGD) waste and rejected fly ash in waste stabilization/solidification systems.* Waste Management, 2006. 26(2): p. 141-149.
254. Puertas, F., S. Martinez-Ramirez, S. Alonso, and T. Vazquez, *Alkali-activated fly ash/slag cement - Strength behaviour and hydration products.* Cement and Concrete Research, 2000. 30(10): p. 1625-1632.
255. Shi, C.J. and R.L. Day, *Acceleration of strength gain of lime-pozzolan cements by thermal-activation.* Cement and Concrete Research, 1993. 23(4): p. 824-832.
256. Wang, K., S.P. Shah, and A. Mishulovich, *Effects of curing temperature and NaOH addition on hydration and strength development of clinker-free CKD-fly ash binders.* Cement and Concrete Research, 2004. 34(2): p. 299-309.
257. Kjellsen, K.O., R.J. Detwiler, and O.E. Gjorv, *Pore structure of plain cement pastes hydrated at different temperatures.* Cement and Concrete Research, 1990. 20(6): p. 927-933.
258. Kjellsen, K.O. and R.J. Detwiler, *Reaction-kinetics of Portland cement mortars hydrated at different temperatures.* Cement and Concrete Research, 1992. 22(1): p. 112-120.

259. Shao, Y., C.J. Lynsdale, C.D. Lawrence, and J.H. Sharp, *Deterioration of heat-cured mortars due to the combined effect of delayed ettringite formation and freeze/thaw cycles.* Cement and Concrete Research, 1997. 27(11): p. 1761-1771.
260. Glasser, F.P., *Properties of cement waste composites.* Waste Management, 1996. 16(1-3): p. 159-168.
261. Fraay, A.L.A., J.M. Bijen, and Y.M. Dehaan, *The reaction of fly-ash in concrete-a critical examination.* Cement and Concrete Research, 1989. 19(2): p. 235-246.
262. Albino, V., R. Cioffi, L. Santoro, and G.L. Valenti, *Stabilization of residue containing heavy metals by means of matrices generating calcium trisulphoaluminate and silicate hydrates.* Waste Management & Research, 1996. 14(1): p. 29-41.
263. Lampris, C., J.A. Stegemann, and C. Cheeseman, *Comparison of the physical properties and leaching characteristics of APC residues solidified using Protland cement and ground granulated blast furnace slag.* available online at http://www.srcosmos.gr/srcosmos/showpub.aspx?aa=13101, 2009.
264. British Standards Institution, *BS EN 12457-2 Characterisation of waste — Leaching —Compliance test for leaching of granular waste materials and sludges.* 2002.
265. Shi, C.J. and A. Fernandez-Jimenez, *Stabilization/solidification of hazardous and radioactive wastes with alkali-activated cements.* Journal of Hazardous Materials, 2006. 137(3): p. 1656-1663.
266. Lu, P., Q. Li, and J.P. Zhai, *Mineralogical characterizations and reaction path modeling of the pozzolanic reaction of fly ash-lime systems.* Journal of the American Ceramic Society, 2008. 91(3): p. 955-964.
267. Shi, C.J. and R.L. Day, *A calorimetric study of early hydration of alkali-slag cements.* Cement and Concrete Research, 1995. 25(6): p. 1333-1346.
268. Allahverdi, A. and J. Ghorbani, *Chemical activation and set acceleration of lime-natural pozzolan cement.* Ceramics – Silikáty, 2006. 50(4): p. 193-199.
269. Roy, D.M., W.M. Jiang, and M.R. Silsbee, *Chloride diffusion in ordinary, blended, and alkali-activated cement pastes and its relation to other properties.* Cement and Concrete Research, 2000. 30(12): p. 1879-1884.
270. Poon, C.S., X.C. Qiao, and Z.S. Lin, *Effects of flue gas desulphurization sludge on the pozzolanic reaction of reject-fly-ash-blended cement pastes.* Cement and Concrete Research, 2004. 34(10): p. 1907-1918.
271. Shi, C.J., *Early microstructure development of activated lime-fly ash pastes.* Cement and Concrete Research, 1996. 26(9): p. 1351-1359.
272. Shi, C.J. and R.L. Day, *Acceleration of the reactivity of fly-ash by chemical activation.* Cement and Concrete Research, 1995. 25(1): p. 15-21.
273. Alonso, S. and A. Palomo, *Calorimetric study of alkaline activation of calcium hydroxide-metakaolin solid mixtures.* Cement and Concrete Research, 2001. 31(1): p. 25-30.

274. Shi, C.J. and R.L. Day, *Some factors affecting early hydration of alkali-slag cements.* Cement and Concrete Research, 1996. 26(3): p. 439-447.
275. Wang, S.D., K.L. Scrivener, and P.L. Pratt, *Factors affecting the strength of alkali-activated slag.* Cement and Concrete Research, 1994. 24(6): p. 1033-1043.
276. Shi, C.J., *Strength, pore structure and permeability of alkali-activated slag mortars.* Cement and Concrete Research, 1996. 26(12): p. 1789-1799.
277. Richardson, I.G., A.R. Brough, G.W. Groves, and C.M. Dobson, *The characterization of hardened alkali-activated blast-furnace slag pastes and the nature of the calcium silicate hydrate (C-S-H).* Cement and Concrete Research, 1994. 24(5): p. 813-829.
278. Roy, A., P.J. Schilling, H.C. Eaton, P.G. Malone, W.N. Brabston, and L.D. Wakeley, *Activation of ground blast-furnace slag by alkali-metal and alkaline-earth hydroxides.* Journal of the American Ceramic Society, 1992. 75(12): p. 3233-3240.
279. Wang, S.D. and K.L. Scrivener, *Hydration products of alkali-activated slag cement.* Cement and Concrete Research, 1995. 25(3): p. 561-571.
280. Granizo, M.L., S. Alonso, M.T. Blanco-Varela, and A. Palomo, *Alkaline activation of metakaolin: Effect of calcium hydroxide in the products of reaction.* Journal of the American Ceramic Society, 2002. 85(1): p. 225-231.
281. Cho, J.W., K. Ioku, and S. Goto, *Effect of Pb-II and Cr-VI ions on the hydration of slag alkaline cement and the immobilization of these heavy metal ions.* Advances in Cement Research, 1999. 11(3): p. 111-118.
282. Deja, J., *Immobilization of Cr^{6+}, Cd^{2+}, Zn^{2+} and Pb^{2+} in alkali-activated slag binders.* Cement and Concrete Research, 2002. 32(12): p. 1971-1979.
283. Qian, G., D.D. Sun, and J.H. Tay, *Characterization of mercury- and zinc-doped alkali-activated slag matrix - Part I. Mercury.* Cement and Concrete Research, 2003. 33(8): p. 1251-1256.
284. Qian, G.R., D.D. Sun, and J.H. Tay, *Characterization of mercury- and zinc-doped alkali-activated slag matrix - Part II. Zinc.* Cement and Concrete Research, 2003. 33(8): p. 1257-1262.
285. Shi, C.J., J. Stegemann, and R. Caldwell, *An examination of interference in waste solidification through measurement of heat signature.* Waste Management, 1997. 17(4): p. 249-255.
286. Shi, C.J. and R.L. Day, *Chemical activation of blended cements made with lime and natural pozzolans.* Cement and Concrete Research, 1993. 23(6): p. 1389-1396.
287. Querol, X., N. Moreno, J.C. Umana, A. Alastuey, E. Hernandez, A. Lopez-Soler, and F. Plana, *Synthesis of zeolites from coal fly ash: an overview.* International Journal of Coal Geology, 2002. 50(1-4): p. 413-423.
288. Alonso, S. and A. Palomo, *Alkaline activation of metakaolin and calcium hydroxide mixtures: influence of temperature, activator*

concentration and solids ratio. Materials Letters, 2001. 47(1-2): p. 55-62.
289. Yip, C.K., G.C. Lukey, and J.S.J. van Deventer, *The coexistence of geopolymeric gel and calcium silicate hydrate at the early stage of alkaline activation.* Cement and Concrete Research, 2005. 35(9): p. 1688-1697.
290. Shi, C. and R.L. Day, *Comparison of different methods for enhancing reactivity of pozzolans.* Cement and Concrete Research, 2001. 31(5): p. 813-818.
291. Jiminez, A.M.F., E.E. Lachowski, A. Palomo, and D.E. Macphee, *Microstructural characterisation of alkali-activated PFA matrices for waste immobilisation.* Cement & Concrete Composites, 2004. 26(8): p. 1001-1006.
292. Xu, J.Z., Y.L. Zhou, Q. Chang, and H.Q. Qu, *Study on the factors affecting the immobilization of heavy metals in fly ash-based geopolymers.* Materials Letters, 2006. 60(6): p. 820-822.
293. Lee, W.K.W. and J.S.J. van Deventer, *The effects of inorganic salt contamination on the strength and durability of geopolymers.* Colloids and Surfaces a-Physicochemical and Engineering Aspects, 2002. 211(2-3): p. 115-126.
294. Miranda, J.M., A. Fernandez-Jimenez, J.A. Gonzalez, and A. Palomo, *Corrosion resistance in activated fly ash mortars.* Cement and Concrete Research, 2005. 35(6): p. 1210-1217.
295. Atkins, M., F.P. Glasser, and J.J. Jack, *Zeolite-P in cements-its potential for immobilizing toxic and radioactive-waste species.* Waste Management, 1995. 15(2): p. 127-135.
296. Castaldi, P., L. Santona, S. Enzo, and P. Melis, *Sorption processes and XRD analysis of a natural zeolite exchanged with Pb^{2+}, Cd^{2+} and Zn^{2+} cations.* Journal of Hazardous Materials, 2008. 156(1-3): p. 428-434.
297. Fernández-Pereira, C., Y.L. Galiano, M.A. Rodríguez-Piñero, J. Vale, and X. Querol, *Utilisation of zeolitised coal fly ash as immobilising agent of a metallurgical waste.* Journal of Chemical Technology & Biotechnology, 2002. 77(3): p. 305-310.
298. Larosa, J.L., S. Kwan, and M.W. Grutzeck, *Zeolite formation in class-F fly-ash blended cement pastes.* Journal of the American Ceramic Society, 1992. 75(6): p. 1574-1580.
299. Terzano, R., M. Spagnuolo, L. Medici, W. Dorrine, K. Janssens, and P. Ruggiero, *Microscopic single particle characterization of zeolites synthesized in a soil polluted by copper or cadmium and treated with coal fly ash.* Applied Clay Science, 2007. 35(1-2): p. 128-138.
300. Mertens, G., R. Snellings, K. Van Balen, B. Bicer-Simsir, P. Verlooy, and J. Elsen, *Pozzolanic reactions of common natural zeolites with lime and parameters affecting their reactivity.* Cement and Concrete Research, 2009. 39(3): p. 233-240.
301. Snellings, R., G. Mertens, and J. Elsen, *Calorimetric evolution of the early pozzolanic reaction of natural zeolites.* Journal of Thermal Analysis and Calorimetry, 2010. 101(1): p. 97-105.

302. Grutzeck, M., S. Kwan, and M. DiCola, *Zeolite formation in alkali-activated cementitious systems.* Cement and Concrete Research, 2004. 34(6): p. 949-955.
303. Oh, J.E., J. Moon, M. Mancio, S.M. Clark, and P.J.M. Monteiro, *Bulk modulus of basic sodalite, $Na_8[AlSiO_4]_6(OH)_2$-$2H_2O$, a possible zeolitic precursor in coal-fly-ash-based geopolymers.* Cement and Concrete Research, 2011. 41(1): p. 107-112.
304. Galiano, Y.L., C.F. Pereira, and J. Vale, *Stabilization/solidification of a municipal solid waste incineration residue using fly ash-based geopolymers.* Journal of Hazardous Materials, 2011. 185(1): p. 373-381.
305. Lancellotti, I., E. Kamseu, M. Michelazzi, L. Barbieri, A. Corradi, and C. Leonelli, *Chemical stability of geopolymers containing municipal solid waste incinerator fly ash.* Waste Management, 2010. 30(4): p. 673-679.
306. Aubert, J.E., B. Husson, and N. Sarramone, *Utilization of municipal solid waste incineration (MSWI) fly ash in blended cement. Part 1: Processing and characterization of MSWI fly ash.* Journal of Hazardous Materials, 2006. 136(3): p. 624-631.
307. Aubert, J.E., B. Husson, and N. Sarramone, *Utilization of municipal solid waste incineration (MSWI) fly ash in blended cement Part 2. Mechanical strength of mortars and environmental impact.* Journal of Hazardous Materials, 2007. 146(1-2): p. 12-19.
308. Massardier, V., P. Moszkowicz, and M. Taha, *Fly ash stabilization-solidification using polymer-concrete double matrices.* European Polymer Journal, 1997. 33(7): p. 1081-1086.
309. Mulder, E., *Pre-treatment of MSWI fly ash for useful application.* Waste Management, 1996. 16(1-3): p. 181-184.
310. Remond, S., P. Pimienta, and D.P. Bentz, *Effects of the incorporation of Municipal Solid Waste Incineration fly ash in cement pastes and mortars I. Experimental study.* Cement and Concrete Research, 2002. 32(2): p. 303-311.
311. Shi, H.S. and L.L. Kan, *Leaching behavior of heavy metals from municipal solid wastes incineration (MSWI) fly ash used in concrete.* Journal of Hazardous Materials, 2009. 164(2-3): p. 750-754.
312. Ubbriaco, P. and D. Calabrese, *Solidification and stabilization of cement paste containing fly ash from municipal solid waste.* Thermochimica Acta, 1998. 321(1-2): p. 143-150.
313. Ubbriaco, P. and D. Calabrese, *Hydration behaviour of mixtures of cement and fly ash with high sulphate and chloride content.* Journal of Thermal Analysis and Calorimetry, 2000. 61(2): p. 615-623.
314. Wang, K.S., K.L. Lin, and Z.Q. Huang, *Hydraulic activity of municipal solid waste incinerator fly-ash-slag-blended eco-cement.* Cement and Concrete Research, 2001. 31(1): p. 97-103.
315. Collier, N.C., J.H. Sharp, N.B. Milestone, J. Hill, and I.H. Godfrey, *The influence of water removal techniques on the composition and microstructure of hardened cement pastes.* Cement and Concrete Research, 2008. 38(6): p. 737-744.
316. Day, R.L., *Reactions between methanol and Portland cement paste.* Cement and Concrete Research, 1981. 11(3): p. 341-349.

317. Feldman, R.F., *Diffusion measurements in cement paste by water replacement using propan-2-ol.* Cement and Concrete Research, 1987. 17(4): p. 602-612.
318. Knapen, E., O. Cizer, K. Van Balen, and D. Van Gemert, *Effect of free water removal from early-age hydrated cement pastes on thermal analysis.* Construction and Building Materials, 2009. 23(11): p. 3431-3438.
319. Mitchell, L.D. and J.C. Margeson, *The effects of solvents on C-S-H as determined by thermal analysis.* Journal of Thermal Analysis and Calorimetry, 2006. 86(3): p. 591-594.
320. Parrott, L.J., *Novel methods of processing cement gel to examine and control microstructure and properties.* Philosophical Transactions of the Royal Society of London Series a-Mathematical Physical and Engineering Sciences, 1983. 310(1511): p. 155-166.
321. Taylor, H.F.W. and A.B. Turner, *Reactions of tricalcium silicate paste with organic liquids.* Cement and Concrete Research, 1987. 17(4): p. 613-623.
322. British Standards Institution, *BS 1924-2 Stabilized materials for civil engineering purposes — Part 2: Methods of test for cement-stabilized and lime-stabilized materials.* 1990.
323. Vogel, A.I. and J. Mendham, *Vogel's textbook of quantitative chemical analysis,*2000: Prentice Hall.
324. Paya, J., J. Monzo, M.V. Borrachero, S. Velazquez, and A. Bonilla, *Determination of the pozzolanic activity of fluid catalytic cracking residue. Thermogravimetric analysis studies on FC3R-lime pastes.* Cement and Concrete Research, 2003. 33(7): p. 1085-1091.
325. Ubbriaco, P. and F. Tasselli, *A study of the hydration of lime-pozzolan binders.* Journal of Thermal Analysis and Calorimetry, 1998. 52(3): p. 1047-1054.
326. Vedalakshmi, R., A.S. Raj, S. Srinivasan, and K.G. Babu, *Quantification of hydrated cement products of blended cements in low and medium strength concrete using TG and DTA technique.* Thermochimica Acta, 2003. 407(1-2): p. 49-60.
327. Paya, J., J. Monzo, M.V. Borrachero, E. Perris, and F. Amahjour, *Thermogravimetric methods for determining carbon content in fly ashes.* Cement and Concrete Research, 1998. 28(5): p. 675-686.
328. Criado, J.M. and A. Ortega, *A study of the influence of particle-size on the thermal-decomposition of $CaCO_3$ by means of constant rate thermal analysis.* Thermochimica Acta, 1992. 195: p. 163-167.
329. Klug, H.P. and L.E. Alexander, *X-ray diffraction procedures for polycrystalline and amorphous materials,*1974: Wiley.
330. Ramachandran, V.S. and J.J. Beaudoin, *Handbook of analytical techniques in concrete science and technology: principles, techniques, and applications,*2001: Noyes Publications.
331. Morris, M.C., H.F. McMurdie, E.H. Evans, B. Paretzkin, C.R. Hubbard, and S.J. Carmel, *Standard X-ray diffraction powder patterns, Section 17. Data for 54 Substances.* National Bureau of Standards Monograph 25, 1980: p. 1-4.
332. Chung, F.H., *Quantitative interpretation of x-ray diffraction patterns of mixtures. 1. Matrix-flushing method for quantitative multicomponent*

analysis. Journal of Applied Crystallography, 1974. 7(DEC1): p. 519-525.
333. Lipson, H. and H. Steeple, *Interpretation of X-Ray Powder Diffraction Patterns,*1970: Macmillan Publishers Limited.
334. Connolly, J., *Systematic errors and sample preparation for x-ray powder diffraction.* available online at http://epswww.unm.edu/xrd/xrdclass/07-Errors-Sample-Prep-PPT.pdf 2010.
335. Denker, R., N. Oosten-Nienhuis, and R. Meier, *Sample preparation for X-ray analysis, the critical first step.* Global cement magazine, May 2008: p. 17-18.
336. De La Torre, A.G., S. Bruque, and M.A.G. Aranda, *Rietveld quantitative amorphous content analysis.* Journal of Applied Crystallography, 2001. 34: p. 196-202.
337. Diamond, S., *On the glass present in low-calcium and in high-calcium fly ashes.* Cement and Concrete Research, 1983. 13(4): p. 459-464.
338. Guthrie, J.M., *Overview of X-ray fluorescene.* available online at http://archaeometry.missouri.edu/xrf_overview.html, accessed January 2012.
339. Schlotz, R. and S. Uhlig, *An overview of XRF basics, Introduction to X-ray Fluorescence (XRF).* available online at http://www.bruker-axs.de/fileadmin/user_upload/xrfintro/index.html, 2006.
340. Scrivener, K.L., *Backscattered electron imaging of cementitious microstructures: understanding and quantification.* Cement & Concrete Composites, 2004. 26(8): p. 935-945.
341. Bensted, J. and P. Barnes, *Structure and performance of cements,*2002: Spon Press.
342. Meredith, P., A.M. Donald, and K. Luke, *Preinduction and induction hydration of tricalcium silicate-an environmental scanning electron-microscopy study.* Journal of Materials Science, 1995. 30(8): p. 1921-1930.
343. Richardson, I.G., J. Skibsted, L. Black, and R.J. Kirkpatrick, *Characterisation of cement hydrate phases by TEM, NMR and Raman spectroscopy.* Advances in Cement Research, 2010. 22(4): p. 233-248.
344. Girao, A.V., I.G. Richardson, C.B. Porteneuve, and R.M.D. Brydson, *Composition, morphology and nanostructure of C-S-H in white Portland cement-fly ash blends hydrated at 85 degrees C.* Advances in Applied Ceramics, 2007. 106(6): p. 283-293.
345. Mostafa, N.Y. and P.W. Brown, *Heat of hydration of high reactive pozzolans in blended cements: Isothermal conduction calorimetry.* Thermochimica Acta, 2005. 435(2): p. 162-167.
346. Popovics, S., *Concrete materials: properties, specifications, and testing,*1992: Noyes Publications.
347. Dollimore, D. and R.J. Mangabhai, *Effect of mixing time on heat evolution pattern of cement pastes.* Thermochimica Acta, 1985. 85(APR): p. 223-226.
348. Thomas, J.J. and H.M. Jennings, *Effects of D_2O and mixing on the early hydration kinetics of tricalcium silicate.* Chemistry of Materials, 1999. 11(7): p. 1907-1914.

349. British Standards Institution, *BS EN 1015-3 Methods of test for mortar for masonry — Part 3: Determination of consistence of fresh mortar (by flow table).* 1999.
350. British Standards Institution, *BS EN 480-2 Admixtures for concrete, mortar and grout — Test methods — Part 2: Determination of setting time.* 2006.
351. British Standards Institution, *BS EN 196-3 Methods of testing cement — Part 3: Determination of setting times and soundness.* 2005.
352. British Standards Institution, *BS EN 12390-3 Testing hardened concrete Part 3: Compressive strength of test specimens.* 2009.
353. British Standards Institution, *ISO 11465 Soil quality — Part 3: Chemical methods —Section 3.1 Determination of dry matter and water content on a mass basis by a gravimetric method.* 1993.
354. Cabrera, J.G. and P.A. Claisse, *Oxygen and water vapour transport in cement-silica fume pastes.* Construction and Building Materials, 1999. 13(7): p. 405-414.
355. Environment Agency, *EA NEN 7375 Leaching characteristics of moulded or monolithic building and waste materials. Determination of leaching of inroganic components with the diffusion test. 'The tank test'.* 2004.
356. British Standards Institution, *BS EN 12457-1 Characterisation of waste — Leaching — Compliance test for leaching of granular waste materials and sludges — Part 1: One stage batch test at a liquid to solid ratio of 2 l/kg for materials with high solid content and with particle size below 4 mm (without or with size reduction).* 2002.
357. British Standards Institution, *BS EN 12457-2 Characterisation of waste — Leaching — Compliance test for leaching of granular waste materials and sludges — Part 2: One stage batch test at a liquid to solid ratio of 10 l/kg for materials with particle size below 4 mm (without or with size reduction).* 2002.
358. British Standards Institution, *BS EN 12457-3 Characterisation of waste — Leaching — Compliance test for leaching of granular waste materials and sludges — Part 3: Two stage batch test at a liquid to solid ratio of 2 l/kg and 8 l/kg for materials with a high solid content and with a particle size below 4 mm (without or with size reduction).* 2002.
359. British Standards Institution, *BS EN 15216 Characterization of waste — Determination of total dissolved solids (TDS) in water and eluates.* 2007.
360. British Standards Institution, *BS EN ISO 5667-3 Water quality — Sampling — Part 3: Guidance on the preservation and handling of water samples.* 2003.
361. Dionex corporation, *Ion chromatography 'The chromatography of ions' training course manual.* unknown year.
362. Dionex corporation, *Ion chromatography cookbook. A practical guide to quantitative analysis by ion chromatography.* 1987.
363. Environmental protection agency, *SW-846 Test Methods for Evaluating Solid Waste, Physical/Chemical Methods. Method 9056A Determination of inorganic anions by ion chromatography*
2007.

364. Mudgal, P.K., S.P. Bansal, and K.S. Gupta, *Kinetics of atmospheric oxidation of nitrous acid by oxygen in aqueous medium.* Atmospheric Environment, 2007. 41(19): p. 4097-4105.
365. British Standards Institution, *DD CEN/TS 15364 Characterization of waste — Leaching behaviour tests — Acid and base neutralization capacity test.* 2006.
366. Young, J.R., M.J. How, A.P. Walker, and W.M.H. Worth, *Classification as corrosive or irritant to skin of preparations containing acidic or alkaline substances, without testing on animals.* Toxicology in Vitro, 1988. 2(1): p. 19-26.
367. Poon, C.S., A.I. Clark, R. Perry, A.P. Barker, and P. Barnes, *Permeability study on the cement based solidification process for the disposal of hazardous wastes.* Cement and Concrete Research, 1986. 16(2): p. 161-172.
368. Neville, A.M., *Properties of concrete*. 4th ed, 1996, Harlow: John Wiley & Sons.
369. Feldman, R.F., *Pore structure, permeability and diffusivity as related to durability*, in *8th International congress on the chemistry of cement*1986: Rio de Janeiro, Brazil. p. 1-21.
370. Ganjian, E., P. Claisse, M. Tyrer, and A. Atkinson, *Factors affecting measurement of hydraulic conductivity in low-strength cementitious materials.* Cement and Concrete Research, 2006. 36(12): p. 2109-2114.
371. Hearn, N., *Effect of shrinkage and load-induced cracking on water permeability of concrete.* ACI Materials Journal, 1999. 96(2): p. 234-241.
372. Collins, R.E., *Flow of fluids through porous materials,*1961: Reinhold.
373. Dullien, F.A.L., *Porous media: fluid transport and pore structure,*1992: Academic Press.
374. Bamforth, P.B., *The relationship between permeability coefficients for concrete obtained using liquid and gas.* Magazine of concrete research, 1987. 39(138): p. 3-11.
375. Lynsdale, C.J., *The influence of superplasticisers on the engineering properties and performance of concrete.* Civil Engineering, University of Leeds, 1989. PhD thesis.
376. Sanjuan, M.A. and R. MunozMartialay, *Oven-drying as a preconditioning method for air permeability test on concrete.* Materials Letters, 1996. 27(4-5): p. 263-268.
377. Konecny, L. and S.J. Naqvi, *The effect of different drying techniques on the pore-size distribution of blended cement mortars.* Cement and Concrete Research, 1993. 23(5): p. 1223-1228.
378. Claisse, P.A., E. Ganjian, and T.A. Adham, *In situ measurement of the intrinsic permeability of concrete.* Magazine of concrete research, 2003. 55(2): p. 125-132.
379. Shafiq, N. and J.G. Cabrera, *Effects of initial curing condition on the fluid transport properties in OPC and fly ash blended cement concrete.* Cement & Concrete Composites, 2004. 26(4): p. 381-387.
380. Cabrera, J.G. and C.J. Lynsdale, *A new gas permeameter for measuring the permeability of mortar and concrete.* Magazine of concrete research, 1988. 40(144): p. 177-182.

381. Claisse, P.A., H.I. Elsayad, and E. Ganjian, *Water vapour and liquid permeability measurements in cementitious samples.* Advances in Cement Research, 2009. 21(2): p. 83-89.
382. Schwertmann, U., *The double dehyrdoxylation peak of goethite.* Thermochimica Acta, 1984. 78(1-3): p. 39-46.
383. Environment agency, *How to comply with your environmental permit. Additional guidance for clinical waste (EPR 5.07) (Version 1.1).* 2011.
384. Blenkharn, J.I., *Safe disposal and effective destruction of clinical wastes.* Journal of Hospital Infection, 2005. 60(4): p. 295-297.
385. Daschner, F.D. and M. Dettenkofer, *Protecting the patient and the environment - New aspects and challenges in hospital infection control.* Journal of Hospital Infection, 1997. 36(1): p. 7-15.
386. DEFRA, *Waste data overview.* 2011.
387. Hyks, J., T. Astrup, and T.H. Christensen, *Prediction of leaching from air pollution control residues*, in *Sardinia 2007, Eleventh international waste management and landfill symposium*2007: S.Margherita di Pula, Cagliari, Italy.
388. Lee, C.C. and G.L. Huffman, *Medical waste management incineration.* Journal of Hazardous Materials, 1996. 48(1-3): p. 1-30.
389. Baxter, L., *Biomass-coal co-combustion: opportunity for affordable renewable energy.* Fuel, 2005. 84(10): p. 1295-1302.
390. Woods, J., R. Tipper, G. Brown, R. Diaz-Chavez, J. Lovell, and P. de Groot, *URN 06/1960 Evaluating the sustainability of co-firing in the UK.* Report for the DTI, 2006.
391. IPA Energy Consulting, *URN 06/1959 The economics of co-firing.* Report for the DTI, 2006.
392. Diamond, S., *Intimate association of coal particles and inorganic spheres in fly-ash.* Cement and Concrete Research, 1982. 12(3): p. 405-407.
393. Diamond, S., *Particle morphologies in fly-ash.* Cement and Concrete Research, 1986. 16(4): p. 569-579.
394. Dhir, R.K., F.H. Hubbard, J.G.L. Munday, M.R. Jones, and S.L. Duerden, *Contribution of PFA to concrete workability and strength development.* Cement and Concrete Research, 1988. 18(2): p. 277-289.
395. Poon, C.S., X.C. Qiao, and Z.S. Lin, *Pozzolanic properties of reject fly ash in blended cement pastes.* Cement and Concrete Research, 2003. 33(11): p. 1857-1865.
396. Grammelis, P., G. Skodras, and E. Kakaras, *Effects of biomass co-firing with coal on ash properties. Part I: Characterisation and PSD.* Fuel, 2006. 85(16): p. 2310-2315.
397. Wang, S.Z., L. Baxter, and F. Fonseca, *Biomass fly ash in concrete: SEM, EDX and ESEM analysis.* Fuel, 2008. 87(3): p. 372-379.
398. Koukouzas, N., J. Hamalainen, D. Papanikolaou, A. Tourunen, and T. Jantti, *Mineralogical and elemental composition of fly ash from pilot scale fluidised bed combustion of lignite, bituminous coal, wood chips and their blends.* Fuel, 2007. 86(14): p. 2186-2193.
399. Shearer, C.R., N. Yeboah, K.E. Kurtis, and S.E. Burns, *Investigation of biomass co-fired fly ash properties: Characterization and concrete durability performance* in *Second international conference on*

*sustainableconstruction materials and technologies*2010: Universita politecnica delle Marche, Ancona, Italy.
400. Bao, L.M., J. Lin, W. Liu, W.-Z. Lu, and G.L. Zhang, *Investigation of sulfur speciation in particles from small coal-burning boiler by XANES spectroscopy.* Chinese Physics C, 2009. 33(11): p. 1001-1005.
401. Fernandez-Jimenez, A. and A. Palomo, *Characterisation of fly ashes. Potential reactivity as alkaline cements.* Fuel, 2003. 82(18): p. 2259-2265.
402. Wang, S.Z., A. Miller, E. Llamazos, F. Fonseca, and L. Baxter, *Biomass fly ash in concrete: Mixture proportioning and mechanical properties.* Fuel, 2008. 87(3): p. 365-371.
403. Alvarez-Ayuso, E. and H.W. Nugteren, *Synthesis of ettringite: a way to deal with the acid wastewaters of aluminium anodising industry.* Water Research, 2005. 39(1): p. 65-72.
404. La Iglesia, A., M.V. Gonzalez, and J. Dufour, *Zeolite synthesis employing alkaline waste effluents from the aluminum industry.* Environmental Progress, 2002. 21(2): p. 105-110.
405. Tansens, P., A.T. Rodal, C.M.M. Machado, and H. Soares, *Recycling of aluminum and caustic soda solution from waste effluents generated during the cleaning of the extruder matrixes of the aluminum industry.* Journal of Hazardous Materials, 2011. 187(1-3): p. 459-465.
406. Bushey, A.H., *Acidimetric determination of aluminum.* Analytical Chemistry, 1948. 20(2): p. 169-172.
407. Kowalski, Z., W. Kubiak, and A. Kowalska, *Potentiometric titration of hydroxide, aluminate and carbonate in sodium aluminate solutions.* Analytica Chimica Acta, 1982. 140(1): p. 115-121.
408. Naykki, T., A. Raimo, P. Paavo, K. Antero, and N. Paivi, *Determination of Na2O from sodium aluminate NaAlO2.* Talanta, 2000. 52(4): p. 755-760.
409. Benjamin, S.E., *Paper 671. Effects of temperature and pH on the binding of chloirde by calcium aluminate*, in *Pakistan engineering congress, 70th annual session proceedings. Available online at* http://pecongress.org.pk/2007.
410. Renaudin, G., F. Kubel, J.P. Rivera, and M. Francois, *Structural phase transition and high temperature phase structure of Friedels salt, $3CaO\text{-}Al_2O_3\text{-}CaCl_2\text{-}10H_2O$.* Cement and Concrete Research, 1999. 29(12): p. 1937-1942.
411. Rivas-Mercury, J.M., P. Pena, A.H. de Aza, and X. Turrillas, *Dehydration of $Ca_3Al_2(SiO_4)_y(OH)_{4(3-y)}$ ($0 < y < 0.176$) studied by neutron thermodiffractometry.* Journal of the European Ceramic Society, 2008. 28(9): p. 1737-1748.
412. Shih, W.H. and H.L. Chang, *Conversion of fly ash into zeolites for ion-exchange applications.* Materials Letters, 1996. 28(4-6): p. 263-268.
413. Mondragon, F., F. Rincon, L. Sierra, J. Escobar, J. Ramirez, and J. Fernandez, *New perspective for coal ash utilization-synthesis of zeolitic materials.* Fuel, 1990. 69(2): p. 263-266.
414. Lewis, A.E., O. Lahav, and R.E. Loewenthal, *Chemical considerations of sulphur recovery from acid mine drainage*, in *Water Institute of South Africa Biennial Conference*2000: Sun City, South Africa.

415. Fernandez-Jimenez, A., A. Palomo, and M. Criado, *Microstructure development of alkali-activated fly ash cement: a descriptive model.* Cement and Concrete Research, 2005. 35(6): p. 1204-1209.
416. Tajuelo Rodriguez, E., *TEM images of synthesised C-S-H (I)*, 2011, University of Leeds.
417. Ezziane, K., A. Bougara, A. Kadri, H. Khelafi, and E. Kadri, *Compressive strength of mortar containing natural pozzolan under various curing temperature.* Cement & Concrete Composites, 2007. 29(8): p. 587-593.
418. Smith, R.H. and P. Bayliss, *Interlayer desorption of CSH(1).* Cement and Concrete Research, 1972. 2(6): p. 643-646.
419. Dombrowski, K., A. Buchwald, and M. Weil, *The influence of calcium content on the structure and thermal performance of fly ash based geopolymers.* Journal of Materials Science, 2007. 42(9): p. 3033-3043.
420. Balonis, M., *The influence of inorganic chemical accelerators and corrosion inhibitors on the mineralogy of hydrated portland cement systems*, in *Department of chemistry*2010, PhD Thesis: University of Aberdeen.
421. Black, L., C. Breen, J. Yarwood, K. Garbev, P. Stemmermann, and B. Gasharova, *Structural features of C-S-H(I) and its carbonation in air - A Raman spectroscopic study. Part II: Carbonated phases.* Journal of the American Ceramic Society, 2007. 90(3): p. 908-917.
422. Bentz, D.P., M.A. Peltz, and J. Winpigler, *Early-age properties of cement-based materials: II. Influence of water-to-cement ratio* ASCE Journal of Materials in Civil Engineering, 2009. 21 (9): p. 512-517.
423. Willey, J.D., *Effect of ionic strength on the solubility of an electrolyte.* Journal of chemical education, 2004. 81(11): p. 1644-1646.
424. Duchesne, J. and E.J. Reardon, *Measurement and prediction of portlandite solubility in alkali solutions.* Cement and Concrete Research, 1995. 25(5): p. 1043-1053.
425. Hampson, C.J. and J.E. Bailey, *On the structure of some precipitated calcium alumino-sulfate hydrates.* Journal of Materials Science, 1982. 17(11): p. 3341-3346.
426. Wardle, M., *Co-fired PFA in cement*, 2009, BEng Dissertation: University of Leeds.
427. Hwang, C.L. and D.H. Shen, *The effects of blast-furnace slag and fly-ash on the hydration of Portland-cement.* Cement and Concrete Research, 1991. 21(4): p. 410-425.
428. Poellmann, H., H.J. Kuzel, and R. Wenda, *Solid-solution of ettringites. 1. Incorporation of OH- and CO_3^{2-} in $3CaO\text{-}Al_2O_3\text{-}3CaSO_4\text{-}32H_2O$.* Cement and Concrete Research, 1990. 20(6): p. 941-947.
429. Odler, I., J. Schoppstuhl, and H. Dorr, *Thermoanalytical studies on hydrated tricalcium silicate.* Thermochimica Acta, 1979. 29(2): p. 283-287.